(2)
OV 30 1982
830-4410
NAS 1.55:2249
ORIGINAL

NASA Conference Publication 2249

COMPLETED
[redacted] 341

Tenth NASTRAN® Users' Colloquium

Proceedings of a colloquium held at
New Orleans, Louisiana
May 13-14, 1982

NASA

I

NASA Conference Publication 2249

Tenth NASTRAN® Users' Colloquium

Proceedings of a colloquium held at
New Orleans, Louisiana
May 13-14, 1982

NASA
National Aeronautics
and Space Administration

**Scientific and Technical
Information Branch**

1982

II

FOREWORD

NASTRAN® (NASA STRUCTURAL ANALYSIS) is a large, comprehensive, nonproprietary, general purpose finite element computer code for structural analysis which was developed under NASA sponsorship and became available to the public in late 1970. It can be obtained through COSMIC (Computer Software Management and Information Center), Athens, Georgia, and is widely used by NASA, other government agencies, and industry.

NASA currently provides continuing maintenance of NASTRAN® through COSMIC. Because of the widespread interest in NASTRAN®, and finite element methods in general, the Tenth NASTRAN® Users' Colloquium was organized and held at the Marriott Hotel, New Orleans, May 13-14, 1982. (Papers from previous colloquia held in 1971, 1972, 1973, 1975, 1977, 1978, 1979, and 1980, are published in NASA Technical Memorandums X-2378, X-2637, X-2378, X-2893, X-3278, X-3428, and NASA Conference Publications 2018, 2062, 2131, and 2151.) The Tenth Colloquium provides some comprehensive general papers on the application of finite element methods in engineering, comparisons with other approaches, unique applications, pre- and post-processing or auxiliary programs, and new methods of analysis with NASTRAN®.

Individuals actively engaged in the use of finite elements or NASTRAN® were invited to prepare papers for presentation at the Colloquium. These papers are included in this volume. No editorial review was provided by NASA or COSMIC, however, detailed instructions were provided each author to achieve reasonably consistent paper format and content. The opinions and data presented are the sole responsibility of the authors and their respective organizations.

CONTENTS

Page

FOREWORD iii

1. OPERATING IN THE AGE OF NASTRAN 1
by Thomas G. Butler (Butler Analyses)

2. RECENT IMPROVEMENTS AND ENHANCEMENTS TO NASTRAN 12
by P. R. Pamidi (Computer Sciences Corporation)

3. RECENT DEVELOPMENTS OF NASTRAN PRE- AND POST-PROCESSORS: RESPONSE SPECTRUM ANALYSIS (RESPAN) AND INTERACTIVE GRAPHICS (GIFTS) 18
by Eric F. Hirt and Gary L. Fox (NKF Engineering Associates, Inc.)

4. AN INTERACTIVE REVIEW SYSTEM FOR NASTRAN 45
by Lawrence L. Durocher (University of Bridgeport) and
Andrew F. Gasper (Hamilton Standard)

5. ON THE USE OF HARMONIC EXPANSIONS IN MAGNETIC FIELD PROBLEMS IN NASTRAN 65
by Myles M. Hurwitz, Delores R. Wallace, and Ernest W. Brooks
(David W. Taylor Naval Ship Research and Development Center)

6. IMPROVING A NASTRAN DYNAMIC MODEL WITH TEST DATA USING LINWOOD . . . 74
by B. H. Ujihara, M. M. Dosoky, and E. T. Tong (Rockwell International)

7. SOLUTION OF AXISYMMETRIC FLUID STRUCTURE INTERACTION PROBLEMS WITH NASTRAN 87
by A. J. Kalinowski and C. W. Nebelung
(Naval Underwater Systems Center)

8. LARGE DISPLACEMENTS AND STABILITY ANALYSIS OF NONLINEAR PROPELLER STRUCTURES 112
by Robert A. Aiello and Christos C. Chamis
(NASA Lewis Research Center)

9. PREDICTION OF BEAD AREA CONTACT LOAD AT THE TIRE-WHEEL INTERFACE USING NASTRAN 133
By C. H. S. Chen (The B.F. Goodrich Company)

10. ON ELASTIC-PLASTIC ANALYSIS OF AN OVERLOADED BREECH RING USING NASTRAN 143
by P. C. T. Chen (U. S. Army Armament Research and Development Command
Benet Weapons Laboratory)

11. FINITE ELEMENT SOLUTION OF TORSION AND OTHER 2-D POISSON EQUATIONS . 153
by Gordon C. Everstine (David W. Taylor Naval Ship Research and
Development Center)

12. A NEW CAPABILITY FOR ELASTIC AIRCRAFT AIRLOADS VIA NASTRAN 165
by Hugh C. Briggs and Lance E. Chrisinger
(Air Force Institute of Technology)

13. NASTRAN ON THE HEP 187
by W. Keith Brown (RPK Corporation)

14. THE USAGE OF SUBSTRUCTURING ANALYSES IN THE GET AWAY SPECIAL (GAS) PROGRAM 204
by Nelson J. Ferragut (NASA Goddard Space Flight Center)

15. USING NASTRAN TO SOLVE SYMMETRIC STRUCTURES WITH NONSYMMETRIC LOADS . 216
by Thomas G. Butler (Butler Analyses)

16. EVALUATION AND REDUCTION OF ERRORS INDUCED BY THE GUYAN TRANSFORMATION 233
by Gary L. Fox (NKF Engineering Associates, Inc.)

17. ON RESTARTS IN NASTRAN 249
by P. R. Pamidi and M. M. Lin (Computer Sciences Corporat

OPERATING IN THE AGE OF NASTRAN

T. G. Butler, BUTLER ANALYSES

NASTRAN was born at a time when technology was advancing rapidly. It is interesting to reflect on conditions prevailing then. At year zero in the age of NASTRAN (1964) the role of analysis in mechanical design was to make rough estimates. Testing was relied on for proof of design. Analysts were known as intellectual eggheads, but test people were called practical, down-to-earth types. Popular analytical methods at the time were Hardy-Cross and Hrenikoff for statics; for shaft vibrations they were Mykelstad and Holzer. Analog computers were the most advanced analytical tools. Electrical engineers were doing remarkable things with network analyzers, and similar success was enjoyed with hydraulic networks. Finite elements had only recently appeared, and all programs were company-proprietary and limited in solution range. Aerospace companies dominated the finite element scene. The workhorse computer was the IBM 7094, but third-generation computers were developing a competition between IBM 360, CDC 6600, and UNIVAC 1108. Time sharing was on the drawing boards. Terminal inputs used card readers. Universities were preoccupied with solving boundary value problems, but a small nucleus of about 20 professors worldwide were taking finite elements seriously.

NASA's Office of Advanced Research and Technology (OART) under Dr. Raymond Bisplinghoff sponsored a considerable amount of research in the area of flight structures through its operating centers. Representatives from the centers who managed research in structures convened annually to exchange ideas. I was one of the representatives from Goddard Space Flight Center at the meeting in January 1964. I detected a pattern that seemed to need redirection. Center after center described research programs to improve analysis of structures. Shells of different kinds were logical for NASA to analyze at the time because rockets are shell-like. Each research concentrated on a different aspect of shells. Some were closed with discontinuous boundaries. Other shells had cutouts. Others were noncircular. Others were partial spans of less than 360°. This all seemed quite worthwhile if the products of the research resulted in exact closed-form solutions. However, all of them were geared toward making some simplifying assumption that made it possible to write a computer program to give numerical solutions for their behavior. The popular phrase at the time was "solutions to within engineering accuracy." Each of these computer programs required data organization different from every other program; e.g., they were not compatible. Each was intended for exploring localized conditions rather than complete shell-like structures, such as a whole rocket. My reaction to these programs was that if the end products were all accurate only to within engineering accuracy, technology was currently available to give engineering solutions to not just localized shells but to whole, highly varied structures. The method was finite elements. I proposed that finite elements be used for obtaining engineering solutions and research be upgraded to making fewer simplifications and aim for closed-form solutions, which are always needed. This caused a furor, but Headquarters responded by setting up a committee to investigate the subject of numerical analysis of structures.

The ad hoc committee was composed of a representative from each NASA Center. There was some change of personnel before the committee's work was completed. Names of members were:

Center	Representative
Ames	Dick Beam and Perry Polentz
Flight	Dick Rosecrans
Goddard	Tom Butler (Chairman) and Pete Smidinger
JPL	Mickey Alper and Bob Bamford
Langley	Herb Cunningham
Lewis	Bill Scott and Jim McAleese
Manned	Tom Modlin
Marshall	Bob McComas

The committee was commissioned to investigate what the state of analysis was in the aerospace industry at the time. We were to determine if analog computing should be promoted more or if the finite elements method was more suited to NASA's analyses. We were to try to find an existing finite element program of a quality that would be worth recommending to all NASA Centers.

We wanted to visit all aerospace companies, but under out-time and budgetary constraints we were obliged to limit ourselves. We visited Boeing in Seattle, Lockheed in Burbank, Douglas in Santa Monica, Philco in Pasadena, North American in Columbus, Bell in Buffalo, and Martin in Baltimore. All these companies were extremely cooperative and candid. At the completion of the investigation we felt assured that there was enough information at hand to come to a consensus.

The committee's recommendation to Dr. Bisplinghoff, Mel Rosche, and Doug Michel at NASA Headquarters was that NASA sponsor the development of its own finite element program to update the analytical capability of the whole aerospace community. The program should incorporate the best of the state of the arts, which were currently splintered, and incorporate them into a single program. Headquarters endorsed the committee's recommendation and asked the committee to draw up specifications. The committee convened in a stormy session at Manned Space Flight Center to hammer out a rough set of specifications. Then Headquarters asked three NASA Centers -- Ames, Goddard, and Langley -- to submit proposals to manage the program. Headquarters selected Goddard. Goddard appointed me to manage the project, which was then called the General Purpose Structural Analysis Program.

After our Goddard office refined the specifications, teams of aerospace companies were asked to propose on design plans for the program with the stipulation that the two top companies from the design phase would then compete for the implementation contract. Much credit goes to Bill Doles of the Goddard Computing Support Contracting Office for displaying extreme skill in getting this program under contract smoothly and in record time. Computer Sciences, Martin Company, and MacNeal Schwendler Corporation formed the winning team that started coding in July 1966. Parts of the program were first put into operation at Goddard in May 1968. By autumn of 1968 deliveries of the statics portion were made to other NASA Centers. A year later all centers had the complete program and had been given onsite instruction on how to analyze with it. A debugging period followed before the release of NASTRAN to the general public began in 1970. This was year 6 in the age of NASTRAN.

What was accomplished? It lived up to all its promises and more by a long shot:

> It gathered together all the best in the state of the arts and incorporated them into a single program.
>
> It pioneered the concept of the General Purpose Program, which is to say that all parts of the program were commensurable for structural models up to 2,000 degrees of freedom (d.o.f.) and beyond. This meant that a model of a large structure could be started with a static analysis and finish with a transient analysis without having to reduce its size to accommodate dynamics.
>
> It demolished many barriers that had curtailed the early programs.
>
> It opened static analysis from a size of 100-600 d.o.f. to sizes beyond the specified 2,000 d.o.f. and out to 10,000 d.o.f. by using spill logic.
>
> It opened eigenvalue analysis from core-sized problems of 100 d.o.f. yielding 15 roots to hundreds of reliable roots from problems beyond order 2,000 d.o.f.
>
> It advanced the solution of matrices in the complex domain from order 25 d.o.f. far beyond the specified 2,000 d.o.f.
>
> It introduced the use of nested sets of displacement variables.
>
> It pioneered the concept of a general purpose plotter (independent of any particular piece of hardware).
>
> It closed the door on the force method, regrettably.
>
> It set new standards of input data formats.
>
> It separated the handling of problem control data from the data describing the structural model.
>
> It incorporated a matrix abstraction node (DMAP) so that structural modules could be addressed through other than rigid formats.
>
> It set new standards for documentation. Distinct manuals were published for users, programmers, theory, and demonstration problems.

It abounded with service code to provide user conveniences. Service code exceeded operational code in the ratio of 10 : 1. No redundant information was required.

It was modular. Internal parts of the program could be changed without disrupting other parts.

It was open ended. New elements, new modules, and new rigid formats could be added.

It was maintainable and capable of being updated, both for advances in computers and in the science of mechanics.

It had its own execution log so that aborts could be related to the structural phase of solution.

It had its own measures of solution integrity (Epsilon sub E).

It put finite elements into the public domain. It was free to anyone.

It promoted the use of finite elements in the auto and machinery industries.

It introduced an entirely new method of eigenvalue extraction, inverse power with shifts, which allowed a root of any harmonic to be calculated with equal accuracy over the frequency range so that errors were due to modeling, not to computing.

It provided transient analysis of structures by means of the direct integration of coupled equations without having to transform to the modal approach.

It contained multipoint constraints, which was novel for its time but is taken for granted today.

It contained scalar elements distinct from geometrically based elements.

So much was accomplished by this devoted team of engineers and programmers, it is fitting that they be remembered for their accomplishments. Individual attention is given to the people who were the prime developers.

Bob Peabody was the architect of NASTRAN's system design. It was his perception that limited a small section to interface with the computer so all else is machine independent. No communication within core lets all modules be sequence independent. The internal management of tapes, discs, and memory optimizes resources at each step. The importance of parameter control of operations gives flexibility and keeps overhead low. The famous OSCAR (Operating Sequence Control Array) was entirely his invention. He was head of the team during the design phase.

Dick MacNeal designed the solution structure of NASTRAN. He blended the mathematical operations with the physics for each type of solution. He invented the concept of nested displacement sets. He originated the inverse power method as a stand-alone technique for eigenvalue extraction. He included modules beyond the specification for multipoint constraints, scalar elements, and individual nonlinear elements. He was the author of the theoretical manual.

Keith Redner was the master programmer of NASTRAN and head of the implementation team. He spearheaded the coring of FORTRAN for compatibility on all computers. He designed the internal input/output concept. He designed the overlays and links. He saved the single program concept when he wrote the loader for the CDC 6600. He set the high coding standards that everyone emulated. He coauthored the CHKPNT/RSTRT design.

Mac McCormick was the author of the decomposition technique for banded matrices with active columns. He was a pioneer in finite element analysis, a programmer of finite element code, and highly involved with computer hardware. As such, he was an all-round man who oversaw the transformation of the engineering mathematics into algorithms suitable for programming specifications. He was constantly concerned with efficiency, both programming-wise and hardware-wise. He supervised the installation of NASTRAN on the computers at the NASA Centers and supervised the training of center engineers in the use of NASTRAN. He was the author of the user's manual.

Tom Clark was the inventor of the general purpose plotter. He devised spill logic for handling large matrices. He was the author of the Givens eigenvalue extraction technique. He was instrumental in devising the overlay structure. He was highly involved with matrix packing.

Steve Wall and Dick Pyle were tireless programmers. They were the chief lieutenants to Keith Redner. They were prime implementors and innovators, getting solutions to knotty problems daily as they came up: adapting to new computers, adapting to operating system changes, adapting to new issues of compilers, setting up hierarchies of memory management, handling machine language conversions, building overlays, managing update levels, and handling liaison with many computing centers.

Carl Hennrich set up the engineering data inputs, wrote demonstration problems, coauthored CHKPNT/RSTRT design, set up training, and ran the engineering check problems.

Ken Yale wrote the DMAP language that put such a singular stamp on NASTRAN.

Dave Herting is an unsung hero who was busily engaged in transcribing the engineering design concepts of Dick MacNeal into step-by-step working operations. He was involved in the engineering mathematics from statics, buckling, eigenvalues, transients, random, and many others. He organized the rigid formats for various solutions.

Frank Douglas had the important job of coding all the elastic element routines in NASTRAN. He was the author of the programmer's manual. He designed the expansion concepts of dummy elements and dummy modules.

Howard Diehlman's work was pivotal for the whole program. He wrote the code for the workhorse routine within NASTRAN, the decomposition for symmetric, nonsymmetric, real, complex matrices. It was under constant modification as it was applied to statics, to eigenvalues, to buckling, and to transients. He also did much of the machine-dependent aspects of adapting NASTRAN to the UNIVAC 1108.

Howard Longacre developed the general purpose output file processor that was adaptable to any module. He wrote the code for the X-Y plotter. He teamed with Keith Redner to write the CDC 6600 loader.

Loren Kuusinen, Don McLean, and Howard McCoy were utility men that did the 101 things of a technical nature that always needed doing. They smoothed the way for the principals.

Betty Dunbar nee Reisinger and Grace Hunter were the secretaries who were so indispensable for the voluminous documentation, for travel accommodations all over the country, and for report preparation.

Bob Schwendler, Erwin Allen, and Ron Deiss were the administrators that took all the heat for all the irregularities that are bound to creep up in a vast enterprise such as this.

Before the completion of this project, Goddard management overruled me and amputated the force method part from NASTRAN. The team at the Martin Company, who had labored so long and hard, had all their work aborted. They were Dave Hall, Stan Kaufman, Bo Bata, and Skip Wenk.

Later in the development some of the unique axisymmetric elements from the Bell Company were added to NASTRAN. The people from Bell included Steve Jordan and J. Batt.

The Goddard NASTRAN project staff, who worked for me, were Bill Case, Bill Cooke, Jim Mason, Dick McConnell, Reg Mitchell, and Ed Puccinelli.

The Goddard Award Fee Review Panel, to whom I reported, were Eugene Wasielewski, Jim Fleming, John New, Bill Huston, Cliff Shorter, and Buddy Payne.

The NASA Headquarters people were Ray Bisplinghoff, Mel Rosche, Doug Michel, Milton Ames, Red Rowsome, Harry Rowell, Martha Dwyer, and John Stern.

One thing that must be mentioned about the project, that is remarkable, pertains to the spirit that infused it everywhere. Every man thought that he was the key man on the whole project. As it turned out, every man was key because for the whole to mesh no effort was inconsequential. The marvelous thing was that every man felt it inside. There was a feeling of destiny on the project. We knew that we were doing something big and important that was due to have lasting effects. It turned out that we were right. When Keith Redner's sons asked him what he was doing, his reply was, "I am helping to build the world's largest computer program." Keith invented a phrase that gave flesh to that spirit. When anyone tried to submit ordinary code to him he would say, "Not up to the NASTRAN standard." This became a catchphrase on the project. The other catchphrase that we used was "Think general."

The past has many wonderful stories connected with it that are tempting to dwell on, but that temptation must be suppressed to keep this article from becoming shaggy dog in character. The next topic is the present, year 18 in the age of NASTRAN. It commemorates the 12th anniversary of the public release and the 10th colloquium. What is the climate of analysis at present? One of the most remarkable and hopeful signs that has occurred is that testing does not monopolize design certification. A lion's share of designs are now proven by analysis. Testing still has exclusive control over fatigue predictions and damped transient responses. There is a revolution in analysis. It used to be that decisions were based upon extrapolations from too little analytical information. Now the tables have turned and decisions are being made from a flood of information so that skills have to be developed for culling the essentials from the distractions of a surplus of information. Analysts are now respected members of the profession and are no longer disdained as fuzzy-minded, egghead intellectuals. Analyses run the full range from quick and dirty, coarse estimates to single large runs of 8,000 to 10,000 d.o.f., then out to substructuring runs embracing from 80,000 to 100,000 d.o.f. The displacement method of finite element analysis definitely dominates the scene. The number of finite element programs available to the analyst has mushroomed. They are listed here and start with the many versions of NASTRAN:

COSMIC NASTRAN	The current public domain version
MSC/NASTRAN	MacNeal Schwendler proprietary version
UAI/NASTRAN	Universal Analytics proprietary version
UNIVAC NASTRAN	Sperry UNIVAC proprietary version
DTNSRDC NASTRAN	David Taylor Naval Ship Research & Development Center version
MARC NASTRAN	Marc Analysis & Research proprietary version
NKF NASTRAN	NKF Engineering Associates proprietary version

Other than NASTRAN, the finite element programs being rented commercially in order of vintage are:

ASKA
STRUDL
DET VERITAS NORSKE
STARDYNE
MARC
SPAR
ANSYS
SAP
ATLAS
EASE
SUPERB

What does this competition amount to in terms of total solution capability? As a point of reference, examine the solution capability of Level 17.7 of NASTRAN in terms of major types of analyses:

Mechanical structures:	Linear stress, weight, eigenvalue, transient, random, acoustic, hydroelastic
Thermal structures:	Steady state, radiation, transient
Aerodynamic loads:	Subsonic, transonic, supersonic, gust
Extended capability:	Substructuring, modal synthesis, DMAP matrix solutions of any discipline

Viewed from the standpoint of the tools that an analyst needs today to solve the problems with which he is confronted on a day-by-day basis, NASTRAN Level 17.7 can accommodate him with 95 percent of those tools.

During the period in which NASTRAN maintenance decisions emphasized the intensive debugging of existing capability in preference to adding new capabilities and conveniences, the competitive programs strove hard to excel in something that NASTRAN didn't. They succeeded. They added some elastic elements, e.g.:

Bending plate with offsets, tapered thickness, and a 10 : 1 aspect ratio
Pipe elbow element
Tapered beam element
Membrane without excessive stiffness
High-order hexagon

These new elements make it a bit easier to do some analyses in the category of mechanical structures, listed above. They added an additional feature called dynamic reduction, which can take some of the guesswork out of condensing a large-order model to a small-order one before engaging in eigenvalue analysis in the mechanical structures category above. They added a distinct new solution category called nonlinear analysis. They are marketing tutorial manuals to help the neophyte get familiar with finite element methods.

The effect of delaying the addition of new capability during this "scrubbing up" period is to temporarily lose the ability to serve the analyst in about 5 percent of his work with the tools that he needs. In the meantime NASTRAN has achieved a good state of health due to the caring efforts of P. R. Pamidi and Bob Brugh.

In year 18 what is the status of NASTRAN vis-a-vis the rapidly moving computer hardware field? NASTRAN adopts to the large mainframe computers with a configuration using overlay 7 deep within each array of 15 links. NASTRAN adopts to the minicomputer in either an interactive or an overlay configuration. Editors for refining and correcting model input data have become indispensable to the analyst as we have moved away from card input to remote terminal input. There has always been dog-work associated with the assembling of engineering data to create the mathematical model for analyzing a structure. To us who had hungered to be able to obtain accurate analytical results, the penance of dog-work was a small price for the sweet satisfaction of having reliable answers. Then came the inheritors of our legacy. I am peeved. The ingrates never hungered so they don't appreciate the treasure at their disposal. They would rather not have good analysis if they have to be burdened with all that dog-work. Well, I did get over my peevishness and came eventually to be glad for these ingrates. They created a market. Aggressive entrepreneurs are fulfilling a need to take the drudgery out of data preparation, to speed up its preparation, and to take the confusion out of extracting the significance of voluminous output. Such activity goes by the general heading of pre- and post-processors. By far the most vigorous aspect of these is in the field of graphics, as opposed to the pure software packages. However, I would compare the state of graphics pre- and post-processors today with the state that finite elements were in before NASTRAN came on the scene in 1964. Many good features exist. There is much to be desired in each available package. Each operates under a cloak of proprietary secrecy. There is much duplication of effort that could be redirected toward advancing the whole field in general.

In year 18 what is now being offered in the public domain? NASTRAN through COSMIC is one. There is a promise that the G-Prime graphics program will be offered to COSMIC for distribution by DTNSRDC. Documentation appears to be the only thing holding up this promise. Now we come to a disgrace. There is a graphics program called PATRAN that is uniquely versatile. NASA paid for this around 1978. It was delivered to NASA. It was given an official announcement at the Sixth NASTRAN Colloquium held in 1977 at the Lewis Research Center. The public has been waiting to subscribe to it through COSMIC ever since. It can't. It is being peddled commercially! How is this possible? It sounds like it ought to be investigated.

Finally, how does the academic world compare in year 18 to the times in year zero? Finite element courses are being offered. Finite element analyses are being performed. Academic research embraces finite element support. Finite element modeling is still an art; there is no text that teaches how to come to grips with the decisions that an analyst has to make in ensuring that elasticity, mass, constraints, and loads are faithfully represented vis-a-vis the limitations that the finite elements have built into them. If the academics don't publish one soon, one of us will have to come forward to fill the gap.

I have been asked to make some predictions about the future. At the outset I will tender a disclaimer for any ability to predict the future based upon my poor record of the past. I began using digital computers as soon as they became commercially available. In 1950 I wired my own boards for the control of three algebraic steps at a time on the IBM 402 with card input and card output. Fifty boards for a problem was a respectable size. When the CPC (Card Programmed Calculator) was marketed in 1951 it was such an extraordinary improvement over hand wiring of boards that I predicted we couldn't go any further. In 1953 when the IBM 650 drum computer replaced all those cards it was like magic. I predicted we couldn't go further. In 1955 when IBM called its electron tube computer the GIANT, it solved problems so fast that it boggled the mind. I predicted we couldn't go further. In 1957 when solid state replaced the electron tubes in the computer, the speed and size were staggering. I predicted we couldn't go further. In 1963 when computers were used to control computers, like the coupling of the IBM 7044 to an IBM 7094, it sounded like Big Brother was finally taking over. I predicted we couldn't go further. When in 1965 third-generation 360, 6600, and 1108 computers surpassed the predecessors again by orders of magnitude, I gave up doubting; so I predicted that the manufacturers would ultimately give up binary logic and escalate to trinary logic. It hasn't happened. In 1965, when I was asked to take on the NASTRAN project, I predicted that finite elements would survive only 10 years before design synthesis would supersede analysis. When the 10 years were up in 1975, not only was analysis not superseded, it was entrenched. With such a record I offer predictions tongue in cheek.

I predict that a new professional society will be born to represent the community of interest amongst engineering analysis over all of the traditional societies. It will be called ASEA--the American Society of Engineering Analysis.

I predict that there will be a handbook reference on damping, such that analysts will be able to model damping distribution at the element level so that transient response can be performed with confidence.

I predict that when a piece of machinery such as a pump is delivered it will be expected that a finite element analysis of that machine will be made a routine part of that delivery. When a company like Eastman Kodak has a system problem, they can perform a substructure analysis by lifting the analytical model for each component off the shelf and model the linkages between major components.

I predict that NASTRAN will become operational on a microcomputer. Every engineer will have his own microcomputer as he now has his own hand calculator. These microcomputers will solve problems of increasing size by starting at the local level, pooling micros into a network for larger problems, then dispatching them to big mainframes for huge problems. Input of model data will be directly from graphics data bases in response to interactive prompts. Help references will be available on call.

I predict that NASTRAN maintenance updates will be delivered by small ROM cards. There will be enough competition amongst finite element computer programs that COSMIC will satisfy some of its enhancements commercially, similar to the way that competing automobile manufacturers sell to each other. Documentation will not be delivered in printed volumes. It will be available for access as a data base by dialing COSMIC or a local central computer.

I predict that NASTRAN will be available to undergraduate engineers on microcomputers. Finite elements will be used to demonstrate engineering principles in the lecture hall.

I predict that there will be an evolution away from finite element analysis as we know it today toward one of three or maybe to all three of three different channels. One possibility will be to have a network analyzer of passive analog elements and constraints that can be set by buttons and read out any response at any network node. Another possibility is that computer memory will grow so large and cheap that a direct assault on the differential equations could be considered without having to corrupt the problem with finite elements approximations. The third possibility will be the advancement of design synthesis to the simultaneous consideration of multiple merit functions wherein current finite element codes will be embedded as a callable utility.

However the future goes, it promises to be as exciting as the past 18 years.

RECENT IMPROVEMENTS AND ENHANCEMENTS TO NASTRAN

P. R. Pamidi*
Computer Sciences Corporation

ABSTRACT

Several improvements and enhancements made to NASTRAN recently are discussed in this paper.

INTRODUCTION

Many improvements and enhancements have been made to NASTRAN recently with a view to increasing its usefulness. These are all incorporated in the latest release of the program (Release Apr. 1982). Some important features resulting from these changes are discussed in this paper. This discussion will be incorporated in the NASTRAN documentation soon.

STREAMLINED RIGID FORMATS

This represents one of the most significant and noticeable improvements made to NASTRAN in recent years. As part of this effort, all 20 of the Rigid Formats in NASTRAN were completely revamped. The result is a set of Rigid Formats that incorporate all of the features of the improved DMAP capability and that are both elegant and streamlined in appearance. The important features incorporated into all of the Rigid Formats as part of this work are as follows:

1. All CHKPNT instructions were deleted from the DMAP and replaced by a single global PRECHK ALL instruction resulting in automatic checkpointing of all output data blocks. (See Reference 1 for a detailed discussion of this feature).

2. ALL SAVE instructions of the form SAVE FLAG in the DMAP were replaced by automatic SAVE features of the form /S,N,FLAG/ in the immediately preceding DMAP instructions.

3. All numerical constant parameters of the form /C,N,M/ in the DMAP were replaced by /M/.

4. All BCD constant parameters of the form /C,N,B/ in the DMAP were replaced by /*B*/.

---

*Present affiliation: RPK Corporation

IMPROVED RIGID FORMATS

The effort to streamline all Rigid Formats (discussed above) was utilized to incorporate several improvements to the Rigid Formats. Some of these are listed below.

1. Heat R. F. 9 was expanded to handle multiple dynamic loading cases in a manner similar to that in DISP R. F. 9.
2. The processing of OMITs in AERO Rigid Formats 10 and 11 was made more efficient.
3. HEAT R. F. 1 and R. F. 3 were modified to yield contour plots of temperatures.
4. DISP R. F. 8 was expanded to yield plots of frequency deformations.
5. PURGE instructions were inserted at several appropriate locations in the DMAPs of all Rigid Formats. This, in conjunction with the PRECHK ALL instruction discussed earlier, results in more efficient restarts. (See Reference 1 for a detailed discussion of this feature).

CHANGES RELATED TO PLOTTING

Several changes have been made in the program with regard to the plotting capability. Some of these are summarized below.

1. The CALCOMP and SC plotters are no longer supported in NASTRAN; only the NASTRAN General Purpose Plotter (NASTPLT) is supported. This relieves NASTRAN of the need and burden of keeping up with changes and developments in plotter hardware.
2. The default plotter is a NASTPLT microfilm plotter with typing capability.
3. The CSCALE feature has been made fully operational both in structure plotting and in XY plotting. However, instead of being a real value, the CSCALE parameter is now an integer value. This integer is the factor by which the normal (or default) size of the characters is multiplied before plotting. (Each character is, by default, assigned a space of 0.08" width x 0.16" height and within this space the character is derived from a 0.06" square). Note that this factor is used to multiply both the width

and the height of the characters. Thus, a CSCALE value of 2 gives a character which takes up an area that is four times the area taken up by the default size.

4. The CSCALE value is made available in the PLT2 plotter output if the plotter has typing capability so that this value can be used by the external translator program.

5. The plot summary now shows not only the plotter name (NASTPLT), but also the model (microfilm, drum or table) as well as the typing capability (with or without typing capability). In addition, the CSCALE value used is also indicated.

6. Structure plotting data is now checked for errors much more extensively than was being done earlier. (In many ways, this is similar to the manner in which XY plotting data has all along been checked for errors). As a result, conditions that earlier resulted in cancellation of plots but continuation of the job or creation of erroneous plots now result in cancellation of the job with appropriate user fatal messages.

CHECKING OF REQUIRED PARAM BULK DATA CARDS

Several Rigid Formats require that certain PARAM bulk data cards be present, but this was never checked by the program. This checking is now done in the preface so that if the required PARAM bulk data cards are not present in the data, the program terminates with appropriate user fatal messages.

CHECKPOINT/RESTART CAPABILITY

Several improvements and enhancements have been made to the checkpoint/restart capability in the program. These are discussed in detail in Reference 1.

UNSORTED AND SORTED BULK DATA DECK ECHO

ECHO=BOTH (in the Case Control Deck) has been made the default for restart runs and for runs employing the UMF. Since the only bulk data cards that the user submits in a restart run or in a run using the UMF are those that represent deletions from and/or additions to the Bulk Data Deck already on the OPTP (Old Problem Tape) or the UMF, the unsorted echo of the Bulk Data Deck is the only way of identifying these deletions and/or additions. (The user can, of course, override the default by specifying, for example, ECHO=SORT or ECHO=NONE).

AUTOMATIC OUTPUT OF THE DMAP SOURCE LISTING

The LIST option on the XDMAP card (see page 5.7-14 of Reference 2) has been made the default for restart runs and for runs using the DMAP approach (APP DMAP) or the substructure capability (APP DISP,SUBS). This causes the DMAP source listing to be automatically output on the print file in these cases. There is no longer any need, therefore, to turn on DIAG 14 (in the Executive Control Deck) for this purpose.

The DMAP source listing is useful in restart runs since the user can identify the DMAP instructions that are initially flagged for execution (see Reference 1). In the case of APP DMAP runs, the DMAP is part of the input data submitted by the user. In the case of runs using the substructure capability, DMAP ALTERs are automatically generated by the program. It is, therefore, useful to obtain a listing of the DMAP resulting from these ALTERs.

ELIMINATION OF LINK SWITCHING CAUSED BY USE OF UTILITY MODULES

Certain utility modules like MATPRN, TABPT and others have so far been a part of only Link 8 in the program. As a result, use of these modules by means of ALTERs in Rigid Formats or in DMAP runs has almost always caused additional link switching during execution. This unnecessary link swithing has now been completely eliminated (and the program therefore made more efficient) by incorporating these modules in all links but Link 1.

PAGING OF THE NASTRAN OUTPUT

Proper paging of the NASTRAN output, while simple in concept, is difficult to achieve fully in practice because of the size of the program and the fact that the output is generated in so many areas of the code. Considerable work has been done in this regard recently so that proper paging is now done much more extensively than was the case in earlier versions of the program.

PROCESSING OF MIXED-RECORD DATA BLOCKS BY INPUTT2/OUTPUT2 MODULES

The INPUTT2/OUTPUT2 modules were designed to process tables and matrices, but not mixed-record data blocks (that is, data blocks in which non-string-formatted and string-formatted records occur alternately). An example of such a data block is the PPHIG data block generated by the SDR2 module in DISP R. F. 3. The logic in these modules has been expanded so that they can now process mixed-record data blocks as well as tables and matrices.

MODULE EXECUTE FLAG INCLUDED IN OSCAR LISTING

The OSCAR (Operation Sequence Control ARray) listing resulting from the use of DIAG 4 (in the Executive Control Deck) or the use of an XDMAP card with OSCAR option has been expanded so that it now includes the additional important information as to whether a module (or DMAP instruction) is flagged for execution or not. This is of interest and relevance in restart runs.

USE OF MULTIPLE XDMAP CARDS IN THE DMAP

Multiple XDMAP cards are permitted in the DMAP. Thus, by using multiple XDMAP cards with LIST and NOLIST options, the user can selectively obtain listings of only portions of a DMAP. Similarly, by using multiple XDMAP cards with DECK and NODECK options, the user can obtain punched output of only selected portions of a DMAP.

SUMMARY

Several improvements and enhancements have been made to NASTRAN recently. Some of the more important of these features are described in the paper. These changes increase the usefulness of the program.

REFERENCES

1. Pamidi, P. R., and Lin, M. M., "On Restarts in NASTRAN." Presented at the Tenth NASTRAN Users' Colloquium, New Orleans, Louisiana, May 13-14, 1982.

2. The NASTRAN User's Manual, (Level 17.5), NASA SP-222(05), December 1978.

RECENT DEVELOPMENTS OF NASTRAN
PRE- AND POST-PROCESSORS:
RESPONSE SPECTRUM ANALYSIS (RESPAN)
AND
INTERACTIVE GRAPHICS (GIFTS)

ERIC F. HIRT
and
GARY L. FOX

Engineering and Computational
Sciences Division

NKF Engineering Associates, Inc.

ABSTRACT

This paper presents two specific NASTRAN pre- and post-processors. The first section of this report presents a post-processor for dynamic analysis; the second, a graphical interactive package for model generation and review of results.

Section 1

RESPONSE SPECTRUM ANALYSIS

INTRODUCTION

Many dynamic analysis procedures used today are statistical in nature rather than deterministic. Of these methods, there exists a shock analysis technique in which a response spectrum is used in place of a force or motion time history. Two common examples are the U.S. Navy Dynamic Design Analysis Method (DDAM) and the procedures used in the design of earthquake-resistant structures.

Described below is a computer program that provides this analysis capability based on data obtained from a NASTRAN finite element model. A brief development of the theoretical basis is provided for completeness.

THEORETICAL DEVELOPMENT

The relative displacement of a linear elastic undamped structure subjected to arbitrary independent multiple support motion, $\{X\}$ (Reference 1), is:

$$\{X\} = -\sum_{a} \frac{\{\bar{X}\}^a \quad \lfloor\bar{X}\rfloor^a[M][A]\int_{0}^{t} \{\ddot{Z}(\tau)\} \sin \omega^a (t-\tau)d\tau}{\omega^a \lfloor\bar{X}\rfloor^a [M]\{\bar{X}\}^a} \qquad (1-1)$$

where: $\{\bar{X}\}^a$ = eigenvector associated with mode a (column vector)

$\lfloor\bar{X}\rfloor^a$ = transpose of $\{\bar{X}\}^a$ (row vector)

ω^a = circular frequency associated with mode a

$[M]$ = mass matrix of structure

$[A]$ = matrix relating motion at a free degree of freedom due to a unit motion of a foundation degree of freedom

$\{\ddot{Z}(\tau)\}$ = acceleration of foundation degree of freedoms

The notation used here, {] indicates a row vector, { } indicates a scalar quanity, [} indicates a column vector, and [ ] indicates a general matrix. A matrix multiplication, {][ ][} results in a scalar, as indicated by the left and right elements; similarly, [} {] would indicate a matrix result. In the text a scalar will often be written without the braces.

In many situations the integral in Equation (1-1) is replaced by a "design" shock response spectrum. The design shock spectrum is derived from test data. An excellent discussion of test data interpretation for the purposes of deriving a design shock spectrum is given in Reference 2. Since this spectra is commonly defined in terms of velocity versus frequency, let:

$$[V\}^a = \left| \int_0^t [\ddot{Z}(\tau)\} \sin \omega^a (t - \tau) d\tau \right| \quad \text{(design max over time)} \qquad (1-2)$$

Utilizing this definition, the response equation can be rewritten as:

$$[X\} = \sum_a \frac{1}{\omega^a} [\bar{X}\}^a \sum_{i=1}^{f} P_i^a V_i^a \qquad (1-3)$$

where:

$$\{P]^a = \frac{\{\bar{X}]^a [M] [A]}{\{\bar{X}]^a [M] [\bar{X}\}^a} \qquad (1-4)$$

The sums indicated by Equation (1-3) are no longer algebraic since the phase information has been lost by taking the absolute value as indicated in Equation (1-2). Various types of summing schemes are commonly used as discussed below.

The matrix denoted by $\{P]^a$, as defined by Equation (1-4), may be considered a modified participation factor in the a^{th} mode; it is a row matrix with one entry for each degree of freedom of foundation input.

Equation (1-3) presents a means to determine the probable maximum displacement of a structure due to arbitrary multiple support motion. The use of the term "probable" is a result of the response spectra approach being statistical in nature rather than deterministic. The summing convention used will determine how conservative the calculated response is.

The forces and stresses of a structure resulting from a shock input can be computed from the modal forces and modal stresses by the following:

$$\{F\} = \sum_{a} \frac{1}{\omega^{a}} \{\bar{F}\}^{a} \sum_{i=1}^{f} P_i^a V_i^a \tag{1-5}$$

$$\{\sigma\} = \sum_{a} \frac{1}{\omega^{a}} \{\bar{\sigma}\}^{a} \sum_{i=1}^{f} P_i^a V_i^a \tag{1-6}$$

If the required modal response values are made available and the shock response spectra at each foundation degree of freedom is defined, the remaining question in determining the response of the structure is how to perform the summations in a manner which is conservative but not excessively so. Common summation types currently used in industry and defense are the square root of the sum of the squares (SRSS), sum of the absolute values (ABS), and the Naval Research Laboratory (NRL) sum,

$$F = (F_i)_{max} + \sqrt{[\sum_{i}(F_i^2)\ ] - [(F_i)_{max}]}$$

Reference 3. With these three types of summation available, there exist nine possible methods of determining the response of a structure because two summations must be performed. One summation must be performed over the foundation inputs and another over the modes.

GENERAL OVERVIEW OF RESPAN

RESPAN uses as input the results of a NASTRAN modal analysis (Displacement Solution 3). The results of the NASTRAN modal analysis are made available to RESPAN by the use of the OUTPUT2 module inserted into the rigid format by a DMAP alter. This alter is shown in Figure 1-1.

RESPAN is able to account for the modification of the response spectra due to the effective modal mass of a structure. This influence is discussed in Reference 2. For a structure subjected to independent multiple support motion, the effective modal mass in the a^th mode is given by:

$$[M^{a}] = [R][M]\{\bar{X}\}^{a}\ \{P\}^{a} \tag{1-7}$$

where: [R] = matrix relating the reaction force at a foundation degree of freedom due to a unit force at a free degree of freedom.

The effective modal weight associated with the a^th mode at the f^th foundation degree of freedom is given by:

$$W_f^a = (\sum_{i=1}^{f} M_{fi}) * \text{acceleration due to gravity}$$

The effect on the spectral velocity, V_o, of the effective modal mass is assumed to have a general form of

$$V_o = c_o \frac{a_o + a_1 W_f^a + a_2 (W_f^a)^2}{b_o + b_1 W_f^a + b_2 (W_f^a)^2} \qquad (1\text{-}8)$$

where: a_i, b_i, c_o = user-defined coefficients for a specific problem

For a system with a single input (i.e., a rigid foundation no rotation), the response equations reduce to the following:

$$\{X\} = \sum_a \frac{1}{\omega^a} \{\bar{X}\}^a \; P^a \; V^a \qquad (1\text{-}9)$$

$$\{F\} = \sum_a \frac{1}{\omega^a} \{\bar{F}\}^a \; P^a \; V^a \qquad (1\text{-}10)$$

$$\{\sigma\} = \sum_a \frac{1}{\omega^a} \{\bar{\sigma}\}^a \; P^a \; V^a \qquad (1\text{-}11)$$

with:

$$P^a = \frac{\lfloor \bar{X} \rfloor^a \; [M]\{C\}}{\lfloor \bar{X} \rfloor^a \; [M]\{\bar{X}\}^a} \quad ([A] = 1) \qquad (1\text{-}12)$$

where: $\{C\}$ = direction cosines relating shock direction to the structure coordinate system

For this single input system, the effective modal mass reduces to:

$$M^a = \lfloor \bar{X} \rfloor^a [M]\{C\} \quad P^a \qquad ([R] = 1) \qquad (1\text{-}13)$$

Inputs to RESPAN

The inputs to RESPAN are provided in two segments. The first input segment, the Control Deck, allows for input of the parameters required to control the analysis and the output of the shock analysis. The second input segment, the Data Deck, is used to define the specific response shock spectra to be input at each foundation degree of freedom.

Analysis Control Deck

Inputs to RESPAN in this segment are accomplished by the use of identification mnemonics. The valid mnemonics are shown in Figure 1-2. These mnemonics allow for the above-mentioned functions of controlling the analysis and the output of the shock analysis. Also, several of these mnemonics are utilized to define parameters which are in the analysis.

Input Data Deck

The Data Deck defines the shock response spectra that will be input through the foundations into the structure. The shock response spectra can be described in two ways. The spectral values may be determined by tables of spectral value pairs of frequency and acceleration, displacement, or acceleration. In multiple support analysis, multiple spectra may be input along with identifying which input spectra are to be applied to each foundation degree of freedom. In addition, the shock response spectra can be formed or modified by the procedure defined in Reference 2 and generalized as Equation (1-8).

This weighting function is based upon the effective modal weight of each mode and is input by providing the seven coefficients of Equation (1-8). If both this weighting function and a table of spectral values are input, then the product of the value from the spectral table and this weighting function are used to define the input to each foundation degree of freedom.

Outputs from RESPAN

Through the use of the Control Deck mnemonics, the user specifies the type and amount of output that results from a RESPAN analysis. The output of RESPAN is also controlled by the modal data produced by NASTRAN.

The Control Deck controls the following outputs: the geometry of the NASTRAN model, the resulting modal shock accelerations, displacements, reactions (spc forces), elemental forces and elemental stresses, the SRSS, NRL or ABS summation of the modal results (accelerations, displacements, etc.)

```
  ALTER 7
  OUTPUT 2    GPL,GPDT,GEOM2,EPT,MPT//C,N,-1/C,N,11/V,N,LABL=SMODES    $
  ALTER 74,74
  READ   KLL,MLL,,,EED,,CASECC/LAMA,PHIL,MI,OEIGS/*MODES*/S,N,NEIGV   $
  UMERGE USETD,PHIL,/PHIA/V,N,MAJOR=A/V,N,SUBO=L/V,N,SUB1=R            $
  MPYAD  PHIL,MLL,  /TEMP  /V,N,T=1 /V,N,SIGNAB=1 /V,N,SIGNC=0 /
                           V,N,PREC=0     $
  MPYAD  TEMP,DM,  /PARTFC/V,N,T1=0/V,N,SIGNAB1=1/V,N,SIGNC1=0/
                           V,N,PREC1=0    $
  MPYAD  DM,MLL,/TEMP1/V,N,T4=1/V,N,SIGNAB4=-1/V,N,SIGNC4=0/
                           V,N,PREC4=0    $
  MPYAD  TEMP1,PHIL,/MMASS/V,N,T5=0/V,N,SIGNAB5=1/V,N,SIGNC5=0/
                           V,N,PREC5=0    $
  ALTER 84,84
  DIAGONAL  MGG/DMGG//                                              $
  OUTPUT2   OGPWG,OEIGS,LAMA,PHIG,DMGG//C,N,0/C,N,11/V,N,LABL       $
  OUTPUT2   PARTFC,GENMS1,MMASS,USET,//C,N,0/C,N,11/V,N,LABL        $
  OUTPUT 2  OQG1,OEF1,OES1,,//C,N,0/C,N,11/V,N,LABL                 $

$
$ THE USE OF THE FOLLOWING TWO LINES ALLOW FOR OUTPUT OF ONLY THE
$   EIGENVECTORS BY NASTRAN
$
   OFP       OPHIG,,,,,//V,N,CARDNO                                 $
   EXIT                                                             $

ENDALTER
```

Figure 1-1. NASTRAN DMAP Alter

TITLE - Allows for a 64-character title to be printed with the page header

SYMFACT - Assigns a value to the symmetry factor parameter

WTMASS - Assigns a value to the WTMASS parameter

SAMPLE - Identifies a mode to be output as a sample of the modal computations

GEOMETRY - Controls geometry output

CUTOFF - Controls the percentage of structural weight to be used

SELECT - Selects the minimum or maximum value of Equation (1-8)

SUM - Controls the types of summations to be performed

GRAVITY - Assigns a value to gravity

ABS, MODAL, NRL and SRSS - Selects items for output

Figure 1-2. Analysis Control Deck Mnemonics

Section 2

INTERACTIVE GRAPHICS PACKAGE - GIFTS

INTRODUCTION

The NASTRAN program is capable of analyzing very large and complex structures. Models of large structures require large amounts of data to be input and result in an equally large amount of output. The model generation process is time consuming, error prone, and requires extensive checking to assure an accurate model. In addition, the review of printed output is, at best, difficult. Over the past several years several graphic processors have been provided to facilitate this data handling. One of these processors that has been introduced to augment NASTRAN is the GIFTS system. The following section is intended to acquaint the reader with the GIFTS/NASTRAN program.

BACKGROUND

The Graphics-oriented Interactive Finite Element Time-sharing System, "GIFTS", is a finite element package that has been developed in recent years at the Interactive Graphics Engineering Laboratory of the University of Arizona, Tucson, Arizona, under research efforts sponsored by the Office of Naval Research and by the United States Coast Guard. This finite element package encompasses finite element pre-processing, analysis, and post-processing that has been designed to run on a large variety of minicomputers and mainframes.

The GIFTS system is not a single program; instead, it is a collection of several program modules that reside in a program library. Each program module has been designed to perform a specific task and to run independently of other program modules. Communication between the various modules is accomplished through the use of a United Data Base, UDB. A complete finite element analysis utilizing the GIFTS system requires that the user execute a number of these program modules in a specified order. Program modules allow for model generation, display, editing, verification, model analysis, and the display of resulting displacements and stresses.

One consideration addresed during the design of the GIFTS system was the availability of a large number of finite element codes, each with a different capability. In general, each finite element code has its own input scheme; and if a model is initially built in a form acceptable to one finite element code, a considerable amount of effort is required to reformat the data if it decided to perform analysis using a different finite element code. Because the GIFTS system stores data in a data base for communication within its program modules, all that is required to utilize this system as a pre- and post-processor for any finite element code is two interface programs. One interface program would read the GIFTS UDB and reformat the data into the input form acceptable to a given finite element analysis code, and the other interface program would take the analysis results and store these results into the GIFTS UDB for post-processing. This ability to readily interface the GIFTS system of program modules with any available finite element code allows the finite element modeller to utilize several finite element codes with one standardized input.

CAPABILITIES OF THE GIFTS-NASTRAN INTERFACE

The current GIFTS-NASTRAN interface examines the GIFTS UDB and produces a NASTRAN input deck. The NASTRAN elements that this interface will produce are ROD, BAR, TRMEM, TR1A2, QDMEM1, and QUAD2. The NASTRAN input deck produced requires no modifications for a static analysis utilizing NASTRAN Rigid Form 1, assuming that the loads and boundary conditions were defined utilizing the appropriate GIFTS module.

The storage of the NASTRAN analysis results for accessing via the NASTRAN-GIFTS interface is accomplished via the use of the NASTRAN OUTPUT2 module through a DMAP alter. This DMAP alter is automatically inserted into the NASTRAN input deck by the GIFTS-NASTRAN interface. The NASTRAN-GIFTS interface currently recognizes the results of a Displacement Solution 1 analysis.

To summarize, the GIFTS-NASTRAN interfacing allows for elimination of much of the time necessary to produce error-free NASTRAN finite element models utilizing a user friendly graphical package.

REFERENCES

1. Blake, R.E., and G.J. O'Hara, "Dynamic Response in Three Dimensions of Linear Elastic Structures to Independent Motions of Multiple Supports," NRL Report 4739, May 15, 1956.

2. O'Hara, G.J., "Effect Upon Shock Spectra of the Dynamic Reaction of Structures," NRL Report 5236, December 16, 1958.

3. "Shock Design Criteria for Surface Ships," NAVSEA 0908-LP-000-3010, May 1976.

4. "Shock Design Values (U)," NAVSHIPS DDS 072-1, 15 September 1973, CONFIDENTIAL.

5. Wu, R.W., F.A. Hussain, and L.K. Liu, "Seismic Response Analysis of Structural System Subject to Multiple Support Excitation," Nuclear Engineering and Design, 47, 1978, pp. 273-282.

6. Kamel, H.A., M.W. McCabe, and K.A. Hunter, "GIFTS Version 5.03 User's Reference Manual," University of Arizona, April 17, 1981.

7. Kamel, H.A., and R.M. Osgood, "A First Introduction to the GIFTS-5 System," University of Arizona, December 1979.

Appendix A

SAMPLE RESPAN ANALYSIS

Figure A-1 shows the spring and mass problem that was used for this sample. A model of this system was constructed; and following a NASTRAN modal analysis of this model, a RESPAN analysis was performed. The following pages of this appendix show the output obtained from RESPAN.

BEST DOCUMENT AVAILABLE

```
*****************************************************************************************************
*                                  NKF ENGINEERING ASSOCIATES, INC.                                 *
*                          ENGINEERING AND COMPUTATIONAL SCIENCES DIVISION                          *
*                                         RESPAN LEVEL 1.0                                          *
*                        TRIAL OF RESPAN PROGRAM USING SPRING-MASS SAMPLE                           *
*****************************************************************************************************


                                  -----  ANALYSIS CONTROL DECK  -----

                     TITLE     =        TRIAL OF RESPAN PROGRAM USING SPRING-MASS SAMPLE
                     $
                     $ COMMENTS
                     $
                     MODAL =  ALL
                     NRL = ALL
                     $
                     $ MORE COMMENTS
                     $
                     WTMASS = 0.002588
                     GEOMETRY = YES
                     SUM = 1
                     CUT=98.
                     BEGIN DATA
```

```
****************************************************************************************************
*                                 NKF ENGINEERING ASSOCIATES, INC.                                 *
*                       ENGINEERING AND COMPUTATIONAL SCIENCES DIVISION                            *
*                                        RESPAN LEVEL 1.0                                          *
*                         TRIAL OF RESPAN PROGRAM USING SPRING-MASS SAMPLE                         *
****************************************************************************************************


                                   -----  INPUT DATA DECK -----

                 1       2       3       4       5       6       7       8       9       10
                 1234567 1234567 1234567 1234567 1234567 1234567 1234567 1234567 1234567 1234567
                 ORIENT   0.7071  0.7071  0.0
                 SPECA       2       0.0     0.0    10.0     0.50      10000.   50.0    END
                 ENDDATA
```

```
****************************************************************************************************
*                                 NKF ENGINEERING ASSOCIATES, INC.                                 *
*                          ENGINEERING AND COMPUTATIONAL SCIENCES DIVISION                         *
*                                        RESPAN LEVEL 1.0                                          *
*                          TRIAL OF RESPAN PROGRAM USING SPRING-MASS SAMPLE                        *
****************************************************************************************************

                                  ****  NASTRAN GEOMETRY  ****

                    CODE FOR                                                   CODE FOR
                    LOCATION                GRID COORDINATE,                   RESTRAINT
                   COORDINATE                                                 COORDINATE    RESTRAINT
CODE GRID ID.        SYSTEM         X1              X2              X3          SYSTEM

           1              0    0.00000E+00     0.00000E+00     0.00000E+00         0          23456
           2              0    0.25000E+02     0.00000E+00     0.00000E+00         0          23456
           3              0    0.50000E+02     0.00000E+00     0.00000E+00         0          23456
           4              0    0.60000E+02     0.00000E+00     0.00000E+00         0          23456
           5              0    0.75000E+02     0.00000E+00     0.00000E+00         0          23456
           6              0    0.10000E+03     0.00000E+00     0.00000E+00         0          23456
```

```
***************************************************************************************************
*                                  NKF ENGINEERING ASSOCIATES, INC.                               *
*                          ENGINEERING AND COMPUTATIONAL SCIENCES DIVISION                        *
*                                        RESPAN LEVEL 1.0                                         *
*                         TRIAL OF RESPAN PROGRAM USING SPRING-MASS SAMPLE                        *
***************************************************************************************************

                                     ****  NASTRAN GEOMETRY  ****

                      GRID POINTS            COMPONENT
  CELAS1 ID         END A    END B       END A    END B     ELASTIC  VALUE     DAMPING COEFFICIENT       STRESS COEFFICIENT


      1                1        2           1        1       0.10000E+03         0.00000E+00              0.00000E+00
      2                2        3           1        1       0.75000E+02         0.00000E+00              0.00000E+00
      3                3        4           1        1       0.12500E+03         0.00000E+00              0.00000E+00
      4                3        5           1        1       0.75000E+02         0.00000E+00              0.00000E+00
      5                4        6           1        1       0.10000E+03         0.00000E+00              0.00000E+00
```

```
*****************************************************************************************************
*                                 NKF ENGINEERING ASSOCIATES, INC.                                  *
*                         ENGINEERING AND COMPUTATIONAL SCIENCES DIVISION                           *
*                                        RESPAN LEVEL 1.0                                           *
*                         TRIAL OF RESPAN PROGRAM USING SPRING-MASS SAMPLE                          *
*****************************************************************************************************


                                                      CUMULATIVE
                    MODE    FREQUENCY    MODAL WEIGHT  MODAL WEIGHT    PARTICIPATION      SHOCK FACTOR
                    (CPS)                   (KIPS)      (PERCENT)                            (GEES)

                      1       4.5674      0.29508E-01     90.7967       0.102192E+01      0.22837E+00
                      2       8.9773      0.18587E-02     96.5159      -0.301426E+00      0.44886E+00
                      3      11.8822      0.49200E-03     98.0297       0.161330E+00      0.50933E+00

  **** NUMBER OF MODES REQUIRED TO ACHIEVE 98.0 PER CENT OF WEIGHT IS    3 MODES ****
```

```
************************************************************************************************************
*                                      NKF ENGINEERING ASSOCIATES, INC.                                    *
*                               ENGINEERING AND COMPUTATIONAL SCIENCES DIVISION                            *
*                                            RESPAN LEVEL 1.0                                              *
*                            TRIAL OF RESPAN PROGRAM USING SPRING-MASS SAMPLE                              *
************************************************************************************************************

                                      NRL DISPLACEMENTS DUE TO SHOCK

     GRID ID                          DISPLACEMENTS
                     T1                    T2                    T3


        1        0.00000E+00          0.00000E+00          0.00000E+00
        2        0.44092E-01          0.00000E+00          0.00000E+00
        3        0.81213E-01          0.00000E+00          0.00000E+00
        4        0.67771E-01          0.00000E+00          0.00000E+00
        5        0.12612E+00          0.00000E+00          0.00000E+00
        6        0.00000E+00          0.00000E+00          0.00000E+00
```

```
************************************************************************************************************
*                                    NKF ENGINEERING ASSOCIATES, INC.                                      *
*                             ENGINEERING AND COMPUTATIONAL SCIENCES DIVISION                              *
*                                           RESPAN LEVEL 1.0                                               *
*                              TRIAL OF RESPAN PROGRAM USING SPRING-MASS SAMPLE                            *
************************************************************************************************************

                                      NRL ACCELERATIONS DUE TO SHOCK


         GRID ID                        ACCELERATIONS
                       T1                    T2                    T3


            1      0.00000E+00          0.00000E+00          0.00000E+00
            2      0.17441E+00          0.00000E+00          0.00000E+00
            3      0.21399E+00          0.00000E+00          0.00000E+00
            4      0.23909E+00          0.00000E+00          0.00000E+00
            5      0.40516E+00          0.00000E+00          0.00000E+00
            6      0.00000E+00          0.00000E+00          0.00000E+00
```

```
*******************************************************************************************************
*                                   NKF ENGINEERING ASSOCIATES, INC.                                  *
*                             ENGINEERING AND COMPUTATIONAL SCIENCES DIVISION                         *
*                                          RESPAN LEVEL 1.0                                           *
*                              TRIAL OF RESPAN PROGRAM USING SPRING-MASS SAMPLE                       *
*******************************************************************************************************

                                        NRL CELAS1 FORCES DUE TO SHOCK
ELEMENT         FORCES


     1     0.440918E+01
     2     0.326274E+01
     3     0.391000E+01
     4     0.373512E+01
     5     0.677706E+01
```

Appendix B

SAMPLE OF GIFTS/NASTRAN

Figure B-1 shows the commands required to construct the model used for this sample, along with a brief description of each command. The model is shown in Figure B-2. For clarity, only one-half of the model is shown in this figure.

Figure B-3 shows the commands required to define the boundary conditions and three separate loading cases. One of these loading cases, loading case 2, is shown on Figures B-4 and B-5.

Figure B-6 shows the stress contours resulting from loading case 2 superimposed on the deflected structure as computed by NASTRAN. Each contour is labeled by a letter, and the table identifies the percentage of the yield strength that the stress level associated with each letter represents.

```
$
$ BULKM SOURCE FOR PIPET DEMO
$ EFHIRT 4-MAY-1982
$
ETH,1/1/.50/                    Defines element thickness group number 1 as 0.5 inch
MSTEEL/1/                       Defines element material group number 1 as mild steel
KPOINT
1  / 6.5,  1.0,  0.0
2  / 6.5,  0.0, -1.0
3  / 6.5, -1.0,  0.0
4  / 6.5,  0.0,  1.0
5  / 2.5,  1.0,  0.0
6  / 2.5,  0.0, -1.0
7  / 2.5, -1.0,  0.0
8  / 2.5,  0.0,  1.0           Defines the location of 16 grid points
9  / 2.5,  5.0,  0.0
10 / 0.0,  5.0, -2.5
11 /-2.5,  5.0,  0.0
12 / 0.0,  5.0,  2.5
13 / 2.5, -5.0,  0.0
14 / 0.0, -5.0, -2.5
15 /-2.5, -5.0,  0.0
16 / 0.0, -5.0,  2.5/
CARC
C11/1,2,3,7
C12/3,4,1,7
C21/5,6,7,7
C22/7,8,5,7                     Connects grids using circular arcs (8 circular arcs
C31/9,10,11,11                  defined)
C32/11,12,9,11
C41/13,14,15,11
C42/15,16,13,11/
SLINE
L15/1,5,7
L37/3,7,7                       Connects grids with straight lines (5 straight lines
L59/9,5,3                       defined)
L713/7,13,3
L1115/11,15,11/
CONE
BRANCH
2.5,  0.0,  0.0/1.0
6.5,  0.0,  0.0/1.0             Identifies 2 right circular cones
MAIN
0.0,  5.0,  0.0/2.5
0.0, -5.0,  0.0/2.5/
LPROJECT                        Projects lines "C21" and "C22" onto the intersection
C21/BRANCH,MAIN                 of the previously defined cones
C22/BRANCH,MAIN/
COMPLINE
LA/L59,C22,L713                 Forms two single lines from previously defined lines
LB/L59,C21,L713/
GETY                            Indicates that triangular bending elements are to be
TB3                             used with material group 1 and thickness group 1
1,1
GRID4
BRANCH1/C11,L37,C21,L15
BRANCH2/C12,L37,C22,L15         Generates 4 four-sided grids by defining boundary lines
MAIN1/C31,L1115,C41,LB
MAIN2/C32,L1115,C42,LA/
GPROJECT
MAIN1/MAIN                      Projects grids onto right circular cones
MAIN2/MAIN/
END
```

Figure B-1. GIFTS Commands for Model Generation

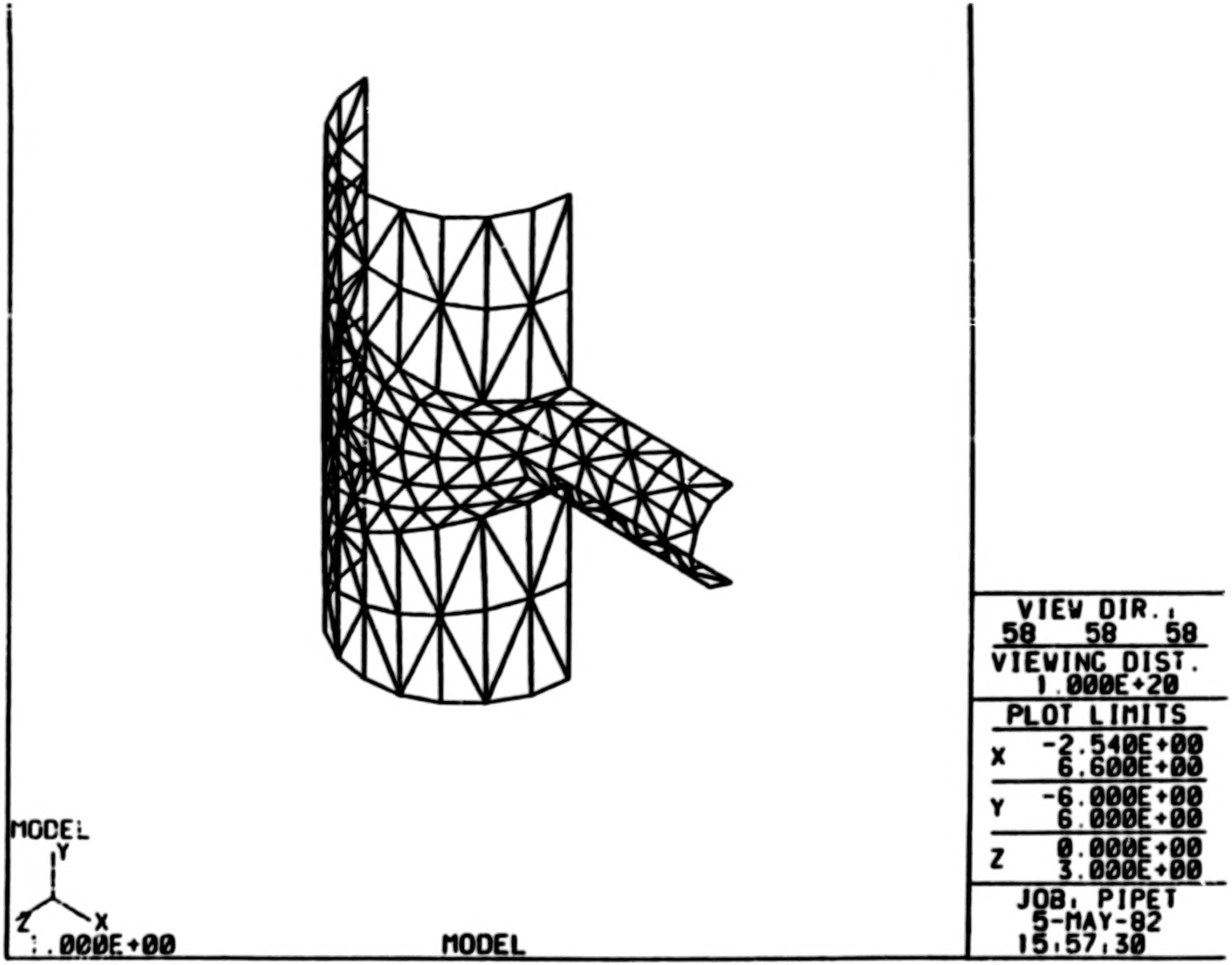

Figure B-2. One-Half of GIFTS Model

```
$
$ BULKLB SOURCE FOR PIPET DEMO
$
$ EFHIRT 4-MAY-1982
$
SUPL,0
C31
C32                                  Suppress all degrees of freedom along 4 lines
C41
C42/
LOADL,1                              Applies a 1000-pound load in direction 1 to two lines
C11/1000.,1000.                      for loading case 1
C12/1000.,1000./
LDCASE/2
LOADL,2                              Applies a 1000-pound load in direction 2 to two lines
C11/1000.,1000.                      for loading case 2
C12/1000.,1000./
LDCASE/3
LOADL,3                              Applies a 1000-pound load in direction 3 to two lines
C11/1000.,1000.                      for loading case 3
C12/1000.,1000./
END
```

Figure B-3. GIFTS Commands for Loading and Constraining

BLANK PAGE

BLANK PAGE

BLANK PAGE

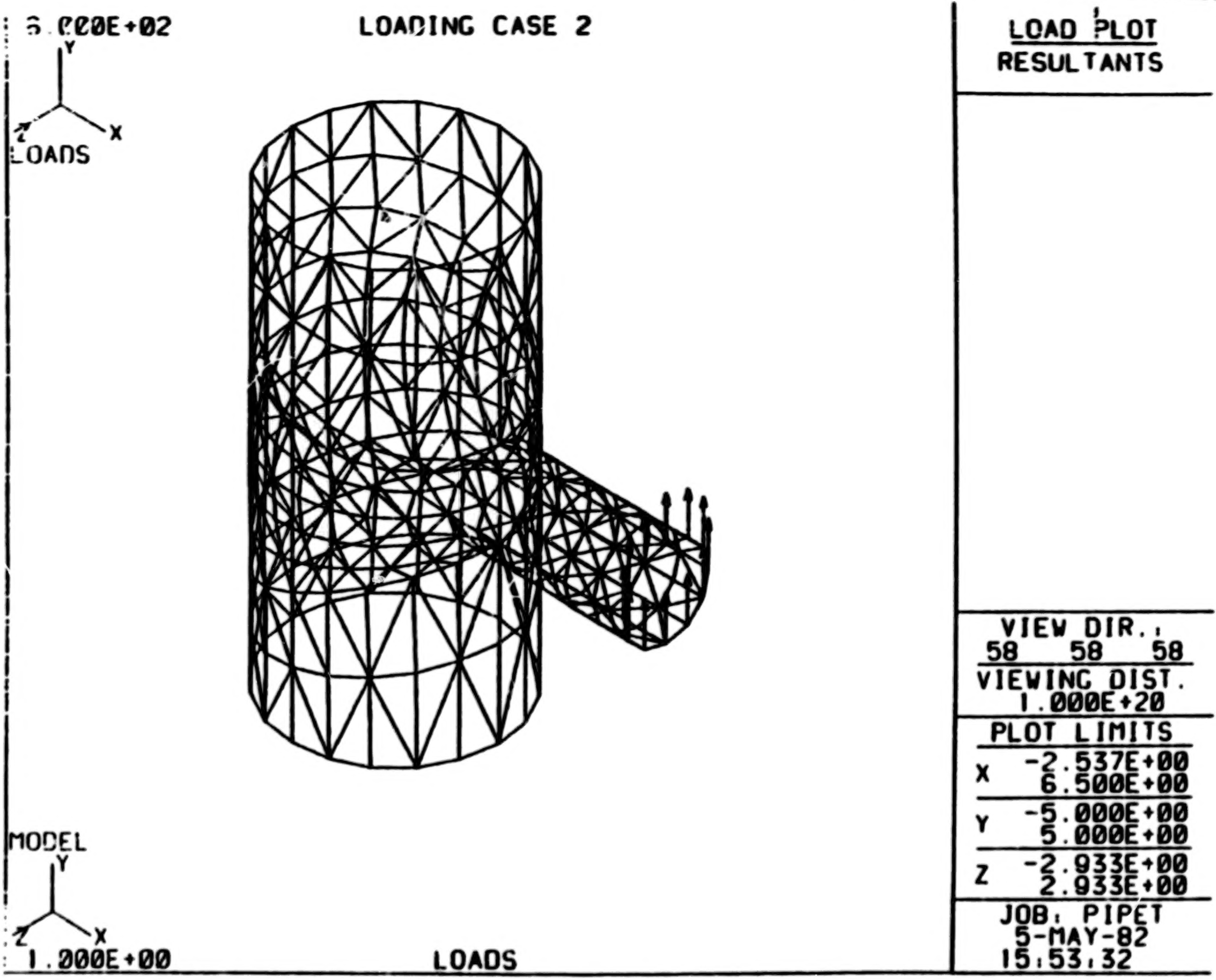

Figure B-4. Applied Loads

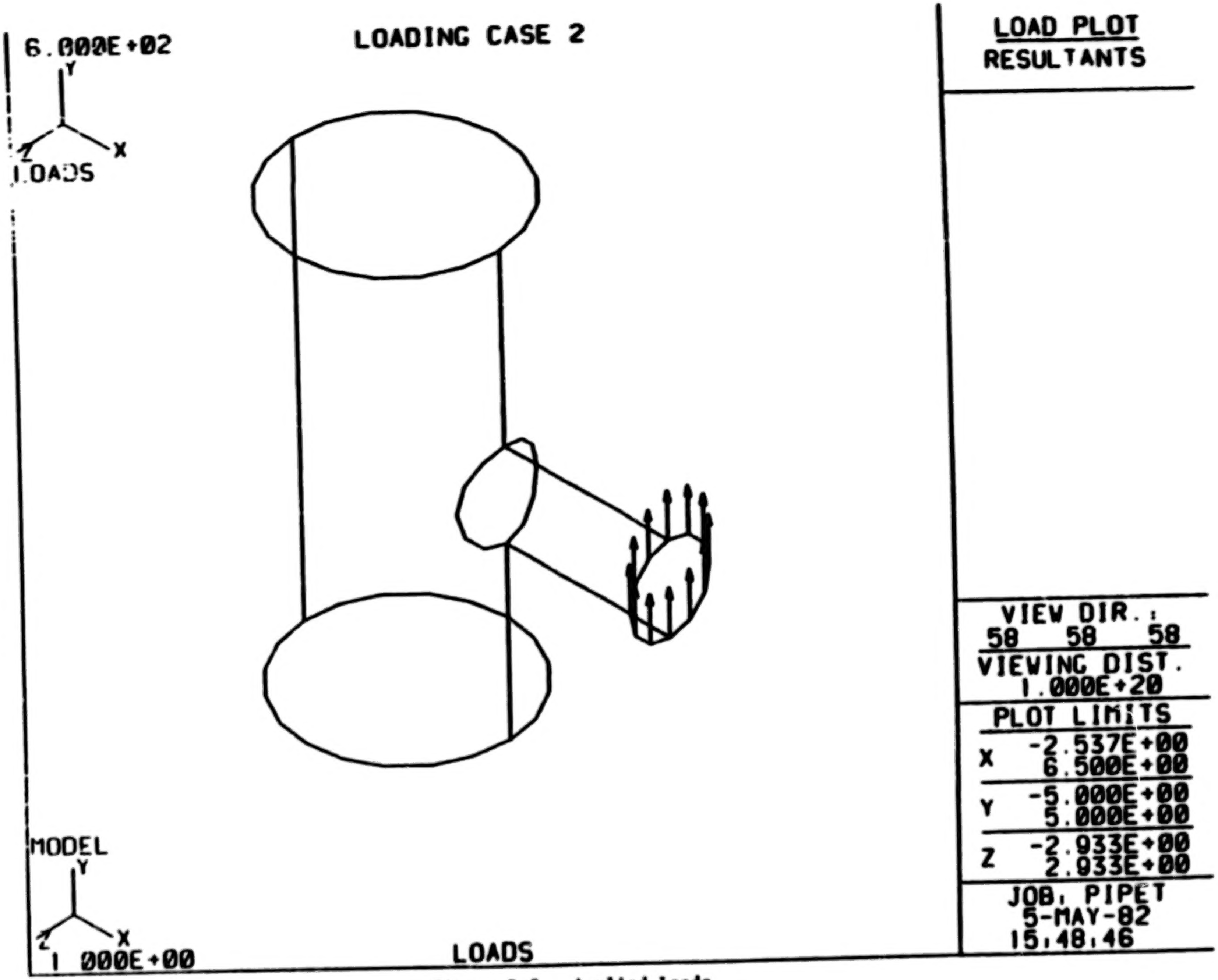

Figure B-5. Applied Loads

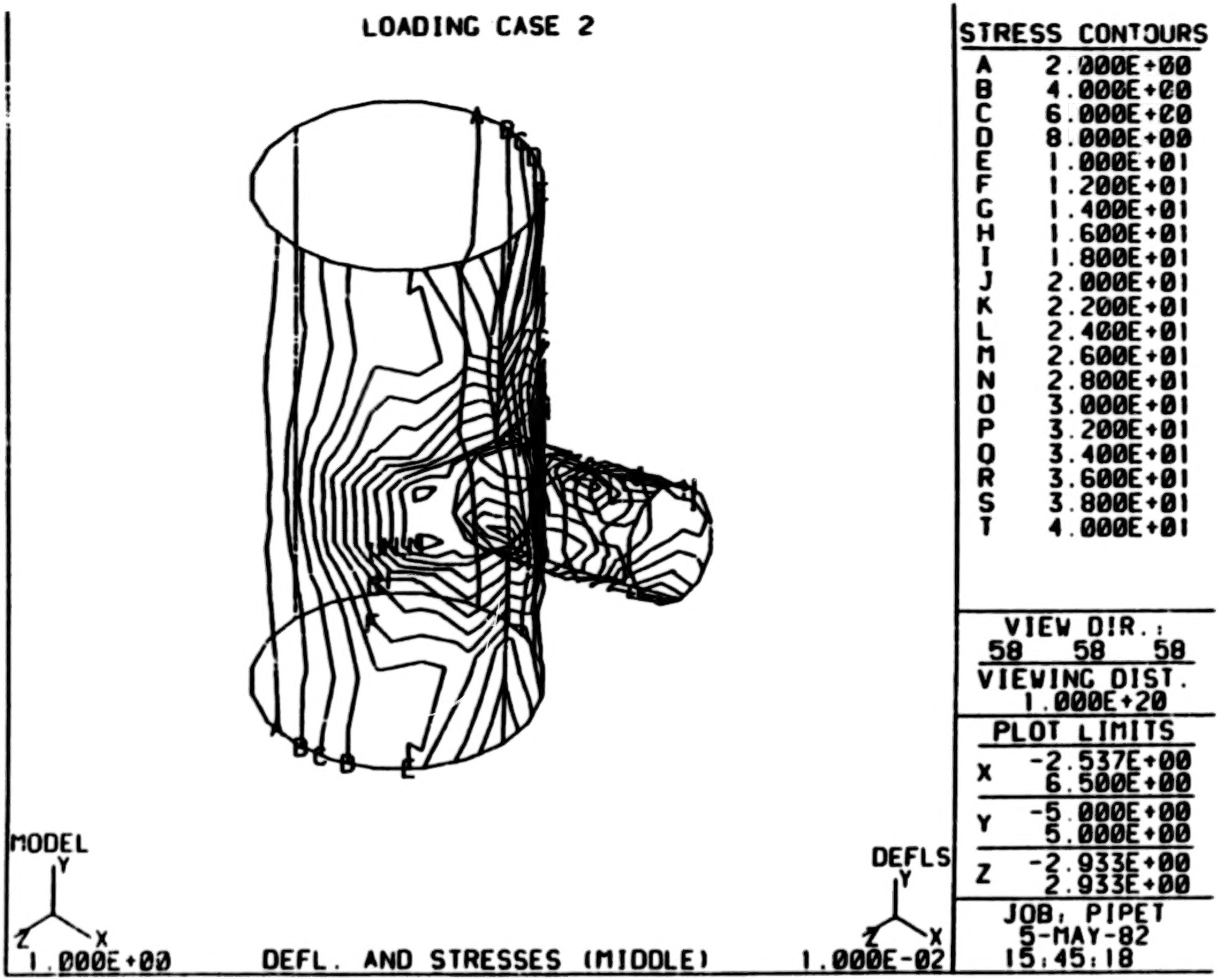

Figure B-6. Resulting Stress Analysis

AN INTERACTIVE REVIEW SYSTEM FOR NASTRAN

Lawrence L. Durocher
University of Bridgeport
Bridgeport, CT 06601

Andrew F. Gasper
Hamilton Standard
Division of United Technologies Corporation
Windsor Locks, CT 06096

SUMMARY

An interactive review system that addresses the problems of model display, model error-checking, and postprocessing has been described. The menu-driven system consists of four distinct programs whose advantages and limitations are detailed. In particular the interface between NASTRAN and MOVIE-BYU, the modifications required to make MOVIE usable in a finite element context, and the resulting capabilities of MOVIE as a graphics postprocessor for NASTRAN are illustrated.

INTRODUCTION

While the linear analysis capabilities of NASTRAN are excellent, its effective use is hampered by the lack of several essential, general purpose software modules; namely (a) a mesh generator, (b) a model display and preliminary error-checker, and (c) a postprocessor for interrogating and graphically displaying the analysis results. Considerable effort has been devoted to mesh generation; however, items (b) and (c) warrant as much, if not more, attention.

A menu-driven, interactive system that addresses the problems of model display and verification and postprocessing is described herein. The system consists of several distinct programs outlined below:

1. NASTVIEW-bulk data review program,

2. PLANIT-three-dimensional sectioning program,

3. SUPERPOS-output superposition and postprocessing program, and

4. MOVIE-BYU-hidden-line graphics display program.

The interface problems and the advantages and limitations associated with the various software packages are discussed. In particular the interface between NASTRAN, SUPERPOS, and MOVIE-BYU is discussed in detail. The modifications required to make MOVIE usable in a finite element context are detailed and the resulting capabilities of MOVIE are illustrated.

THE SYSTEM

The review system at United Technologies' Hamilton Standard Division is part of a larger, more general Finite Element Analysis (FEA) System which includes mesh generators, programs to create JCL for various analysis programs, etc. The system is operational on an IBM 370/168 and is menu-driven via IBM command procedures. Figures 1 and 2 illustrate the overall (FEA) and review systems, respectively. The individual programs associated with the review subsystem are discussed in some detail in the following sections.

NASTVIEW

NASTVIEW is a commercially-available program supplied, by the first author of this paper, in FORTRAN source form for a one-time fee. This program is a menu-driven, interactive, NASTRAN (COSMIC and MSC) bulk data review utility and is currently available for use with Tektronix 40XX series terminals (with cross-hair cursor) or IBM 32XX terminals with attached graphics units. It will read and interpret any NASTRAN deck, perform basic error-checking, and display the geometry of any NASTRAN model comprised of 2-D and/or 3-D elements.

The standard scene manipulation capabilities are available (window definition, scaling, rotation, clipping, etc.). Further, selected groups of elements may be displayed with or without element and node numbers.

In addition, the user can rotate the model to get the correct orientation for NASTRAN output plotting; the proper viewing angles to be used in the case control VIEW card are listed on the graphics screen with each view. This feature eliminates many reruns and restarts due to incorrect viewing angles.

In addition to interpreting the bulk data and displaying the model, NASTVIEW performs the following functions:

(a) bulk data syntax checking,

(b) fundamental error-checking of model,

(c) display of correct NASTRAN viewing angles for any given view of a model, and

(d) display of fundamental model statistics.

A significant amount of syntax checking is performed on all supported element cards, GRID cards, GRDSET, and coordinate system definition cards. NASTVIEW checks all the fields needed to define the geometry of the problem to ensure that the correct data type is in the field; in addition, continuation fields are checked for compatibility. If any type of inconsistency and/or data conversion error is found an appropriate message and the card image will be displayed.

The model can be checked for the following types of modelling errors:

(a) missing GRID card,

(b) disconnected GRID point,

(c) duplicate GRID and/or element identification numbers,

(d) inconsistent coordinate systems, and

(e) coincident nodes, i.e. nodes within a user-specified capture radius.

The number of nodes, number of elements, and number of auxiliary coordinate systems are listed if the user selects the statistics option.

Representative samples of NASTVIEW displays are shown in Figures 3, 4, and 5. Figure 3 is a view of an impeller, Figure 4 is a window view for detail examination of one portion of the impeller, and Figure 5 is a view of the gearbox from Figure 7 showing only selected elements.

NASTVIEW has a number of competitive features that may be absent in other display programs:

(a) code is ANSI standard (1966) FORTRAN and can be run on virtually any mainframe or mega-minicomputer;

(b) JCL, EXECUTIVE, CASE CONTROL do not have to be removed before reading the file;

(c) bulk data does not have to be any specified order;

(d) both COSMIC and MSC/NASTRAN are supported by same program;

(e) essentially all structural element types (including new MSC elements such as CHEXA, CQUAD8, etc.) are supported;

(f) GRID coordinates do not have to be in the basic system, all NASTRAN coordinate system definition cards are interpreted and grid coordinates are converted to basic system;

(g) any selected elements or groups of elements can be kept or deleted from the display;

(h) NASTRAN viewing angles are listed on every view;

(i) node and/or element numbers can be shown on any view of the model;

(j) arbitrary node and element numbering is accommodated by NASTVIEW; and

(k) all user responses are prompted, no commands or mnemonics must be remembered.

Since the code is virtually machine-independent no conversion and/or interface problems exist. While the software is extremely useful, some limitations should be mentioned:

(a) all continuation cards must follow their parent card;

(b) only continuation data is allowed in field 10;

(c) only small field (8-column) data is currently supported; and

(d) model displays do not incorporate hidden-line removal techniques.

The primary use of NASTVIEW is to debug the geometric model definition prior to execution of NASTRAN and verify that element definition, node definition, and coordinate system definition have been correctly specified.

PLANIT

PLANIT is an interactive FORTRAN program developed, under the support of the Air Force Office of Scientific Research, by the Department of Mathematics and Statistics at the University of Pittsburgh. The primary function of PLANIT is to interactively interrogate 20-noded brick finite element models to detect modelling errors. The user is allowed to define any sequence of planes and to view the intersection of each plane with the finite element model on a Tektronix 40XX graphics terminal. Interior voids and grossly distorted or overlapping elements may be detected and corrected prior to costly analysis.

The general strategy employed is as follows (reference 1):

(a) A geometry file for the proposed finite element idealization is constructed (NASTRAN format to PLANIT format conversion).

(b) The user views this idealization and chooses a cross-sectional plane of the structure for close scrutiny.

(c) The user can specify those brick elements he wishes scanned or the program will consider all the bricks from the geometry file.

(d) The intersection of each brick with the specified plane is determined (if such exists) and is displayed.

(e) The user labels each component of the intersection which is then appended to a master plot file.

(f) After considering the totality of bricks to be scrutinized, the master plot file is displayed. Voids between elements, or overlapping of elements will appear as unlabelled or multiply-labelled subregions.

(g) The NASTRAN bulk data file is corrected if errors are found.

An additional option, that is not currently supported at Hamilton Standard, is to have PLANIT build a geometry file for a companion program, STRSIT (reference 2), which plots stress contours on the intersections determined by PLANIT.

PLANIT was written for a DEC-SYSTEM-10 computer and requires an initial programming effort to eliminate nonstandard FORTRAN. PLANIT'S input format is straight-forward and the conversion between NASTRAN CIHEX2 element and PLANIT format is an easy task.

The primary disadvantages of PLANIT are:

(a) considerable amount of user interaction, and

(b) point plots rather than line plots are obtained.

In spite of these disadvantages the program can be very effective in locating geometric modelling errors in very complex models. Figure 6 shows a point plot of a typical intersection, in this case a section through the impeller, also shown in Figures 8 and 10.

SUPERPOS

SUPERPOS is an interactive FORTRAN and PL/I program developed by the Scientific Programming Group at Hamilton Standard and the Computer Aided Design and Manufacturing Center at the University of Bridgeport. The program serves two distinct functions:

(a) NASTRAN postprocessor, and

(b) MOVIE-BYU preprocessor. (MOVIE-BYU is described in the next section)

The program name, SUPERPOS, was chosen because in addition to postprocessing a given NASTRAN output, the user is allowed to superpose a sequence of NASTRAN OUTPUT2 files in an interactive manner.

Before postprocessing the output the user interactively creates a review (superposition) table indicating the files to be combined, the subcase(s) from each file, and the scalar multiple by which each subcase is to be multiplied. The commands by which the review table is created allow a user to review what NASTRAN files are available and to combine scalar multiples of subcases from the same or different NASTRAN runs, assuming the geometry and boundary conditions are compatible.

Superposition is particularly important when used in conjunction with a flexibility type of approach to the selection of applied loads. This approach can eliminate reruns, restarts, or laborious hand calculations when the exact ratio of loads applied in different directions is unknown or uncertain in the early stages of analysis.

Many postprocessors focus exclusively on employing computer graphics to:

(a) display the finite element model and

(b) illustrate the analysis results.

While graphic displays of this type are absolutely necessary they are insufficient by themselves. In most cases more detailed quantitative information is needed after the stress and displacement fields have been visualized. The analyst then frequently is required to pour over great stacks of printed output to locate important characteristics. The SUPERPOS-MOVIE combination gives the user more interactive capabilities beyond those of model and output displays.

In general the user will use SUPERPOS for one or more of the following purposes:

1. Combine scalar multiples of subcases of various NASTRAN runs.
2. Obtain averaged nodal stresses.
3. Obtain all displacements in basic coordinate system.
4. Postprocess the NASTRAN output to create a MOVIE-BYU file for later viewing (perspective, 3-D, hidden-line views with or without scalar contours).
5. Interrogate displacement data, locate nodes where displacement component is in specified range.
6. Interrogate averaged nodal stresses, locate nodes where stress component is in specified range.
7. Interrogate element stresses, locate elements where stress component is in specified range.
8. Calculate net applied force vector or component in any direction and net applied moment vector about any point.

By the list of uses it should be clear that after combining NASTRAN runs, an analyst will employ SUPERPOS to interrogate the output and/or to create MOVIE files for later display.

SUPERPOS provides an effective interface between NASTRAN and MOVIE-BYU and resolved the following problem areas.

1. NASTRAN OUTPUT2 files must be allocated, read, interpreted, and combined "on the fly", via the superposition table and stored in a compact but usable form.
2. To overcome the interpretation phase of item #1, general purpose

NASTRAN OUTPUT2 table read routines must be created to interpret the unformatted output and place it in high speed memory in a usable form.

3. MOVIE requires sequential node numbering and NASTRAN models with nonsequential node numbering must be renumbered, transparent to the user. In addition the correspondence between the original and sequential schemes must be passed to MOVIE.

4. MOVIE requires nodal values of any scalars to be contoured; nodal stresses must be calculated.

5. MOVIE employs displacements in the basic system; nonbasic displacements must be transformed.

6. MOVIE uses "parts", where a part is a group of MOVIE "elements"; an element is a polygon or "warped polygon". All NASTRAN elements must be converted to polygons and the resulting polygons grouped as parts.

7. Elements with nonplanar faces (CIHEX2) must have center node data, i.e. coordinates, displacements, and stresses, calculated and passed to MOVIE.

8. If the MOVIE "poor-man" hidden line technique is to used, element-polygon conversion must result in consistent directions for polygon normals.

The following elements are currently supported by SUPERPOS: CBAR, CQUAD1, CQUAD2, CTRIA1, CTRIA2, CIHEX1 and CIHEX2. Other elements are ignored for display and calculation purposes.

In calculating averaged nodal stresses, the following decisions were made:

1. CBAR stresses are ignored.

2. Plate stresses:

    (a) membrane stresses are calculated in addition to $Z = Z_1$, $Z = Z_2$ stresses.

    (b) element stresses are transformed to six fundamental components in basic system.

    (c) element stresses are distributed equally to all element nodes.

    (d) Z - variations between adjacent elements are ignored.

3. Brick nodal values are simply allocated to appropriate nodes and then averaged.

For models containing plates, three sets ($Z = 0$, Z_1, Z_2) of nodal stresses are calculated and passed to MOVIE. Each set contains seven stresses, the six fundamental components of the stress tensor and the equivalent stress.

Only the plate stresses require some additional computations before the stresses can be lumped to the nodes and averaged. The direction cosines between the local element axes and the basic system must be calculated and then the stresses can be transformed to the basic system.

In most cases the user will employ SUPERPOS in both a listing and a MOVIE mode, that is the user will want to interrogate the NASTRAN output to create printed summaries and create MOVIE files for later display and/or plots. After the user has defined the review table and the program has done all the preliminary phases of postprocessing, the user is asked to choose one of two nonexclusive options, PRINT or MOVIE.

In the PRINT option the user can interrogate the output to get printed listings or terminal display of the following quantities:

1. Node numbers and displacements where a nodal component (selectable) or the magnitude of the displacement is in a user-specified range; displacements can be bounded in original or basic systems.

2. Element numbers and stresses of those elements where an element stress component (selectable) or equivalent stress is in a user-specified range. For plate stresses the user can bound the membrane or membrane-bending stress at $Z = Z_1$ or Z_2. For bar elements the bound can be on axial or axial-bending stresses.

The PRINT option allows the user to interrogate the NASTRAN output in a very efficient manner and can essentially eliminate the need for NASTRAN output listings. SUPERPOS, used in conjunction with MOVIE-BYU, has proved to be a very effective tool for postprocessing NASTRAN output.

MOVIE-BYU

MOVIE-BYU is a system of FORTRAN programs available from Brigham Young University (Provo, Utah). The primary function of the MOVIE system is to provide continuous tone shading and hidden surface representations of mathematical models. The system consists of six programs (DISPLAY, MOSAIC, SECTION, TITLE, UPDATE, and UTILITY) which allow creation, editing,reformatting, and scene manipulation (rotation, scaling, etc.) of data shared in a common data file.

SUPERPOS, the finite element interface to MOVIE-BYU, is a seventh program which transforms the finite elements to one of the MOVIE display primatives (n-sided polygons) and outputs the polygons and scalar functions of interest (displacement and stress components) in the required central file format.

The MOVIE-BYU source is FORTRAN and was written for a DEC-SYSTEM-10 computer. The early versions (prior to version 3.6) required considerable effort to eliminate nonstandard FORTRAN. The newest release (3.7) apparently is much less machine-dependent.

A number of modifications are required to make the MOVIE-BYU DISPLAY program usable in a finite element context:

(a) MOVIE employs a sequential node numbering scheme and to display the actual node numbers on plots the input data format of the central file must be changed to include the correspondence between the original and sequential set.

(b) Contour selection is not user oriented and it is necessary to add menus for contour selection, (for example for the x-stress contour). The plot modules also must be expanded to label the plots as to which contour is being plotted and what numerical value is associated with each contour. Hamilton Standard added the CONTOUR command to choose contour data and NOCONTOUR to stop contour display.

(c) During the conversion from elements to polygons, when brick elements are present, correspondence between element numbers and part numbers is lost. There is no remedy, short of making each brick a part (collection of polygons), for this problem.

(d) The display program is part oriented and it is useful to change the central file format to contain a list of which finite elements belong to which part. The ELEMENT command was added to display a list of the elements belonging to each part.

(e) The display program and the associated data reside in high speed memory and the available memory limits the problem size. Hamilton Standards' version of MOVIE-BYU allows a maximum of 500 parts and 7500 polygons.

(f) It is not possible to draw the deflected geometry on top of the undeformed geometry. The SUPER command was added to achieve this effect.

With these changes implemented, MOVIE-BYU, used in conjunction with the NASTRAN postprocessor (SUPERPOS), has proved to be a very attractive graphical interrogation tool for three-dimensional analysis. Figures 7 and 8 illustrate the hidden surface removal for plate and brick meshes, respectively. Figures 9 and 10 demonstrate stress contours drawn on visible surfaces. Figure 9 shows that users may use the MOVIE-BYU explode feature to render internal parts usable.

Figures 7-10 would be a meaningless jumble of lines without the hidden lines removed; model verification and stress interpretation are clearly an order-of-magnitude easier by the use of the MOVIE system.

POSSIBLE ENHANCEMENTS

While the review system is very effective, a number of enhancements, particularly in the SUPERPOS-MOVIE combination, are possible:

(a) Recovery and interrogation of constraint actions and element forces.

(b) Support of other element types and other rigid formats (only rigid formats 1, 3 are currently supported).

(c) Recovery, interrogation, calculation, and contouring of other quantities such as strain energy density, element strain energy, temperatures, etc.

(d) Interface with "rebreak" and "patch" programs for model refinement.

(e) Interface with a "semi-automatic" report generation program.

(f) Merger of several NASTRAN models and results into one MOVIE file.

(g) SUPERPOS interface to model generation programs.

(h) Interactive stress axes definition and subsequent contouring and/or listings.

(i) Use of some type(s) of economizing techniques to minimize the number of MOVIE polygons.

CONCLUDING REMARKS

An interactive review system for NASTRAN has been described in as much detail as space allows. This system has proven to be very effective in locating errors in models prior to analysis and interpreting the stress and displacement output from very complex models.

REFERENCES

1. Frey, A.E., Hall, C.A., and Porsching, T.A.: PLANIT: Plane Intersections of 20-node Brick Elements. Department of Mathematics and Statistics, Report No. AF 78-1, University of Pittsburgh, May, 1978.

2. Hall, C.A., Porsching, T.A., and Sledge, F.: STRSIT: Contour Plotting of Stresses on Planes of Intersection. Department of Mathematics and Statistics, Technical Report ICMA-79-06, University of Pittsburgh, July, 1979.

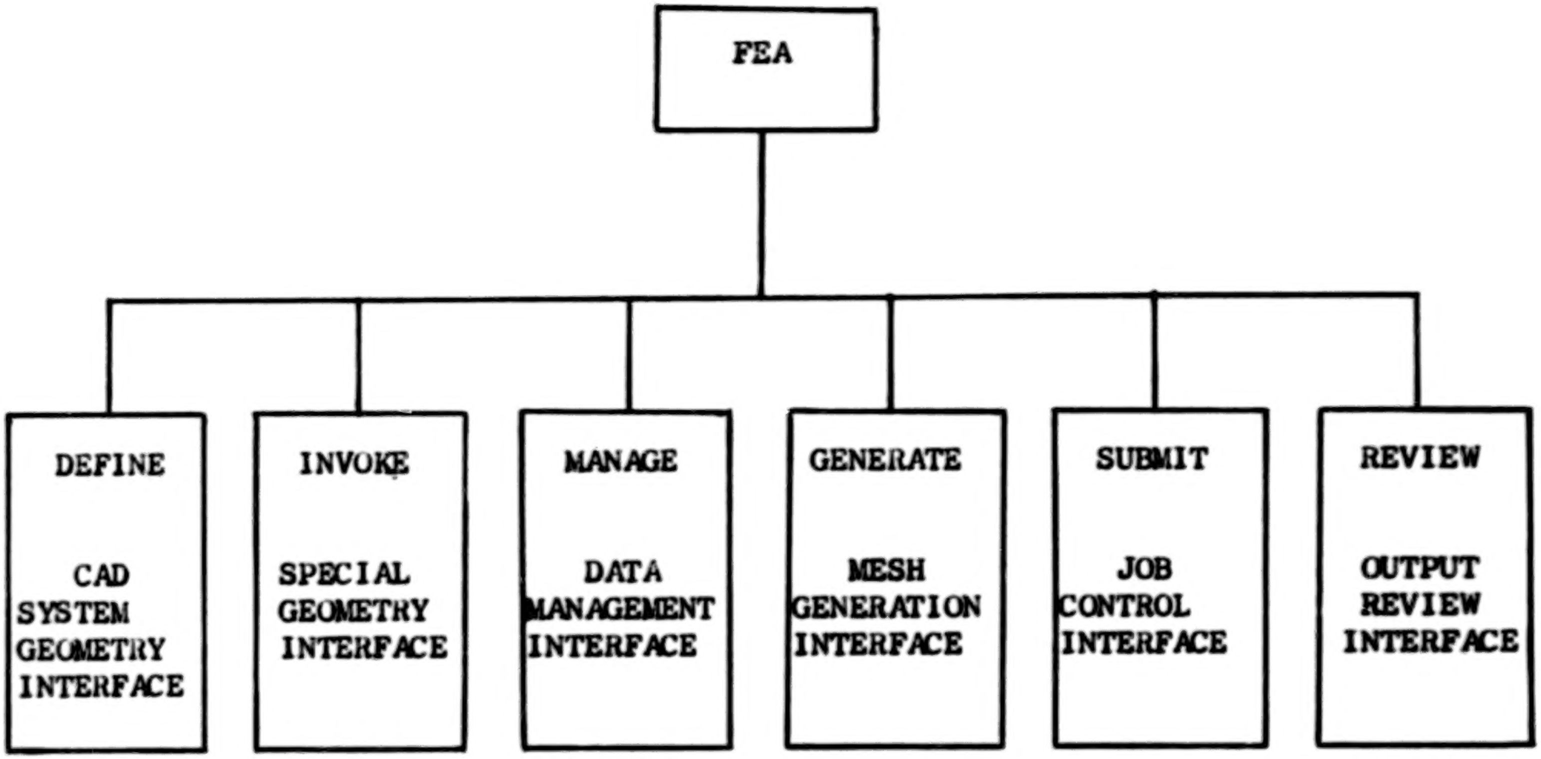
FEA
DEFINE
CAD SYSTEM GEOMETRY INTERFACE
INVOKE
SPECIAL GEOMETRY INTERFACE
MANAGE
DATA MANAGEMENT INTERFACE
GENERATE
MESH GENERATION INTERFACE
SUBMIT
JOB CONTROL INTERFACE
REVIEW
OUTPUT REVIEW INTERFACE

FIGURE 1

Finite Element Analysis System

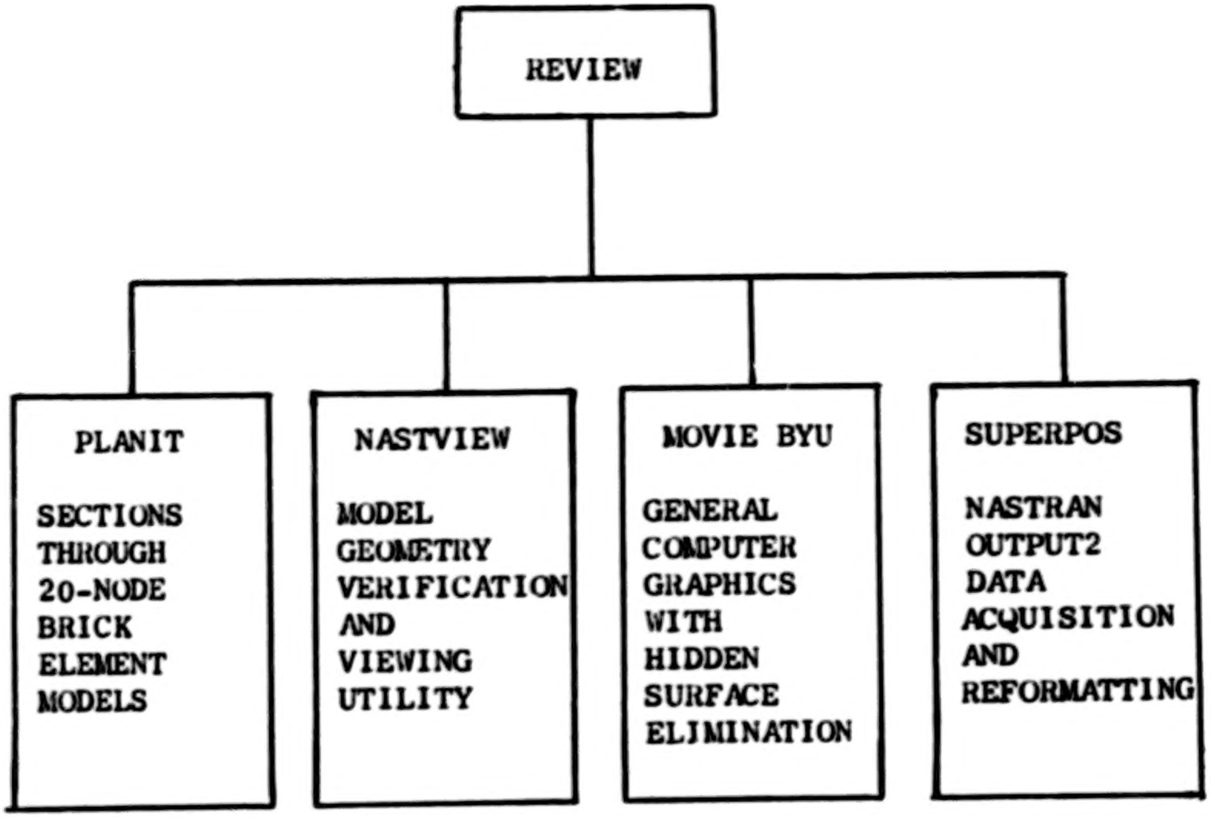
REVIEW
PLANIT
SECTIONS THROUGH 20-NODE BRICK ELEMENT MODELS
NASTVIEW
MODEL GEOMETRY VERIFICATION AND VIEWING UTILITY
MOVIE BYU
GENERAL COMPUTER GRAPHICS WITH HIDDEN SURFACE ELIMINATION
SUPERPOS
NASTRAN OUTPUT2 DATA ACQUISITION AND REFORMATTING

FIGURE 2

Review Subsystem

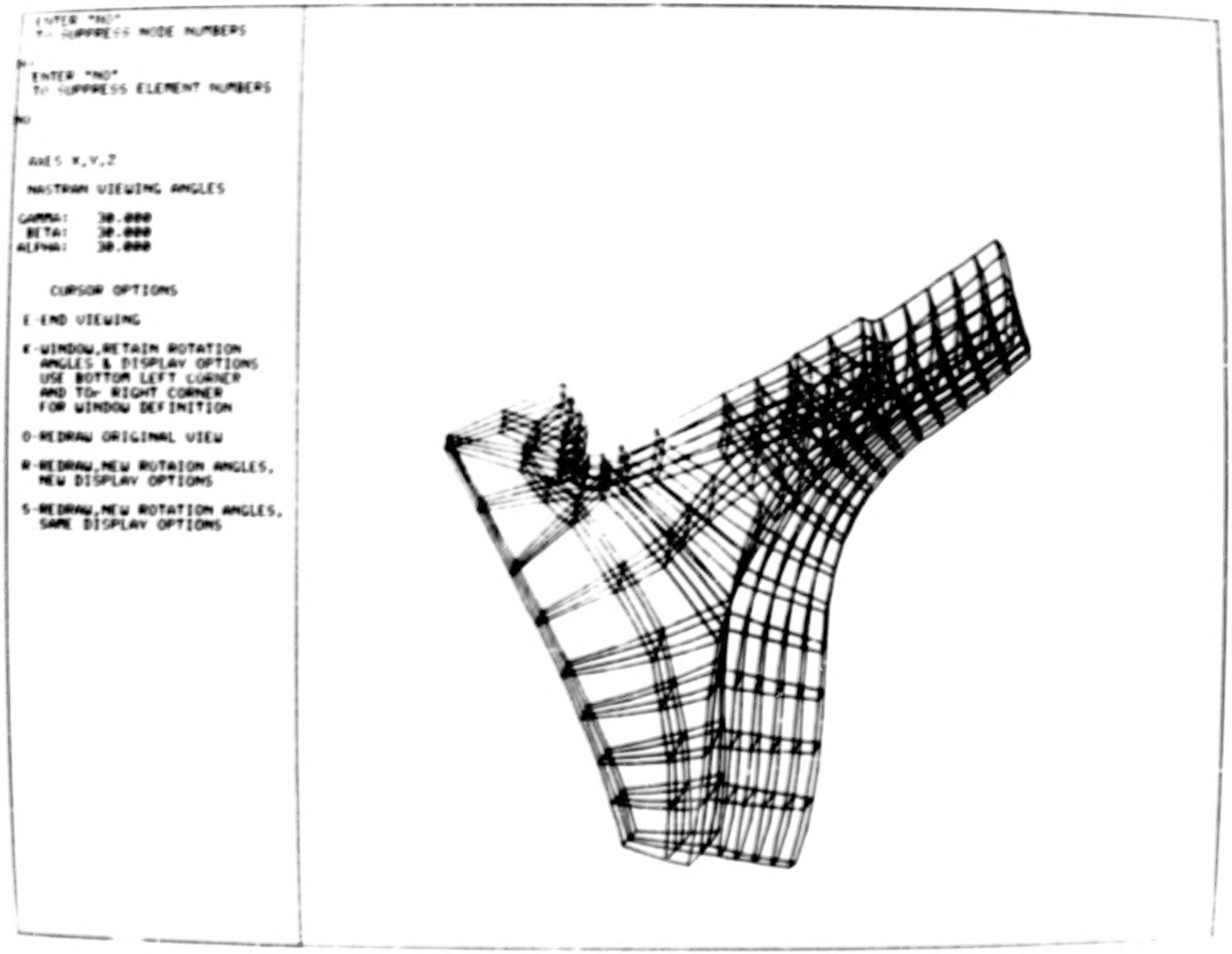

```
ENTER "NO"
TO SUPPRESS NODE NUMBERS

N
ENTER "NO"
TO SUPPRESS ELEMENT NUMBERS

NO


AXES X,Y,Z

NASTRAN VIEWING ANGLES

GAMMA:    30.000
 BETA:    30.000
ALPHA:    30.000


   CURSOR OPTIONS

E-END VIEWING

K-WINDOW,RETAIN ROTATION
  ANGLES & DISPLAY OPTIONS
  USE BOTTOM LEFT CORNER
  AND TOP RIGHT CORNER
  FOR WINDOW DEFINITION

O-REDRAW ORIGINAL VIEW

R-REDRAW,NEW ROTAION ANGLES,
  NEW DISPLAY OPTIONS

S-REDRAW,NEW ROTATION ANGLES,
  SAME DISPLAY OPTIONS
```

FIGURE 3

NASTVIEW Display of Impeller

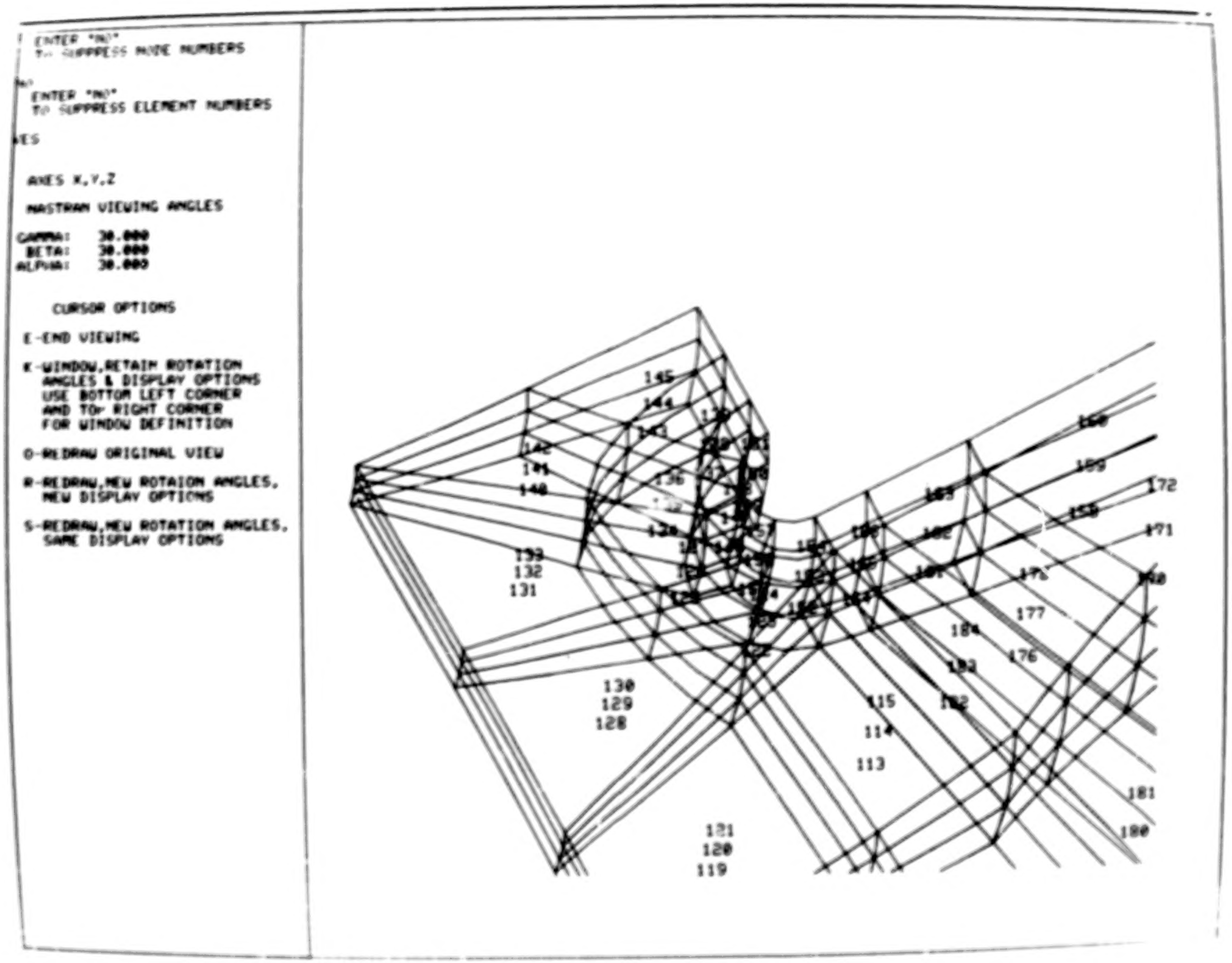

```
ENTER "NO"
TO SUPPRESS NODE NUMBERS

NO
ENTER "NO"
TO SUPPRESS ELEMENT NUMBERS

YES

AXES X,Y,Z

NASTRAN VIEWING ANGLES

GAMMA:    30.000
 BETA:    30.000
ALPHA:    30.000

   CURSOR OPTIONS

E-END VIEWING

K-WINDOW,RETAIN ROTATION
  ANGLES & DISPLAY OPTIONS
  USE BOTTOM LEFT CORNER
  AND TOP RIGHT CORNER
  FOR WINDOW DEFINITION

O-REDRAW ORIGINAL VIEW

R-REDRAW,NEW ROTAION ANGLES,
  NEW DISPLAY OPTIONS

S-REDRAW,NEW ROTATION ANGLES,
  SAME DISPLAY OPTIONS
```

FIGURE 4

NASTVIEW Window of Impeller

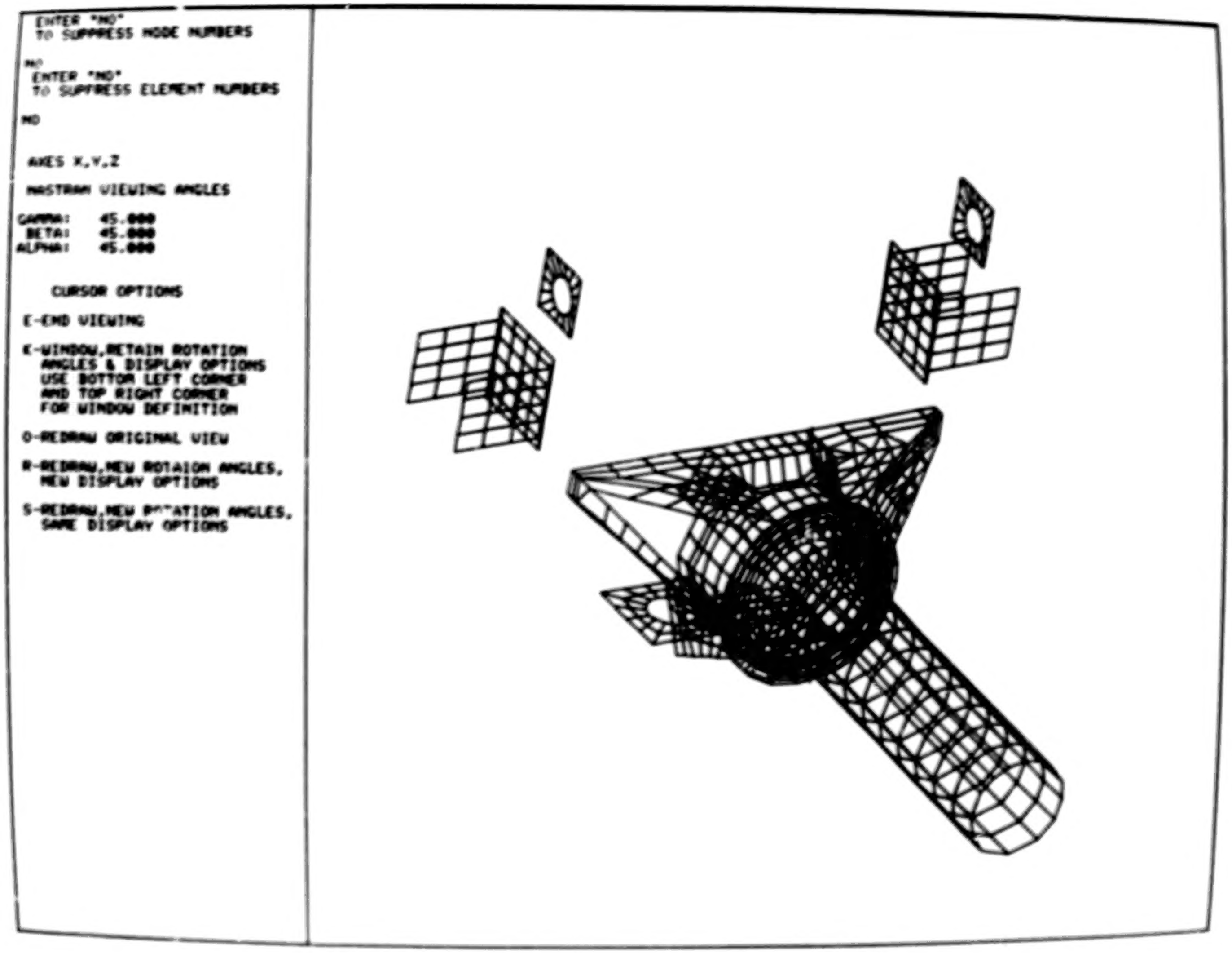

```
ENTER "NO"
TO SUPPRESS NODE NUMBERS

NO
ENTER "NO"
TO SUPPRESS ELEMENT NUMBERS

NO


AXES X,Y,Z

NASTRAN VIEWING ANGLES

GAMMA:    45.000
 BETA:    45.000
ALPHA:    45.000


   CURSOR OPTIONS

E-END VIEWING

K-WINDOW,RETAIN ROTATION
  ANGLES & DISPLAY OPTIONS
  USE BOTTOM LEFT CORNER
  AND TOP RIGHT CORNER
  FOR WINDOW DEFINITION

O-REDRAW ORIGINAL VIEW

R-REDRAW,NEW ROTAION ANGLES,
  NEW DISPLAY OPTIONS

S-REDRAW,NEW ROTATION ANGLES,
  SAME DISPLAY OPTIONS
```

FIGURE 5

NASTVIEW Display of Selected Elements

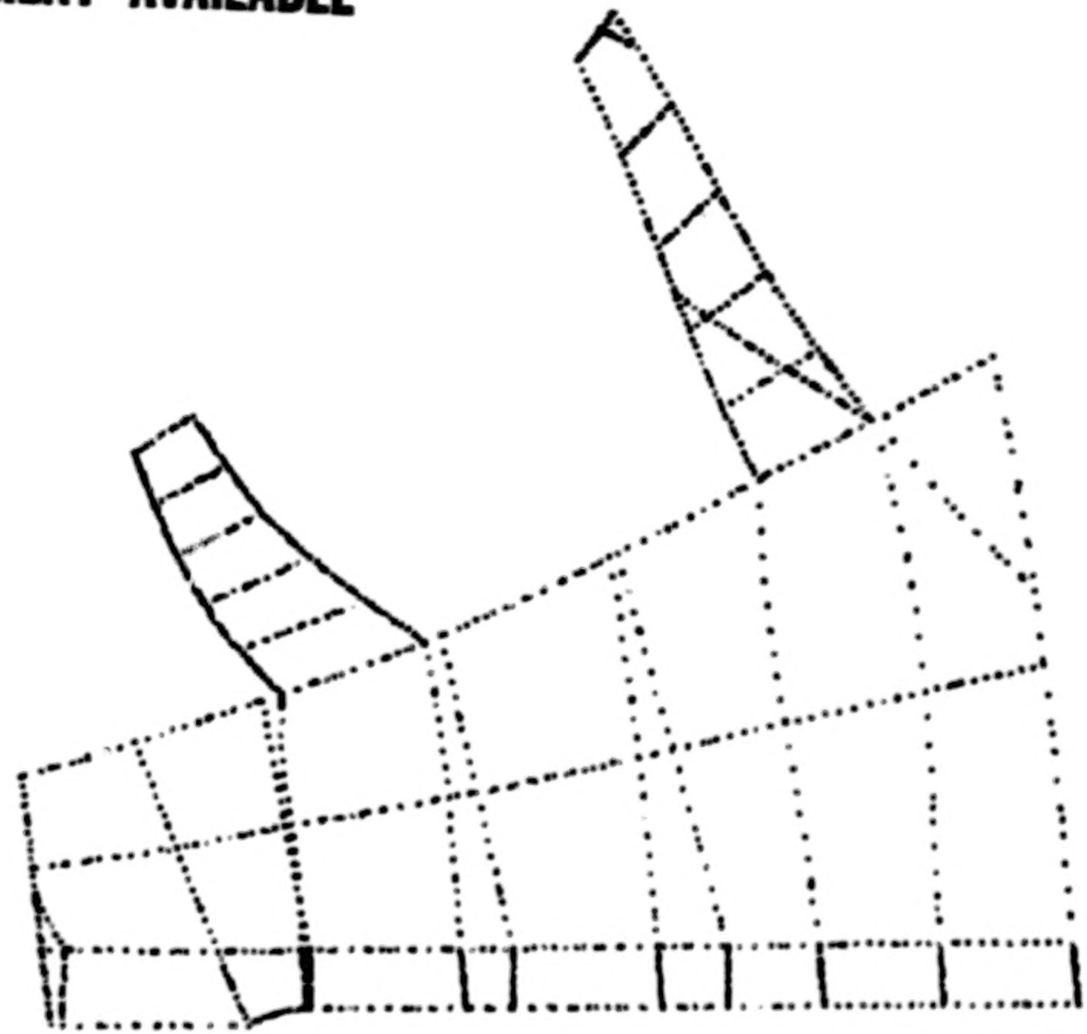

FIGURE 6

Impeller Section Via PLANIT

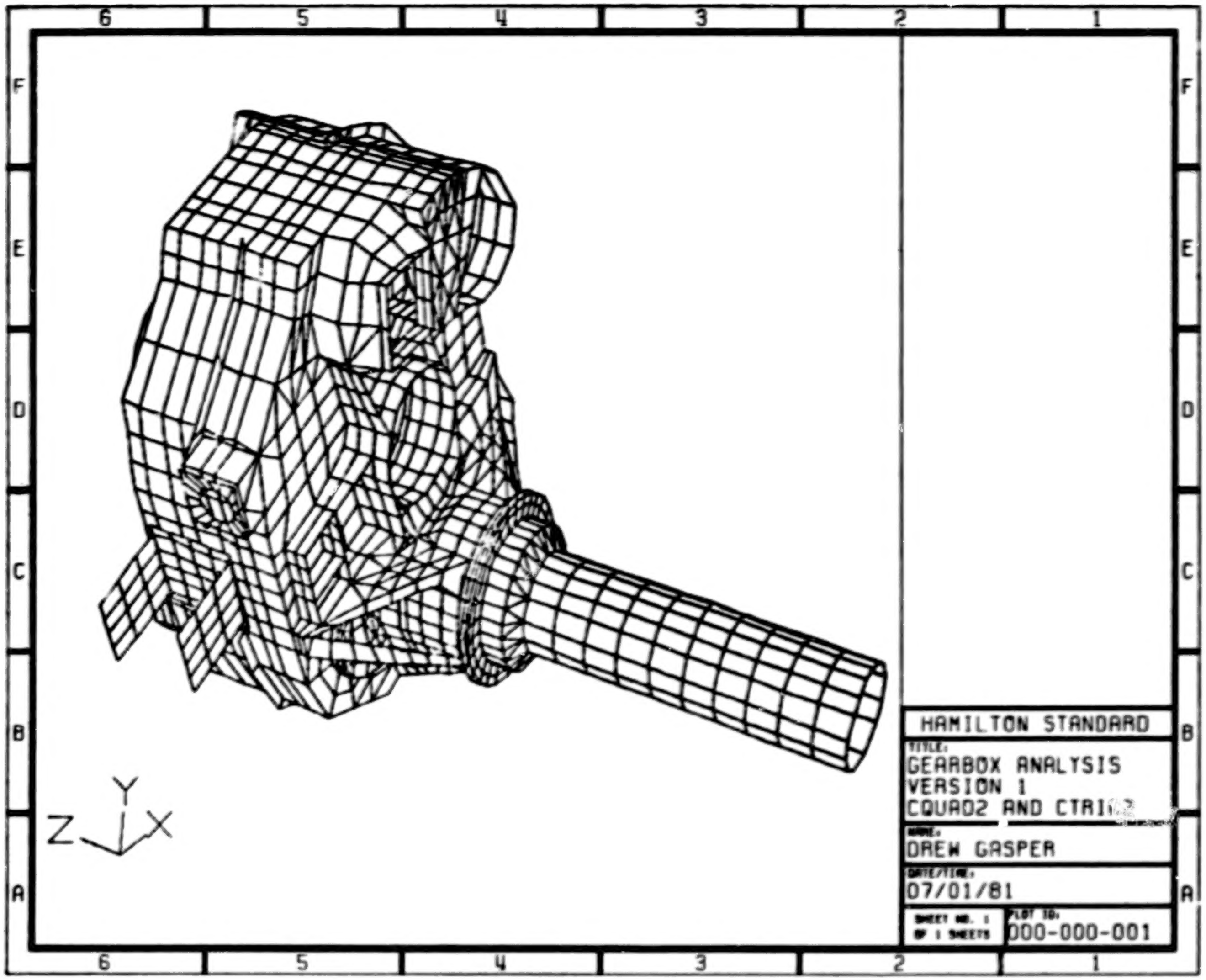

FIGURE 7

MOVIE-BYU Display of Gearbox

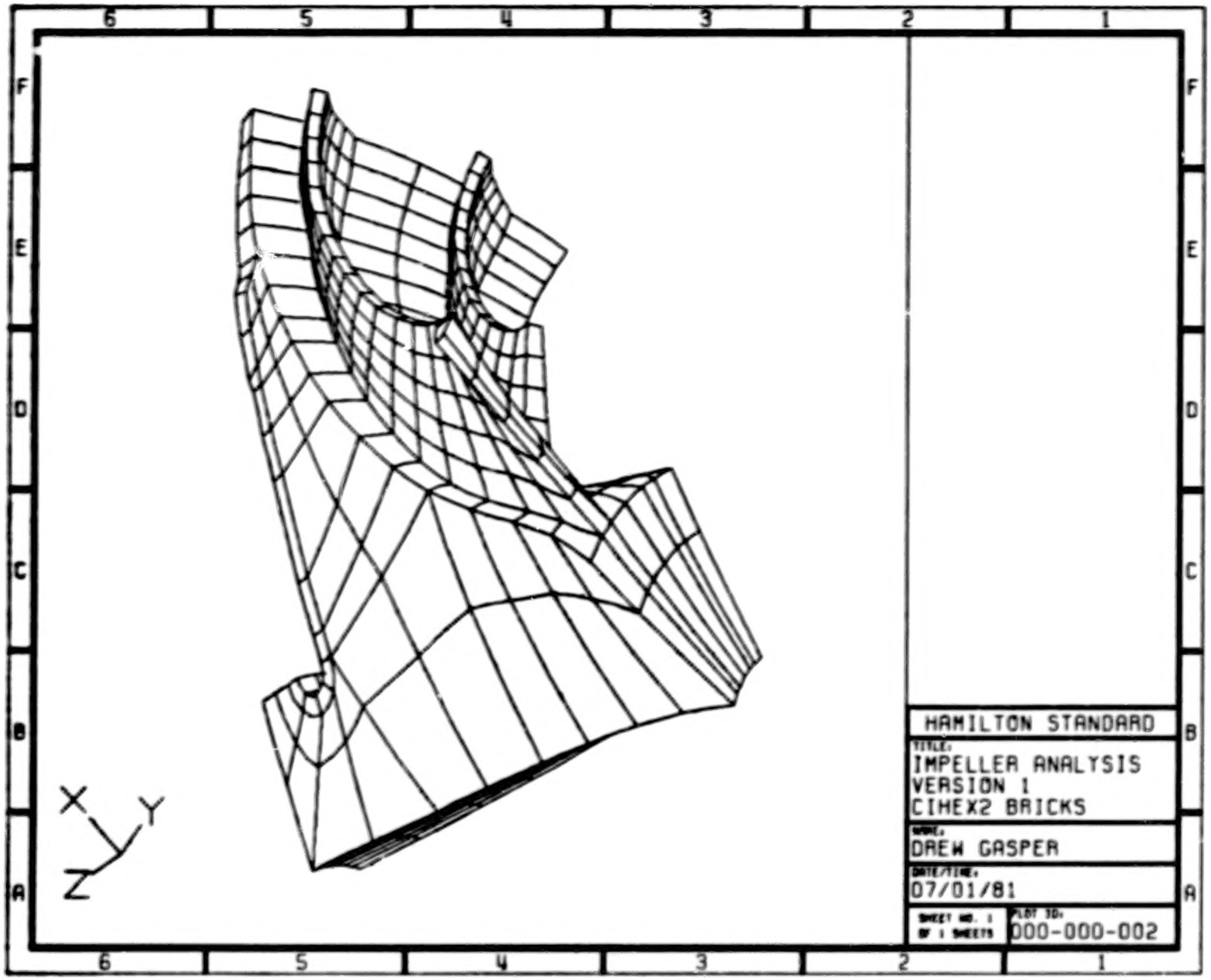

FIGURE 8

MOVIE-BYU Display of Impeller

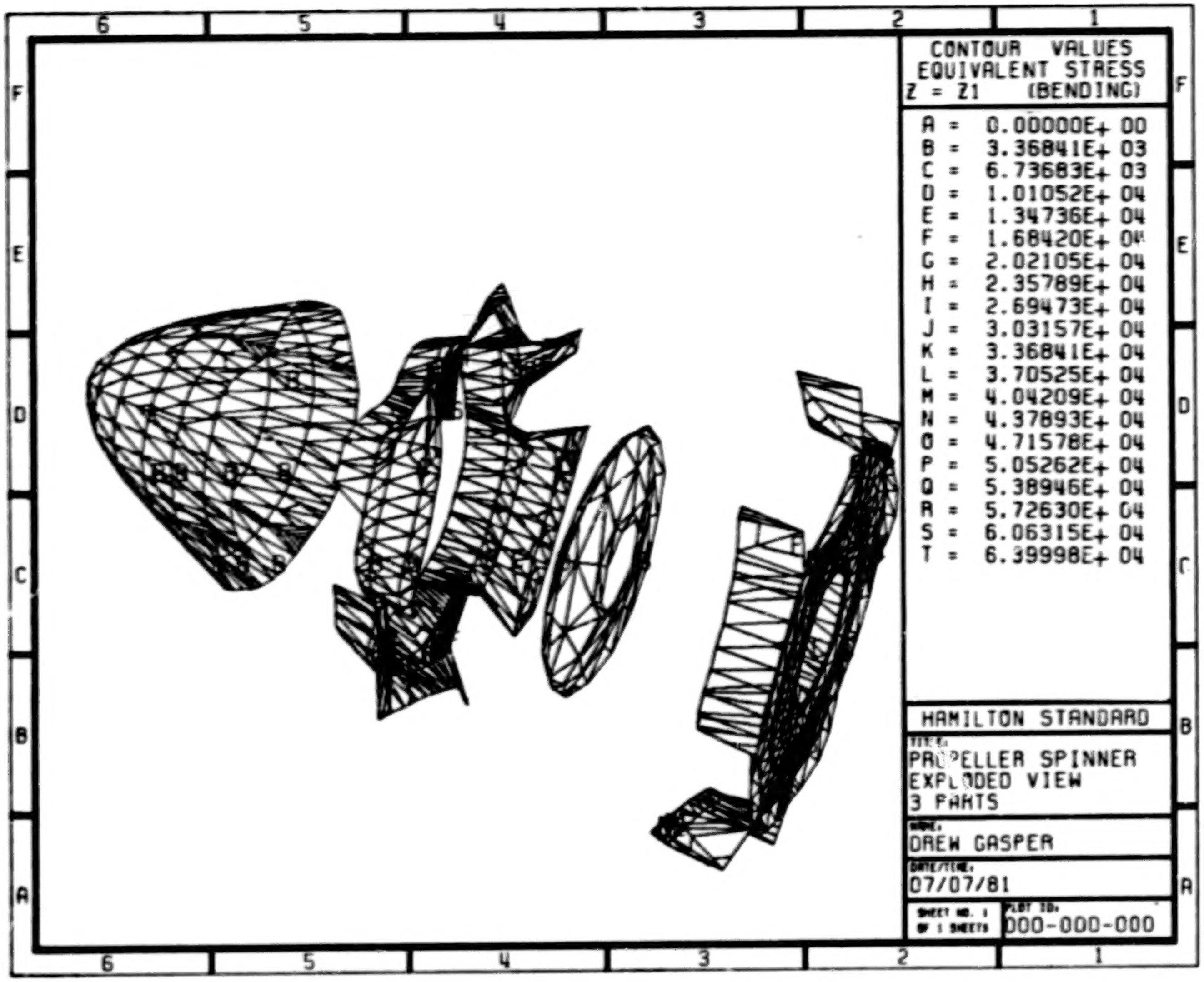

FIGURE 9

MOVIE-BYU Exploded View

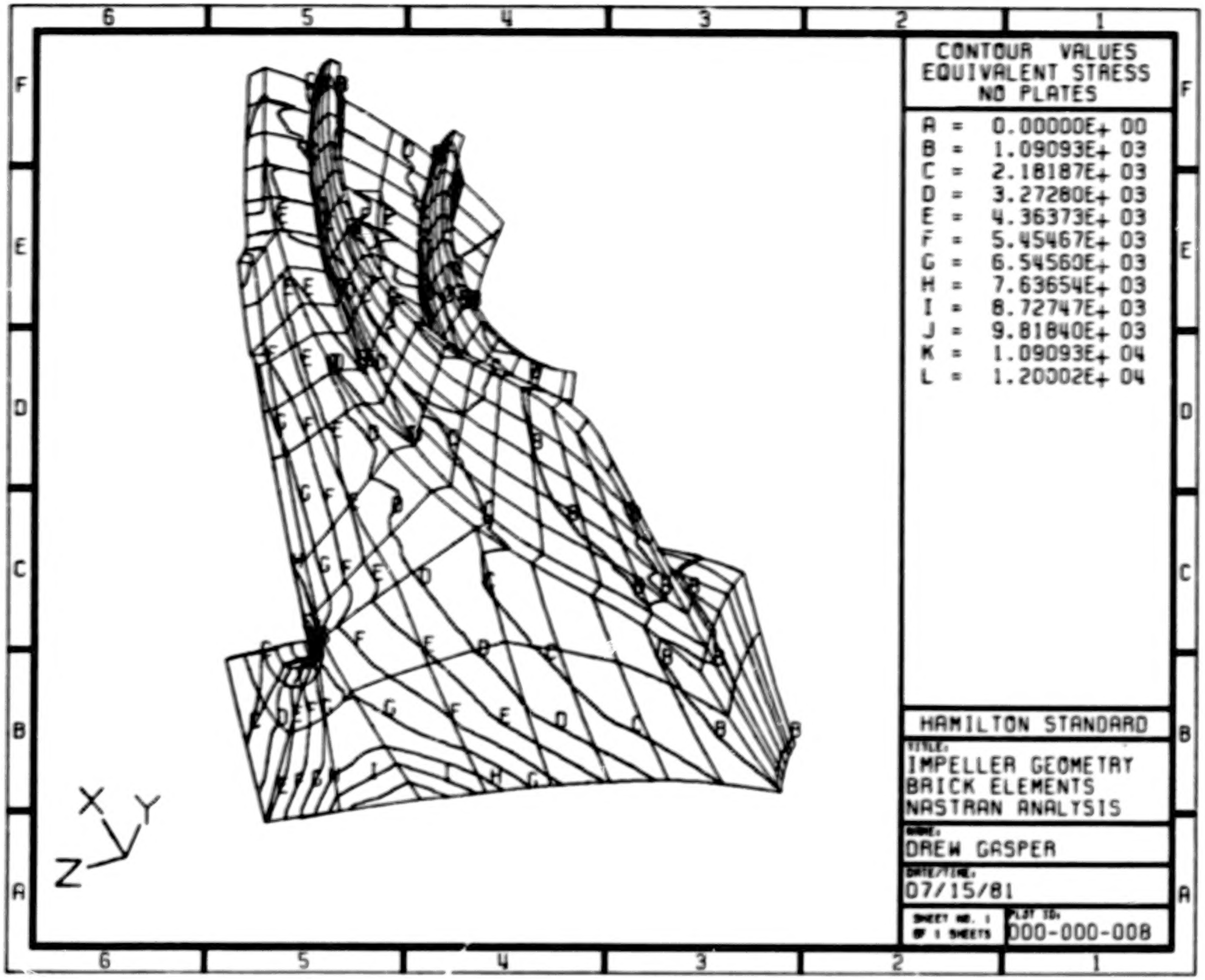

FIGURE 10

MOVIE-BYU Contours on Visible Surfaces

ON THE USE OF HARMONIC EXPANSIONS IN MAGNETIC FIELD PROBLEMS IN NASTRAN

Myles M. Hurwitz, Dolores R. Wallace and Ernest W. Brooks
David W. Taylor Naval Ship R&D Center

SUMMARY

When field problems with infinite exterior domains are solved by the finite element method, the domain must be modeled to "infinity," i.e., to a boundary far enough away from the structure so that the boundary condition does not distort the solution near the structure. For economic reasons, the density of the finite element mesh usually decreases as the distance from the structure increases, thus degrading the results in the far field. This paper demonstrates the use of a prolate spheroidal harmonic expansion to compute far field results in magnetics problems with the DTNSRDC version of NASTRAN.

INTRODUCTION

The determination of the magnetic field in and about ferromagnetic bodies is an important computation in both government and industry. In commercial applications, knowledge of the fields in and near transformers and electrical machinery is often desired. In naval applications, the ability to determine the magnetic field about a naval vessel could lead to methods for reducing the field.

The governing equations of classical electromagnetic wave theory are Maxwell's equations:

$$\nabla \cdot D = \rho \tag{1}$$

$$\nabla \cdot B = 0 \tag{2}$$

$$\nabla \times E = -\frac{\partial B}{\partial t} \tag{3}$$

$$\nabla \times H = J + \frac{\partial D}{\partial t} \tag{4}$$

where

D = electric displacement
B = magnetic flux density
E = electric field intensity
H = magnetic field intensity
J = current density
ρ = charge density
t = time

(Upper case letters denote vectors; lower case, scalars.) The present work is concerned only with time-independent fields, thereby decoupling equations (1)-(4) into one pair of equations governing the electrostatic field ((1) and (3)) and a second pair governing the magnetostatic field ((2) and (4)). Interest here is in the latter pair and the appropriate constitutive equation:

$$\nabla \times H = J \tag{5}$$

$$\nabla \cdot B = 0 \tag{6}$$

$$B = \mu H \tag{7}$$

where μ is the magnetic permeability.

Numerical techniques for solving equations (5)-(7) include integral equations (ref. 1) and differential equations (ref. 2). A summary of the advantages and disadvantages of the two techniques is given in reference 3. The present work uses the differential equation approach which was incorporated into NASTRAN as described in reference 4.

In the theoretical aspects of the analysis as presented in reference 4, ϕ was defined as the scalar potential of the magnetic field anomaly H_m, i.e.,

$$H_m = \nabla \phi \tag{8}$$

where H_m is the modification, or anomaly, due to the presence of ferromagnetic material, to a Biot-Savart field. It is ϕ which is solved for by NASTRAN's heat transfer approach.

In the anticipated applications of this method, accurate values of ϕ will be required in both the near field and far field. A major drawback of using the finite element method for solving magnetostatic problems is that the infinite domain surrounding the ferromagnetic material must be modeled (at least, to the point at which ϕ may be considered small). These accuracy and modeling requirements mean that the finite element mesh must be very fine in all regions. In addition, the results near the finite element boundary may not be as precise as desired because of the imposed $\phi = 0$ boundary condition.

Two methods which could avoid the need for modeling the vast majority of the exterior domain are the use of infinite elements (ref. 5) and the coupling of integral and differential techniques (ref. 6). These methods are presently being investigated, but meanwhile a third method, harmonic expansions, is being used to avoid fine modeling to "infinity". In the present applications, all ferromagnetic material and sources are enclosed by a suitably shaped surface, usually spherical or prolate spheroidal. Then, NASTRAN is used to solve for the potentials ϕ at the grid points on the enclosing surface. Finally, Laplace's equation

$$\nabla^2 \phi = 0 \tag{9}$$

may be solved, in the proper coordinates, using the potentials on the enclosing surface as an interior boundary condition.

PROLATE SPHEROIDAL HARMONIC EXPANSIONS

Most naval applications require only prolate spheroidal coordinates. The solution of Laplace's equation in these coordinates is (ref. 7):

$$\phi = \sum_{n=0}^{\infty} \sum_{m=0}^{n} [A_{mn} \cos (m\theta) + B_{mn} \sin (m\theta)] P_n^m (\eta) \left[\frac{Q_n^m (\xi)}{Q_n^m (\xi_o)} \right] \tag{10}$$

where

$$\left. \begin{matrix} A_{mn} \\ B_{mn} \end{matrix} \right\} = \frac{\epsilon_m}{4\pi} (2n+1) \frac{(n-m)!}{(n+m)!} \int_0^{2\pi} \begin{matrix} \cos \\ \sin \end{matrix} (m\theta) d\theta \int_{-1}^{+1} \phi_o (\eta, \phi) P_n^m(\eta) d\eta$$

P, Q = associated Legendre functions of the first and second kinds, respectively

$$\epsilon_m = \left\{ \begin{matrix} 1, & m = 0 \\ 2, & m > 0 \end{matrix} \right.$$

ξ, η, θ = prolate spheroidal coordinates (See Figure 1)

ϕ_o = potential on prolate spheroidal reference surface $\xi = \xi_o$

With the use of this expansion, the finite element model can become coarser as the distance from the prolate spheroidal reference surface increases. In addition, the model need not extend "too far", since the concept requires an accurate potential distribution only on the reference surface, which is placed as close as possible to the ferromagnetic material. However, the discretization of the reference surface itself must be fine enough to allow for an accurate representation of the integrals in the computation of the coefficients A_{mn} and B_{mn}.

As indicated in reference 4, the DTNSRDC version of NASTRAN was modified to perform the magnetostatic analysis. It has since been further modified to include the computation of the series coefficients A_{mn}, B_{mn} of equation (10). The coefficients are placed on an external file using the OUTPUT2 functional module and are used in a separate post-processor to compute the potential at selected points exterior to the prolate spheroidal reference surface. The magnetic field at the point is computed from the potential using a simple differencing scheme.

SAMPLE PROBLEM

At the time this paper was being prepared, a finite element mesh of a magnetostatics problem with an enclosing prolate spheroidal reference surface was still being generated. However, to demonstrate the concept, 461 grid points were generated so that they represent half a prolate spheroidal reference surface of $\xi = 1.02$ from $\theta = 0^{\circ}$ to $\theta = 180^{\circ}$. The intersection of the X-Y plane and the prolate spheroid is an ellipse with a major axis of 10 meters and a minor axis of 2 meters. A circular loop with a radius of .5 meters and a current of 2 amperes is assumed to lie in the X-Z plane centered about the Y-axis.

The scalar potential at a point, due to a current loop of radius a with current I at a distance r from the center of the loop and at an angle ψ from the axis of the loop, is (ref. 8):

$$\phi = \frac{I}{2}\left[\frac{a^{2}\cos\psi}{2r^{2}} - \frac{3a^{4}}{16r^{4}}\left(5\cos^{3}\psi - 3\cos\psi\right) + \text{---}\right] \qquad (11)$$

This potential was enforced at each of the 461 grid points with SPC cards and the prolate spheroidal harmonic coefficients were computed. One measure of accuracy is to compare computed coefficient A_{11} with the analytical coefficient obtained by using the magnetic dipole moment of the current loop (ref. 9). (The magnetic dipole moment is equal to the product of the current and the area enclosed by the loop). In the present case, the analytical coefficient is .035407 and the computed coefficient was .034946, an error of 1.3%. Table I shows the comparison of the exact potential at various points as given by equation (11) and the potential computed by the series expansion of equation (10). Also included is a comparison of the magnetic field components H_x , H_y , H_z and magnitude $|H|$. It can be seen from Table I that the only questionable results are at points which are both very close to the prolate spheroidal reference surface and which have relatively small potential values. As soon as we start moving away from the surface, the results improve dramatically. In fact, at distances far from the current loop, the loop appears as a magnetic dipole, allowing very accurate computations with only the dipole coefficient A_{11}. However, being very close to the surface requires many accurate coefficients. Therefore, it is anticipated that the poor results could be improved by a finer modeling of the reference surface and by the use of more series coefficients. However, it should be remembered that the major purpose of the series expansion is to provide accurate results in the far field. In the near field, accurate results should be expected in the finite element analysis because of the finer modeling.

REFERENCES

1. Trowbridge, C.W.: Applications of Integral Equation Methods for the Numerical Solution of Magnetostatic and Eddy Current Problems. Rutherford Laboratory Report RL-76-071, June 1976.

2. Zienkiewicz, O.C.; Lyness, John; and Owen, D.R.J.: Three-Dimensional Magnetic Field Determination Using a Scalar Potential - A Finite Element Solution. IEEE Transactions on Magnetics, Vol. MAG-13, No. 5, Sept. 1977.

3. Simkin, J.; and Trowbridge, C.W.: Three-Dimensional Nonlinear Electromagnetic Field Computations, Using Scalar Potentials. IEE Proceedings, Vol. 127, Part B, No. 6, Nov. 1980.

4. Hurwitz, M.M.; and Schroeder, E.A.: Solving Magnetostatic Field Problems with NASTRAN. Seventh NASTRAN Users' Colloquium, NASA CP-2062, Oct. 1978.

5. Bettess, P.: More on Infinite Elements. Int'l Journal for Num. Methods in Eng., Vol. 15, 1980.

6. Zienkiewicz, O.C.; Kelly, D.W.; and Bettess, P.: Marriage a la mode - The Best of Both Worlds (Finite Elements and Boundary Integrals). Int'l Symposium on Innovative Numerical Analysis in Applied Engineering Science, Versailles, France, May 1977.

7. Morse, P.M.; and Feshbach, H.: Methods of Theoretical Physics. McGraw-Hill, New York, 1953.

8. Corson, D.; and Lorrain, P.: Introduction to Electromagnetic Fields and Waves. W.H. Freeman and Co., San Francisco, 1962.

9. Nixon, D.A.; and Baker, F.E.: Using Prolate Spheroidal Magnetization Distributions for Magnetic Modeling. J. Appl. Physics, 52(2), Feb. 1981.

TABLE I - COMPARISON BETWEEN ANALYTICAL AND COMPUTED RESULTS

Point				% Error				
No.	x	y	z	Φ	H_x	H_y	H_z	$\lvert H \rvert$
1	0.	1.	0.	0.5		1.4		1.4
2	0.	1.1	0.	0.9		0.2		0.2
3	0.	1.5	0.	1.3		1.9		1.9
4	0.	2.	0.	1.3		2.0		2.0
5	0.	5.	0.	1.3		1.6		1.6
6	0.	20.	0.	1.3		1.4		1.4
7	5.	0.	0.			65.6		65.6
8	5.	0.	0.1			2.3		2.3
9	5.	0.	0.2			8.5		8.5
10	5.	0.	0.5			1.4		1.4
11	5.	0.	1.			1.1		1.1
12	5.	0.	2.			1.1		1.1
13	5.	0.1	0.	43.9	1306.	9.5		24.2
14	5.	0.2	0.	8.4	40.4	20.8		20.1
15	5.	0.3	0.	2.4	6.1	1.5		1.7
16	5.	0.4	0.	1.7	1.8	0.1		0.2
17	5.	0.5	0.	1.4	1.5	0.5		0.6
18	5.	0.6	0.	1.2	1.3	0.8		0.9
19	5.	0.7	0.	1.2	1.3	1.0		1.0
20	5.	0.8	0.	1.1	1.3	1.1		1.1

TABLE I - (Continued)

Point				% Error				
No.	x	y	z	ϕ	H_x	H_y	H_z	$\|H\|$
21	5.	0.9	0.	1.1	1.3	1.1		1.2
22	5.	1.	0.	1.1	1.3	1.2		1.2
23	5.	5.	0.	1.2	1.4	0.9		1.3
24	5.	20.	0.	1.3	1.2	1.4		1.4
25	5.1	0.	0.			9.1		9.1
26	5.2	0.	0.			4.1		4.1
27	5.5	0.	0.			1.5		1.5
28	6.	0.	0.			1.2		1.2
29	2.	1.	0.	0.2	1.5	7.3		2.0
30	2.	2.	0.	1.0	1.4	0.7		1.2
31	2.	5.	0.	1.3	1.3	1.5		1.4
32	2.	20.	0.	1.3	1.1	1.4		1.4
33	3.	1.	0.	0.7	0.2	1.2		0.6
34	3.5	0.85	0.	0.6	1.9	2.4		0.6
35	4.	0.61	0.	0.4	29.5	1.8		4.9
36	4.	0.65	0.	0.5	15.6	2.7		1.5
37	4.	1.	0.	0.9	1.0	1.5		1.3
38	4.	5.	0.	1.3	1.4	1.1		1.3
39	4.	20.	0.	1.3	1.2	1.4		1.4
40	4.5	0.44	0.	5.0	32.0	30.5		26.5
41	4.5	0.5	0.	2.2	3.2	9.0		8.4
42	2.	0.	1.				0.5	0.5
43	2.	0.	2.				1.2	1.2
44	2.	0.	5.				1.4	1.4
45	2.	0.	20.				1.3	1.3

A blank indicates an analytical quantity of 0.

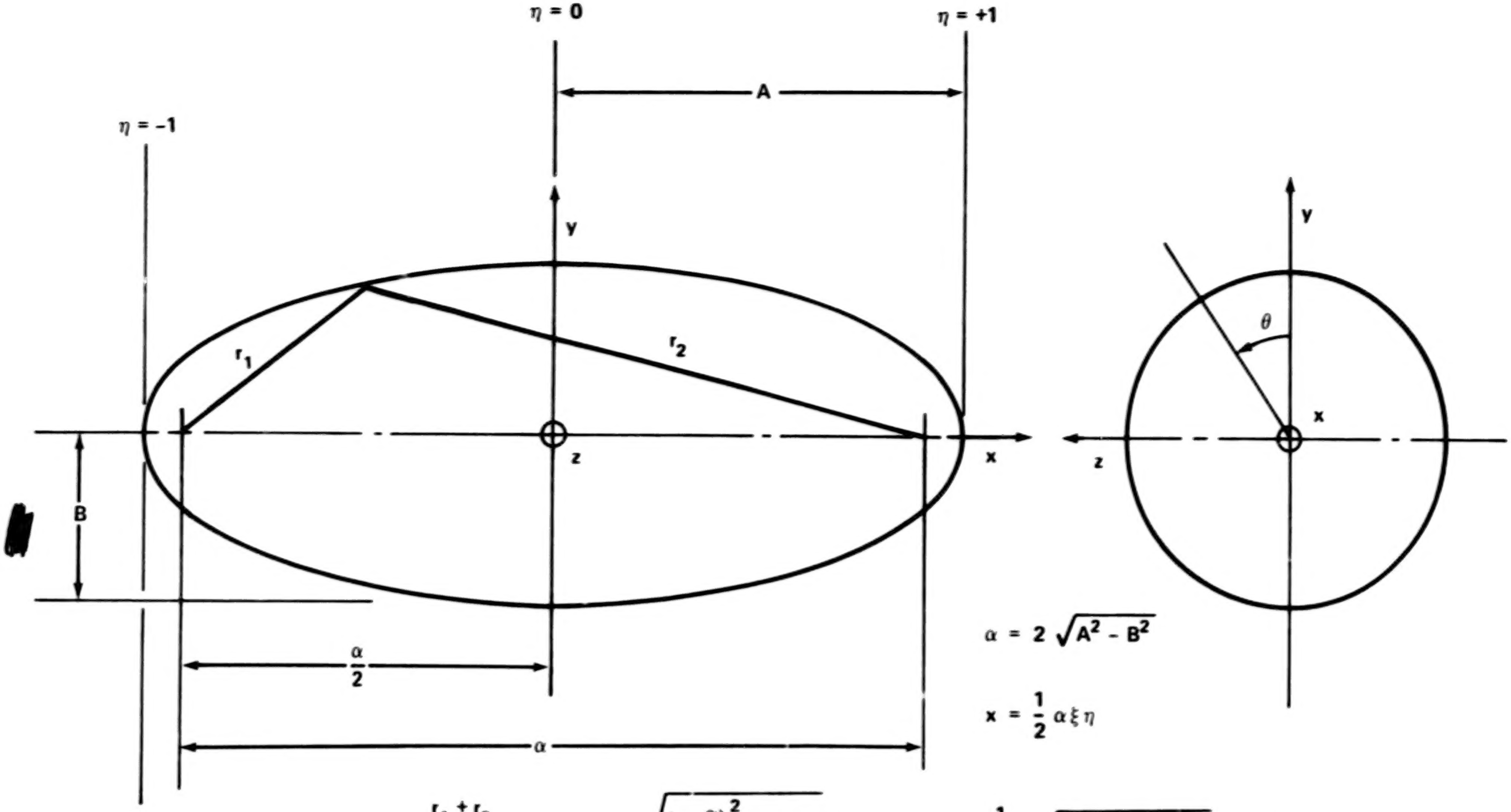

$$\alpha = 2\sqrt{A^2 - B^2}$$

$$x = \frac{1}{2}\alpha\xi\eta$$

$$\xi = \frac{r_1 + r_2}{\alpha} \qquad r_1 = \sqrt{\left(x + \frac{\alpha}{2}\right)^2 + y^2 + z^2} \qquad y = \frac{1}{2}\alpha\sqrt{(\xi^2 - 1)(1 - \eta^2)}\cos\theta$$

$$\eta = \frac{r_1 - r_2}{\alpha} \qquad r_2 = \sqrt{\left(x - \frac{\alpha}{2}\right)^2 + y^2 + z^2} \qquad z = \frac{1}{2}\alpha\sqrt{(\xi^2 - 1)(1 - \eta^2)}\sin\theta$$

FIGURE 1 - PROLATE SPHEROIDAL COORDINATE SYSTEM

IMPROVING A NASTRAN DYNAMIC MODEL
WITH TEST DATA USING LINWOOD

B.H. Ujihara, M.M. Dosoky, and E.T. Tong
Shuttle Orbiter Division
Rockwell International

SUMMARY

A recent concept expresses a test-measured mode as a linear combination of analytical modes for the same prototype. This approach is extended to predict associated changes to math model mass and stiffness. Success in its application depends upon selection of the right "unit" structures upon which corrections are based. The method is demonstrated by application to test data/math model of the quarter-scale solid rocket booster model of the Space Shuttle.

INTRODUCTION

Ground vibration testing (GVT) affords an important means of verifying structural dynamic math models. Such testing seeks to establish natural frequencies and mode shapes in the frequency range of interest. These characteristics, in turn, form the basis for assessing math model acceptability. Depending upon circumstances, this may be either "pass" or "no pass." Correspondingly, the corrective course of action may range from a simple "as is," to a drastic rework of the entire finite element model.

A simple comparison of frequencies and mode shapes may suffice for a "pass" rating of acceptability. It is only with a rating of "no pass" that the problem begins to demand concern. Even so, a substantial percentage of such "no pass" judgments may often be tracked by "eyeball" to areas of specific stiffness and/or mass distributions. In such cases, enough clues of a circumstantial nature may be evident that math model improvements can be efficiently incorporated. The remaining "no pass" judgments stem from discrepancies for which the cure is not immediately obvious.

This paper describes a method intended for application to this last area. It is an extension of a recently introduced modal correlation technique (ref. 1). Essentially, it expresses a given test mode as a least-squared error linear combination of analytical modes (LCM). The present extension lies in the use of LCM to predict dynamic math model corrections based upon test data.

The nonuniqueness of these predictive corrections are a result of limitations of the test data in describing all the eigenvectors of the math model. Presumably, if these limitations could be eliminated, the predicted eigenvectors and frequencies could, in principle, be uniquely corrected to the experimental values.

The application is intended for linear systems whose dynamic math models are nearly correct. Their modification must, therefore, be of a perturbative nature. By virtue of the least-squares technique employed, gross errors in the test data may be systematically detected by their lack of fit. On the other hand, effects of real world nonlinearities, nonproportionality of damping, etc., remain unaccounted for. As already noted, the method assumes a test mode shape is expressible as an LCM.

For this assumption to be meaningful, the analytical set must be "nearly correct." That is, one mode of the analytical set must correspond closely with the experimental mode being considered. In statistical terms, a single mode correlation in excess of 0.7 or so would be desirable. Supplemental modes in the selected linear combination would then be expected to produce a multiple correlation near 1.0.

Interestingly, the math models of today can contain dynamic degrees of freedom far in excess of the number used for experimental mode definition. Then, the task of modal correlation by this scheme would appear to be one of underspecification; that is, more modes would be available than data points. However, in the perturbation sense described above, only a few modes are needed to achieve high correlation (say, half a dozen). In an extreme case of perfect correlation, only one mode (the correct one) would be needed. Adding more modes would not improve the correlation. It should be clear that by its very nature the correlation becomes one of overspecification leading naturally to the present approach.

METHOD OF ANALYSIS

Ref. 2 describes the least-squared error expression of a test mode in terms of a linear combination of analytical modes. For continuity, the pertinent features of that concept are summarized.

Known in statistics as linear regression in multiple variables, ref. 3 states that four inherent assumptions are involved. Of these, the first two are:

(1) A linear relationship exists between the independent variables, x_{ij}, and the estimated displacement

$$Y_i = b_o + X_{i1}b_1 + X_{i2}b_2 + \cdots + X_{in}b_n^* \qquad (1)$$

(2) The observed value, y_i, is related to Y_i by

$$y_i = Y_i + e_i \qquad (2)$$

where e_i is a random error

Then the residual, or sum of differences between observed and estimated displacement is

$$R = \sum_{i=1}^{m} \left(y_i - Y\right) \qquad (2)$$

with i being summed over all m accelerometers.

The sum of their squares is

$$RSQ = \sum_{i=1}^{m} \left(y_i - Y\right)^2 \qquad (4)$$

Inclusion of a weighting parameter leads to

$$RR = \sum_{i=1}^{m} M_i\left(y_i - Y_i\right)^2 \qquad (5)$$

Substituting eqs. (1) into (5)

$$RR = \sum_{i=1}^{m} M_i \left(y_i - X_{i1b1} - X_{i2b2} - \cdots - X_{inbn}\right)^2 \qquad (6)$$

Minimization of RR with respect to each bj results in n linear simultaneous equations in the coefficients b_j, $j = 1,2 \cdots n$.

$$[X_{ij}]^T [M_i]\ [X_{ij}]\ \left|b_j\right| = [X_{ij}]^T [M_i]\ \left|y_i\right| \qquad (7)$$

The multiple correlation coefficient for independent variable, i, is

$$R_i^2 = \frac{\sum_{J=1}^{m} M_j \left(Y_j - y\right)^2}{\sum_{J=1}^{m} \left(y_j - y\right)^2} \qquad (8)$$

summed over all m accelerometers.

As noted in ref. 1, a sophisticated IBM Share program (LINWOOD) performs this linear regression analysis. LINWOOD has been incorporated into NASTRAN via Dummy Module, (ref. 2).

Selection of analytical modes to represent a given test mode is a matter of judgment by the analyst. Several trial combinations may be required. Kinetic energy tables are useful in this process. The number of test modes with which LCM are to be fitted is also up to the analyst of the problem at hand. At any rate, determination of the LCM constitutes the first phase in the process of modal correlation. The second and final phase, described here, is directed towards the isolation of specific math model deficiencies. Of first concern are naturally those responsible for the greatest observed differences between experimental and analytical data.

If an eigenvector, ϕ, and corresponding frequency ω are known for a given K and M, then

$$\left| [K]\ \{\phi\}\ --\ [M]\ \{\phi\}\ \omega^2 \right| = 0 \tag{9}$$

[K] and [M] are analytically derived; but suppose a certain number of test modes have been obtained from a prototype. Suppose further that each test mode has been matched with "acceptable accuracy" by a linear combination of a subset of the math model modes.

$$\{\phi_{TEST}\} = [\phi_{ANALYT}]\ \{b\} \equiv \{LCM\} \tag{10}$$

Various ramifications of LCM have already been discussed. Then an expression similar to eq. 9 may be written for an LCM in which changes to [K] and [M] are inferred

$$\left| [K + k]\ \{LCM\} - [M + m]\ \{LCM\}\ \omega_T^2 \right| = 0 \tag{11}$$

Separating the incremental quantities,

$$\left| [k]\ \{LCM\} - [m]\ \{LCM\}\ \omega_T^2 \right| = - \left| [K]\ \{LCM\} - [M]\ \{LCM\}\ \omega_T^2 \right| = \left| R_o \right| \tag{12}$$

where $\{R_o\}$ are the residual forces required of the incremental [k] and [m] to satisfy eq. 11.

For simplicity, the case first considered is that with a correct mass matrix, i.e., [m] = NULL

$$\text{then } [k]\ \{LCM\} = \{R_o\} \tag{13}$$

$\{R_o\}$, the residual force vector, is the primary source of information defining degrees of freedom at which stiffnesses need to be changed. It should be safe to assume that those with the largest residual forces are the ones to be changed first. Further, any stiffness changes invoked must not affect physical realizability of the resulting system, symmetry, and other known requirements.

Rather than the deficiency of individual degrees of freedom, the objective is to define characteristic deficiencies. These may involve specific structural areas or types of stiffness (i.e., bending, axial, etc.). If a few such characteristic deficiencies can explain the major differences, the correction task is correspondingly easier. Realistic stiffness distributions covering the characteristic deficiencies may then be matched against $\{R_o\}$ in the least-squared error sense. The multiplication constants which result then determine the level of stiffness corrections.

For lack of a better name, the realistic stiffness distributions required here are identified as incremental unit structures (IUS). They are essentially partial derivatives of the correction stiffness matrix. The independent variables are selected generalized degrees of freedom, α_i representing the characteristic deficiencies. In a physical sense, the IUS α_i represent actual structure to be either added to or removed from the existing structure.

$$[k] = [IUS_1]\ \alpha_1 + [IUS_2]\ \alpha_2 + \cdots + [IUS_n]\ \alpha_n \tag{14}$$

substituting eq. 14 into eq. 13

$$[IUS_1]\ \{LCM\}\ \alpha_1 + [IUS_2]\ \{LCM\}\ \alpha_2$$

$$+ \cdots + [IUS_n]\ \{LCM\}\ \alpha_n = \{R_o\} \tag{15}$$

with $\{C_i\} = [IUS_i]\ \{LCM\}$, eq. 15 becomes (16)

$$\{C_1\}\ \alpha_1 + \{C_2\}\ \alpha_2 + \ldots + \{C_n\}\ \alpha_n = \{R_o\} \tag{17}$$

In matrix form,

$$m\ \overset{n}{[C_{ij}]}\ \{\alpha_j\} = \{R_o\} \tag{18}$$

In simple cases wherein the unreduced stiffness matrix is also the dynamic stiffness matrix, it may be possible to solve eq. 18 in closed form. For practical cases, however, eq. 18 is best satisfied by a least-squared error fit, since n>>m generally. Then

$$m\ \overset{n}{[C_{ij}]}\ \{\alpha_j\} \cong \{R_o\} \tag{18a}$$

It would seem intuitively that the correlation coefficient for this fit should be fairly high. Otherwise the selected IUS would be suspected of not telling the full story. Once the IUS are acceptably determined, eq. 14 may be used to construct [K].

The case of corrective mass terms follows similar lines. Analogous to eq. 14.

$$[m] = [IUM_1]\ \beta_1 + [IUM_2]\ \beta_2 + \cdots + [IUM_n]\ \beta_n \tag{19}$$

where [IUM] is "incremental unit mass." Going back to eq. 12

$$\begin{aligned}
&\Big|[IUS_1]\ \{LCM\}\ \alpha_1 + [IUS_2]\ \{LCM\}\ \alpha_2 \\
&+ \cdots + [IUS_n]\ \{LCM\}\ \alpha_n\Big| \\
&- \ \Big|[IUM_1]\ \{LCM\}\ \omega^2\beta_1 + [IUM_2]\ \{LCM\}\ \omega^2\beta_2 \\
&+ \cdots + [IUM_n]\ \{LCM\}\ \omega^2\beta_n\Big| = \Big|R_o\Big|
\end{aligned} \tag{20}$$

with $\{D_i\} = -\ [IUM]\ \{LCM\}\ \omega^2$ together with eq. 16 (21)

$$\left|C_{ij} \;\vdots\; D_{i(j+N)}\right| \begin{Bmatrix} \alpha_j \\ \hdashline \beta_{j+N} \end{Bmatrix} = \left|R_o\right| \tag{22}$$

By induction, the case of several test modes becomes

$$\begin{bmatrix} \overset{1}{C}_{ij} & \overset{1}{D}_{ij} \\ \overset{2}{C}_{ij} & \overset{2}{D}_{ij} \\ \bullet & \\ \bullet & \\ \bullet & \\ \overset{n}{C}_{ij} & \overset{n}{D}_{ij} \end{bmatrix} \begin{Bmatrix} \alpha_j \\ \beta_{j+N} \end{Bmatrix} \begin{Bmatrix} \overset{1}{R}_o \\ \overset{2}{R}_o \\ \bullet \\ \bullet \\ \bullet \\ \overset{n}{R}_o \end{Bmatrix} \tag{23}$$

A SIMPLIFIED EXAMPLE

For further clarification, a simple example is treated. In the two-degree of freedom system, the equations of motion in one of its two normal modes is

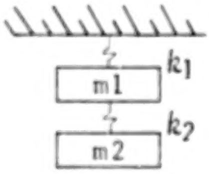

$$\begin{bmatrix} -m_1\omega 2 & 0 \\ 0 & -m2\omega 2 \end{bmatrix} \begin{Bmatrix} X1 \\ X2 \end{Bmatrix} + \begin{bmatrix} k1+k2 & -k2 \\ -k2 & k2 \end{bmatrix} \begin{Bmatrix} X1 \\ X2 \end{Bmatrix} = 0 \tag{24}$$

Let the math model values be

$$k_1 = K_2 = 1.2 \tag{25}$$

$$m_1 = m_2 = 0.8 \tag{26}$$

Without bothering to compute the eigen solutions, let it be assumed that a "test measured" mode is

$$\begin{Bmatrix} X_1 \\ X_2 \end{Bmatrix} = \begin{Bmatrix} 0.6 \\ 1.0 \end{Bmatrix} \tag{27}$$

and the "measured" frequency is $\sqrt{1.5}$. In this simple case, there is no need for an LCM since "measurements" exist at all math model degrees of freedom. So eq. 11 becomes

$$\begin{bmatrix} 2.4 & -1.2 \\ -1.2 & 1.2 \end{bmatrix} \begin{Bmatrix} 0.6 \\ 1.0 \end{Bmatrix} - \begin{bmatrix} 0.8 & 0 \\ 0 & 0.8 \end{bmatrix} \begin{Bmatrix} 0.6 \\ 1.0 \end{Bmatrix} (1.5) = \begin{vmatrix} R_o \end{vmatrix} \qquad (28)$$

$$\begin{Bmatrix} 0.48 \\ 0.72 \end{Bmatrix} = \begin{vmatrix} Ro \end{vmatrix} \qquad (29)$$

Assuming for the present that $m = 0$

$$\begin{bmatrix} k_1 \end{bmatrix} \begin{Bmatrix} X_1 \\ X_2 \end{Bmatrix} = \begin{bmatrix} 1.0 & 0 \\ 0 & 0 \end{bmatrix} \begin{Bmatrix} 0.6 \\ 1.0 \end{Bmatrix} = \begin{Bmatrix} 0.6 \\ 0 \end{Bmatrix} \qquad (30)$$

$$\begin{bmatrix} k_2 \end{bmatrix} \begin{Bmatrix} X1 \\ X2 \end{Bmatrix} = \begin{bmatrix} 1.0 & -1.0 \\ -1.0 & 1.0 \end{bmatrix} \begin{Bmatrix} 0.6 \\ 1.0 \end{Bmatrix} = \begin{Bmatrix} -0.4 \\ 0.4 \end{Bmatrix} \qquad (31)$$

Combining eqs. 30 and 31 with 29 in 18

$$\begin{bmatrix} 0.6 & -0.4 \\ 0 & 0.4 \end{bmatrix} \begin{Bmatrix} \alpha 1 \\ \alpha_2 \end{Bmatrix} = \begin{Bmatrix} 0.48 \\ 0.72 \end{Bmatrix} \qquad (32)$$

Simultaneous solution of eq. 32 yields

$$\alpha_1 = 2.0 \qquad (33)$$

$$\alpha_2 = 1.8 \qquad (34)$$

so that

$$k_1 \, \alpha_1 = \begin{bmatrix} 1.0 & 0 \\ 0 & 0.0 \end{bmatrix} (2.0) = \begin{bmatrix} 2.0 & 0.0 \\ 0.0 & 0.0 \end{bmatrix} \qquad (35)$$

$$k_2 \;\; \alpha_2 = \begin{bmatrix} 1 & -1 \\ -1 & 1 \end{bmatrix} (1.8) = \begin{bmatrix} 1.8 & -1.8 \\ -1.8 & 1.8 \end{bmatrix} \qquad (36)$$

Adding these to the original [K] matrix shown in eq. 28

$$\begin{vmatrix} K_{FINAL} \end{vmatrix} = \begin{bmatrix} 6.2 & -3.0 \\ -3.0 & 3.0 \end{bmatrix} \qquad (37)$$

This, together with the given [M] does indeed possess the "measured" mode and frequency as eigensolution.

By the same token, an equally valid solution may be obtained by requiring all the adjustment to be in the mass matrix. In order to define unique corrections, it is necessary to obtain "test measurements" for the remaining mode. This would then lead to four equations and four unknowns α_1, α_2, α_1, α_2. In any practical case, this condition cannot be met. Neither is it practical to pull apart a highly reduced stiffness matrix to isolate its separate constituents. These two limitations are what lead to least-squares analysis and the concept of incremental unit structure and mass.

The decisions for selecting particular IUS and IUM are up to the analyst. In conjunction with any contemplated mass corrections, their effects upon rigid body mass coefficients must be kept in mind. Thus the importance of independently verifying rigid body mass coefficients against measured quantities of the prototype cannot be overemphasized. Mass changes may be highly constrained depending upon the precision of this comparison.

APPLICATION TO A SPECIFIC CASE

The Space Shuttle quarter-scale ground vibrations test program included fabrication and test of quarter-scale replica models of all elements of the lift-off configuration. Of these the cantilevered lift-off quarter-scale solid rocket booster (QSSRB) showed puzzling differences between predicted and observed natural frequencies. This configuration was therefore chosen as a test case for the method. The relatively small size of this dynamic model (222 DOF) was also attractive.

Figure 1 is a sketch of the QSSRB with its accelerometer locations. The model is of stainless-steel construction loaded with inert simulated solid propellant. Radius of the cylindrical section is 0.46 meters (18 inches) and overall length is 12.2 meters (480 inches).

A total of 59 accelerometers were installed generally as indicated by the arrows of figure 1. Figure 2 shows sketches of the cantilever support structure in views looking forward. The forward support is a ball and socket taking translational loads in all three coordinate directions. Pin ended struts form the aft attach to react side forces and rolling moment. Taken together, the support system is essentially determinate.

The math model formulated in Cosmic NASTRAN resulted in 222 dynamic degrees of freedom. Initial modal predictions were obtained by simply fixing the attach degrees of freedom. No allowances for tare properties were made. Table I shows measured test frequencies and their modal description. Analytical frequency predictions from the initial model are matched against the test data. Associated simple correlation coefficients based upon modal displacements at accelerometer points are shown in the last column.

Following the method of ref. 1 best fit (least-squared error) linear combinations of these analytical modes were obtained to represent the first y-bending mode at 10.25 Hz, and the Z-translation with roll mode at 5.89 Hz. In selecting candidate analytical modes to form the combination, it was noted that modes 3 and 6 (not shown) contained more than 90 percent of kinetic energy in nozzle rotation. Since the cantilever test configuration contained a pressure bulkhead in place of the nozzle, these two modes were excluded from the combination. Using analytical modes 1, 2, 4, 5, and 7 through 10, the multiple correlation coefficients obtained for these fits were 0.994 and 0.992 for the 5.89 Hz and 10.25 Hz modes respectively.

SELECTION OF INCREMENTAL UNIT STRUCTURE

Substitution of these LCM into the right hand side of eq. 12 resulted in residual forces shown in figures 3a and 3b. An unexpected characteristic noted in the plots of residual forces was that the dominant forces are primarily in plane. This suggested an IUS obtained by reducing the basic stiffness to in-plane DOF only.

The large residual moment in nozzle θ_z at mode 53 figure 3a, was provided for by reducing the basic stiffness to nozzle θ_z and support DOF. Tare stiffness was accounted for by reducing the basic stiffness down to individual strut stiffnesses as separate IUS in y and z directions. Proceeding in this manner, a total of 12 IUS were defined.

With these as independent variables, least-squared error linear combinations were obtained to match residual forces for the two test modes. In turn, the resulting changes to the stiffness matrix were incorporated into the basic stiffness matrix. The entire analysis was accomplished with DMAP in Cosmic NASTRAN and dummy modules for nonmatrix operations.

It is reiterated that the equivalent physical process involved here is the addition or removal of structure. Any known restrictions such as that from symmetry or boundary conditions should be preserved. Inherently, then, it would seem advisable to base IUS on the basic stiffness or mass matrix wherever possible.

The method is still largely untried, but results are encouraging. Lacking at present is a definitive approach to the designation of IUS. Hopefully this would reduce the trial and error involved, and the insight required for their selection.

Figure 4 shows percentage error in predicted frequency relative to test frequency versus test frequency. Predictions both before and after correction are shown. Simple correlation coefficients are shown in a similar way. Although a dramatic improvement is indicated, the simple correlation of 32.2 Hz has actually fallen off. Nevertheless, corrections dictated by only the first two test modes show a consistent improvement with all corrected frequency errors lying in the ±10 percent band.

Surprisingly, one of the more important corrections was shown by this analysis to be stiffnesses of in-plane degrees of freedom. Because these are not directly associated with attachment structure, its incorporation in the unrestrained stiffness matrix should show improvement in frequency correlation with the unrestrained configuration test data.

Figure 5 shows this frequency comparison for the unrestrained QSSRB. The message to be gained here is that predicted corrections are only as good as demonstrated. While some improvement is evident, it is clear that a separate analysis first, of the unrestrained QSSRB, should be made.

CONCLUSIONS

The concept of expressing test modes as a linear combination of analytical modes has been applied to the prediction of corrective terms in math model mass and stiffness. Test data for the Space Shuttle quarter-scale solid rocket booster was analyzed by this method demonstrating significant improvements in frequency and mode shape correlation. In this context, applicability of the method is believed to have been demonstrated.

REFERENCES

1. Fitting Equations to Data; Daniel and Wood, John Wiley & Sons, Inc., 1971.

2. LINWOOD as a NASTRAN Dummy Module for Modal Correlation with Test Data (A Least Squares Algorithm); Ujihara, Guyan, Van Hofwegen, Heckenlaible. Proceedings of First Chautauqua on Finite Element Modeling, Schaeffer Analysis, Inc., Sept. 1980.

Table I. - QS SRB LIFT-OFF CANTILEVERED MODES

Test					Initial Model Analytical Shell Freq.	
Seq. No.	Mode. No.	Description	C/ cc	Freq. Hz	Hz	R
1	1	1st Y bending		9.75	10.13	(0.60)
2	3	1st Y bending		10.25	10.13	(0.60)
3	8	Z-TRANS w/roll	0.073	5.89	7.03	(0.99)
4	13	Z bending	0.018	11.04	12.78	(0.75)
5	18	Y bending	0.022	15.26	20.06	(0.90)
6	27	1st Z bending	0.018	22.25	28.96	(0.89)
7	28	2 Z-B	0.016	31.94	32.33	(0.90)
8	29	2 Y-B	0.022	32.3	36.80	(0.77)
9	30	3rd Y-B	0.022	50.6	65.1	(0.72)
10	31	2 Z-B & $_x$	0.028	53.9	65.1	(0.68)
11	32	Torsion & 3rd Z-B	0.0315	63.25	69.9	(0.63)

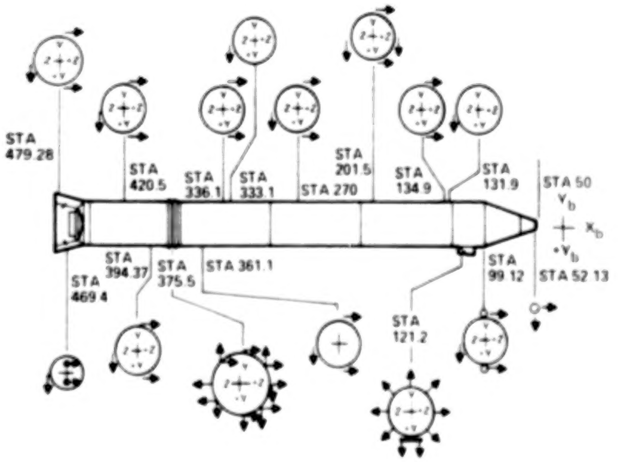

Fig. 1 Side View With Accelerometer Locations

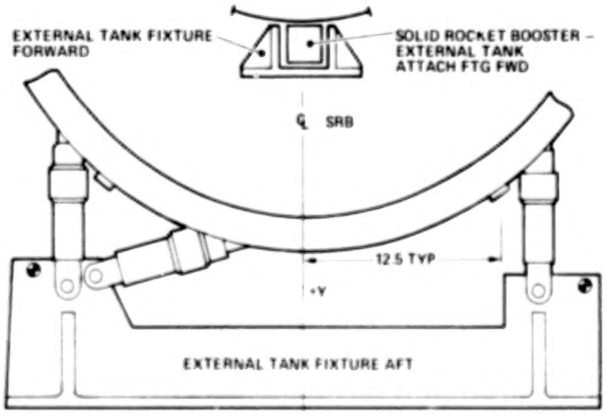
EXTERNAL TANK FIXTURE FORWARD
SOLID ROCKET BOOSTER – EXTERNAL TANK ATTACH FTG FWD
℄ SRB
12.5 TYP
+Y
EXTERNAL TANK FIXTURE AFT

Fig. 2 Sketch of Cantilever Supports

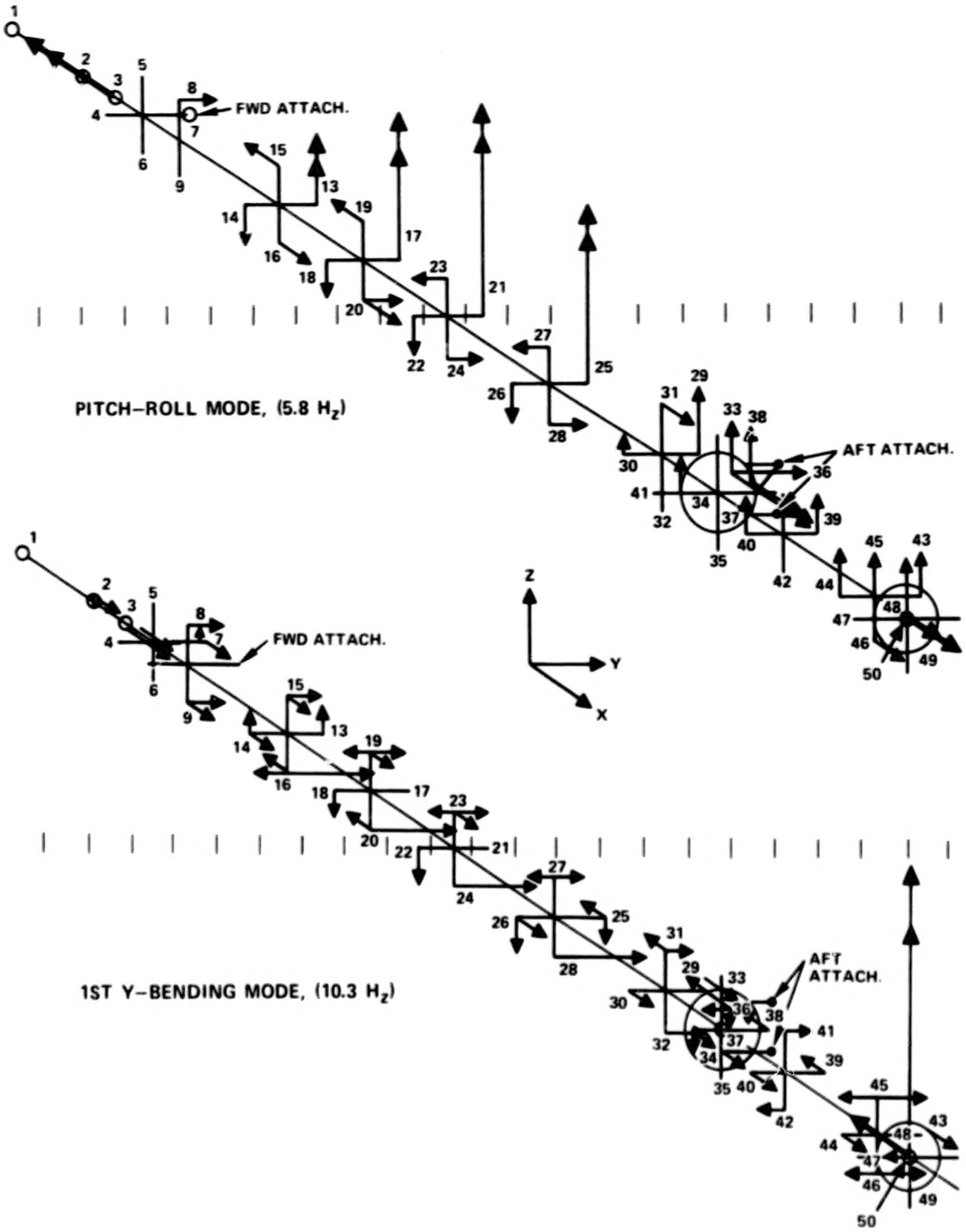

Fig. 3 Sketch of Residual Forces

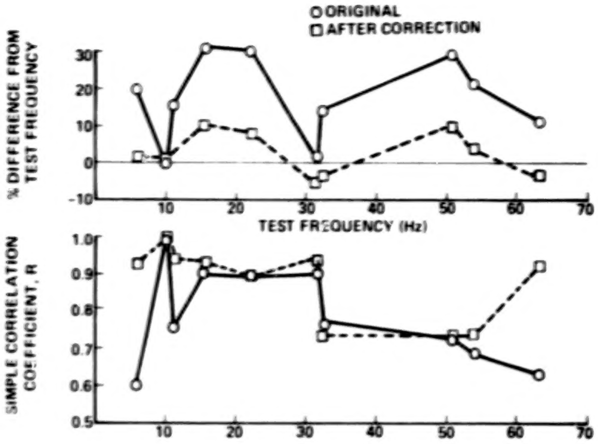

Fig. 4 Comparison of Math Model Frequency Errors and Modal Displacement Correlation Based Upon Test Data (Cantilever Configuration)

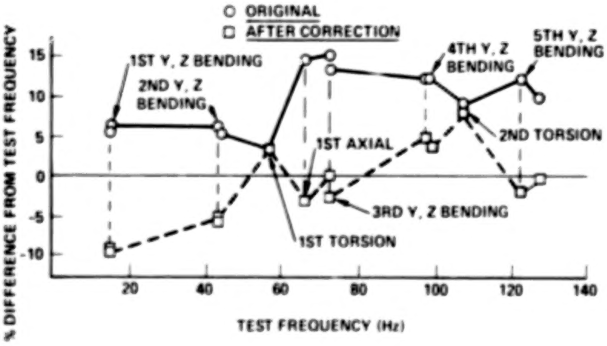

Fig. 5 Comparison of Math Model Frequency Errors Based Upon Test Data (Unrestrained Configuration)

SOLUTION OF AXISYMMETRIC FLUID STRUCTURE INTERACTION PROBLEMS WITH NASTRAN

A. J. KALINOWSKI

and

C. W. NEBELUNG

NAVAL UNDERWATER SYSYEMS CENTER
NEW LONDON, CONNECTICUT 06320

SUMMARY

This paper is concerned with the solution of axisymmetric acoustic fluid-structure interaction problems, employing the NASTRAN computer program. A previously developed 3-D Cartesian Coordinate pressure element formulation is adapted especially for axisymmetric elements. Analogous to the 3-D Cartesian Coordinate predecessor, the fluid portion of the problem is modeled with finite elements wherein one of the displacement components serves as a dummy variable for the pressure unknowns (all other degrees-of-freedom for the node are constrained out). Due to the lack of the 3-D counterpart of a 2-D type MAT2 Card, one cannot exactly input the constants needed to invoke the analogy. Two alternatives for implementation of the analogy are presented: (a) an approximate method by which dummy values of G, and ν (shear modulus and Poisson's ratio) are used to approximately invoke the analogy wherein the accuracy of the approximation can be made as close as desired to the proper analogy within an arbitrary small parameter ε; (2) an exact method whereby the NASTRAN FORTRAN coding is slightly changed to invoke the analogy exactly. Comparison of the finite element solution to the exact solution to the same problem is given.

Also provided, is a procedure for treating the far field boundary in scattering type problems wherein both the input loading and scattered pressure must be accounted for at the same outer boundary nodes.

INTRODUCTION

This paper addresses the topic of solving fluid structure interaction problems with the NASTRAN computer program. Although the material presented here is aimed directly towards the NASTRAN applications, it nevertheless contains general information regarding solving acoustic orientated fluid-structure interaction problems which can be applied to other general purpose finite element computer programs. The presentation focuses on axisymmetrical elastic structures immersed in an acoustic fluid (i.e., a fluid response representable by small deformation theory). The early part of the formulation is valid for both transient or steady state dynamic problems and can be applied to both symmetric and axisymmetric loading. The latter part of the paper which treats scattering and radiation type loadings is orientated more towards steady state axisymmetric loaded problems wherein the limiting factor lies mainly with the accuracy of the wave absorbing boundary at the termination point of the infinite domain of fluid surrounding the submerged structure.

The existing fluid-structure interaction capability resident within the NASTRAN program is designed to handle acoustic fluids constrained to lie in a finite dimension tank. Other extended fluid/structure applications of NASTRAN are summarized in a survey paper, ref. 1. Here focus is placed on expanding one of the above methods surveyed, namely the pressure analogy approach originally presented in ref. 2. Our goal is to develop the pressure analogy method for the particular case of axisymmetrical structures (i.e., in a cylindrical coordinate system) analogous to the Cartesian Coordinate development of ref. 2. Further, specific example problems (along with the corresponding input deck) will be given to clearly illustrate a simple example involving a submerged plate fluid-structure interaction problem. A radial wave problem is also treated.

The application of the pressure analogy for 3-D problems (whether they be 3-D Cartesian Coordinates as in ref. 2; or, 3-D cylindrical coordinates as encountered in axisymmetrical problems) requires some additional explanation with regard to assigning the equivalent material constants needed to invoke the pressure analogy. The problem lies in the fact that there is no direct way to input a general 3-D stress strain law matrix, [D], in the relation

$$\{\sigma\} = [D]\{\varepsilon\} \tag{1}$$

where the $\{\sigma\}$, $\{\varepsilon\}$ relations

$$\{\sigma\} = \begin{Bmatrix} \sigma_{rr} \\ \sigma_{zz} \\ \sigma_{\theta\theta} \\ \sigma_{rz} \\ \sigma_{r\theta} \\ \sigma_{z\theta} \end{Bmatrix} \qquad \{\varepsilon\} = \begin{Bmatrix} \varepsilon_{rr} \\ \varepsilon_{zz} \\ \varepsilon_{\theta\theta} \\ \gamma_{rz} \\ \gamma_{r\theta} \\ \gamma_{z\theta} \end{Bmatrix} = \begin{Bmatrix} \dfrac{\partial u_\theta}{\partial r} \\ \dfrac{\partial u_z}{\partial z} \\ \dfrac{1}{r}\dfrac{\partial u_\theta}{\partial \theta} + u_r/r \\ \dfrac{\partial u_r}{\partial z} + \dfrac{\partial u_z}{\partial r} \\ \dfrac{1}{r}\dfrac{\partial u_r}{\partial \theta} + \dfrac{\partial u_\theta}{\partial r} - v/r \\ \dfrac{\partial u_\theta}{\partial z} + \dfrac{1}{r}\dfrac{\partial u_z}{\partial \theta} \end{Bmatrix} \tag{2}$$

are the stress and strain components for axisymmetric structures. In other words, there is no 3-D counterpart to the general input available on the MAT2 card for 2-D type problems. This paper provides two methods for invoking the 3-D pressure analogy: the first is an approximate method, but can be made without changing the computer coding; the second method involves modifying the element stiffness FORTRAN computer coding.

PRESSURE ANALOGY FROM ELASTICITY EQUATIONS

The first step in implementing the fluid-structure interaction capability, is to reduce axisymmetric elasticity elements (e.g., NASTRAN CTRAPAX, CTRIAAX, CTRAPRG, CTRIARG, elements) down to pressure analogy elements. The field equations for elasticity are given by

$$\frac{\mu_e}{\rho_e} \nabla^2 \vec{u} + \frac{\left(\lambda_e + \mu_e\right)}{\rho_e} \nabla \left(\nabla \cdot \vec{u}\right) = \frac{\partial^2 \vec{u}}{\partial t^2} \qquad (3)$$

and the field equation for the acoustic representation of the fluid is given by

$$\frac{k_f}{\rho_f} \nabla^2 p = \frac{\partial^2 p}{\partial t^2} \qquad (4)$$

where $\nabla^2(\ ) = \frac{\partial^2(\ )}{\partial r^2} + \frac{1}{r^2} \frac{\partial^2(\ )}{\partial \theta^2} + \frac{\partial^2(\ )}{\partial z^2}$

where μ_e, λ_e are the elastic Lame´ constants of the elastic element, ρ_e is the mass density of the elasticity element, $\vec{u}$ is the cylindrical coordinate displacement vector of the elasticity element (i.e., $\vec{u} = [u_r, u_z, u_\theta]^T$), p is the fluid pressure, k_f is the bulk modulus of the fluid, ρ_f is the mass density of the acoustic fluid and k_f is the bulk modulus of the acoustic fluid. By inspection, it is seen that equation (3) can reduce to equation (4) by setting

$$\begin{aligned} \lambda_e &= -k_f \\ \mu_e &= +k_f \\ \rho_e &= \rho_f \\ u_z &= p \\ u_r &= 0 \\ u_\theta &= 0 \end{aligned} \qquad (5)$$

thus the elasticity element will now support the field equation

$$c^2 \nabla^2 u_z^p = \frac{\partial^2 u_z^p}{\partial t^2} \quad , \text{ with } c^2 = k_f/\rho_f \tag{6}$$

where the superscript p on the u_z component of displacement is inserted to remind us that the scalar pressure quantity, p, now occupies the u_z displacement slot once the analogy is invoked through the enforcement of equations (5).

Next we have the task of substituting $\lambda_e = -k_f$ and $\mu_e = +k_f$ into the stiffness formulation for any of the axisymmetric elements mentioned earlier.

Equivalent G_e, ν_e to Invoke Pressure Analogy

The first approach that comes to mind is to simply back calculate, say an E_e, ν_e, that results in an equivalent λ_e, μ_e (recall some combination of any two of the three elastic constants E_e, ν_e, G_e are the raw data input fed in on a MAT1 card, for example). However, $E_e = \mu_e (3\lambda_e + 2\mu_e)/(\lambda_e + \mu_e)$, and $\nu_e = .5\lambda_e/(\lambda_e + \mu_e)$, consequently the insertion of $\lambda_e = -\mu_e = k_f$ would obviously create problems leading to infinite values for E_e and ν_e. An alternate approach is let G_e and ν_e be the two basic input elastic constants where again we start by expressing G_e and ν_e in terms of λ_e, μ_e; thus,

$$\begin{aligned} G_e &= \mu_e \\ \nu_e &= \frac{1}{2\left(1 + \frac{\mu_e}{\lambda_e}\right)} \end{aligned} \tag{7}$$

Next, rather than let $\mu_e = +k_f$, $\lambda_e = -k_f$ as demanded by equation (5), instead, we let

$$\mu_e = +k_f \text{ and } \lambda_e \simeq -k_f \tag{8}$$

More specifically, let the parameter ε be defined as a small parameter that defines the closeness of the near equality in the second of equation (8), where

$$\varepsilon \equiv +\mu_e/\lambda_e + 1 \tag{9}$$

Thus when equation (8) is substituted into equation (9), $\varepsilon = 0$ when λ_e exactly equals $-k_f$ and ε can be made to be arbitrarily close to zero, by making λ_e arbitrarily close, but not equal, to $-k_f$. Thus, substituting equation (9) into equation (7) we have

$$\boxed{\begin{array}{l} G_e = k_f \\ \nu_e = \dfrac{1}{2\varepsilon} \\ \rho_e = \rho_f \end{array}} \qquad \text{Constants Required to Invoke Pressure Analogy} \tag{10}$$

where ε is arbitrarily small, say $\varepsilon = 10^{-5}$.

In terms of the material [D] matrix of equation (1), the exact implementation of the analogy will lead to a [D] matrix of the form

$$[D] = k_f \begin{bmatrix} +1 & -1 & -1 & 0 & 0 & 0 \\ -1 & +1 & -1 & 0 & 0 & 0 \\ -1 & -1 & +1 & 0 & 0 & 0 \\ 0 & 0 & 0 & +1 & 0 & 0 \\ 0 & 0 & 0 & 0 & +1 & 0 \\ 0 & 0 & 0 & 0 & 0 & +1 \end{bmatrix} \tag{11}$$

or in the case of employing equation (10) will implicitly lead to

$$[D] = k_f \begin{bmatrix} \frac{2\varepsilon-1}{\varepsilon-1} & \frac{1}{\varepsilon-1} & \frac{1}{\varepsilon-1} & 0 & 0 & 0 \\ \frac{1}{\varepsilon-1} & \frac{2\varepsilon-1}{\varepsilon-1} & \frac{1}{\varepsilon-1} & 0 & 0 & 0 \\ \frac{1}{\varepsilon-1} & \frac{1}{\varepsilon-1} & \frac{2\varepsilon-1}{\varepsilon-1} & 0 & 0 & 0 \\ 0 & 0 & 0 & +1 & 0 & 0 \\ 0 & 0 & 0 & 0 & +1 & 0 \\ 0 & 0 & 0 & 0 & 0 & +1 \end{bmatrix} \tag{12}$$

Note that as $\varepsilon \to 0$, the approximate [D] matrix, equation (12), reduces exactly to equation (11).

Modification of FORTRAN Coding to Invoke Pressure Analogy

In this case, the pressure analogy is invoked exactly, provided a minor FORTRAN coding change is made in the stiffness generation routine for the axisymmetric element in question. Here, the corresponding fixes for the 17.6 level of NASTRAN (VAX computer version) as applied to TRIAAX and TRAPAX (triangular cross-section and quadralateral cross-section) element is given.

• Modification for TRAPAX Element

In this case the TRAPAD subroutine must be modified. The change suggested herein will both allow the element to perform its normal operation as solid elastic element in addition to the special application of reducing to the pressure analogy element. The material ID (i.e., the MID appearing in field 2 (column 9-16)) on a MAT1 NASTRAN card is used to trigger the special analogy. The user employing a material ID in the range

$$9000 \leq \text{MID} \leq 9100$$

in conjunction with setting $G_e = k_f$ and $\nu_e = 0.0$ on a corresponding MAT1 card will invoke the exact analogy implied by equation (12). The corresponding FORTRAN change is given in Figure 1.

• Modification for TRIAAX Element

The change is installed analogous to the procedure explained above, except here the changes are to be made in the TRIAAD subroutine. Again, the user employing a material ID on a MAT1 card falling anywhere in the range

$$9000 \leq \text{MID} \leq 9100$$

in conjunction with setting $G_e = k_f$ and $\nu_e = 0.0$ on the corresponding MAT1 card will invoke the exact analogy implied by equation (12). The corresponding FORTRAN change is given in Figure 2.

FINITE ELEMENT EQUATIONS FOR PRESSURE ANALOGY

Next, consider the form of the finite element governing equations when the pressure equations of motion are viewed through the eyes of the pressure analogy. For simplification, only axisymmetrical loading will be treated the remainder of this paper. Upon invoking the analogy via the method described earlier, the following assembled matrices will be formed for the fluid domain portion of the interaction problem

```
      IF(MATID.GE.9000.AND.MATID.LE.9100)GO TO 320
      V=  ANU(1)     * E(2)/ E(1)
      VZ = ANU(2)     * E(3)/ E(2)
      VR = ANU(3)     * E(1)/ E(3)
      DEL = 1./(1. - V*ANU(1)  - VZ *ANU(2)- VR*ANU(3) - ANU(1)*ANU(2)*
     X      ANU(3) - V* VZ* VR )
C
C COMPUTE ELASTIC CONSTANTS MATRIX FROM MATERIAL TO ELEMENT AXIS
      DO 510 I = 1,21
  510 TEO(I) = 0.
      TEO(1) = E(1)* (1.- ANU(2)*VZ)* DEL
      TEO(2) = E(1)* (ANU(3)+ VZ* V)* DEL
      TEO(3) = E(3)* (1.- ANU(1)*V )* DEL
      TEO(4) = E(1)* (V+ ANU(3)*ANU(2))* DEL
      TEO(5) = E(3)* (VZ +ANU(1)*ANU(3))* DEL
      TEO(6) = E(2)* (1.-  VR *ANU(3))* DEL
      TEO(10)= G(3)
      TEO(15)= G(1)
      TEO(21)= G(2)
      GO TO 330
  320 CONTINUE
      DO 360 I=1,21
  360 TEO(I)=0.0
      FKF   =G(1)
      TEO(1)=FKF
      TEO(2)=-FKF
      TEO(3)=FKF
      TEO(4)=-FKF
      TEO(5)=-FKF
      TEO(6)=FKF
      TEO(10)=FKF
      TEO(15)=FKF
      TEO(21)=FKF
  330 CONTINUE
```

* In the COSMIC Level 17.6 version of NASTRAN (for VAX computer), replace the lines of coding starting with Sequence Number 2100 through 2270 with the above FORTRAN coding. The sequence numbers we refer to appear in Columns 73 through 80 of the original COSMIC FORTRAN card images.

Fig. 1 FORTRAN Changes for CTRAPAX Elements
(for TRAPAD subroutine)

```
      IF(MATID.GE.9000.AND.MATID.LE.9100)GO TO 321
C
C SET MATERIAL PROPERTIES IN DOUBLE PRECISION VARIABLES
      ER = E(1)
      ET = E(2)
      EZ = E(3)
      VRO = ANU(1)
      VOZ = ANU(2)
      VZR = ANU(3)
      GOR = G(1)
      GZO = G(2)
      GRZ = G(3)
      VOR = VRO * ET / ER
      VZO = VOZ * EZ / ET
      VRZ = VZR * ER / EZ
      DEL = 1.D0/(1.D0 - VRO*VOR  - VOZ*VZO - VZR*VRZ
     1     - VRO * VOZ * VZR - VRZ * VOR * VZO )
C
C COMPUTE ELASTIC CONSTANTS MATRIX FROM MATERIAL TO ELEMENT AXI
C
      DO 250 I=1,21
  250 TEO(I) = 0.D0
C
      TEO(1)=  ER*(1. -  VOZ*VZO)*DEL
      TEO(2) = ER * ( VZR + VZO * VOR ) * DEL
      TEO(3)=  EZ*(1. -  VRO*VOR)*DEL
      TEO (4) = ER * ( VOR + VZR * VOZ) * DEL
      TEO (5) = EZ * (VZO + VRO * VZR ) * DEL
      TEO(6)=  ET*(1. -  VRZ*VZR)*DEL
      TEO (10) = GRZ
      TEO (15) = GOR
      TEO (21) = GZO
      GO TO 330
  321 CONTINUE
      DO 360 I=1,21
  360 TEO(I)=0.0
      FKF   = G(1)
      TEO(1)=FKF
      TEO(2)=-FKF
      TEO(3)=FKF
      TEO(4)=-FKF
      TEO(5)=-FKF
      TEO(6)=FKF
      TEO(10)=FKF
      TEO(15)=FKF
      TEO(21)=FKF
  330 CONTINUE
```

* In the COSMIC Level 17.6 version of NASTRAN (for VAX computer), replace the lines of coding starting with Sequence Numbers 2040 through 2330 with the above FORTRAN coding. The sequence numbers we refer to appear in Columns 73-80 of the original COSMIC FORTRAN card images.

Fig. 2 FORTRAN Changes for CTRIAAX Elements (for TRIAAD subroutine)

$$[m]\{\ddot{U}_z^p\} + [c]\{\dot{U}_z^p\} + [k]\{U_z^p\} = \{f_z\} \tag{13a}$$

or in expanded form

$$\begin{bmatrix} m^{ii} & 0 & 0 \\ 0 & m^{ww} & 0 \\ 0 & 0 & m^{bb} \end{bmatrix} \begin{Bmatrix} \{\ddot{U}_z^p\}^i \\ \{\ddot{U}_z^p\}^w \\ \{\ddot{U}_z^p\}^b \end{Bmatrix} + \begin{bmatrix} c^{ii} & c^{iw} & c^{ib} \\ c^{wi} & c^{ww} & c^{wb} \\ c^{bi} & c^{bw} & c^{bb} \end{bmatrix} \begin{Bmatrix} \{\dot{U}_z^p\}^i \\ \{\dot{U}_z^p\}^w \\ \{\dot{U}_z^p\}^b \end{Bmatrix}$$

$$+ \begin{bmatrix} k^{ii} & k^{iw} & k^{ib} \\ k^{wi} & k^{ww} & k^{wb} \\ k^{bi} & k^{bw} & k^{bb} \end{bmatrix} \begin{Bmatrix} \{U_z^p\}^i \\ \{U_z^p\}^w \\ \{U_z^p\}^b \end{Bmatrix} = \begin{Bmatrix} f_z^i \\ f_z^w \\ f_z^b \end{Bmatrix} \tag{13b}$$

where the displacement vector* $\{U_z^p\}$ and associated load vector $\{f_z\}$ have been partitioned into three parts; namely, into nodes interior to the fluid (superscript "i"), nodes on the wetted surface interfacing the fluid and solid (superscript "w") and nodes lying on the outer truncation boundary of the fluid (superscript "b"). The $[m]$, $[k]$, $[c]$ matrices (employing lower case symbols) are automatically formed by the computer program (e.g., NASTRAN) employing the analogy. The $[m]$, $[c]$, $[k]$ fluid element matrices are constructed automatically by the finite element computer program employing the analogy equation (10), however, the loading vector, $\{f\}$, requires additional explanation. It must be remembered that while employing the analogy with a solid elasticity type element, the expected elasticity loading is the surface traction vector, T_i, (having units of stress in the analogy), thus the force vector, $\{f_z\}$, is given by

$$\{f_z\} = \int_{s_e} [N]^T \{T_z\} ds \tag{14a}$$

for consistently formed distributed load-to-concentrated load formations, or alternatively is given by

$$\{f_z\} = \{\Delta A\ T_z\} \tag{14b}$$

for lumped force applications, where ΔA is a suitable fraction of the area of the neighboring elements surrounding each surface node where the force is to be applied.

---

*Note, the superscript p has been added to the analogy displacement variable to remind us that pressure, p, occupied the z component of the displacement vector.

Next, we must determine how $\{T_z\}$ is related to the fluid pressure p (i.e., u_z^p). From ref. 4, the surface traction vector T_i is related to the stress components through the relation

$$T_i = \sigma_{ji}\, n_j' \tag{15}$$

where n_j' is a positive outward normal unit vector to the *surface of the fluid*. More specifically, the z component of T_i, expressed in cylindrical coordinates, is given by

$$T_z = \sigma_{rz}\, n_r' + \sigma_{zz}\, n_z' + \sigma_{\theta z}\, n_\theta' \tag{16}$$

Upon substituting equations (1) and (11) into (16), we arrive at

$$T_z = k_f\, (\gamma_{rz}\, n_r' + (-\varepsilon_{rr} - \varepsilon_{\theta\theta} + \varepsilon_{zz})\, n_z' + \gamma_{\theta z}\, n_\theta' \tag{17}$$

However, for the analogy, recall $u_r = u_\theta = 0$, thus with the aid of strain - displacement relations from equation (2), equation (17) reduces to

$$T_z = k_f \left(\frac{\partial u_z^p}{\partial r}\, n_r' + \frac{1}{r} \frac{\partial u_z^p}{\partial \theta}\, n_\theta' + \frac{\partial u_z^p}{\partial z}\, n_z' \right) \tag{18}$$

Next the terms inside the parenthesis of equation (18) are recognized to be the gradient of u_z^p in the direction of the outward unit normal $\vec{n}'$, thus equation (18) is rewritten

$$T_z = k_f \vec{\nabla}(u_z^p) \cdot \vec{n}' = k_f \frac{\partial u_z^p}{\partial n'} \tag{19}$$

Therefore equation (19) implies that in the pressure analogy, the elasticity surface traction component, T_z, is related to the fluid bulk modulus times the normal derivative of the fluid pressure.

Evaluation of Load Vector for Pressure Analogy

Now with the aid of equation (19), we are in a position to evaluate the $\{f_z\}$ load vector.

- evaluation of f_z^i

Since we are not considering any body forces, the nodal loading values for nodes interior to the fluid domain are set to zero, thus

$$f_z^i = 0 \tag{19a}$$

- evaluation of f^w_z

This is the key term that relates the fluid pressure variable, u^p_z, to the surface motion of the structure. The equations of motion of an acoustic fluid are given by (ref. 5)

$$\vec{\nabla}(p) = -\rho_f \frac{\partial^2 \vec{u}^f}{\partial t^2} \tag{20}$$

where $\vec{u}^f$ denotes the fluid particle displacement vector. However, at the fluid-structure interface, the boundary condition relating the structure displacement, $\vec{U}^w$ and the fluid particle motion $\vec{u}^f$ is given by (ref. 6)

$$\dot{\vec{U}}^w \cdot \vec{n} = \dot{\vec{u}}^f \cdot \vec{n} \tag{21}$$

(i.e., the normal to the structure surface component of velocity of the fluid and structure are equal). Thus, differentiating equation (21) with respect to time and then substituting equation (20) into (21) it follows

$$\rho_f \ddot{\vec{U}}^w \cdot \vec{n} = -\vec{\nabla} p \cdot \vec{n} \tag{22}$$

or equivalently

$$\rho_f \ddot{U}^w_n = -\frac{\partial p}{\partial n} = +\frac{\partial p}{\partial n'} \tag{22a}$$

since $\vec{n} = -\vec{n}'$, where $\vec{n}'$ is the outward unit normal from the fluid surface. Finally, the lumped version of the $\{f^w_z\}$ vector is given by substituting equation (22a) into equation (19) and then equation (14b) resulting in the expression

$$\{f^w_z\} = \{\Delta A^w k_f \rho_f \ddot{U}^w_n\} \tag{23}$$

However, since normal coordinates are not always available in the finite element program implementing the analogy for axisymmetrical problems, $\ddot{U}_n$ is expressed in the global cylindrical coordinate $\ddot{U}^w_r$, $\ddot{U}^w_z$. Thus, the component of the velocity vector $\vec{U}^w$ pointing in the outward normal to the structure surface is given by $U^w_n = \vec{U}^w \cdot \vec{n}$, thus equation (23) becomes

$$\{f^w_z\} = \{\Delta A^w k_f \rho_f (\ddot{U}^w_r n_r + \ddot{U}^w_z n_z)\} \tag{24}$$

where n_r, n_z are components, direction cosines, of the outward unit vector to the surface at the application of nodal force $\{f^w_z\}$, and ΔA^w is the wetted surface area surrounding the nodal force.

- evaluation of f^b_z

Finally, there remains the evaluation of the outer boundary force f^b_z. Depending on the kind of problem being solved, we consider four types of outer boundaries (i.e., the termination of the fluid mesh surrounding the structure), namely (a) rigid outer fluid boundary, (b) free surface (soft) outer fluid boundary, (c) absorption boundary for scattering problems, and (d) absorption boundary for radiation problems.

a. rigid outer fluid boundary

In this case, the boundary condition is simply $\frac{\partial p}{\partial n'} = 0$, (i.e., $\frac{\partial u_z^p}{\partial n'} = 0$) consequently in view of equations (19) and (14a) the corresponding f_z^w is

$$\{f_z^b\} = 0$$

and the surface degree of freedom, u_z^p are free variables (i.e., are not set = zero).

b. free surface (soft) outer fluid boundary

Here, the boundary condition is $p = 0$ (i.e., $u_z^p = 0$) on the outer boundary. In this case, $\{f_z^b\}$ is not specified by the user, and is computed as a reaction force required to enforce the $u_z^p = 0$ condition. The $u_z^p = 0$ condition is simply applied via SPC constraints in the NASTRAN input data.

c. absorbing boundary for scattering problems

In this type of problem, a traveling pressure wave is incident upon the submerged structure. The problem input forcing function and the absorption of the scattered pressure wave all are enforced at the outer boundary cut in the fluid medium. From ref. 3, the boundary condition in terms of pressure is given by

$$\frac{\partial p}{\partial n'} = -\frac{\mathrm{Cos}\psi}{c_f}\dot{p} + \frac{\partial p_{inc}}{\partial n'} + \frac{\mathrm{Cos}\psi}{c_f}\frac{\partial p_{inc}}{\partial t} \tag{25}$$

where $\frac{\partial(\;)}{\partial n'}$ is the gradient normal to the surface of the cut, p_{inc} is the incident fluid pressure, $\mathrm{Cos}\psi$ is a geoemtric correction factor. If the shape of the fluid outer boundary surrounding the structure is a sphere, $\mathrm{Cos}\psi = 1.0$, however for other shapes, $\mathrm{Cos}\psi$ corresponds to the cosine of the angle between the outward normal, $\vec{n}$, to the surface point, and the unit vector pointing along the average direction of propagation, $\vec{n}^W$. The direction of $\vec{n}^W$ can approximately constructed to be along a line starting at the geometrical center of the structure and terminating at the surface node where the $\{f_z^b\}$ load is applied. The geometrical correction can also be ignored by simply setting $\mathrm{Cos}\psi = 1$, even in cases where the fluid boundary surrounding the structure is not spherical.

Next, substitute equation (25) into (19) and (14b) to obtain

$$\{f_z^b\} = \underbrace{\Delta A^b k_f\left(\frac{-\mathrm{Cos}\psi}{c_f}\right)\dot{u}_z^p}_{\substack{\text{combines (without}\\\text{minus) with damp-}\\\text{ing matrix [C]}}} + \underbrace{\Delta A^b k_f\left(\frac{\partial p_{inc}}{\partial n'} + \frac{\mathrm{Cos}\psi}{c_f}\frac{\partial p_{inc}}{\partial t}\right)}_{\substack{\{f_z^b\}^e \text{ explicit term in}\\\text{loading vector}}} \tag{26}$$

The variable $\{f_z^b\}$ has an implicit portion determined as part of the solution (first term on right) and an explicit term, $\{f_z^b\}^e$, which is completely known since the formula for p_{inc} is explicitly known as a function of space and time.

For example, an incident plane wave traveling in the +z direction is given by the expression $p_{inc} = p_0 \, e^{i(-\omega z/c+\omega t)}$, consequently in this case

$$\{f_z^b\}^e = \left[\Delta A^b k_f \left(\mathrm{Cos}\psi - \mathrm{Cos}\,(n',z)\right) p_o \, e^{i(-(\omega z/c_f) + \pi/2)}\right]_{\omega/c_f} \tag{27}$$

where Cos (n',z) is the cosine of the angle between the plus z axis and the outward normal to the fluid boundary at the point of nodal force application. The $e^{i\omega t}$ portion of the loading is omitted in equation (27) since this factor is never explicitly applied to a NASTRAN load card for steady state SOL 8 rigid formats.

d. absorbing boundary for radiation problems

In this class of problems, the forcing function originates from within the submerged body and emits radiating pressure waves which propagate outward towards the fluid mesh outer boundary. The development follows the example of the previous scattering treatment, except for the fact that $p_{inc} = 0$, thus $\{f_z^b\}^e = 0$. The lumped value damping term,

$$\Delta A^b k_f \left(\frac{\mathrm{Cos}\psi}{c_f}\right) \tag{28}$$

again is combined with the fluid damping matrix $\lfloor c \rfloor$.

FINITE ELEMENT EQUATIONS FOR STRUCTURE

The governing equations of motion for the submerged elastic structure are formed in the usual fashion. For example, with the NASTRAN program, one can employ CTRAPAX, CTRIAAX and CCONEAX elements for the n = 0 harmonic. It will be convenient to partition the displacement vector (and consequently the mass, stiffness and damping matrices) into the form $[U^I, U_r^W, U_z^W]^T$ wherein the partition blocks refer to any node displacement component interior to the structure (superscript "I"), global radial component of a wet fluid-structure interface node and global axial component of a wet fluid-structure interface node respectively. Consequently the equations of motion for the structure in finite element form become

$$[M]\{\ddot{U}\} + [C]\{\dot{U}\} + [K]\{U\} = \{F\} \tag{29a}$$

or more specifically in expanded form are expressed in the form

$$\begin{bmatrix} M^{II} & 0 & 0 \\ 0 & M_r^{WW} & 0 \\ 0 & 0 & M_z^{WW} \end{bmatrix} \begin{Bmatrix} \ddot{U}^I \\ \ddot{U}_r^W \\ \ddot{U}_z^W \end{Bmatrix} + \begin{bmatrix} C^{II} & C^{IR} & C^{IZ} \\ C^{RI} & C^{RR} & C^{RZ} \\ C^{ZI} & C^{ZR} & C^{ZZ} \end{bmatrix} \begin{Bmatrix} \dot{U}^I \\ \dot{U}_r^W \\ \dot{U}_z^W \end{Bmatrix}$$

$$+ \begin{bmatrix} K^{II} & K^{IR} & K^{IZ} \\ K^{RI} & K^{RR} & K^{RZ} \\ K^{ZI} & K^{ZR} & K^{ZZ} \end{bmatrix} \begin{Bmatrix} U^I \\ U_r^W \\ U_z^W \end{Bmatrix} = \begin{Bmatrix} F^I \\ F_r^W \\ F_z^W \end{Bmatrix} \tag{29b}$$

where [M], [C], [K] are the structural mass, damping and stiffness matrices and {F} is the force vector. The F^I portion of the structural load vector corresponds to any internal forces that are generated within the structure. The F_r^w and F_z^w forces are a combination of interaction forces existing between the structure and fluid, plus any additional external forces that happen to lie on the surface (usually these additional values are zero for scattering problems), thus

$$\begin{aligned} \{F_r^w\} &= \{- n_r \, \Delta A^w \, p^w\} + \{F_r^w\}^e \\ \{F_z^w\} &= \{- n_z \, \Delta A^w \, p^w\} + \{F_z^w\}^e \end{aligned} \qquad (30)$$

where n_r, n_z are the components (direction cosines) of a vector to the point of nodal force application, ΔA^w is the appropriate nodal force (distributed load-to-nodal force area conversion) and $\{F_r^w\}^e$, $\{F_z^w\}^e$ are any explicitly known nodal forces that exist at the fluid-structure interface in addition to the yet unknown interaction nodal forces. For example, in the case of acoustic radiation problems involving shells submerged in water, it would not be unusual to have explicity applied nodal loads acting at the wet fluid-structure interface nodes. Note that n_r, n_z are components of an outward unit normal to the structure surface.

COMBINED FINITE ELEMENT FLUID-STRUCTURE EQUATIONS

Now we are in a position to combine the fluid and structure finite element equations. The scattering problem is the most complicated situation and will be the one we use to setup the coupled equations of motion. All other cases such as a rigid outer boundary, soft outer boundary or a wave absorption outer boundary for purely radiation problems, can be obtained as a subset of the more general scattering case by simply dropping the appropriate terms from the scattering case.

Scattering Interaction Case

The coupled system of equations is achieved by substituting equations (30) into (29b) and then substituting equations (26), (24), (19a) into equation (13b), thus obtaining the result

$$
\begin{gathered}
\begin{bmatrix}
M^{II} & 0 & 0 & 0 & 0 & 0 \\
0 & M_r^{ww} & 0 & 0 & 0 & 0 \\
0 & 0 & M_z^{ww} & 0 & 0 & 0 \\
0 & 0 & 0 & m^{ii} & 0 & 0 \\
0 & -\Delta A^w \rho_f k_f n_r & -\Delta A^w \rho_f k_f n_z & 0 & m^{ww} & 0 \\
0 & 0 & 0 & 0 & 0 & m^{bb}
\end{bmatrix}
\begin{Bmatrix}
\ddot{U}^I \\ \ddot{U}_r^w \\ \ddot{U}_z^w \\ (\ddot{U}_z^p)^i \\ (\ddot{U}_z^p)^w \\ (\ddot{U}_z^p)^b
\end{Bmatrix} + \\
\begin{bmatrix}
C^{II} & C^{IR} & C^{IZ} & 0 & 0 & 0 \\
C^{RI} & C^{RR} & C^{RZ} & 0 & 0 & 0 \\
C^{ZI} & C^{RR} & C^{ZZ} & 0 & 0 & 0 \\
0 & 0 & 0 & c^{ii} & c^{iw} & c^{ib} \\
0 & 0 & 0 & c^{wi} & c^{ww} & c^{wb} \\
0 & 0 & 0 & c^{bi} & c^{bw} & c^{bb} + \Delta A^b k_f \dfrac{\mathrm{Cos}\psi}{c_f}
\end{bmatrix}
\begin{Bmatrix}
\dot{U}^I \\ \dot{U}_r^w \\ \dot{U}_z^w \\ (\dot{U}_z^p)^i \\ (\dot{U}_z^p)^w \\ (\dot{U}_z^p)^b
\end{Bmatrix} + \\
\begin{bmatrix}
K^{II} & K^{IR} & K^{IZ} & 0 & 0 & 0 \\
K^{RI} & K^{RR} & K^{RZ} & 0 & \Delta A^w\, n_r & 0 \\
K^{ZI} & K^{ZR} & K^{ZZ} & 0 & \Delta A^w\, n_z & 0 \\
0 & 0 & 0 & k^{ii} & k^{iw} & k^{ib} \\
0 & 0 & 0 & k^{wi} & k^{ww} & k^{wb} \\
0 & 0 & 0 & k^{bi} & k^{bw} & k^{bb}
\end{bmatrix}
\begin{Bmatrix}
U^I \\ U_r^w \\ U_z^w \\ (U_z^p)^i \\ (U_z^p)^w \\ (U_z^p)^b
\end{Bmatrix}
=
\begin{Bmatrix}
F^I \\ (F_r^w)^e \\ (F_z^w)^e \\ 0 \\ 0 \\ (f_z^b)^e
\end{Bmatrix}
\end{gathered}
\tag{31}
$$

Thus to solve a scattering problem, follow the steps given below

1. Build the structure with axisymmetrical elements in the usual manner.
2. Model the fluid surrounding the structure with axisymmetrical solid elasticity elements (such as CTRAPAX and CTRIAAX elements), where the material constants are entered according to equation (10) and all displacement components are constrained to zero except u_z.
3. Allow for a double set of node numbers (occupying the same grid coordinates) between the fluid and structure interface. In order to avoid undesirable large bandwidths in the equation solver, it is advisable to have the node numbers of the neighboring

node points across the fluid-to-structure gap be in the same neighborhood.

4. Assign dashpots into the fluid damping matrix (i.e., dampers are assigned to the outer fluid boundary nodes according to equation (28a)); these are implemented through DMIG cards in NASTRAN.

5. Add off-diagonal terms in mass matrix of equation (31) through DMIG cards. In the column corresponding to wet node radial structural component $\ddot{U}_r^W$ and row corresponding to wet node pressure variable $(\ddot{U}_z^p)^W$, insert value $-\Delta A^W \rho_f k_f n_r$; similarly, in the column corresponding to wet node axial structural component U_z^W and row corresponding to wet node pressure variable $(\ddot{U}_z^p)^W$, insert value $-\Delta A^W \rho_f k_f n_z$. When using the DMIG cards, the column and row number are defined indirectly via the node number and associated component number of the wet node in question. Sample problem illustrate the use of this feature.

6. Add off-diagonal terms in stiffness matrix of equation (31) through DMIG cards. In the column corresponding to wet node pressure variable $(U_z^p)^W$ and row corresponding to wet radial structural component U_r^W, insert the value $\Delta A^W n_r$. Similarly, in the column corresponding to wet node pressure variable $(U_z^p)^W$ and row corresponding to wet axial structural component U_z^W, insert the value $\Delta A^W n_z$.

7. Apply the explicitly known structural loads internal to the structure, F^I, and any explicitly known loads on the wetted fluid-structure interface surface, $(F_r^W)^e$, $(F_z^W)^e$. We emphasize that these latter two surface loads are not the fluid-structure interaction forces (they are accounted for implicitly in the formulation). For most scattering problems the F^I, $(F_r^W)^e$, $(F_z^W)^e$ forces are zero. Typically, these quantities come into play only for radiation loaded problems considered later.

8. Apply the explicitly known incident wave driving force, $(f_z^b)^e$. The general lumped version formula for this expression is given by the second portion of equation (26). The most common case for axisymmetrical loading would be for a plane wave propagating in the +z direction wherein an explicit formula for the driving force is given in equation (27) and is applied to all fluid outer boundary mesh surface modes.

Radiation Interaction Case

The formulation for radiation problems follows the previous scattering formulation except for some small differences, namely the fact that the radiated field is due only to explicit dynamic loads on the structure (F^I, $(F_r^W)^e$, $(F_z^W)^e$ whereas $(f_z^b)^e = 0$. Consequently, to implement the analogy method for radiation problems, simply follow Steps 1 through 7 as explained in the previous scattering explanation, with $(f_z^b)^e = 0$ in the final Step 8.

Rigid Outer Boundary

For this type problem, consider the outer boundary of the fluid mesh to be a rigid surface (e.g., a containment wall). This problem only applies to radiation type situations. Here, follow the steps outlined in the previous radiation explanation, except omit Step 4. The $\partial p/\partial n' = 0$ rigid boundary condition is automatically satisfied by leaving the outer boundary free of loads.

Soft Outer Boundary

This type problem also only applied to radiation problems and is implemented by following the steps of the previous radiation explanation, except omitting Step 4. Also $p = 0$ is enforced by setting the z-component of the analogy variable (i.e., $u_z^p = 0$) equal to zero on the outer boundary of the fluid mesh with SPC cards, for example.

DEMONSTRATION PROBLEMS

The implementation of the pressure analogy is perhaps best illustrated with the aid of simple demonstration problems. The philosophy of these problems is to keep the example as simple as possible so that all the data concerning the problem set up is available and at the same time, the simple example can be checked against the exact solution for accuracy comparison purposes.

Axial Wave Demonstration Problem

In this example, consider the fluid-structure interaction problem of a plane wave normally incident upon a 1/4 inch steel plate which is totally submerged in an infinite fluid domain (e.g., see Fig. 3). Since the particle motion transverse to the direction of wave propagation is zero, we need only model a single strip of elements in the z-direction. The physical properties of the materials involved are as follows: for the steel plate, the mass density, Young's modulus and Poisson's ratio are, $\rho = .000735$ lb-sec^2/in^4, $E = 29.0 \times 10^6$ psi, $\nu = .30$ respectively and for the fluid, the bulk modulus and mass density are given by $k_f = 345600.$ psi, $\rho_f = .000096$ lb-sec^2/in^4. The driving frequency is 6000 Hz, consequently, the plate thickness is small compared to the compressional speed of steel. Therefore, the plate can be modeled with "plate theory" and the need

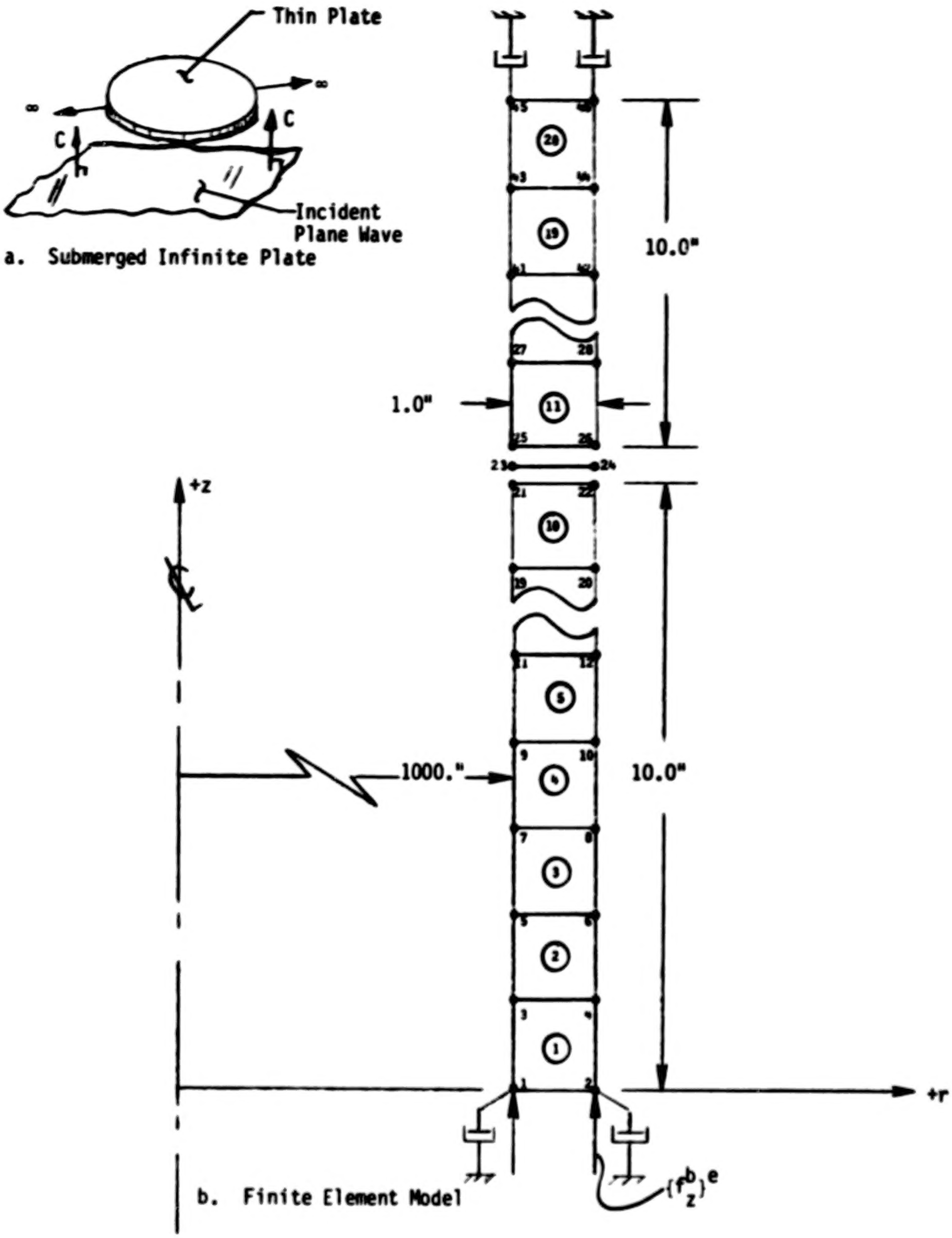

a. Submerged Infinite Plate

b. Finite Element Model

Fig. 3 Axial Wave Demonstration Problem

to model through-the-thickness of the actual plate is not required in this particular example. Based on prior experience, ten elements per fluid wavelength in the direction of wave propagation is sufficient to model a traveling wave. The finite element model is shown in Fig. 3 and the corresponding NASTRAN input deck is shown in Fig. 4. The loading is computed employing equation (27). The Fig. 3 finite element model has four fluid outer boundaries which we refer to as the lower end face ($z = 0$); upper end face ($z = 20.0$ in.); outer end face ($r = 1001.$ in.) and inner end face ($r = 1000.$ in.). With respect to applying equation (27) to this particular problem, we note that the plane wave strength is $p_0 = 1.0$ psi and also on the lower end face, $\text{Cos}\psi = 1.0$, $\text{Cos}(n',z) = -1.0$; on the upper end face, $\text{Cos}\psi = 1.0$, $\text{Cos}(n',z) = +1.0$; on the outer end face, $\text{Cos}\psi = 0.0$, $\text{Cos}(n',z) = 0.0$ and on the inner face, $\text{Cos}\psi = 0.0$, $\text{Cos}(n',z) = 0.0$.

For the zeroth harmonic, the loads, dampers, mass matrix entries, stiffness matrix entries are entered in a total applied force, total damping force, etc. sense. Thus the ΔA^b and ΔA^w factors employed in applying Steps 1-8 refer to the total area surrounding the node (e.g., $\Delta A^b = 2\pi r \cdot \Delta z$ for element faces parallel with the z axis).

The exact solution (see ref. 7) vs. NASTRAN solution is given below for magnitude of the pressure on the incident side and back side of the steel plate.

QUANTITY SOLUTION	AMPLITUDE OF TOTAL PRESSURE ON INCIDENT SIDE	AMPLITUDE OF TRANSMITTED BACK SIDE PRESSURE
EXACT SOL	1.25	.857
NASTRAN	1.34	.854

The user is cautioned to check for a factor of 2.0 error in the lumped mass matrix formed when employing CTRAPAX elements for the level 17.6 version of NASTRAN on the VAX or 1108. We have fixed the FORTRAN coding so that the matrix is properly formed. Users without a FORTRAN fix can compensate by artificially multiplying the mass density input by 2.0. Since the FORTRAN coding has been fixed in the version corresponding to the sample problems used to generate the demonstration problems, the density employed on the MAT1 cards correspond to actual mass densities on the materials involved in the analysis.

The FORTRAN fix to avoid the factor of 2.0 density error is as follows: at column 73 card sequence number 2620 in the subroutine TRAPAD, replace the two lines

```
IECPT(1) = IECPT(1) - (IECPT(1)/1000)*1000 -1  and  AJH0 = IECPT(1)
```

with the two lines

```
IECP = IECPT(1) - (IECPT(1)/1000)*1000 - 1
AJH0 = IECP
```

also, replace the one line (starting at column 73 sequence number 5430)

```
          830 AJH0 = IECPT(1) - (IECPT(1)/1000)*1000 - 1
```

with the two lines

```
          830 IECP = IECPT(1) - (IECPT(1)/1000)*1000 - 1
              AJH0 = IECP
```

Radial Wave Demonstration Problem

In this example, consider the fluid-structure interaction problem of an inward propagating cylindrical wave incident upon a 1.5 inch thick walled infinitely long silver cylinder, which has fluid on the outside and has a void on the inside (see Fig. 5). Since the incident wave front is parallel with the z-axis, the solution only depends on r, consequently one needs only model a one element thick strip of elements as shown in Fig. 5. In this problem both the fluid and the cylinder are modeled with CTRAPAX elements. The physical properties of the materials involved are as follows: for the silver cylinder, the mass density, Young's modulus and Poisson's ratio are $\rho = .000982$, $E = 1.13 \times 10^7$, $\nu = .36999$, respectively and for the fluid, the bulk modulus and mass density are given by $k_f = 345600.$ psi and $\rho_f = .000096$ lb-sec^2/in^4. The driving frequency for the problem is f = 6000.0 Hz. The finite element model is shown in Fig. 5 and the corresponding NASTRAN input deck is shown in Fig. 6. The structure (cylinder) is in a state of plain strain, thus $u_z = 0$ for the silver cylinder. The model has three outer fluid boundaries which we refer to as the lower end face (z = 0); upper end face (z = 1.0); and outer end face (r = 18.0"). Since all response quantities do not vary with z, $\frac{\partial p}{\partial z} = 0$, thus in view of equations (14b) and (19), it follows that in the analogy, $\frac{\partial u_z^p}{\partial z} = 0$ on the upper and lower end faces by simply not applying any force values to these nodes (i.e., they are free nodes w.r.t. the u_z^p degree-of-freedom in the pressure analogy). In the case of the outer boundary, we substitute the formula for a cylindrical wave propagating in the -r direction (wave front is prarllel to the z axis) into the second part of equation (26), where the applied loading at $r = r_b$ is given by

$$\{f_z^b\}^e = \frac{\Delta A^b k_f \omega}{c_f\, H_0^{(1)}(\omega r_W/c_f)} \left[-H_1^{(1)}(\omega r/c_f) + i\, H_0^{(1)}(\omega r/c_f) \right] \Bigg|_{r=r_b} \tag{32}$$

where $H_0^{(1)}(\ )$ and $H_1^{(1)}(\ )$ are the zeroth and 1st order Hankel functions of the first kind, r_W is the outer radius of the cylinder, and $r = r_b$ is the outer boundary of the fluid mesh (18.0").

The above exact form is approximately given by

$$\{f_z^b\}^e \approx i\, \Delta A^b k_f\, ? \sqrt{r_w/r}\, \frac{\omega}{c_f} e^{i(r-r_w)\omega/c_f} \Bigg|_{r=18.0} \tag{33}$$

```
ID NUSC AXIAL WAVE EXAMPLE
APP DISP
SOL 8
TIME 10
CEND
TITLE=AXIAL WAVE EXAMPLE
AXISYMMETRIC = COSINE
K2PP=STIFF
M2PP=MASS
B2PP=DASHPOTS
DISPLACEMENT(PHASE) = ALL
FREQ = 1
MAXLINES = 30000
DLOAD = 200
BEGIN BULK
AXIC    0
CCONEAX 1       150     23      24
CTRAPAX 1       100     1       2       4       3
CTRAPAX 2       100     3       4       6       5
CTRAPAX 3       100     5       6       8       7
CTRAPAX 4       100     7       8       10      9
CTRAPAX 5       100     9       10      12      11
CTRAPAX 6       100     11      12      14      13
CTRAPAX 7       100     13      14      16      15
CTRAPAX 8       100     15      16      18      17
CTRAPAX 9       100     17      18      20      19
CTRAPAX 10      100     19      20      22      21
CTRAPAX 11      100     25      26      28      27
CTRAPAX 12      100     27      28      30      29
CTRAPAX 13      100     29      30      32      31
CTRAPAX 14      100     31      32      34      33
CTRAPAX 15      100     33      34      36      35
CTRAPAX 16      100     35      36      38      37
CTRAPAX 17      100     37      38      40      39
CTRAPAX 18      100     39      40      42      41
CTRAPAX 19      100     41      42      44      43
CTRAPAX 20      100     43      44      46      45
DAREA   201     1000001 3       1.885+9 1000002 3       1.885+9
DMIG    DASHPOTS        1       1       1
DMIG    DASHPOTS1000001 3               1000001 3       10104.67
DMIG    DASHPOTS1000002 3               1000002 3       10104.67
DMIG    DASHPOTS1000045 3               1000045 3       10104.67
DMIG    DASHPOTS1000046 3               1000046 3       10104.67
DMIG    MASS    0       1       1       1
DMIG    MASS    1000023 1               1000023 3       .0
DMIG    MASS    1000023 1               1000025 3       .0
DMIG    MASS    1000023 3               1000023 3       1.043+5
DMIG    MASS    1000023 3               1000025 3       -1.043+5
DMIG    MASS    1000024 1               1000023 3       .0
DMIG    MASS    1000024 1               1000025 3       .0
DMIG    MASS    1000024 3               1000024 3       1.043+5
DMIG    MASS    1000024 3               1000026 3       -1.043+5
DMIG    STIFF   0       1       1       1
DMIG    STIFF   1000023 3               1000023 1       .0
DMIG    STIFF   1000023 3               1000023 3       -3143.16
DMIG    STIFF   1000024 3               1000024 1       .0
DMIG    STIFF   1000024 3               1000024 3       -3143.16
DMIG    STIFF   1000025 3               1000023 1       .0
DMIG    STIFF   1000025 3               1000023 3       3143.16
DMIG    STIFF   1000026 3               1000024 1       .0
DMIG    STIFF   1000026 3               1000024 3       3143.16
```

```
DPHASE  203     1000001 3       90.0    1000002 3       90.0
FREQ    1       6000.
MAT1    100             345600. 50000.  .000096
MAT1    150     29.+6           .3      .000735
PCONEAX 150     150     .25     150     1.302-3 150     .2
PTRAPAX 100             100     .0      90.0    180.0   270.0
RINGAX  1               1000.0  .0                      12456
RINGAX  2               1001.0  .0                      12456
RINGAX  3               1000.0  1.0                     12456
RINGAX  4               1001.0  1.0                     12456
RINGAX  5               1000.0  2.0                     12456
RINGAX  6               1001.0  2.0                     12456
RINGAX  7               1000.0  3.0                     12456
RINGAX  8               1001.0  3.0                     12456
RINGAX  9               1000.0  4.0                     12456
RINGAX  10              1001.0  4.0                     12456
RINGAX  11              1000.0  5.0                     12456
RINGAX  12              1001.0  5.0                     12456
RINGAX  13              1000.0  6.0                     12456
RINGAX  14              1001.0  6.0                     12456
RINGAX  15              1000.0  7.0                     12456
RINGAX  16              1001.0  7.0                     12456
RINGAX  17              1000.0  8.0                     12456
RINGAX  18              1001.0  8.0                     12456
RINGAX  19              1000.0  9.0                     12456
RINGAX  20              1001.0  9.0                     12456
RINGAX  21              1000.0  10.0                    12456
RINGAX  22              1001.0  10.0                    12456
RINGAX  23              1000.0  10.0                    12456
RINGAX  24              1001.0  10.0                    12456
RINGAX  25              1000.0  10.0                    12456
RINGAX  26              1001.0  10.0                    12456
RINGAX  27              1000.0  11.0                    12456
RINGAX  28              1001.0  11.0                    12456
RINGAX  29              1000.0  12.0                    12456
RINGAX  30              1001.0  12.0                    12456
RINGAX  31              1000.0  13.0                    12456
RINGAX  32              1001.0  13.0                    12456
RINGAX  33              1000.0  14.0                    12456
RINGAX  34              1001.0  14.0                    12456
RINGAX  35              1000.0  15.0                    12456
RINGAX  36              1001.0  15.0                    12456
RINGAX  37              1000.0  16.0                    12456
RINGAX  38              1001.0  16.0                    12456
RINGAX  39              1000.0  17.0                    12456
RINGAX  40              1001.0  17.0                    12456
RINGAX  41              1000.0  18.0                    12456
RINGAX  42              1001.0  18.0                    12456
RINGAX  43              1000.0  19.0                    12456
RINGAX  44              1001.0  19.0                    12456
RINGAX  45              1000.0  20.0                    12456
RINGAX  46              1001.0  20.0                    12456
RLOAD2  200     201             203     202
TABLED1 202                                                     +TAB1
+TAB1   1.0     1.0     10000.0 1.0     ENDT
ENDDATA
```

Fig. 4 NASTRAN Input for Axial Wave Demonstration Problem

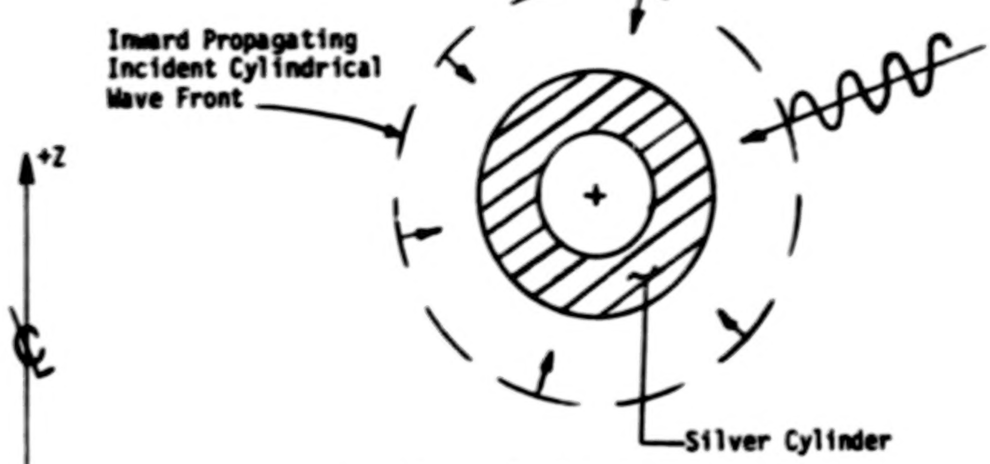

a. View of Problem in r,θ plane

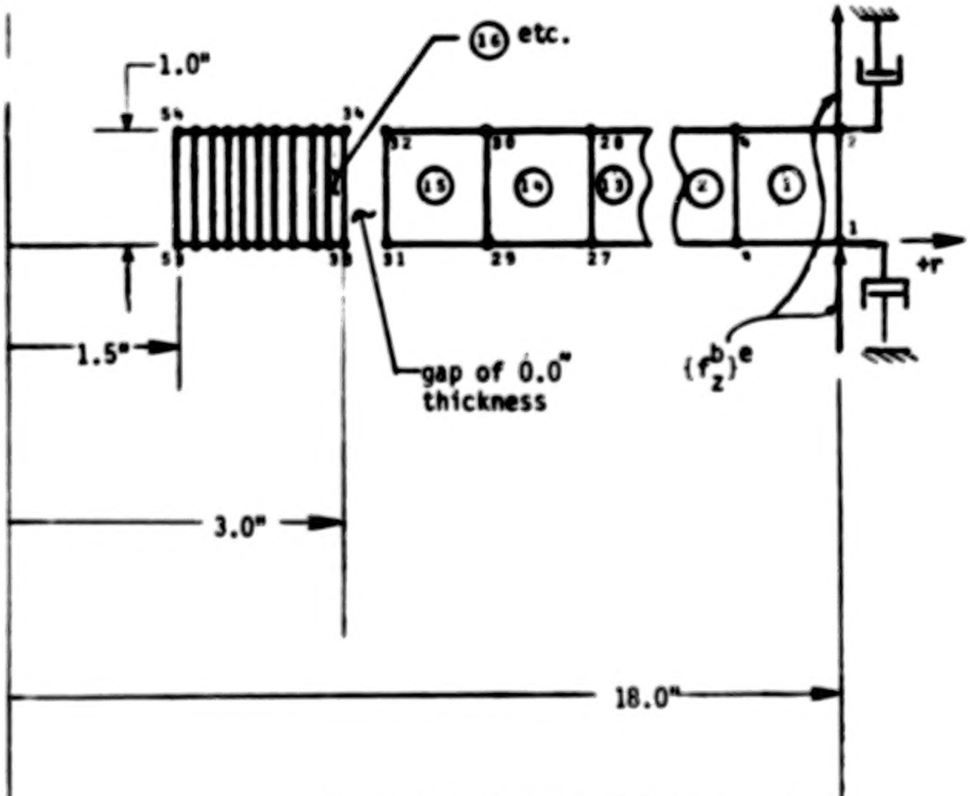

b. Finite Element Model in r-z plane

Fig. 5 Radial Wave Demonstration Problem

```
ID NUSC RADIAL WAVE EXAMPLE
APP DISP
SOL 8
TIME 10


CEND
TITLE=RADIAL WAVE EXAMPLE
AXISYMMETRIC = COSINE
K2PP=STIFF
B2PP=DASHPOTS
M2PP=MASS
DISPLACEMENT(PHASE) = ALL
FREQ = 1
MAXLINES = 100000
OLOAD=ALL
SPCFORCES=ALL
DLOAD = 200
BEGIN BULK
AXIC    0
CTRAPAX 1       100     3       1       2       4
CTRAPAX 2       100     5       3       4       6
CTRAPAX 3       100     7       5       6       8
CTRAPAX 4       100     9       7       8       10
CTRAPAX 5       100     11      9       10      12
CTRAPAX 6       100     13      11      12      14
CTRAPAX 7       100     15      13      14      16
CTRAPAX 8       100     17      15      16      18
CTRAPAX 9       100     19      17      18      20
CTRAPAX 10      100     21      19      20      22
CTRAPAX 11      100     23      21      22      24
CTRAPAX 12      100     25      23      24      26
CTRAPAX 13      100     27      25      26      28
CTRAPAX 14      100     29      27      28      30
CTRAPAX 15      100     31      29      30      32
CTRAPAX 16      150     35      33      34      36
CTRAPAX 17      150     37      35      36      38
CTRAPAX 18      150     39      37      38      40
CTRAPAX 19      150     41      39      40      42
CTRAPAX 20      150     43      41      42      44
CTRAPAX 21      150     45      43      44      46
CTRAPAX 22      150     47      45      46      48
CTRAPAX 23      150     49      47      48      50
CTRAPAX 24      150     51      49      50      52
CTRAPAX 25      150     53      51      52      54
DAREA   201     1000001 3       1.0     1000002 3       1.0
DMIG    DASHPOTS0       1       1       1
DMIG    DASHPOTS1000001 3               1000001 3       375.772
DMIG    DASHPOTS1000002 3               1000002 3       375.772
DMIG    MASS    0       1       1       1
DMIG    MASS    1000031 1               1000031 3       -317.691
DMIG    MASS    1000031 3               1000031 3       .0
DMIG    MASS    1000032 1               1000032 3       -317.691
DMIG    MASS    1000032 3               1000032 3       .0
DMIG    STIFF   0       1       1       1
DMIG    STIFF   1000031 3               1000031 1       9.4247
DMIG    STIFF   1000031 3               1000031 3       .0
DMIG    STIFF   1000032 3               1000032 1       9.4247
DMIG    STIFF   1000032 3               1000032 3       .0
```

```
FREQ    1       6000.
MAT1    100             345600. 50000.  .000096
MAT1    150     1.11+7          .36999  .000262
PTRAPAX 100             100     0.0     90.     180.    270.
PTRAPAX 150             150     0.0     90.     180.    270.
RINGAX  1               18.0    .0                      12456
RINGAX  2               18.0    1.0                     12456
RINGAX  3               17.0    .0                      12456
RINGAX  4               17.0    1.0                     12456
RINGAX  5               16.0    .0                      12456
RINGAX  6               16.0    1.0                     12456
RINGAX  7               15.0    .0                      12456
RINGAX  8               15.0    1.0                     12456
RINGAX  9               14.0    .0                      12456
RINGAX  10              14.0    1.0                     12456
RINGAX  11              13.0    .0                      12456
RINGAX  12              13.0    1.0                     12456
RINGAX  13              12.0    .0                      12456
RINGAX  14              12.0    1.0                     12456
RINGAX  15              11.0    .0                      12456
RINGAX  16              11.0    1.0                     12456
RINGAX  17              10.0    .0                      12456
RINGAX  18              10.0    1.0                     12456
RINGAX  19              9.0     .0                      12456
RINGAX  20              9.0     1.0                     12456
RINGAX  21              8.0     .0                      12456
RINGAX  22              8.0     1.0                     12456
RINGAX  23              7.0     .0                      12456
RINGAX  24              7.0     1.0                     12456
RINGAX  25              6.0     .0                      12456
RINGAX  26              6.0     1.0                     12456
RINGAX  27              5.0     .0                      12456
RINGAX  28              5.0     1.0                     12456
RINGAX  29              4.0     .0                      12456
RINGAX  30              4.0     1.0                     12456
RINGAX  31              3.0     .0                      12456
RINGAX  32              3.0     1.0                     12456
RINGAX  33              3.0     .0                      23456
RINGAX  34              3.0     1.0                     23456
RINGAX  35              2.85    .0                      23456
RINGAX  36              2.85    1.0                     23456
RINGAX  37              2.7     .0                      23456
RINGAX  38              2.7     1.0                     23456
RINGAX  39              2.55    .0                      23456
RINGAX  40              2.55    1.0                     23456
RINGAX  41              2.4     .0                      23456
RINGAX  42              2.4     1.0                     23456
RINGAX  43              2.25    .0                      23456
RINGAX  44              2.25    1.0                     23456
RINGAX  45              2.1     .0                      23456
RINGAX  46              2.1     1.0                     23456
RINGAX  47              1.95    .0                      23456
RINGAX  48              1.95    1.0                     23456
RINGAX  49              1.8     .0                      23456
RINGAX  50              1.8     1.0                     23456
RINGAX  51              1.65    .0                      23456
RINGAX  52              1.65    1.0                     23456
RINGAX  53              1.5     .0                      23456
RINGAX  54              1.5     1.0                     23456
RLOAD1  200     201                     1       2
TABLED1 1                                                               +ABC
+ABC    6000.0  7.2355+57000.0  1.0+6   ENDT
TABLED1 2                                                               +BCD
+BCD    6000.0  -1.014+77000.0  1.0+6   ENDT
ENDDATA
```

Fig. 6 NASTRAN Input for Radial Wave Demonstration Problem

and is more recognizable as a plane wave with cylindrical spreading. The input is such that the free field pressure has a 1.0 psi strength at the outer radius of the cylinder, $r = r_w = 3.0"$. Equation (32) is used to load the sample problem.

The exact solution (ref. 8) is given below for the magnitude of the total pressure as evaluated at the outer surface of the cylinder.

Exact Solution = 1.977

NASTRAN = 1.979 psi

The cylinder is stiff upon comparing the first mode hoop natural frequency to the driving frequency, thus it is expected that one nearly encounters a doubling of the 1.0 psi incident pressure wave strength at the fluid-solid interface.

CONCLUDING REMARKS

A step-by-step procedure is presented for solving fluid-structure interaction problems for axisymmetrical structures submerged in an acoustic fluid medium. A pressure analogy is used which employs solid elasticity elements that pose as fluid elements. The structural model and fluid variables are connected at the fluid-structure interface through the use of DMIG cards. The methodology presented here has concentrated on axisymmetrical structures with steady state axisymmetrical loading; however, the procedure can be extended to treat non-axisymmetrical loading and/or transient loading, although this situation is not treated herein.

The pressure analogy for 3-D problems can be invoked by one of two alternative methods regarding the setting of the material constants required to implement the method for 3-dimensional problems. The simpler, but approximate method (equivalent G,ν) presented here yields, for all practical purposes, the same numerical results as the exact implementation of the analogy, consequently it is felt that recompolation of the FORTRAN coding is not absolutely necessary as would be required by the exact implementation case.

Finally, the user is warned to check the lumped mass matrix accuracy for the particular version of NASTRAN he may decide to use. We have found that the lumped mass matrix employing (CTRAPAX elements for a COSMIC level 17.6 VAX version of NASTRAN) is too small by a factor of 2.0. The paper gives two possible fixes in order to correct the situation.

REFERENCES

1. Kalinowski, A. J., and Patel, J. S., "A Summary of NASTRAN Fluid/Structure Interaction Capabilities", 5th NASTRAN Users' Colloquium, Ames Research Center, Oct. 1976.

2. Everstine, G. C., Schroeder, E. A., and Marcus, M. S., "The Dynamic Analysis of Submerged Structures", 4th NASTRAN Users' Colloquium, 1975, NASA TM X-3278.

3. Kalinowski, A. J., "Geometrically Corrected Viscous Boundaries for Steady State Acoustic Scattering and Radiation Problems", Computational Methods for Infinite Domain Media-Structure Interaction, edited by A. J. Kalinowski, ASME volume to be released at 1981 ASME Winter Annual Meeting, Nov. 1981, Washington, DC.

4. Sokolnekoff, I. S., Mathematical Theory of Elasticity, Second Edition, McGraw-Hill Book Co.

5. Kinsler, L. E., and Frey, A. R., Fundamentals of Acoustics, Second Edition, John Wiley & Sons, Inc., 1962.

6. Milne-Thomson, L. M., Theoretical Hydrodynamics, MacMilliam Co., 1963.

7. Kalinowski, A. J., "Modeling Structural Damping for Solids Having Distinct Shear and Dilatational Loss Factors", Seventh NASTRAN Users' Colloquium, NASA CP-2062, 1978.

8. Kalinowski, A. J., and Nebelung, C. W., "Media-Structure Interaction Computations Employing Frequency Dependent Mesh Sizes with the Finite Element Method", the 51st Shock and Vibration Bulletin, May 1981.

LARGE DISPLACEMENTS AND STABILITY ANALYSIS OF NONLINEAR PROPELLER STRUCTURES

Robert A. Aiello and Christos C. Chamis

National Aeronautics and Space Administration
Lewis Research Center
Cleveland, Ohio 44135

SUMMARY

This paper describes the use of linear rigid formats in COSMIC NASTRAN without DMAP procedures for the analysis of nonlinear propeller structures. Approaches for updating geometry and applying follower forces for incremental loading are demonstrated. Comparisons are made with COSMIC NASTRAN rigid formats and other independant finite element programs. Specifically, the comparisons include results from the four approaches for updating the geometry using RIGID FORMAT 1, RIGID FORMATS 4 and 13, MARC and MSC/NASTRAN. It is shown that "user friendly" updating approaches (without DMAPS) can be used to predict the large displacements and instability of these nonlinear structures. These "user friendly" approaches can be easily implemented by the user and predict conservative results.

INTRODUCTION

The potential for high propulsive efficiency in the MACH 0.7 to 0.8 speed range has renewed interest in turboprop propulsion in recent years. Advanced turboprop concepts feature thin, highly swept and twisted propeller blades to achieve high efficiency and low noise at cruise. Deflections due to centrifugal loading, for blades of this type, exhibit a high degree of nonlinearity requiring special analysis techniques not automatically available in COSMIC NASTRAN.

As stated in the NASTRAN Theoretical Manual, "An important limitation of the automatic geometric nonlinear procedures provided with (COSMIC) NASTRAN is in the assumption that the applied loads from which the differential stiffness is derived remain fixed in magnitude and direction during deformation of the structure, and that their points of application move with the structure". This assumption is not valid for swept cantilever type structures like turboprop blades in a centrifugal force field where the direction and magnitude of the force vector is determined by the displaced position of the structure.

Highly swept turboprop blades in a centrifugal force field may experience an abrupt reversal of tip deflection or a large change in tip-chord angle as the rotational speed is increased. These sudden changes in position can severely affect aerodynamic performance and are referred to as instability points in this paper. The objective of this paper is to describe a study conducted on a representative advanced turboprop blade configuration. The selected configuration has a sweep angle of 60 degrees which is at the high end of a range of sweep angles being considered for the advance turboprop concept. The purpose of the study was to investigate high tip displacements, inherent in these designs, using NASTRAN without DMAP alters. The study included the use of RIGID FORMATS 1, 4 and 13. Results obtained from these RIGID FORMATS are compared with each other and with other finite element programs. The mathematical description of the various method used is summarized in the Appendix.

TURBOPROP GEOMETRY AND FINITE ELEMENT MODEL

The model of the scaled turboprop blade shown in figure 1 is about 10 inches long, has a tip chord of 2 inches, and a maximum chord at the hump of about 3.5 inches. The thickness varies from 1 inch at mid-chord at the root to 0.040 inches at mid-chord at the tip. The leading edge thickness varies from 0.180 inches at the root to 0.022 inches at the tip. The trailing edge thickness varies from 0.077 inches at the root to 0.016 inches at the tip. The blade has a twist of 33.2 degrees, a sweep angle of 60 degrees and was assumed to be made of titanium. This blade was never built because of predicted high deflections and stresses at operating speeds.

The NASTRAN finite element model is show in figure 2. This model consists of 423 grid points, 744 CTRIA2 elements and 2466 unrestrained degrees of freedom. The model was restrained along the bottom of the shank. The middle node was restrained in all six degrees of freedom and the other six nodes were restrained in five degrees of freedom with translation allowed in the direction of the spin axis.

RIGID FORMAT 1 (STATIC SOLUTION)

RIGID FORMAT 1 was used to investigate the turboprop geometric nonlinearities in four ways;

Case (1) (RF1-1) Updated Geometry/Angular Speed Difference- A centrifugal force field was applied to the model in increments of 1500 revolutions per minute. Nodal displacements and nodal forces (load vectors generated from the applied speed increment plus the summation of load vectors from previous steps) at each increment were stored in computer disc files. After each step grid locations were updated by adding the nodal displacements to the previous grid points and a new summation of force vectors was created by adding the applied load vectors to the previous summation of load vectors. The new set of grid locations defined the deformed model position for the next increment and the force vectors defined the load required to reach that position. the centrifugal force field applied at each step was equal to the square root of the difference of the new speed squared minus the last speed squared. The mathematical description for this case is summarized in section 1 of the Appendix. Seven NASTRAN runs were made from 1500 to 10500 RPM. Tip rotations and positions were used to identify the onset of instability, figure 3. For this case the large tip displacement between 4500 RPM and 6000 RPM (figure 3b) was clearly indicative of the onset of structural instability. The change in tip-chord angle for this case (figure 3a) was not as indicative of instability as the change in tip-chord position. The tip displacement also changes directions as the angular speed increases from 4500 RPM to 6000 RPM (figure 3b). The tip displacement becomes progressively larger as the angular speed is increased to 9000 RPM and then changes direction again at 10500 RPM indicating another region of instability. This method is straight forward and easy to apply using NASTRAN RIGID FORMAT 1. The predicted angular speeds causing instability are conservative (pessimistic) and, if accepted, will lead to design modifications to avoid the speeds causing instability.

Case (2) (RF1-2) Updated Geometry/Angular Speed - A Centrifugal force field was applied to the model in increments of 1500 RPM. Nodal displacements at each increment were stored in computer disc files. After each step grid locations were updated by adding the nodal displacements to the previous grid points. The new set of grid locations defined the deformed model position for the next increment. The total angular speed was applied to this updated position. The mathematical description of this case is summarized in section 2 of the Appendix. Seven NASTRAN runs were made from 1500 to 10500 RPM. Again, tip-chord rotations and positions were used to identify the onset of instability (figure 4). For this case the onset of instability can be noted from the large tip displacement and change in direction between 4500 RPM and 6000 RPM (figure 4b). Again, the change in tip-chord angle was not as indicative of instability as the change in position. The change in tip-chord position from 9000 RPM to 10500 RPM is more dramatic than in case (1). This method, also, is straight forward and very easy to apply using NASTRAN RIGID FORMAT 1. The predicted points of instability onset occur at lower rotor speeds than those using the method of case (1). Compared to the other two cases using RIGID FORMAT 1, this case has the following advantages; (a) provides the most pronounced prediction of instability, (b) requires only one computer disc file for storage of displacements, and (c) is straight forward and easiest to apply.

Case (3) (RF1-3) Updated Geometry/Angular Speed/Restraining Forces - A centrifugal force field was applied to the model in increments of 1500 RPM. Nodal displacements and nodal forces (load vectors generated by the applied rotational speed) at each increment were stored in computer disc files. After each step, grid locations were updated by adding the nodal displacements to the previous grid points. The new set of grid locations defined the deformed model position for the next increment. New force vectors were then created from the NASTRAN generated loads resulting from the current applied rotational speed. These force vectors were applied in the opposite sense at the next speed increment and represented blade internal restraining forces (relative equilibrium with the deformed shape). The full rotational speed was applied at the next increment. The mathematical description of this approach is summarized in section 3 of the Appendix. Seven NASTRAN runs were made from 1500 to 10500 RPM. Tip-chord rotations and positions were used to identify the onset of instability (figure 5). As for the previous two cases, the onset of instability is noted by the large tip displacement between 6000 RPM and 7500 RPM (figure 5b). The change in tip-chord angle was not as indicative of instability as the change in position. The point of instability is indicated by the change in tip-chord position from 6000 RPM to 7500 RPM, figure 5b. This approach does not subject the deformed turboprop to the full angular speed at the end of each increment. Therefore, the turboprop deforms the least compared to the previous two cases and, consequently, has the smallest effect on the predictions for the vibration frequencies. Predictions of blade frequencies will be discussed later.

Case (4) (RF1-4) Updated Geometry (Displacement Increment)/Angular Speed Difference - A centrifugal force field was applied to the model in increments of 1500 revolutions per minute. Nodal displacements and nodal forces (load vectors generated from the applied speed increment plus applied load vectors from previous step) at each increment were stored in disc files. After each step, grid locations were updated by adding the nodal displacement increments (current minus previous) to the previous grid points and new force vectors were created. The new set of grid locations defined the deformed model position for the next increment and the force vectors defined the load required to reach that position. The centrifugal force field applied at each step was equal to the square root of the difference of the new speed squared minus the last speed squared. The mathematical description for this case is summarized in section 4 of the Appendix. Seven NASTRAN runs were made from 1500 RPM to 10500 RPM. Tip rotation and displacements were used to identify the onset of instability, figure 6. For this case the jump in chord position from 9000 RPM to 10500 RPM (figure 3b) is clearly indicative of the onset of structural instability. The change in tip-chord angle for this case (figure 3a) is not at all indicative of instability. It shows possible angle-change leveling-off at higher rotor speeds. The tip-chord also changes direction as the angular speed increases from 3000 RPM to 4500 RPM (figure 3b). The accompanying tip displacements become progressively larger as the angular speed is increased to 9000 RPM and then changes direction again at 10500 RPM indicating another region of instability. This method is also straight forward and easy to apply using NASTRAN RIGID FORMAT 1. The predicted angular speeds causing instability are higher than case (1) or case (2) and about the same as case (3). This is the only case which predicts a possible leveling-off in tip-chord angle. However, intermediate points are needed to ascertain leveling-off in tip-chord angle with increasing rotor speed.

The nonlinear structural response predicted using RF1-4 is judged to be the most accurate of the various methods examined herein. The accuracy of the method relative to error estimates and relative to experimental data remains to be determined.

RIGID FORMAT 4 (RF4) (NONLINEAR SOLUTION)

As stated in the NASTRAN User's Guide, "RIGID FORMAT 4 is a second order approximation to nonlinear effects of large deflections which computes the differential stiffness matrix by an iterative technique and treats the new matrix as a load correction. The internal loads are thus not linearly related to the applied loads". (See NASTRAN User's Guide). The mathematical description for this case is summarized in section 5 of the Appendix.

For each step the load was divided into six increments and the differential stiffness matrix was iterated until the value of the ratio of energy error to total energy was less than 0.001.

The iterative solution for the differential stiffness matrix indicated divergence for speeds above 7500 RPM. For the four load cases, 3000 RPM, 4500 RPM, 6000 RPM and 7500 RPM, the number of iterations required to meet the convergence criteria was 2, 3, 4, and 7 respectively. The results are plotted in figure 7. The points of instability are easily identified in figure 7b where the tip-chord displacement changes direction from 4500 RPM to 6000 RPM. These results are analogous to those for case (1) with the exception that the tip-chord rotation increases less with angular speed up to 7500 RPM.

This method is automatically applied. Its shortcoming is that the new load increment remains fixed in magnitude and direction during deformation of the structure. However, judicious interpretation of the results can provide the instability information needed.

RIGID FORMAT 13 (RF 13)
(Normal Modes with Differential Stiffness)

RIGID FORMAT 13 is a one step differential stiffness solution in which the applied loads are assumed to move with their points of application and remain fixed in magnitude and direction. The differential stiffness matrix is computed from the internal element loads resulting from the static solution. RIGID FORMAT 13 combines the differential stiffness with the original stiffness matrix to solve the eigenvalue problem and obtain the normal modes solution. The mathematical description for this case is summarized in section 5 of the Appendix.

Results for tip-chord rotation and tip-chord position are shown in figure 8. Though a change in tip-chord displacement occurs between 2500 RPM and 5000 RPM, it is difficult to identify points of instability using this RIGID FORMAT. Note that the tip-chord displacement changes more slowly as the angular speed increases above 5000 RPM. Compared to the methods described previously, RIGID FORMAT 13 predicts (1) tip-chord rotation which is somewhat more severe than RF1-4 and (2) tip-chord position change which is less severe. It appears that RF13 will yeld reasonable solutions of the geometry nonlinearities including frequencies with the possible exception of impending structural instabilities.

COMPARISON OF RESULTS

The tip-chord rotation is an important design parameter. It affects the angle of attack which influences the efficiencies, as well as noise and aeroelastic characteristics of the propeller. Predicted tip-chord rotations obtained as described previously are compared with each other and with those predicted by three other methods in figure 9. These three other methods are; (1) ICP-independent contractor program Case 6, Appendix, (2) MSC/NASTRAN (McNEAL-Schwindler Company NASTRAN - new nonlinear geometry capability) obtained at Ames Research Center, private communication, and (3) MARC obtained at Lewis. It is noted that the MSC/NASTRAN and MARC predicted results were obtained using standard formats. These results are shown here for comparison purposes only and not to imply that this is the best that can be done using MSC/NASTRAN and/or MARC.

The tip-chord rotation curves predicted by RF1-3, RF4 and MARC are almost identical up to angular speeds of 7500 RPM. Those predicted by RF1-4, RF13 and MSC are about the same and somewhat higher. Those predicted by using the other methods, (RF1-1, RF1-2 and ICP) are respectively higher. The results of methods RF1-1 and RF1-2 follow almost identical paths for tip-rotation. However, the method of RF1-2 is much easier to apply. It should be noted that both tip-chord rotations and tip-chord positions are required to properly assess the propeller structural dynamic behavior in view of possible instabilities at higher speeds. In addition, changes in tip-chord rotation affect directly the angle of incidence and, consequently, the efficiency of the turboprop.

VIBRATION FREQUENCIES

The natural frequencies of the blade in the design speed range are important design parameters which affect stability and life prediction. The results of RIGID FORMAT 13 (Normal Modes with Differential Stiffness) applied to the initial grid positions and to the updated grid positions of RF1-2 is shown in figure 10. These curves indicate that the instability point near 9000 RPM and the resulting decrease in natural frequencies would be overlooked if position updating procedures are not applied to RIGID FORMAT 13 analyses. Also, the margins for interference with cyclic disturbances could be misinterpreted and, therefore, adversly influence the turboprop design.

Similar results comparing updated-position frequencies with path-independent frequencies are shown in figure 11. The path-independent frequencies decreases rapidly and at lower rotor speeds leading to overly pessimistic frequency predictions and, perhaps, to major design modifications.

CONCLUSIONS

COSMIC NASTRAN RIGID FORMAT 1 can be used, without recourse to DMAP alters, to predict the nonlinear structural response of swept twisted propellers. RIGID FORMAT 1 with geometry updating using total displacements at each step (RF1-1, 2) can be used to predict the onset of structural instabilities versus rotor speeds. These predictions are comparable to those predicted using methods which are independent of load path and over-estimate the nonlinear structural response. The path-independent method predicts frequencies which are overly pessimistic. RIGID FORMAT 1 with geometry updating using displacement increments (RF 1-4) can be used to predict the overall nonlinear structural response. This approach appears to be the most accurate. RF1-4 predicted results for tip-chord rotation are somewhat below those predicted using RF13 and those predicted by the McNeal-Schwindler Company NASTRAN. RIGID FORMAT 1 with geometry updating using total displacements and negative force (RF1-3) appears to predict nonlinear structural response comparable to those predicted by RIGID FORMAT 4 and MARC. Results predicted by RF1-3 are below those predicted by RF1-4 and under- estimate the nonlinear structural response.

APPENDIX

MATHEMATICAL DESCRIPTION

The equations describing the mathematics of the several approaches used to obtain nonlinear solutions are summarized in Sections 1 to 6 below. The equations are presented in matrix form. This is a concise description of the many degrees of freedom (DOF) that these equations represent. The notation of the variables used in the equations is as follows: $\{R\}$ denotes spatial position (geometry); $\{u\}$ denotes deformation from an $\{R\}$ spatial position; $[K]$ denotes stiffness matrix; $[M]$ denotes mass matrix; Ω denotes rotor speed; Δ denotes increment. The subscript "o" denotes initial position; the subscript F denotes final position; the subscript i denotes the current increment; the subscript j denotes a summation index with limits defined in the given equation. All the variables are referred to the global coordinate system (x, y, z). The equations are summarized in the sequence used. The notation is also summarized in section 7 for convenience.

1. RIGID FORMAT 1, Case (1) (RF1-1) Updated Geometry/Angular Speed Difference - The incremental equations at the ith step for this case are:

$$\{R_{i-1}\} = \{R_{i-2} + u_{i-1}\} \tag{1}$$

$$\Delta\Omega_i^2 = \Omega_i^2 - \Omega_{i-1}^2 \tag{2}$$

$$\left[K_{i-1}\right] = \left[K_{i-2}\left(R_{i-1}\right)\right] \tag{3}$$

$$\left[M_{i-1}\right] = \left[M_{i-2}\left(R_{i-1}\right)\right] \tag{4}$$

$$\{u_i\} = \left[K_{i-1}\right]^{-1}\left[M_{i-1}\right]\left\{\Delta\Omega_i^2\{R_{i-1}\} + \left\{\sum_{j=0}^{i-1}\Delta\Omega_j^2\{R_j\}\right\}\right\} \tag{5}$$

At $\Delta\Omega_i = \Delta\Omega_F$, $\{R_i\} = \{R_F\}$ (equations (5) and (1)) which is the final deformed spatial position. The total deformation for this case is given by

$$\{U_F\} = \{R_F\} - \{R_o\} \tag{6}$$

The nonlinear geometric effect accumulate progressively in equations (1) to (5) with successive rotor speed increments $\Delta\Omega_i$. Note that the geometry is updated by adding the displacement obtained from equation (5). This accentuates the nonlinear geometric effects and leads to more severe nonlinear response and, therefore, conservative nonlinear structural response.

2. RIGID FORMAT 1, Case (2) (RF1-2) Updated Geometry/Angular Speed - The incremental equations at the ith step for this case are:

$$\{R_{i-1}\} = \{R_{i-2}\} + \{u_{i-1}\} \tag{7}$$

$$[K_{i-1}] = [K_{i-2}(R_{i-1})] \tag{8}$$

$$[M_{i-1}] = [M_{i-2}(R_{i-1})] \tag{9}$$

$$\{u_i\} = \Omega_i^2 [K_{i-1}]^{-1} [M_{i-1}] \{R_{i-1}\} \tag{10}$$

The final deformed position $\{R_F\}$ is obtained from equations (10) and (7) at $\Omega_i = \Omega_F$. The total deformation is obtained from $\{R_F\} - \{R_0\}$. The nonlinear geometric effects accumulate faster for this case than for RIGID FORMAT 1, Case (1) as can be readily observed by comparing equations (5) and (10). RIGID FORMAT 1, Case (2) will predict more conservative nonlinear structural response than RIGID FORMAT 1 Case (1). However, RIGID FORMAT 1, Case (2) is much easier to implement and will indicate possible unstable spatial positions at lower rotor speeds.

3. RIGID FORMAT 1, Case (3) (RF1-3) Updated Geometry/Angular Speed/Restraining Forces - The incremental equations at the ith step for this case are:

$$\{R_{i-1}\} = \{R_{i-2}\} + \{u_{i-1}\} \tag{11}$$

$$\Omega_i^2 = (\Omega_{i-1} + \Delta\Omega)^2 \tag{12}$$

$$[K_{i-1}] = [K_{i-1}(R_{i-1})] \tag{13}$$

$$[M_{i-1}] = [M_{i-1}(R_{i-1})] \tag{14}$$

$$\{u_i\} = [K_{i-1}]^{-1} [M_{i-1}] \left\{\Omega_i^2 \{R_{i-1}\}\right\} - \Omega_{i-2}^2 [M_{i-2}] \{R_{i-2}\} \tag{15}$$

The final deformed position is obtained from equations (15) and (11) at $\Omega_i = \Omega_F$. The total deformation $\{U_F\} = \{R_F\} - \{R_0\}$. This case differs from the previous two cases in the way the current displacement $\{U_i\}$ is calculated in equation (15). The full centrifugal force field is not applied at the ith step. The first term in the braces in equation (15) is the increment of the rotor speed ($\Delta\Omega$) while the second, which is subtracted from the first, represents the cumulative centrifugal force (Ω_{i-1}). This approach will (1) under predict the geometric nonlinear effects on structural response, (2) predict higher rotational speeds for impending instabilities and, as a consequence, will be nonconservative. Implementation of this case is comparable to RF1-1.

4. RIGID FORMAT 1 Case (4) (RF1-4) Updated Geometry (Displacement Increment)/Angular Speed Difference. The governing equations at the ith

angular speed increment (using the notation defined previously) are given by:

$$\left\{R_{i-1}\right\} = \left\{R_0 + \sum_{j=1}^{i-1} \Delta u_j\right\} \tag{16}$$

$$\Delta \Omega_i^2 = \Omega_i^2 - \Omega_{i-1}^2 \tag{17}$$

$$\left[K_{i-1}\right] = \left[K_0\left(R_0 + \sum_{j=1}^{i-1} \Delta u_j\right)\right] \tag{18}$$

$$\left[M_{i-1}\right] = \left[M_0\left(R_0 + \sum_{j=1}^{i-1} \Delta u_j\right)\right] \tag{19}$$

$$\left\{\Delta u_i\right\} = \left[K_{i-1}\right]^{-1}\left[M_{i-1}\right]\left\{\Delta \Omega_i^2\left\{R_{i-1}\right\} + \left\{\sum_{j=0}^{i-1} \Delta \Omega_j^2 \left\{R\right\}_{R_{i-1}}\right\}\right\} \tag{20}$$

$$\left\{u_i\right\} = \left\{\sum_{j=1}^{i} \Delta u_j\right\} \tag{21}$$

AT $\Delta\Omega_i = \Delta\Omega_F$, $\{\Delta U_F\}$ is obtained from equation (20). Subsequently the total deformation is obtained from equation (21) and the final deformed spatial position is obtained from equation (16). Note in equations (16) to (20) that the nonlinear geometric effects enter the equations progressively with each successive rotor speed increment $\Delta\Omega_i$. Note, also, that the total centrifugal force field is used at each R_{i-1} position (equation (20)) as compared to RIGID FORMAT 1, Case (3) (equation (15)) where only the incremental centrifugal field is applied.

5. RIGID FORMATS 4 (RF4) and 13 (RF13) Standard NASTRAN FORMATS - The differential stiffness is used in the solution for both of these formats. Using the previous notation, the governing equation for the differential stiffness is (See the NASTRAN Theoretical Manual)

$$\left\{u_i\right\} = \left[K_0 + K_d(u_e)\right]^{-1}\left\{\Omega_F^2\left[M_0\right]\left\{R_0\right\} + \left[K_d(u_e - u_{i-1})\right]\left\{u_{i-1}\right\}\right\} \tag{22}$$

where $[K_d]$ is the differential stiffness matrix and $\{U_0\}$ is the initial incremental displacement used to form $[K_d]$. It can be seen in equation (16) that the stiffness matrix $[K] = [K_0 + K_d(U_0)]$ is formed using initial position variables and that Ω_F is applied to the initial position. As a result, the intermediate spatial positions and, therefore, the progressive nonlinear geometric effects are not represented in either $[K]$ or Ω. Consequently, both RIGID FORMAT 4 and RIGID FORMAT 13 will underpredict the nonlinear geometric effects on structural response. These formats will predict higher rotor speeds for impending structural instabilities. Solutions obtained by using either of these FORMATS will be more unconservative than those obtained by using RIGID FORMAT 1, Case (3).

6. Nonlineaer Geometric Solutions Independent of Load Path - The total deformation for his approach is given by

$$\left\{u_F\right\} = \left[\left[K_0\right] - \Omega_0^2\left[M_0\right]\right]^{-1}\left\{\Omega_F^2\left[M_0\right]\left\{R_0\right\}\right\} \tag{23}$$

Equation (23) will predict infinite $\{U_F\}$ if

$$\left[[K_0] - \Omega_0^2 [M_0]\right] = 0 \qquad (24)$$

Equation (24) has the form of an eigenvalue problem and, therefore, will cause equation (23) to predict infinite displacements when

$$\Omega_0^2 = \omega^2 \qquad (25)$$

or when the rotor speed (Ω) equals any of the natural frequencies (w) of the structure. Equation (17) will overpredict the nonlinear geometric effects on structural response as well as impending structural instabilities. Consequently, the results will be overly pessimistic.

7. Summary of the Notation used in this Appendix

$[K]$	global stiffness matrix
$[M]$	global mass matrix
$\{R\}$	spatial position (structure geometry) vector
$\{U\}$	global displacement vector
x,y,z	global coordinates
Δ	increment
Ω	rotor speed
ω	natural frequency

Subscripts

F	final
d	differential
i	increment (solution step) index
j	summation index
o	initial

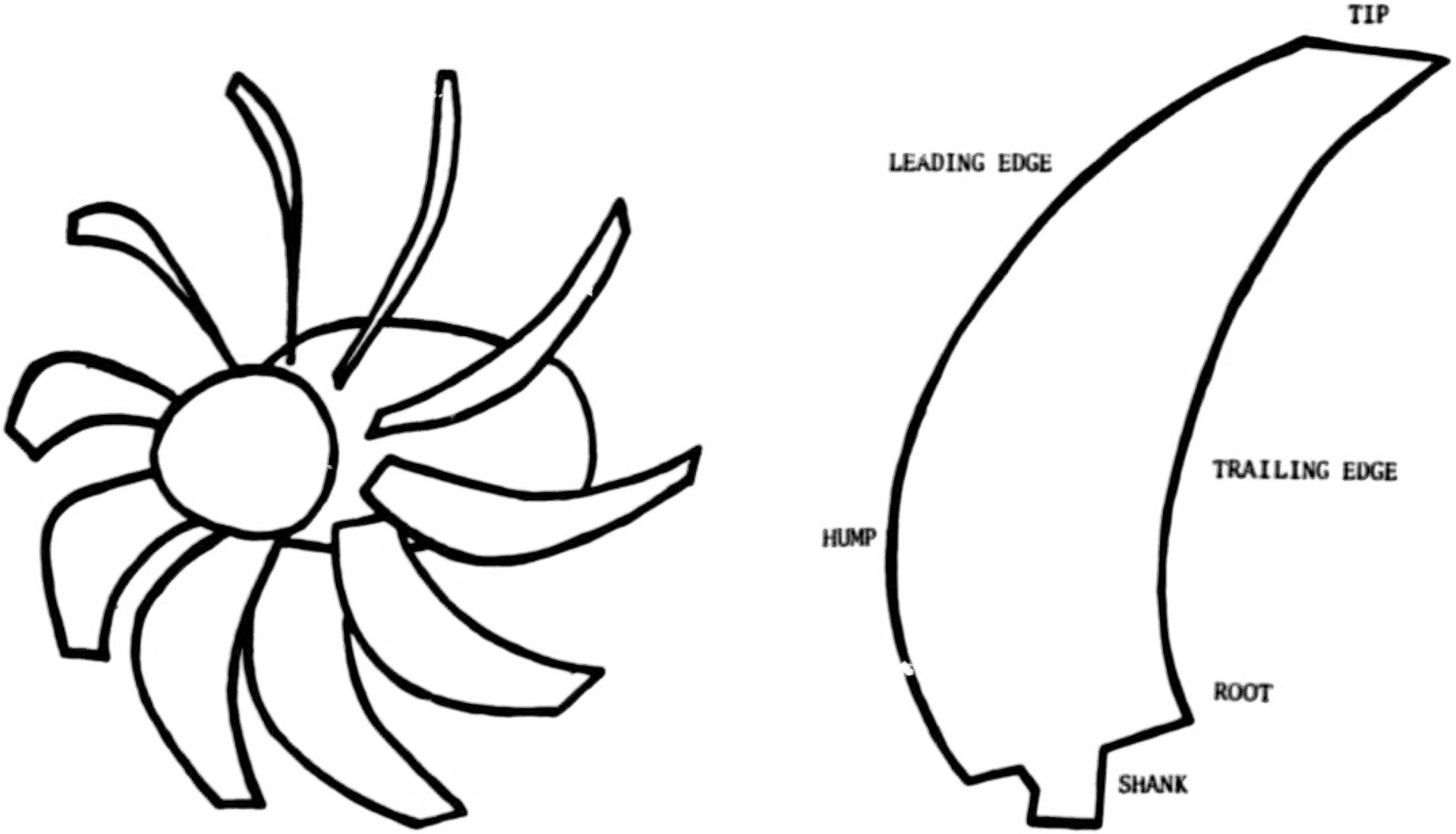

a. STAGE

b. PROPELLER

FIGURE 1 TURBOPROP STAGE AND PROPELLER

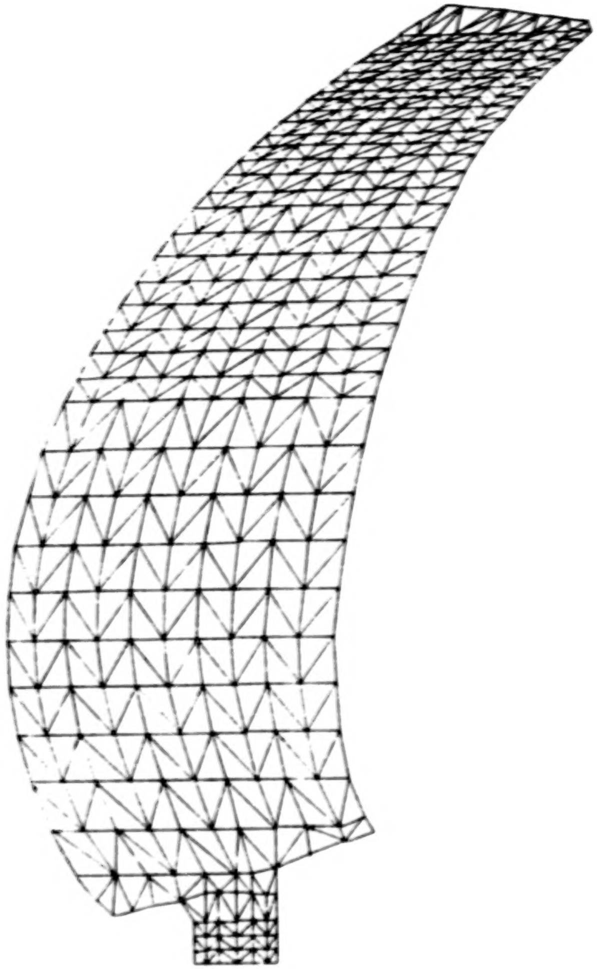

FIGURE 2 TURBOPROP PROPELLER FINITE ELEMENT MODEL
(423 GRID POINTS, 744 ELEMENTS)

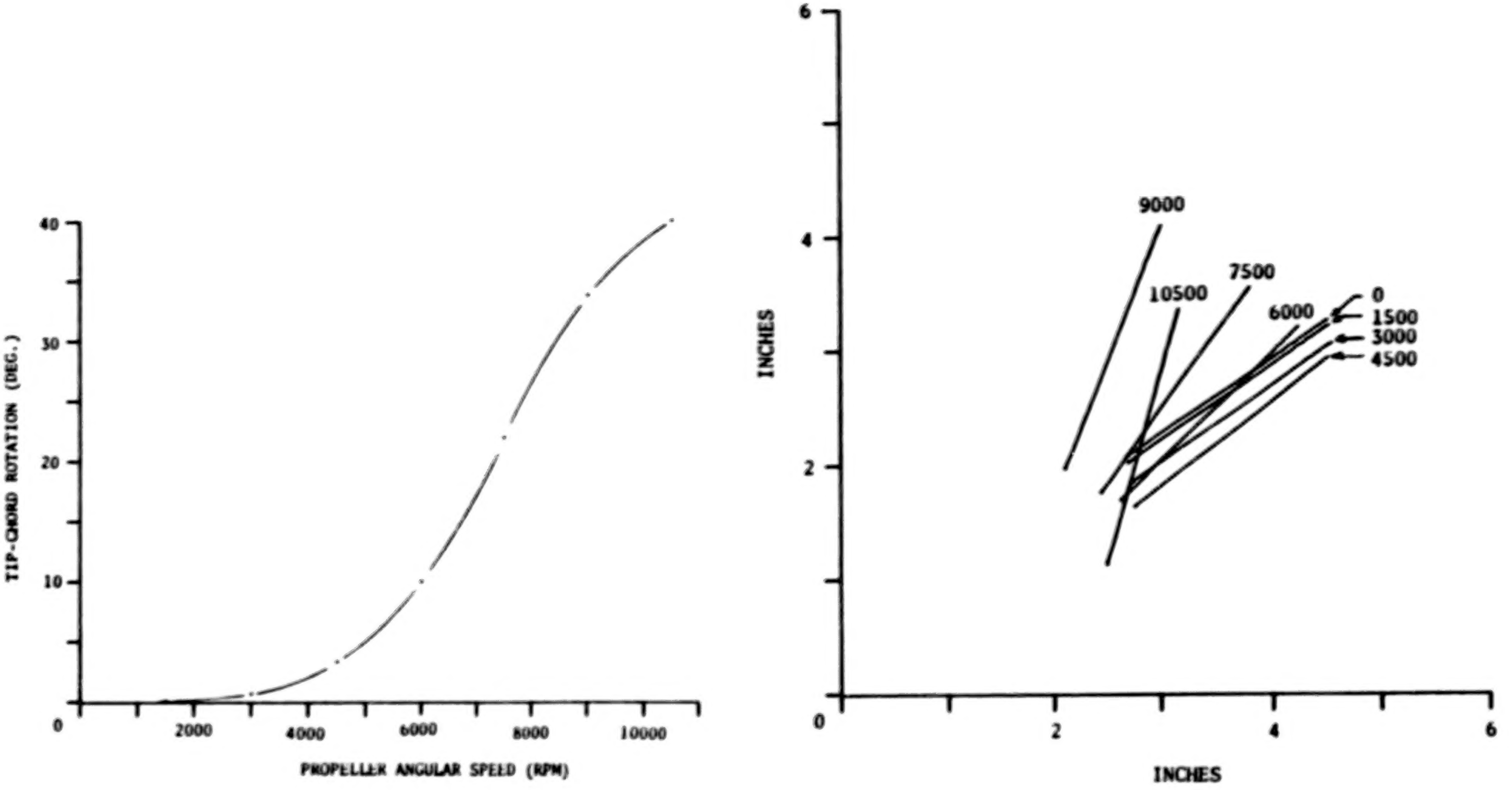

a. TIP-CHORD ROTATION

b. TIP-CHORD DISPLACEMENT

FIGURE 3 RIGID FORMAT 1, CASE (1) - UPDATED GEOMETRY AND FORCES/ANGULAR SPEED DIFFERENCE RESULTS

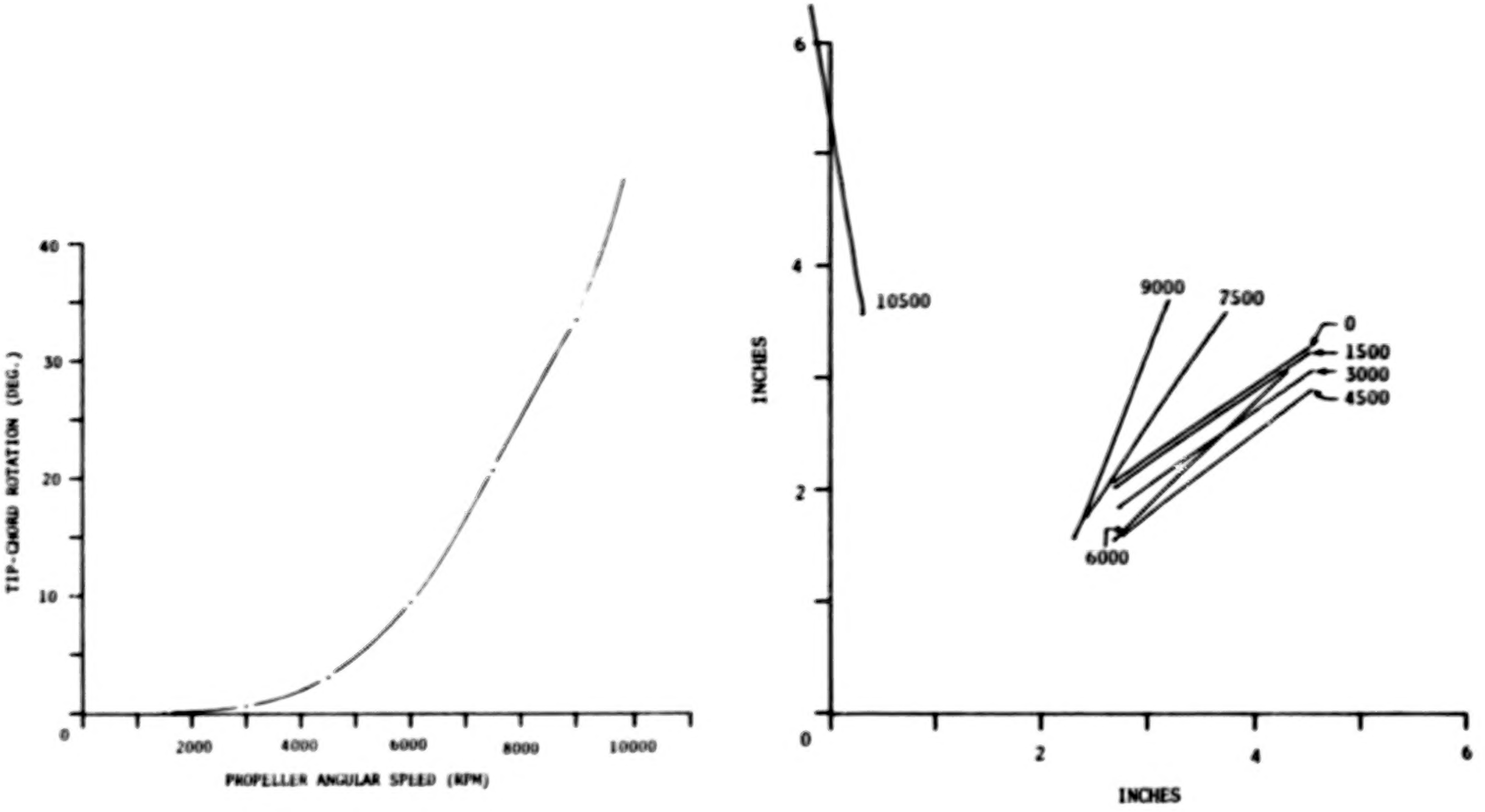

a. TIP-CHORD ROTATION

b. TIP-CHORD DISPLACEMFNT

FIGURE 4 RIGID FORMAT 1, CASE (2) - UPDATED GEOMETRY/ ANGULAR SPEED RESULTS

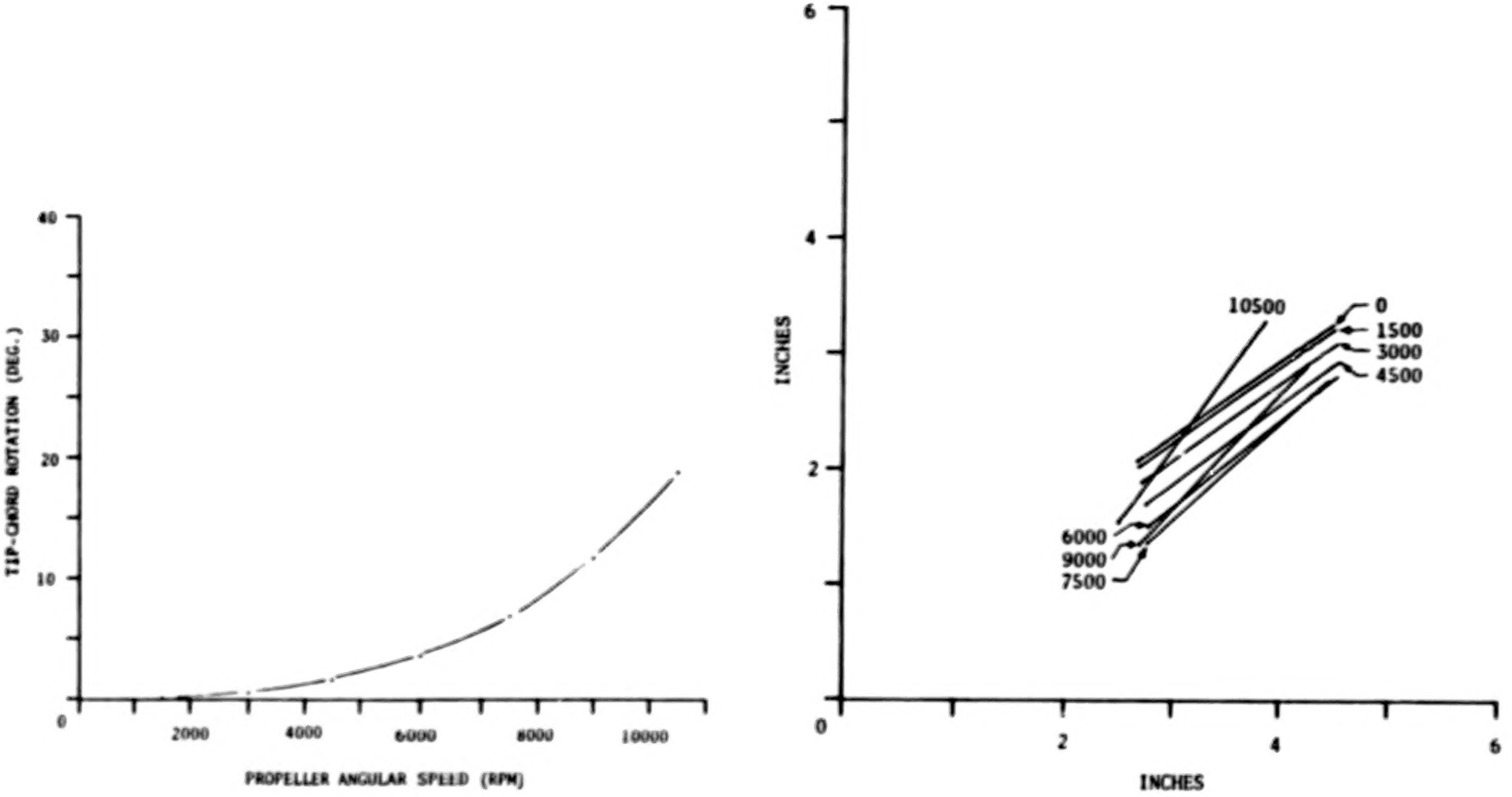

a. TIP-CHORD ROTATION

b. TIP-CHORD DISPLACEMENT

FIGURE 5 RIGID FORMAT 1, CASE (3) - UPDATED GEOMETRY/ANGULAR SPEED/RESTRAINING FORCE RESULTS

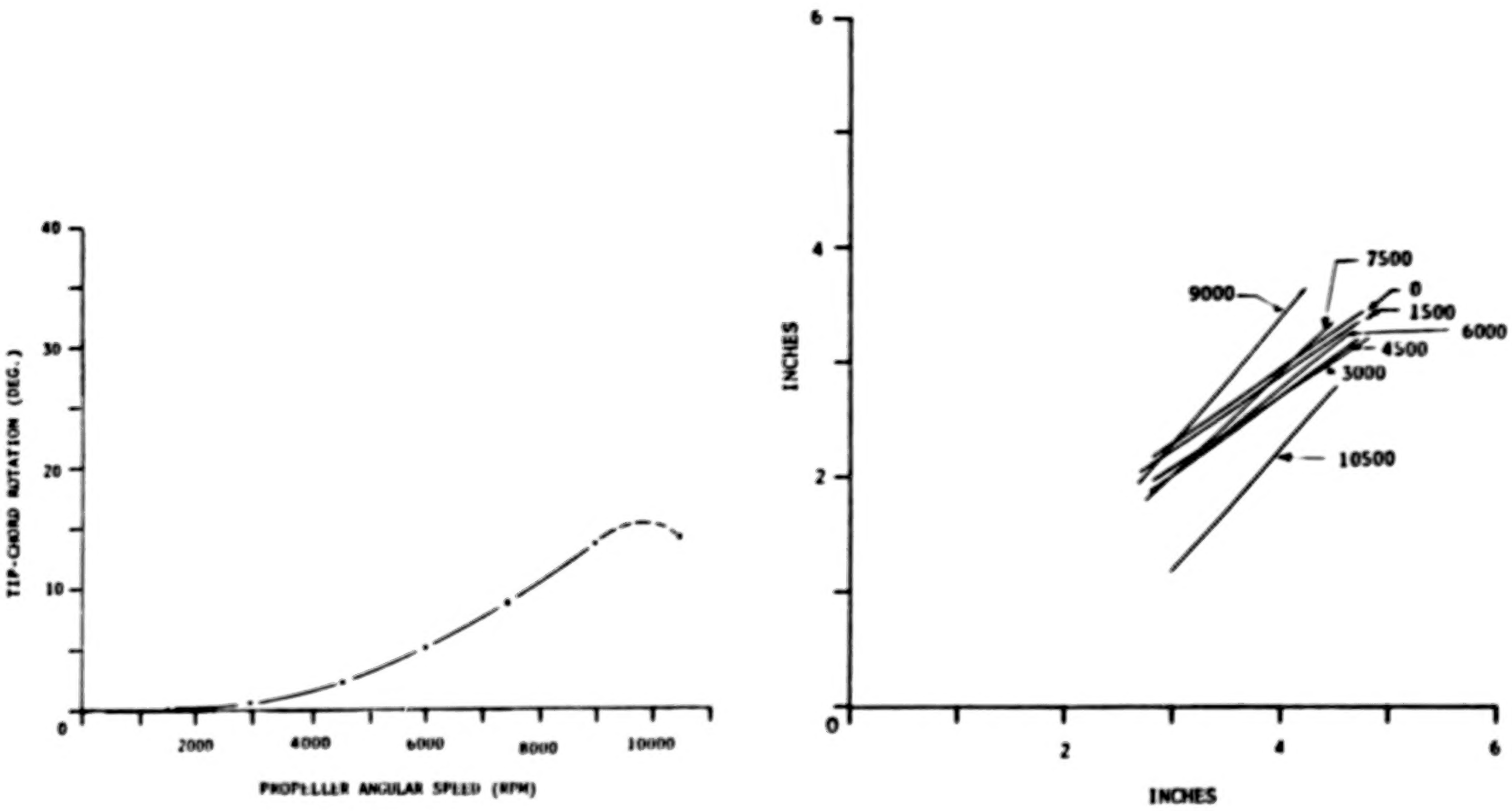

a. TIP-CHORD ROTATION

b. TIP-CHORD DISPLACEMENT

FIGURE 6 RIGID FORMAT 1, CASE (4) - UPDATED GEOMETRY DISPLACEMENT INCREMENT AND FORCES/ANGULAR SPEED DIFFERENCE RESULTS

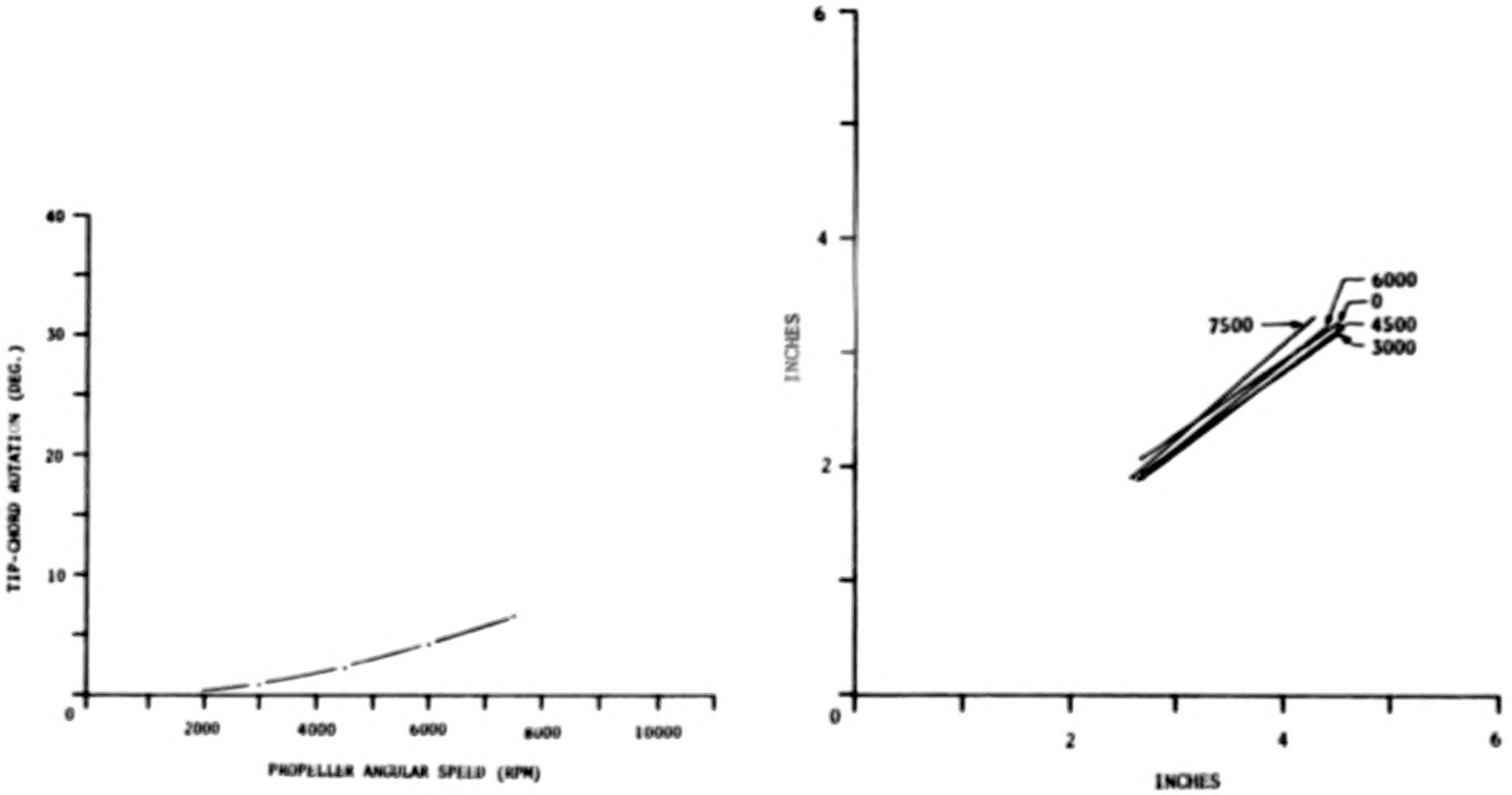

a. TIP-CHORD ROTATION

b. TIP-CHORD DISPLACEMENT

FIGURE 7 RIGID FORMAT 4 SOLUTION RESULTS

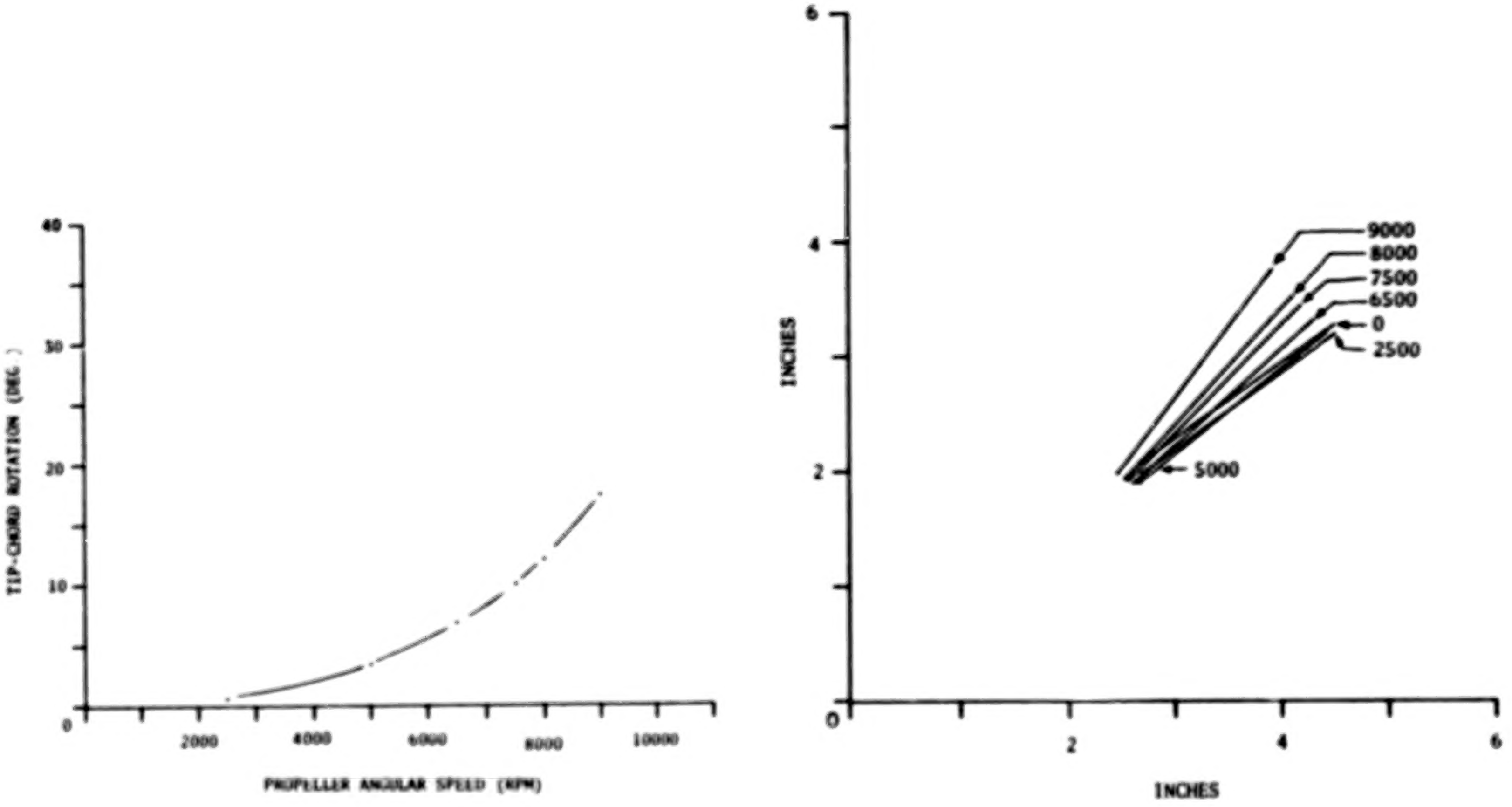

a. TIP-CHORD ROTATION

b. TIP-CHORD DISPLACEMENT

FIGURE 8 RIGID FORMAT 13 SOLUTION RESULTS

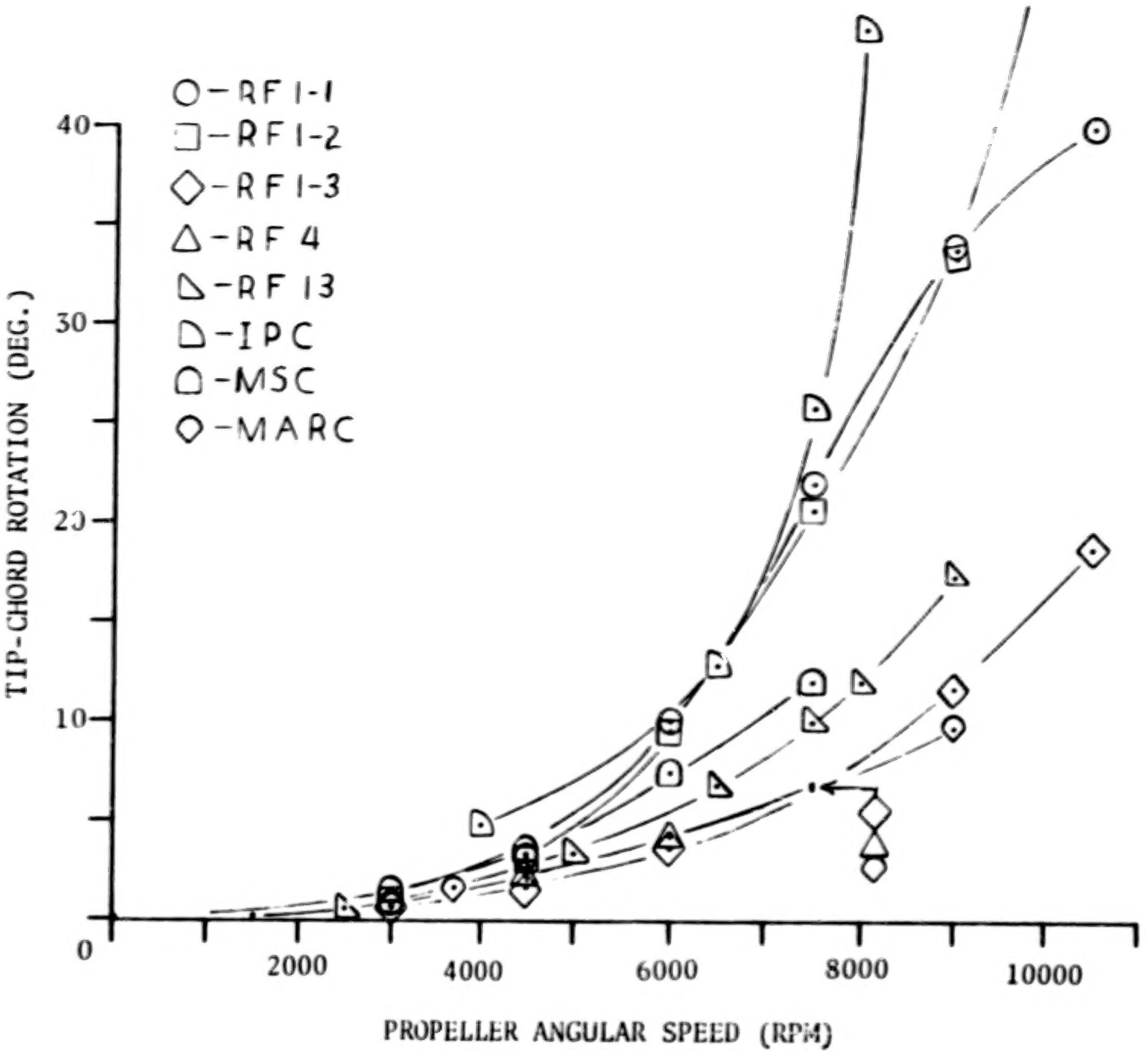

FIGURE 9 COMPARISONS OF PREDICTED TIP-CHORD ROTATION USING VARIOUS METHODS

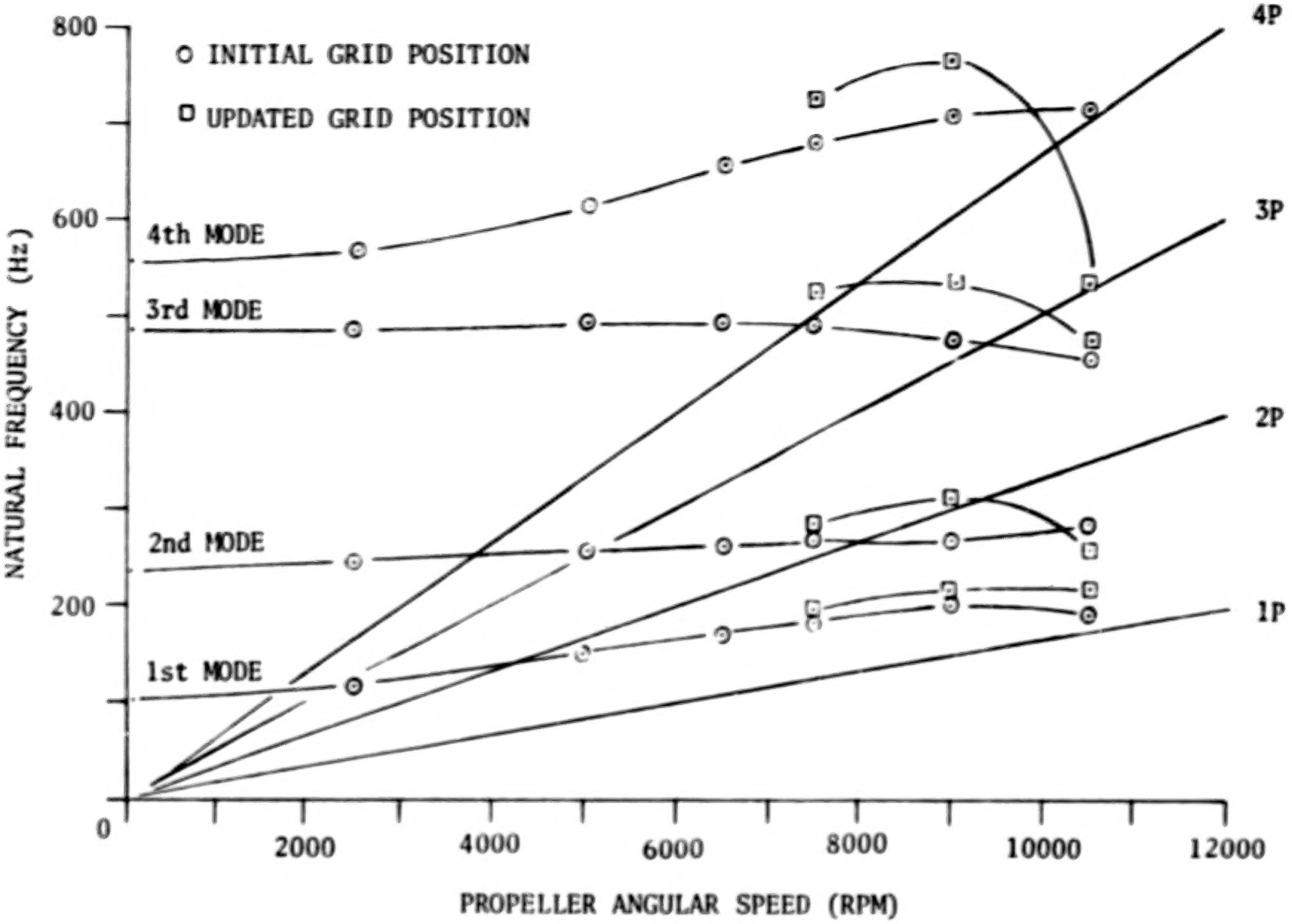

FIGURE 10 CAMPBELL DIAGRAM
COMPARISONS OF PREDICTED NATURAL FREQUENCIES

131

BEST DOCUMENT AVAILABLE

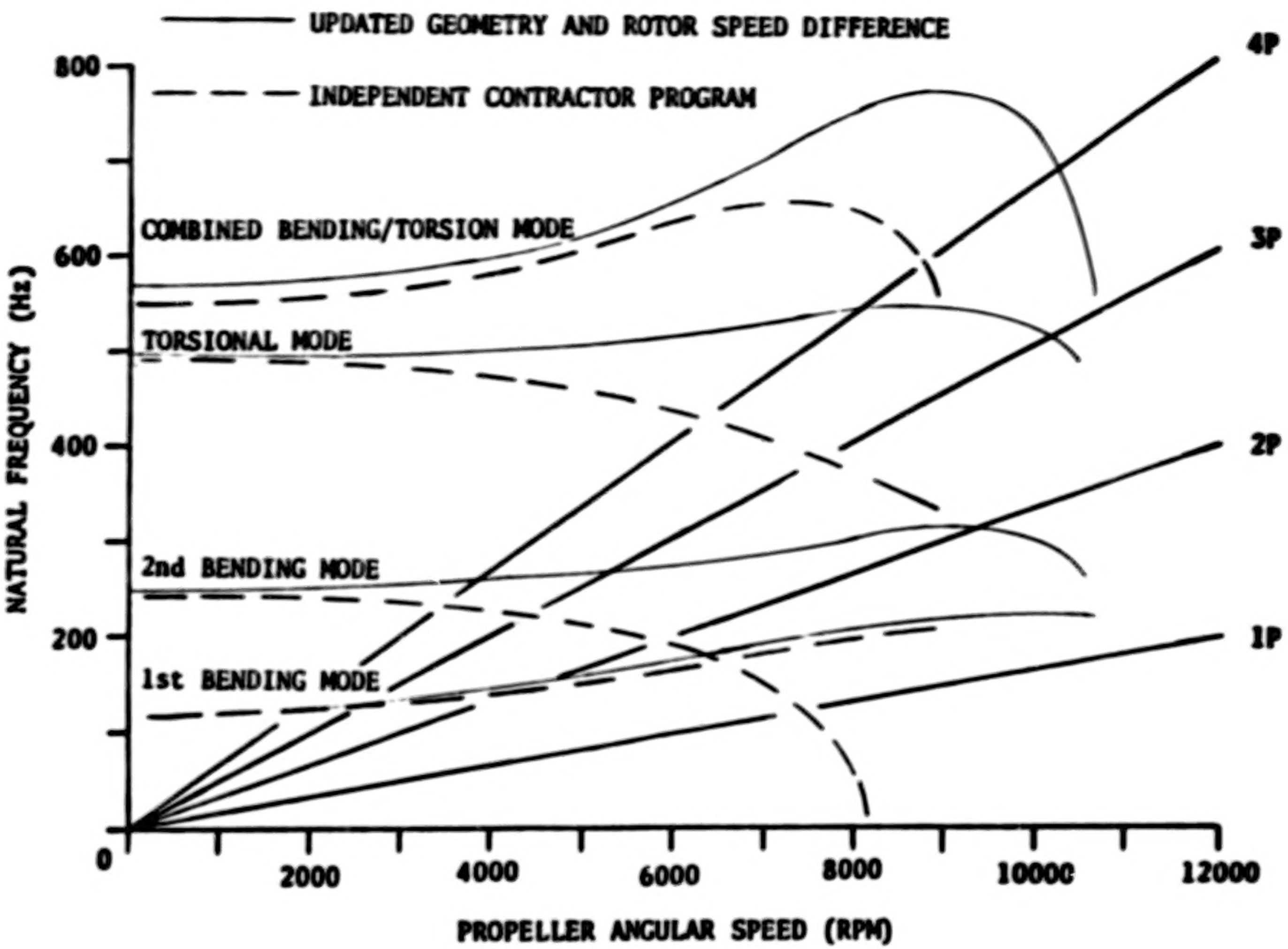

FIGURE 11 CAMPBELL DIAGRAM
COMPARISONS OF PREDICTED NATURAL FREQUENCIES

PREDICTION OF BEAD AREA CONTACT LOAD

AT THE TIRE-WHEEL INTERFACE USING NASTRAN*

C. H. S. Chen
The BFGoodrich Company

SUMMARY

An attempt has been made to theoretically predict the bead area contact load at the tire-wheel interface using NASTRAN. The application of the linear code to a basically nonlinear problem results in excessive deformation of the structure and the tire-wheel contact conditions become impossible to achieve. Therefore a "psuedo-nonlinear" approach was adopted in which the moduli of the cord reinforced composite are increased so that the computed key deformations matched that of the experiment. Some numerical results are presented and are discussed.

INTRODUCTION

Ever since the pneumatic tire was made to be mounted on a wheel, the problem of defining the loads on the wheel due to contact between the tire bead region and the wheel has existed. This information is very much needed in wheel design. Because of the extremely complex nature of the problem, it is not surprising that there is no published theoretical work dealing with this subject. With the introduction of the finite element method, an approximate numerical solution to this problem can now be obtained. Although NASTRAN is not the best program for this purpose, it was available and I explored the possibility of using it to determine the bead contact pressure at the tire-wheel interface. In modeling the tire, the axisymmetric solid of revolution element with triangular cross section (TRIAAX) was selected for two reasons.

1. The TRIAAX element takes either isotropic or orthotropic material. The modeling of a composite structure such as a tire can be made realistically.

2. The TRIAAX composite element can handle an axisymmetric structure undergoing nonaxisymmetric deformation under nonaxisymmetric loading by the technique of Fourier series expansion. Simulation of a loaded tire is thus possible.

The tire and wheel for a Boeing aircraft were used in the present study. In setting up the model, I assumed that the wheel is completely rigid and will not undergo deformation. This simplified assumption eliminated the need for simultaneously analyzing the tire and wheel. Thus, I dealt with a tire sitting on a rigid support which has a well defined profile. This approach was adopted

---

* The author wishes to acknowledge The BFGoodrich Company for the permission to publish this paper.

partly because the wheel, which is not an axisymmetric structure, is best modeled by the three dimensional solid element. But the solid element can not be connected to the axisymmetric ring element. Also, if the deformation of the wheel were small, then the error due to the rigid support assumption should be negligible.

ANALYSES

Tire Modeling

Figures 1 and 2 show the finite element model of the tire. In this model the sidewall rubber and the majority of the inner liner rubber were neglected for simplicity. It should be noted that a rather crude tire model was used as the stress analysis of the tire was not my objective. The tire was divided into a number of regions according to the material type and carcass ply construction. These regions were:

rubber region	: mostly in the tread area, assumed to be isotropic
finishing strip	: along the tire wheel contact, assumed to be isotropic
carcass	: various laminate constructions of Nylon cord reinforced fabric, assumed to be orthotropic
beads	: assumed to be orthotropic/transversely isotropic

Data from the tire specification were used to calculate the cured carcass angles which were used in calculating the elastic properties of the unidirectional composite. The composite properties were calculated by use of Halpin-Tsai equation (ref. 1). The transformation rule (ref.1) was then applied to obtain the bias ply properties.

Loadings

An inflation pressure of 1.10×10^6 Pa (160 psi) was always applied along the inner carcass line. The tire under a vertical load of 22224.9 kg (49000 lb.) was simulated by applying a uniform contact pressure of 1.17×10^6 Pa (170 psi.) to the following regions (refer to Figure 1) which are determined from tire foot print diagram.

From ring	to ring			
1	2	-24.6	θ(degree)	24.6
2	5	-24.72		24.72
5	7	-24.39		24.39
7	9	-23.71		23.71
9	11	-21.96		21.96
11	13	-18.7		18.7
13	15	-8.48		8.48

Bead Fit

The tire diameter is customarily made slightly smaller than the rim diameter so that when the tire is mounted on the wheel the interference fit will prevent air leaks. In the present study the interference fit was simulated by subjecting the bead to a temperature drop of 12.78°C (55°F) which produced about a 12% compression of the material between the bead and the rim.

Nodal Contact Force

Since NASTRAN does not give the SPC as well as MPC forces for TRIAAX element under nonaxisymmetric loading, a post-processing subroutine was written to compute the nodal contact forces at the tire-wheel boundary. Using DMAP alter, the Fourier coefficients of the nodal forces for each element along the boundary are extracted. This was done only for those nodes on the boundary. The subroutine then summed up these coefficients over all the elements which share the common node. Finally the Fourier expansion using those added coefficients gives the nodal contact force at any location along the circumference.

Boundary Condition and Solution Criteria

In Figure 2, the tire-rim contact boundary starts at nodal point 129 and ends at nodal point 142. Fixed point or free boundary condition can be assumed for any of the points from 129 to 142. Sliding boundary condition can be assumed for those points lying on "flat" surfaces. A sliding boundary implies that movement of the point is allowed but the point must stay on the defined surface. This can be achieved by using MPC if the slope of the surface is known. The criteria for an acceptable solution were:

1. Compressive or negligible tensile contact forces at points where the tire remains in contact with the wheel surface.

2. No reaction forces at all points which lift off the contact surface.

3. No boundary point can "sink" below the contact surface and into the wheel.

Since NASTRAN has no contact problem capability, a trial and error process of adjusting boundary conditions at contacting nodal points might be necessary in meeting these requirements.

Difficulty in Linear Analysis

For the element I used, only a linear solution is available from NASTRAN. Therefore, when the loadings were applied, they produced excessive tire deformations. The growth in the crown diameter of the inflated but unloaded tire and the deflection of the inflated and loaded tire were much larger than in tire experiments. This excessive deformation exerted unrealistic requirements on the boundary points. In the case of the loaded tire, the excessive deformations made satisfaction of the solution criteria practically impossible. In order to resolve this problem, an increased moduli approach was adopted.

Increased Moduli Approach

The increased moduli approach may be justified by the following argument. The inflation pressure in a tire produces a pre-stressed condition and that stresses due to mambrane action may cause a considerable decrease of displacements as the structure undergoes geometrically nonlinear behavior. Therefore, since the majority of the load is taken up by the cords in a cord/rubber composite, it seemed logical to increase the moduli of carcass plies. To force the NASTRAN linear solutions at the crown point to fit the experimental data, the following multiplication factors had to be applied to the carcass moduli:

	Multiplication Factor
Inflation only	10
Inflation and loaded	3

NUMERICAL RESULTS

NASTRAN solution using increased moduli were obtained for the following four boundary conditions. In all the four cases the "acceptance" criteria were met. Referring to Figure 2, the four cases were:

Case 1. All nodal points from 129 to 142 were fixed in the r and z directions.

Case 2. Nodal points 129 to 133 were fixed in the r, z directions. Points 134 to 142 were allowed to slide.

Case 3. Nodal points 129 and 132 to 142 were fixed in the r, z directions. Point 130 and 131 were allowed to slide.

Case 4. Nodal points 129, 132 and 133 were fixed in the r and z directions. Points 130, 131 and 134 to 142 were allowed to slide.

In the above, r and z are the radial and axial coordinates repectively.

Only a very limited number of results will be presented. Figure 3 shows the radial and axial contact force profiles under a 1.10×10^6 Pa (160 psi.) inflation pressure for case 1. The contact pressure loading profile was axisymmetric for this loading case. The obtained contact forces are in the unit of force per linear length in the circumference. In general, all four cases **show** substantially similar load variation. Points 130 and 131 are exceptions when they are allowed to slide on a frictionless surface. The results also shoe that the radial load has the highest peak under the inner bead and the lowest peak under the center bead. The axial load is highest at the tip of the flange (point 129). At point 129 the radial load was also appreciably high (about one half that of axial load). Figure 4 shows the nonaxisymmetrical load distribution when the tire is inflated and loaded. Both case 1 and case 2 are shown for node 136 which is under the center bead. For case 1, Figure 5 shows the load distribution in the bead region at the center of the contact patch when the tire is inflated to 1.10×10^6 Pa (160 psi.) and loaded to 22225 kg (49000 lb.). The radial loads under the beads at the center of the contact zone were highest for the center bead and lowest for the inner bead. However, as we move away from the center of the contact zone, the difference between the peaks becomes smaller. Both radial and axial loads at the flange tip (point 129) are of a high magnitude as has been observed in the inflation case. These results are purely theoretical and have to be checked by experiment. The soundness of the increased moduli approach has not been verified.

REFERENCE

1. Jones,r.m., Mechanics of Composite Materials, McGraw-Hill Book Co., 1975.

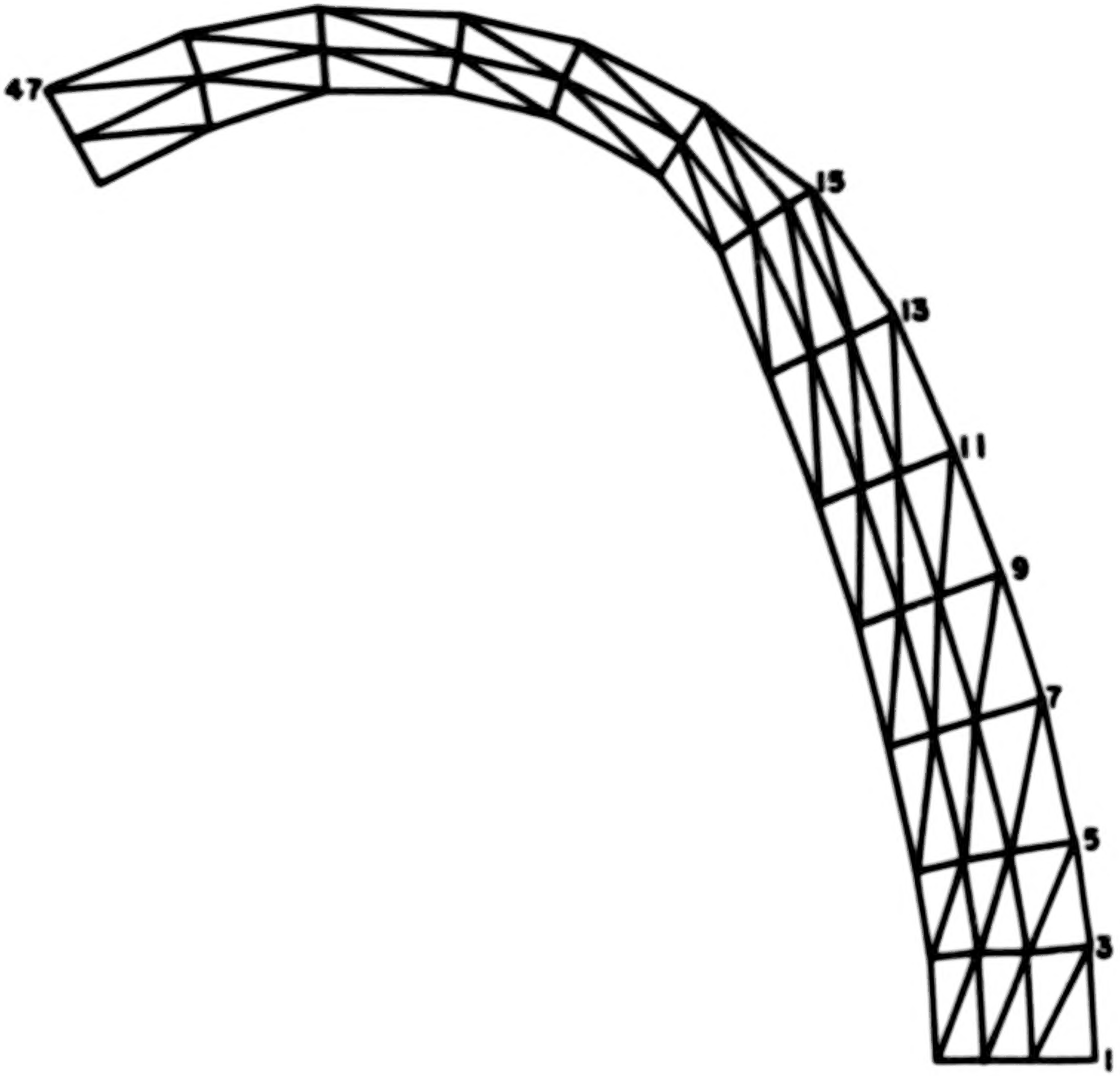

FIGURE 1. TIRE MODEL (PARTIAL)

BLANK PAGE

BLANK PAGE

BLANK PAGE

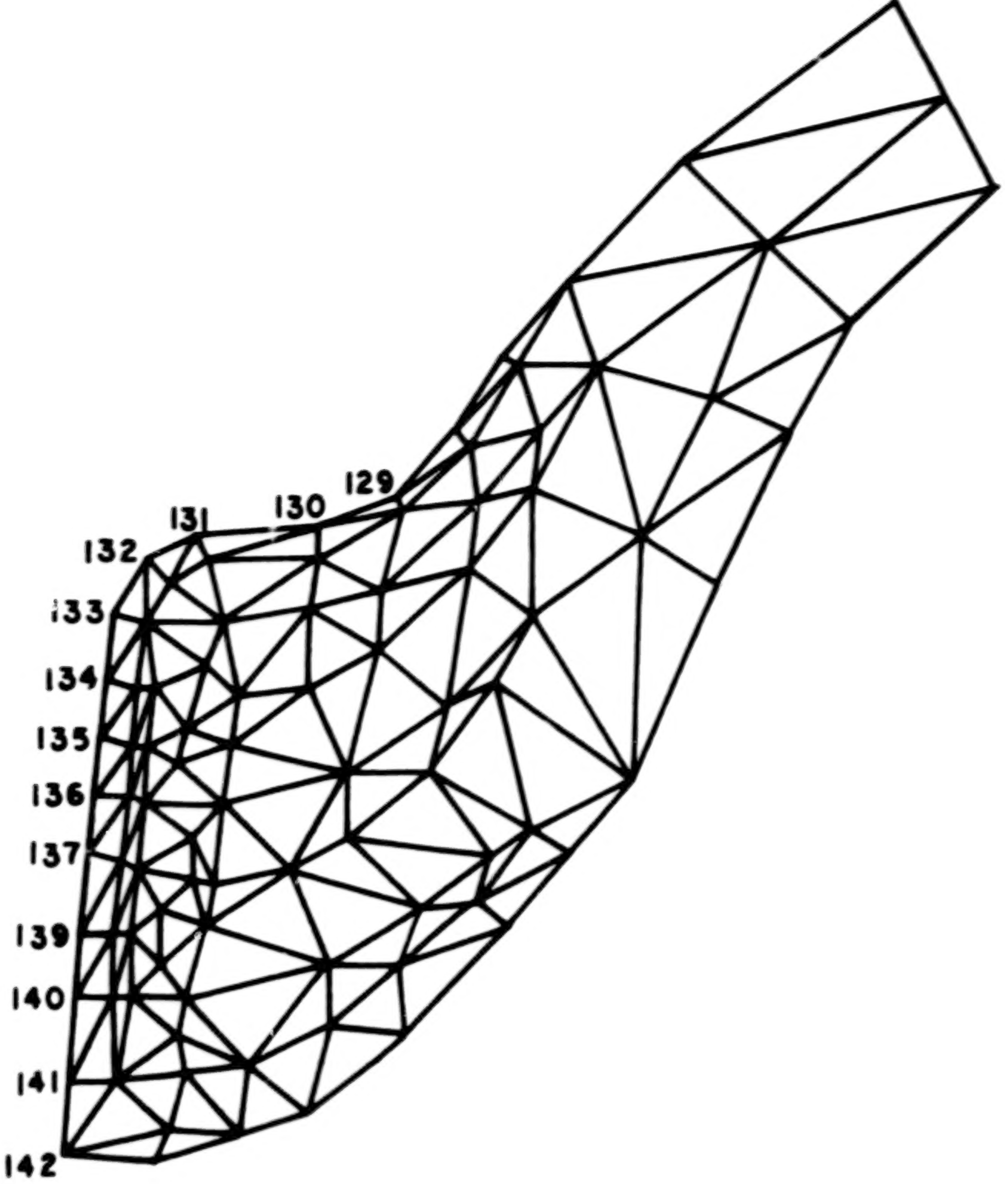

FIGURE 2. TIRE MODEL (PARTIAL)

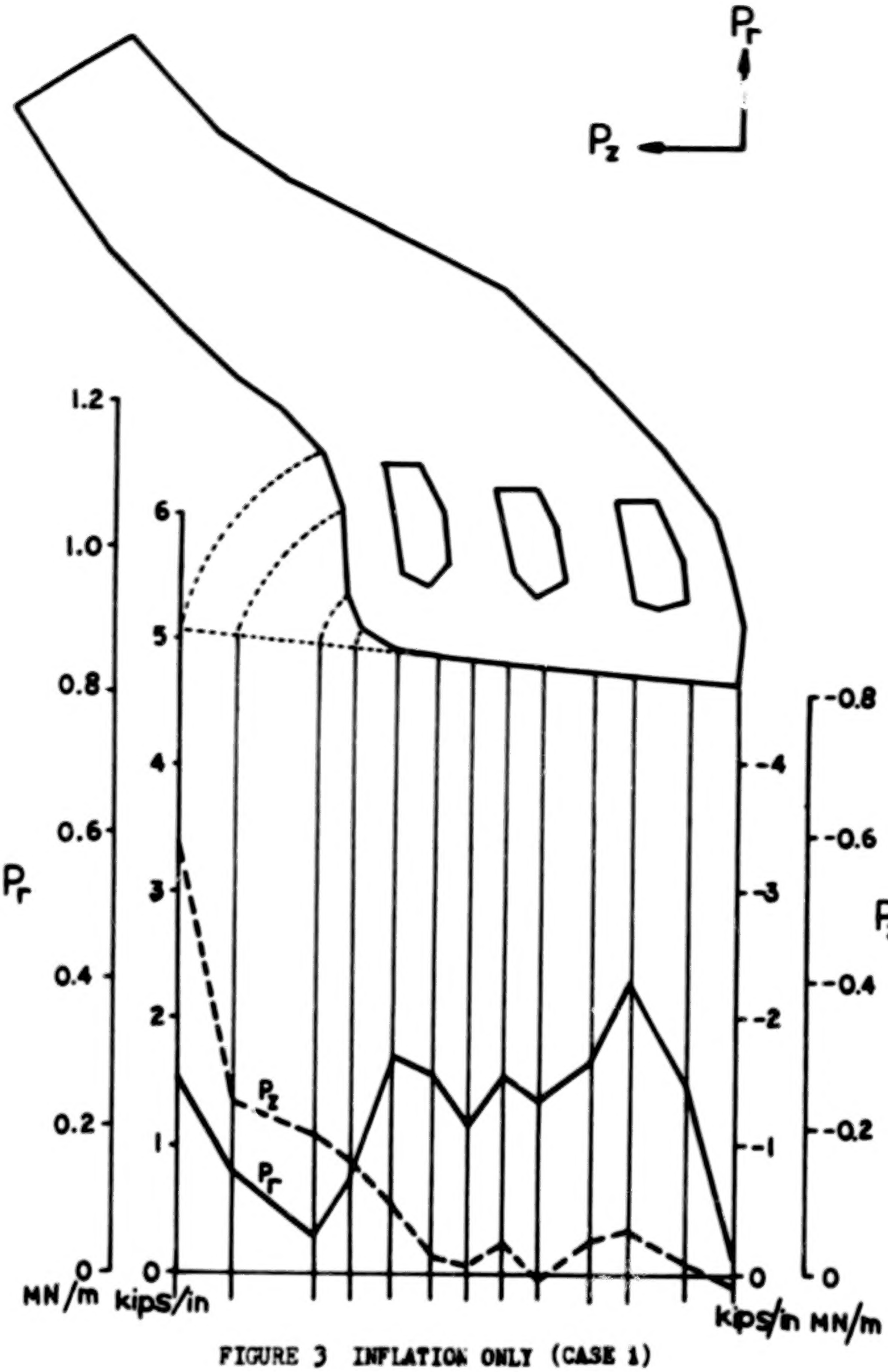

FIGURE 3 INFLATION ONLY (CASE 1)

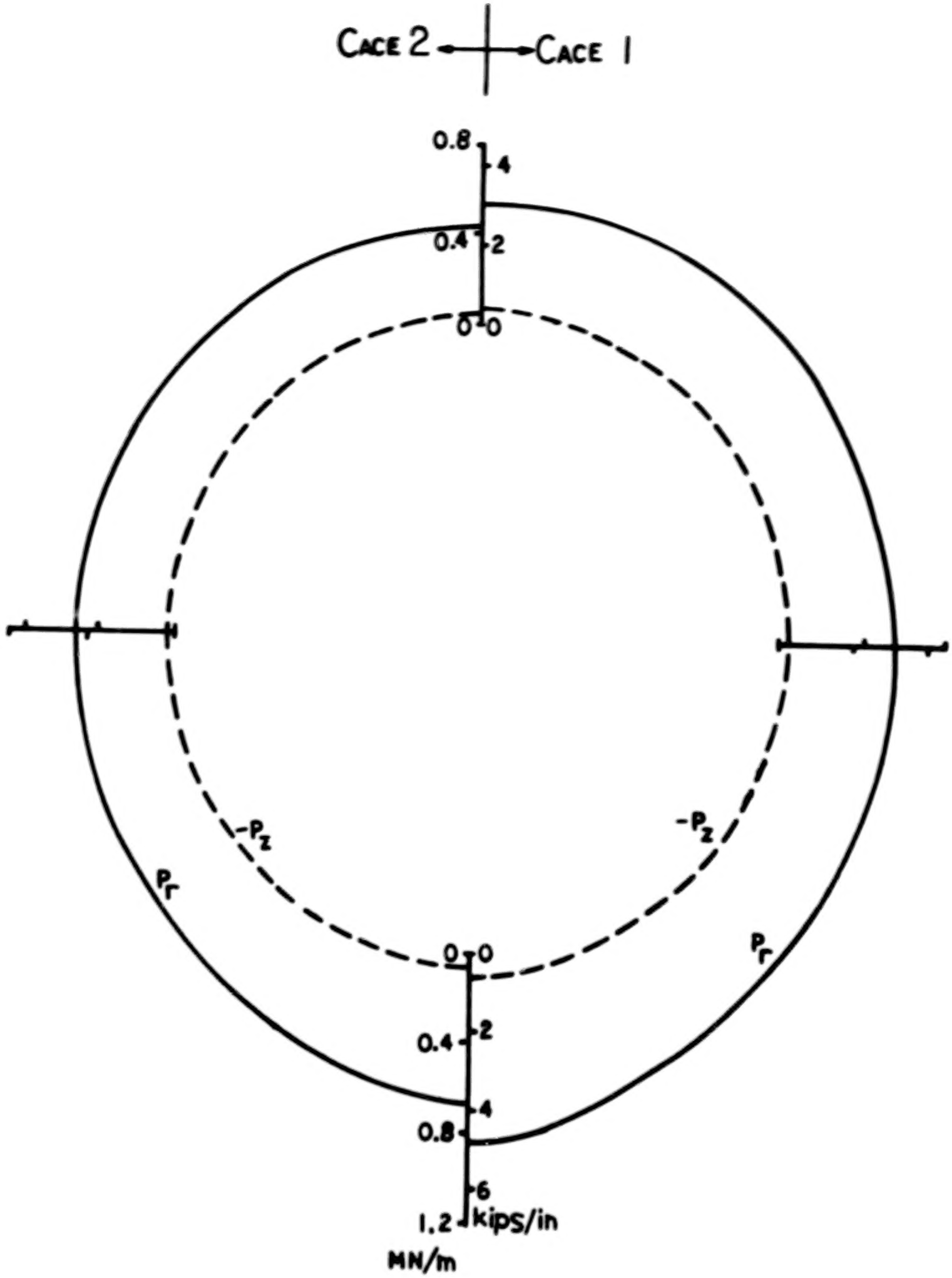

FIGURE 4 INFLATION AND LOADED (NODAL POINT 136)

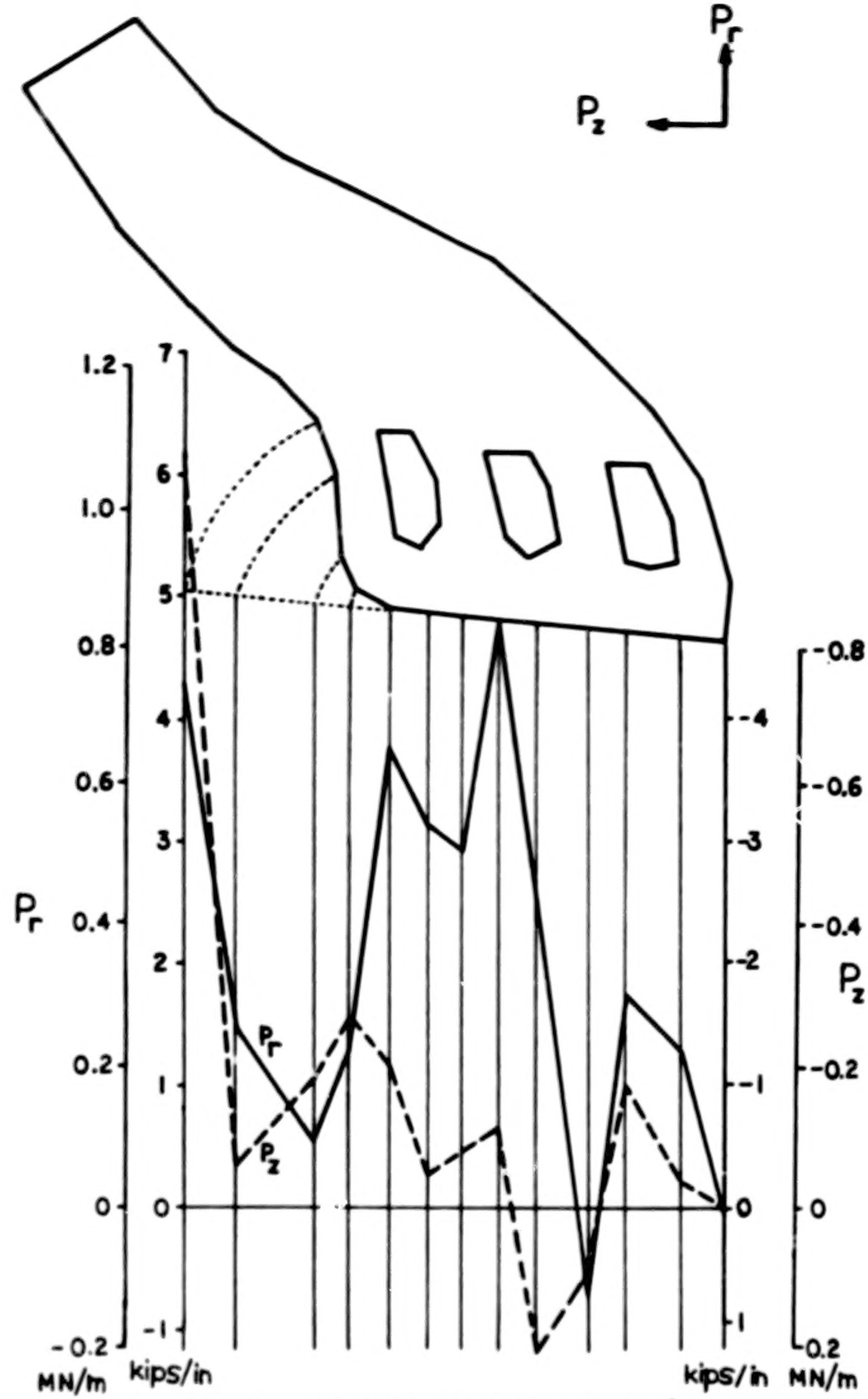

FIGURE 5 INFLATION AND LOADED (CASE 1)

ON ELASTIC-PLASTIC ANALYSIS OF AN OVERLOADED BREECH RING USING NASTRAN

P. C. T. Chen
U.S. Army Armament Research and Development Command
Large Caliber Weapon Systems Laboratory
Benet Weapons Laboratory
Watervliet, NY 12189

SUMMARY

The piece-wise linear analysis option of the NASTRAN code was used to analyze a photoplastic model for sliding breech mechanism. A two-dimensional finite element representation for the breech ring was chosen and the material was made of polycarbonate resin. The aluminum block was regarded as rigid and the width of contact was assumed to remain unchanged during loading. The displacements and stresses in the breech ring were obtained for loading in the elastic as well as plastic range. The maximum tensile stresses before and after complete unloading were obtained and compared with numerical and experimental results.

INTRODUCTION

In guns with a sliding breech mechanism, breech ring failures have been observed originating from the lower fillet in the vicinity of the contact region. The observations indicate that high tensile stress produced by stress concentration at the fillet was responsible for the failure. In order to reduce the chance of failure and extend the fatigue life, an exploratory study was initiated on the autofrettage of a breech mechanism. The technique is based on the production of beneficial residual stresses through coldworking to counteract the high operating stresses induced by firing.

A photoplastic model made of aluminum block and polycarbonate ring was designed (ref. 1). The maximum fillet stresses for an elastic load, as well as an elastoplastic load, were determined experimentally. Residual stress resulting from removing maximum test load was calculated. Two numerical investigations of the photoplastic model were made by using NASTRAN (ref. 2) and a different finite element program (ref. 3). The latter numerical results are in good agreement with the experimental data in the elastic as well as plastic range of loading (ref. 4).

This paper describes the NASTRAN analysis of a photoplastic model and gives an assessment of the NASTRAN code. The NASTRAN results for the maximum tensile stress are determined as a function of loading beyond the elastic limit. The loading range in which the NASTRAN program can be applied has been determined. Beyond this range, the values for the maximum tensile stress and the residual stress are estimated and compared with other numerical (ref. 3) and experimental (ref. 1) results at the maximum load level.

MODEL AND LOADING

A two-dimensional photoplastic model of aluminum block and polycarbonate ring was designed (ref. 1). The breech ring made of 0.12 inch thick LEXAN plate and the top of the ring was fixed. This material has a Poisson's ratio of 0.38 in the elastic state and a limiting value of 0.5 in the plastic state. The stress-strain (σ-ε) curve for LEXAN can also be described by the modified Ramberg-Osgood equation in the following form

$$E\varepsilon/\sigma_B = \sigma/\sigma_B + (3/7)(\sigma/\sigma_B)^n \quad \text{for} \quad \sigma_A < \sigma < \sigma_C \qquad (1)$$

and the values of five parameters are $E = 325$ Ksi, $n = 11.5$, $\sigma_A = 6.2$ Ksi, $\sigma_B = 8.7$ Ksi, $\sigma_C = 9.576$ Ksi, where E is Young's modulus, n is a parameter, σ_A is the proportional limit, σ_B is the secant yield strength having a slope equal to 0.7 E and σ_C is the flow stress at which the slope of the stress-strain is zero.

Figure 1 shows a finite element representation for one half of the breech ring. The other half is not needed because of symmetry. There are 224 grids and 189 quadrilateral elements in this model. The grids 1 through 8 are constrained in x-direction only while grids 233 through 240 are held fixed. The top portion of the breech ring is omitted because this is believed to have little effect on the maximum stress information near the lower fillet. In fact this belief has been confirmed by obtaining the elastic solution for another finite element model with additional 70 quadrilateral elements in the top portion. The differences between these two models for the maximum tensile and compressive stresses are 1.3%, 3.3%, respectively. The aluminum block is regarded as rigid and the load is transmitted to the ring through contact. Initially the block is in full contact with the ring. As load increases, a gap develops in the central portion. The width of the central gap under the full test load of 572 pounds is observed experimentally to be about five inches. NASTRAN program in its present form cannot be used to determine the width of contact and the force distribution as functions of loading. In this numerical investigation, several contact conditions are chosen and assumed to remain unchanged during loading.

ELASTIC SOLUTION

Since the width of contact and the force of distribution are not to be determined as functions of loadings, eight contact conditions under different prescribed displacements or forces are tried. The displacements and stresses in the elastic range for all cases are obtained. Three cases are under uniform prescribed displacements; case 1 at nodes (33,41,49,57), case 2 at nodes (49,57,65), and case 3 at nodes (57,65,81). Five cases are under prescribed forces; case 4 (20,50,30 lbs.) at nodes (49,57,65), case 5 (63.13, 36.87 lbs.) at nodes (57,65), case 6 (100 lbs) at node 65, case 7 (50,50 lbs.) at nodes (65,81), case 8 (12.5, 25,25,25,12.5 lbs.) at nodes (57,65,81,89,97). It is interesting to find out that the location of the maximum tensile stress is in element 155 for all cases and agrees very well with the experimental observation. The constraint forces for the three cases under prescribed displacements are calculated. If the total contact force F is 100 pounds, the magnitudes of the maximum tensile stress for 8 cases are 1801, 1847, 1869, 1842, 1840, 1853, 1873, 1916 psi, respectively. It should be noted that the stresses in the NASTRAN program are calculated at the centroid of each element but only one principal stress at the force boundary can be measured. The experimental result for the maximum tensile stress at the fillet 2222 psi per 100 pounds of load in the elastic range. For the purpose of comparison, the boundary stress is determined by extrapolation using the calculated results for those elements along the radial direction through element 155. This is shown in Figure 2 for case 4. It seems that the numerical result agrees very well with the experimental data in the elastic range of loading.

The stress outputs of the NASTRAN program are σ_x, σ_y, τ_{xy}, β, σ_1, σ_2, τ_m at the centroid of each element where σ_x, σ_y, τ_{xy} are the stresses in element coordinate system (x,y); β is the principal stress angle; σ_1 and σ_2 are the major and minor principal stresses; and τ_m is the maximum shear. Since our stress results are stored on tape, we can retrieve them to calculate the octahedral shear stress (τ_o), the effective stress (σ_o), the stresses in global coordinate system ($\overline{\sigma}_x$, $\overline{\sigma}_y$, and $\overline{\tau}_{xy}$) and we can also calculate the residual stresses after complete unloading from various stages of loadings. The formulas for the above calculations are

$$\tau_o = (\sqrt{2}/3)\sigma_o = (S_x{}^2 + S_y{}^2 + S_2{}^2 + 2\tau_{xy}{}^2)^{1/2} \quad ,$$

$$S_x = (2\sigma_x - \sigma_y)/3 \quad , \quad S_y = (2\sigma_y - \sigma_x)/3 \quad ,$$

$$S_z = -(\sigma_x + \sigma_y)/3 \quad , \quad \theta = \alpha - \beta \quad ,$$

$$\overline{\sigma}_x = 1/2(\sigma_1 + \sigma_2) + 1/2(\sigma_1 - \sigma_2)\cos 2\theta \quad ,$$

$$\overline{\sigma}_y = 1/2(\sigma_1 + \sigma_2) - 1/2(\sigma_1 - \sigma_2)\cos 2\theta \quad ,$$

$$\overline{\tau}_{xy} = - 1/2(\sigma_1 - \sigma_2)\sin 2\,\Theta \qquad (2)$$

where α is the angle of the global coordinate system with respect to the element coordinate system.

ELASTOPLASTIC SOLUTION

Only two of the eight contact conditions considered in the elastic range have been extended into the plastic range. They are case 1 under prescribed displacements and case 4 under prescribed forces. RIDIG FORMAT 6 of the NASTRAN Code is used in both cases. However, for problems under prescribed displacements, the DMAP sequence should be slightly modified. The maximum contact displacement at grid points 33, 41, 49, and 57 is set as 0.089 inch. This magnitude is to be reached in 15 incremental steps defined by PLFACT card. Since no actual applied forces are involved, a dummy force card together with its related information should be provided. The contact force F is the sum of the vertical components of the constraint forces under contact. The results for F at the first 12 load levels are 203, 265, 324, 353, 382, 411, 439, 467, 490, 512, 533, 544. The NASTRAN program stops at load level 13 with the error message - "stiffness matrix singular due to material plasticity". The relation between the contact force and the contact displacement is almost linear as shown in Figure 3. We have examined the stresses in all elements and the results show that the maximum tensile stresses occur in element 155. This location remains unchanged as load increases. Therefore, we plot the stresses in this element as functions of loading history as shown in Figure 3. At F = 544 pounds, $(\sigma_1, \sigma_2, \sigma_o)$ = (10750, 1656, 10025) psi in element 155. Since the NASTRAN program stops at load level 13, it fails to give any information for loading larger than 544 pounds. However, it does show that the stresses in element 155 remain unchanged after the contact force F reaches 533 pounds. The residual stresses after complete unloading from various stages of loadings are calculated and these results for σ_1 in element 155 are shown also in Figure 3. The residual stress σ_1 is still in tension if unloading from the early stages of loadings. This is undesirable. If the contact force is larger than 533 pounds, then the residual stress decreases. The octahedral shear stress τ_o is used to determine the size of the plastic zone under various loading levels. The plastic zone at F = 544 pounds is shown as the dark area in Figure 1.

We have also obtained an elastoplastic solution for the problem under prescribed forces at nodes 49, 57, and 65. The distributions of forces at these three points are assumed to be 20, 50, 30%, respectively. We have applied the forces of F = 240, 300, 350, 400, 450, 500, 524, 548, 572 pounds. The NASTRAN program stops at the last load level with the error message - "stiffness matrix singular due to material plasticity". It is interesting to observe that when the contact force increased from 524 to 548 pounds, the stresses in element 155 remain unchanged and the values for σ_1, σ_2, σ_o, are 10603, 1562, 9914 psi, respectively. We may make a conjecture that a constant state of stress in element 155 is reached after the contact force reaches 524 pounds. The results for the stresses $(\sigma_1, \sigma_2, \tau_o)$ in element 155 as functions of contact forces are shown in Figure 4. The residual stresses after complete unloading from various stages of loading can be calculated and the results for σ_1 are also shown in Figure 4. For the purpose of comparison, this problem under the same loading conditions has been solved using a different finite element program (ref. 3). The results for the maximum tensile stress σ_1 and the residual stress σ_1 are shown by the dotted lines in Figure 4. The results are quite different from those based on the NASTRAN program. The residual stress σ_1 is element 155 after unloading from maximum test load (F = 572 lbs.) is about zero based on the NASTRAN results as shown in Figures 3 and 4 while the other numerical result (ref. 3) is about 2000 psi in compression.

It should be noted that the stresses in the finite element programs were calculated at the centroid of each element but only one principal stress at the boundary was measured. The values of the maximum tensile stress at the fillet based on the experimental approach are 2222 psi at F = 100 pounds and 9300 psi at F = 572 pounds. For comparing with experimental results, the boundary stress is determined by extrapolation using the calculated results for those elements along the radial direction through element 155. This is illustrated in Figure 5 for the fourth case of contact condition using the computer program in reference 3. Four curves are plotted in Figure 5 and they represent the major principal stress for four load levels. The residual stresses after complete unloading are determined by assuming that the unloading process is purely elastic. Our numerical results reveal no reverse yielding. As seen in Figure 5, a satisfactory agreement has been reached between the experimental and numerical results (ref. 3 and 4). The NASTRAN result for the maximum tensile stress in the elastic range is 2220 psi for a force of 100 pounds as shown in Figure 2. Assuming that the maximum tensile stress at F = 572 pounds is 10600 psi, the residual stress after complete unloading is estimated to 2100 psi in compression and the experimental result is 3400 psi in compression as shown in Figure 5. There is a definite need to improve the NASTRAN program for stress analysis in the plastic range especially under large values of loadings.

CONCLUSION

A numerical study on a photoplastic model for sliding breech mechanism has been made by using NASTRAN program. The location and magnitude for the maximum tensile stresses have been determined for loading in the elastic as well as elastoplastic range. In the elastic range of loading, the numerical results are in good agreement with the experimental data. In the elastoplastic range of loading the NASTRAN program can be used only up to a certain load limit. Beyond this limit, the values for the maximum tensile stress and the residual stress after complete unloading can only be estimated. The comparisons with other numerical and experimental results indicate that further investigation on the NASTRAN program is needed for problems involving large plastic deformation.

REFERENCES

1. Cheng, Y. F., "Photoplastic Study of Residual Stress in an Overloaded Breech Ring," ARRADCOM Technical Report No. ARLCB-TR-78018, Benet Weapons Laboratory, Watervliet, NY 12189.

2. Chen, P. C. T., and O'Hara, G. P., "NASTRAN Analysis of a Photoplastic Model for Slding Breech Mechanism," Proceedings Army Numerical Analysis and Computer Conference, pp. 237-254, September 1979.

3. Chen, P. C. T., "Numerical Prediction of Residual Stresses in an Overloaded Breech Ring," Proceedings of the Army Numerical Analysis and Computer Conference, pp. 333-346, August 1980.

4. Chen, P. C. T. and Cheng, Y. F., "Stress Analysis of an Overloaded Breech Ring," Proceedings of the International Conference on Reliability, Stress Analysis, and Failure Prevention, pp. 175-180, August 1980.

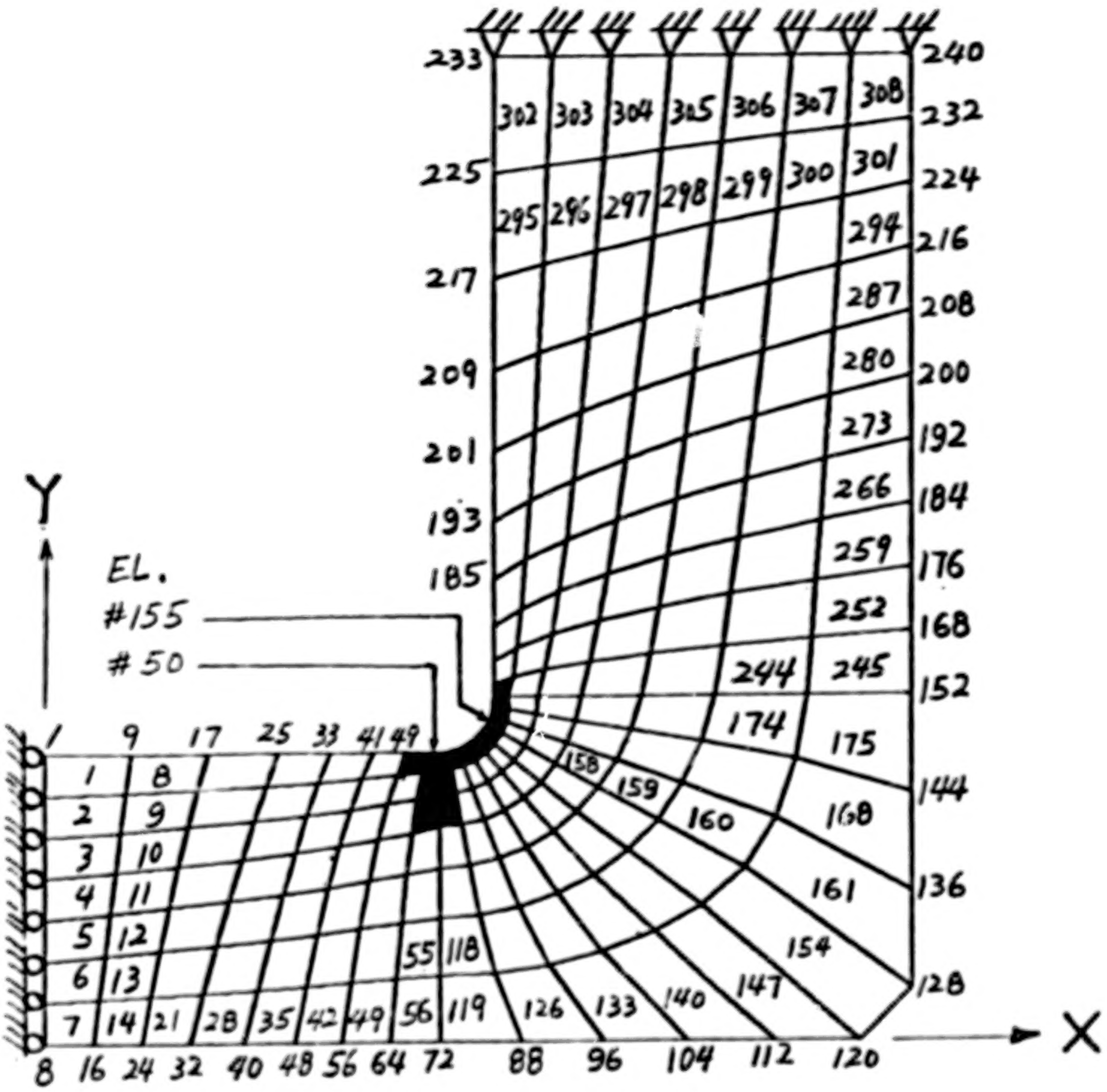

Figure 1. Finite Element Model for Breech Ring.

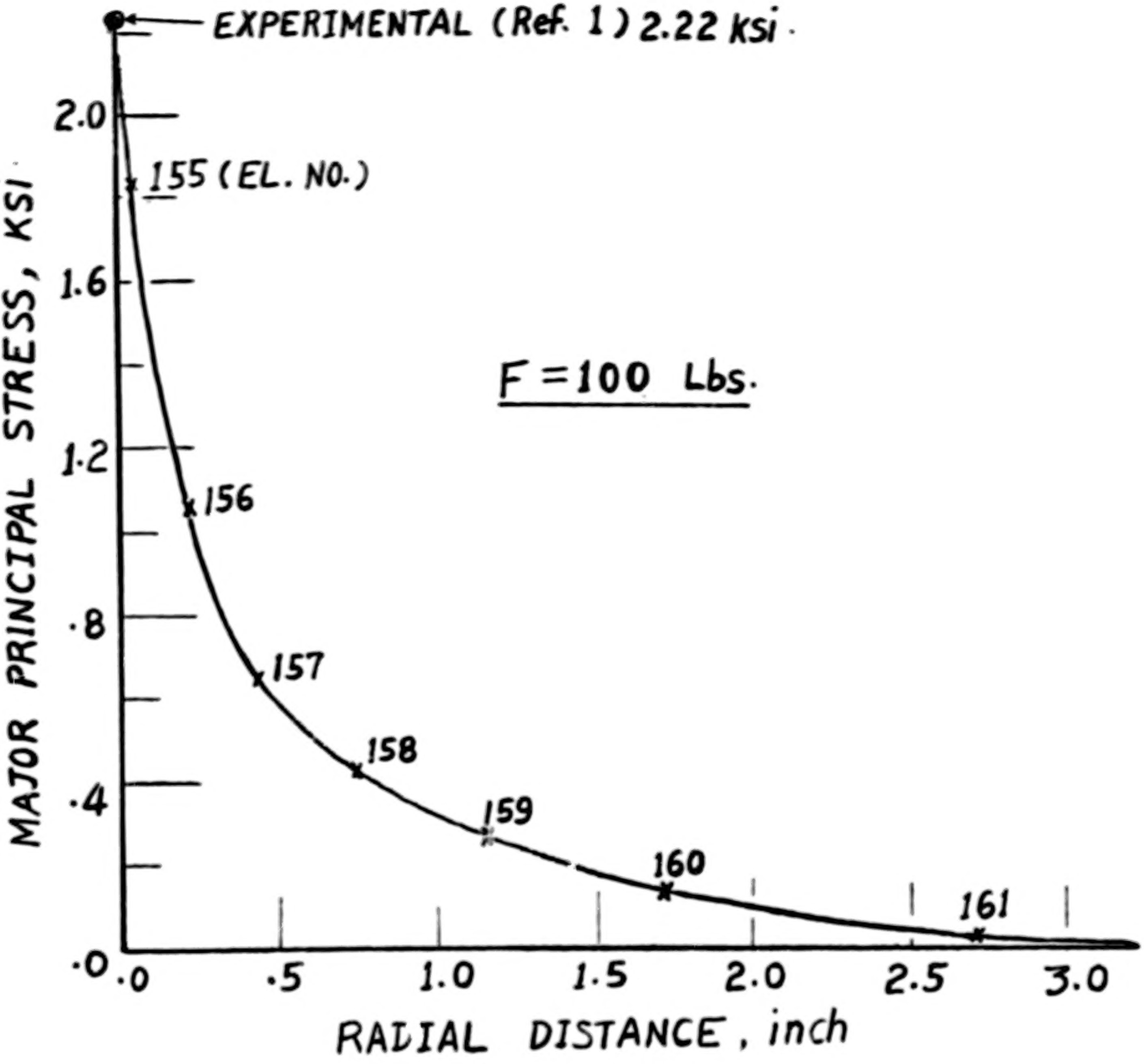

Figure 2. Maximum Tensile Stress for Elastic Loading.

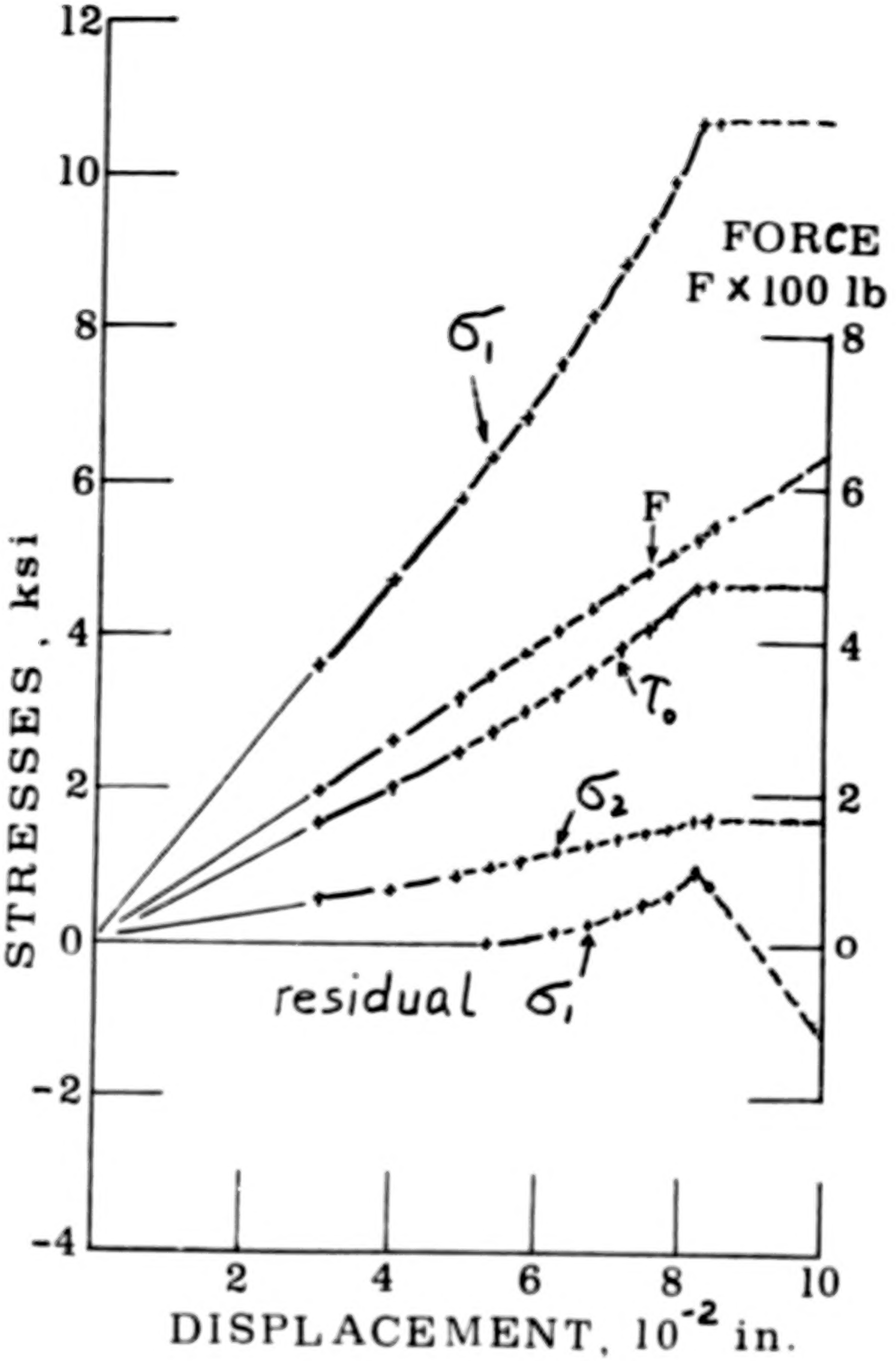

Figure 3. Stresses in Element 155 as Functions of Contact Displacement.

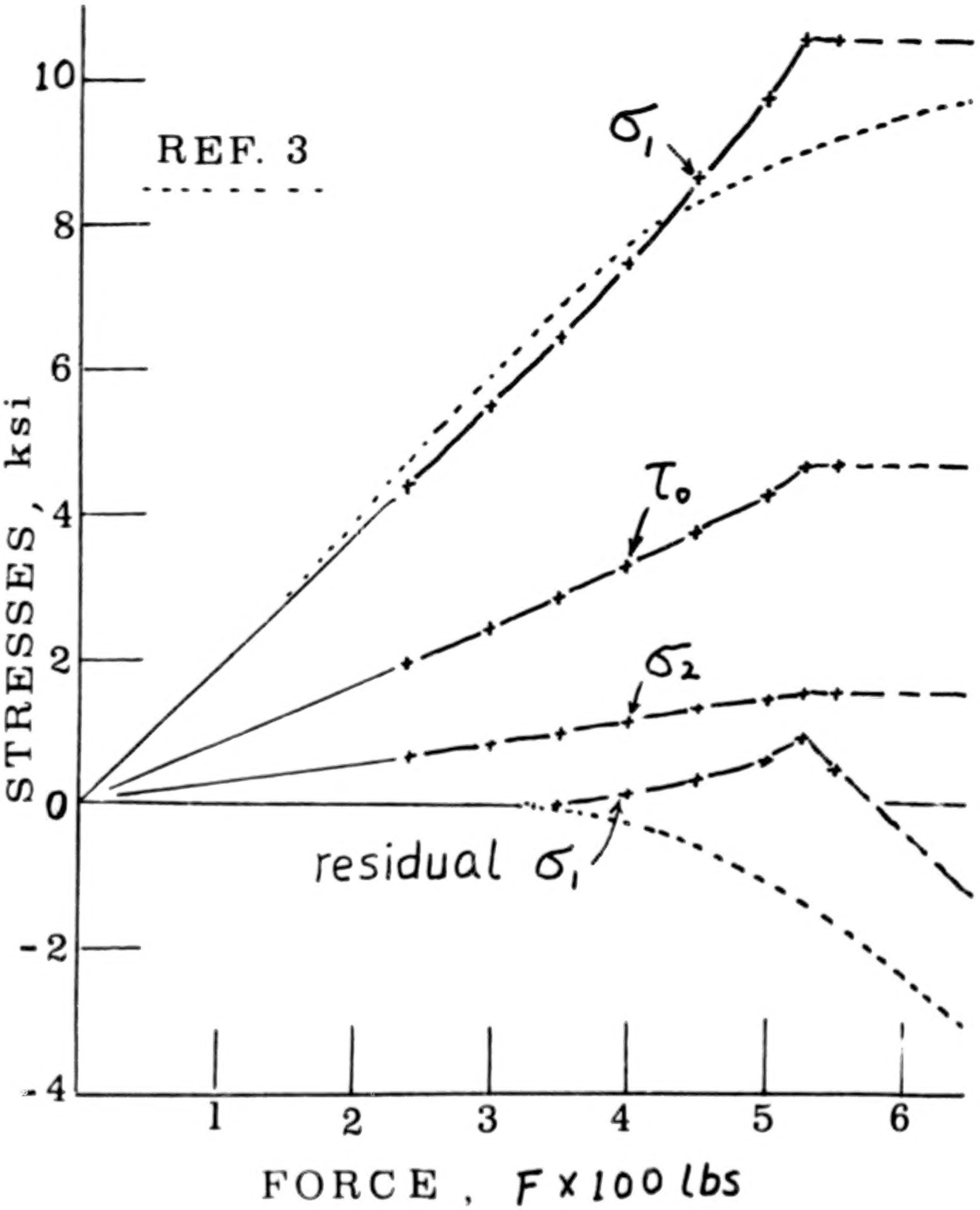

Figure 4. Stresses in Element 155 as Functions of Contact Force.

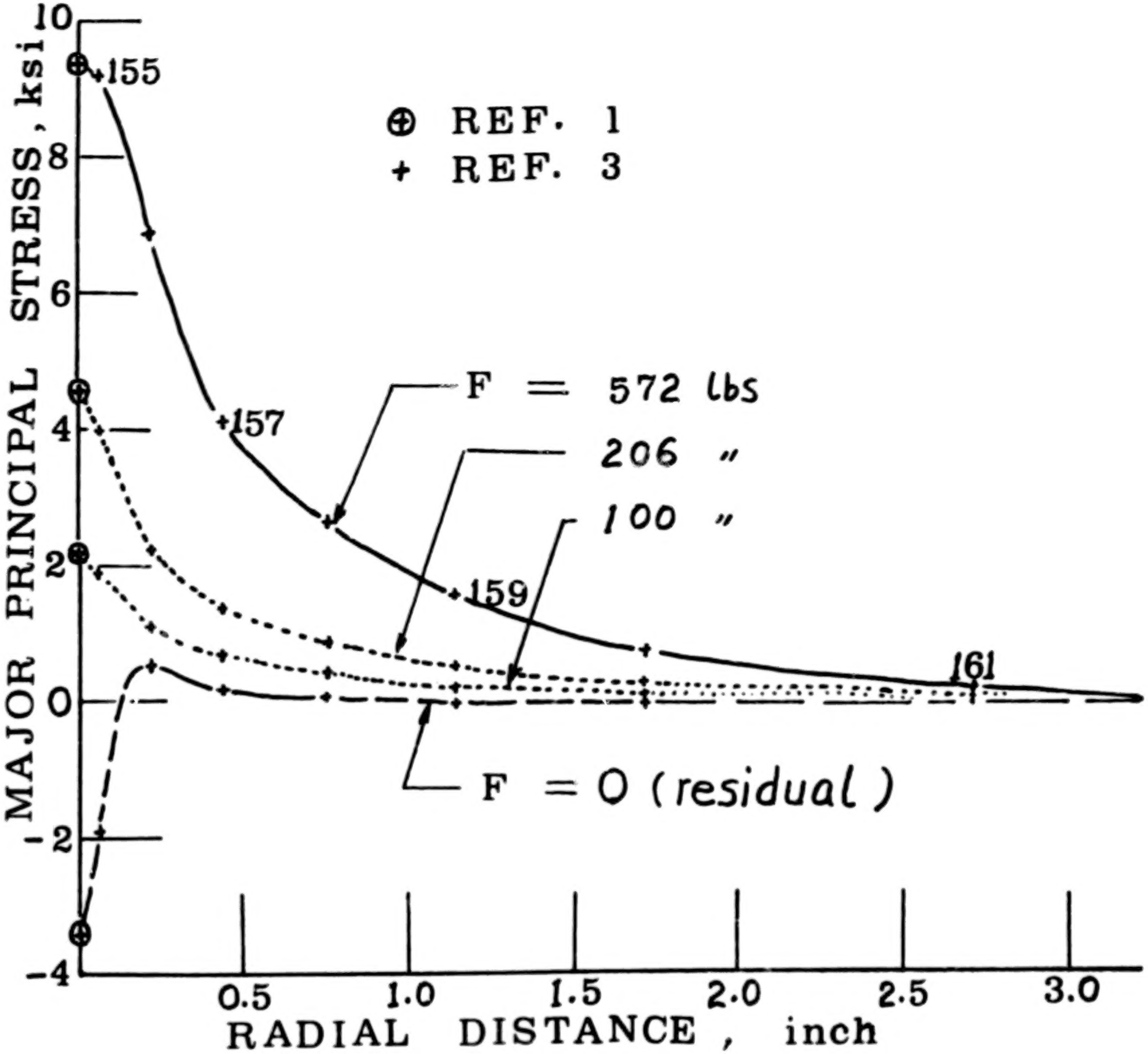

Figure 5. Determination of the Maximum Fillet Stress.

FINITE ELEMENT SOLUTION OF TORSION AND OTHER 2-D POISSON EQUATIONS

Gordon C. Everstine
David W. Taylor Naval Ship R&D Center
Bethesda, Maryland 20084

SUMMARY

The NASTRAN structural analysis computer program may be used, without modification, to solve two-dimensional Poisson equations such as arise in the classical St. Venant torsion problem. The nonhomogeneous term (the right-hand side) in the Poisson equation can be handled conveniently by specifying a gravitational load in a "structural" analysis. The use of an analogy between the equations of elasticity and those of classical mathematical physics is summarized in detail.

BACKGROUND

A computer program like NASTRAN has such wide-ranging capability and versatility that it can be applied in areas other than those for which it was specifically designed by drawing analogies between the equations which NASTRAN solves (e.g., the equations of elasticity) and those of other application areas. For example, before NASTRAN had an explicit heat transfer capability, Mason (Ref. 1) described ways to solve two-dimensional heat conduction problems using the standard structural capabilities. Later, it was shown (Ref. 2-4) that NASTRAN could be directly applied to certain fluid-structure interaction problems such as underwater vibrations and shock. More recently, it has been shown (Ref. 5) that general purpose finite element computer programs can be used, as is, to solve various scalar field equations such as the wave equation, the Helmholtz equation, Laplace's equation, Poisson's equation, the heat equation, and the telegraph equation, as well as mixed field problems (such as coupled structural-acoustic problems) which involve these equations. It was, in particular, shown how to specify the elastic constants, boundary conditions, and applied loads to solve problems involving these equations.

The use of the analogy developed in Ref. 5 will be summarized in detail and illustrated for the classical problem of torsion of prismatic bars, which requires the solution of the two-dimensional Poisson equation.

THE ANALOGY

Many linear problems in mathematical physics involve the solution of an equation obtained by specializing the general form

$$\nabla^2\phi + g = a\,\ddot{\phi} + b\,\dot{\phi} \tag{1}$$

where ∇^2 is the Laplacian operator, dots denote partial time differentiation, the functions g, a, and b are, in general, position-dependent, and the unknown scalar function ϕ depends on both position and time.

Special cases of Equation (1) arise in such diverse applications as heat conduction, acoustics, electrical and magnetic potential problems, torsion of prismatic bars, potential fluid flow, and seepage through porous media. Several common special cases are listed here:

Laplace's equation: $\nabla^2\phi = 0$ (2)

Poisson's equation: $\nabla^2\phi + g = 0$ (3)

wave equation: $\nabla^2\phi = \ddot{\phi}/c^2$ (4)

heat equation: $k\nabla^2\phi + q = \rho\, c\, \dot{\phi}$ (5)

telegraph equation: $\partial^2\phi/\partial x^2 = LC\,\ddot{\phi} + RC\,\dot{\phi}$ (6)

Helmholtz equation: $\nabla^2\phi + k^2\,\phi = 0$ (7)

The Helmholtz equation is the time-harmonic form of the wave equation.

Most boundary conditions likely to be encountered in connection with Equation (1) will probably be special cases of the general form

$$a_1\,\partial\phi/\partial n + a_2\,\phi + a_3\,\dot{\phi} + a_4\,\ddot{\phi} + a_5 = 0 \tag{8}$$

where n is the outward normal at the boundary. For example, in heat conduction problems, a boundary with a prescribed temperature function ϕ_0 satisfies the Dirichlet condition

$$\phi = \phi_0 \tag{9}$$

and a perfectly insulated boundary has the Neumann condition

$$\partial\phi/\partial n = 0 \tag{10}$$

In free surface flow problems, the linearized free surface condition on the velocity potential is (Ref. 6)

$$\ddot{\phi} + g_0 \phi_{,z} = 0 \tag{11}$$

where g_0 is the acceleration due to gravity, the free surface is the plane z=constant, and commas denote partial differentiation. In radiation problems, the one-dimensional (plane wave) radiation condition that the velocity potential must satisfy at a non-reflecting boundary is

$$\phi_{,n} + \dot{\phi}/c = 0 \tag{12}$$

where c is the wave speed.

An example of a boundary condition not of the general form of Equation (8) is the condition which must be satisfied at an accelerating boundary of a fluid

$$p_{,n} + \rho \ddot{u}_n = 0 \tag{13}$$

where p is the fluid pressure, ρ is the mass density, and $\ddot{u}_n$ is the outward normal component of fluid particle acceleration.

According to the analogy (Ref. 5) between Equation (1) and the Navier equations of classical elasticity, Equations (1) and (8) can be solved with elastic finite elements using the following procedure:

1. Select one of the three Cartesian components of displacement (or the z-component in cylindrical coordinates) to represent the scalar field variable ϕ. Constrain all other displacement components everywhere in the field.

2. Model the domain of interest (either 2-D or 3-D) with finite elements having material constants satisfying

$$E_e = \alpha G_e , \qquad \rho_e = a G_e \tag{14}$$

where "a" is the variable appearing in Equation (1), and E_e, G_e, and ρ_e denote the Young's modulus, shear modulus, and mass density assigned to the finite elements on the material card (MAT1 in NASTRAN). The subscript "e" has been added to emphasize that these constants are merely numbers assigned to the elements and may bear no resemblance to any actual material porperties associated with a particular application. The dimensionless constant α in Equation (14) should, for 3-D problems, be chosen large enough to make α+1 numerically indistinguishable from α (Ref. 5). For 2-D problems, α should be small, but not so small that $1+\alpha$ is numerically indistinguishable from unity. Thus, on most computers (Ref. 5),

$$\alpha = \begin{cases} 10^{-5} & \text{(2-D)} \\ 10^{20} & \text{(3-D)} \end{cases} \tag{15}$$

The shear modulus G_e can be selected arbitrarily (Ref. 5). The finite elements eligible for use in the model are those derived from classical elasticity theory rather from the engineering theories involving beams, plates, or shells. Thus, for 2-D problems, the plane stress membrane elements (such as QDMEM1 or TRIM6 in NASTRAN) are appropriate. For 3-D problems, the solid elements (such as IHEXi or TRAPRG in NASTRAN) should be used.

3. Apply to the unconstrained degree of freedom (DOF) at each grid point in the region a "force" given by

$$F = G_e \, g \, V \tag{16}$$

where V is the volume assigned to the point and g is the function appearing in Equation (1). For problems for which the function g in Equation (1) is independent of position (as, for example, in the classical St. Venant torsion problem), this load may be specified conveniently by applying to the "structure" a gravitational field for which the acceleration due to gravity g_0 satisfies

$$\rho_e \, g_0 = G_e \, g \tag{17}$$

4. Connect between ground and the unconstrained DOF at each grid point in the region a scalar dashpot (e.g., DAMP1 in NASTRAN) whose damping constant (the ratio of damping force to velocity) is $G_e bV$, where b is the function appearing in Equation (1) and V is the volume assigned to the point.

5. Enforce the boundary condition (8) by applying to the unconstrained DOF at each grid point on the boundary of the region a "force" given by

$$F = -G_e \, A \, (a_2 \, \phi + a_3 \, \dot{\phi} + a_4 \, \ddot{\phi} + a_5)/a_1 \, , \qquad a_1 \neq 0 \tag{18}$$

where A is the area assigned to the point. (In general (Ref. 5), the outward normal derivative $\partial\phi/\partial n$ is enforced at a boundary point by applying a "force" to the unconstrained DOF at that point equal to $G_e \, A \, \partial\phi/\partial n$. A positive force corresponds to a positive outward normal derivative.) In

Equation (18), the a_2 term is analogous to a scalar spring of constant G_eAa_2/a_1 connected between the point and ground. The a_3 term is analogous to a scalar dashpot of constant G_eAa_3/a_1 connected between the point and ground. The a_4 term is analogous to an added mass of value G_eAa_4/a_1 attached to the point. (Here, one should probably use a consistent, rather than lumped, formulation since Zarda and Marcus (Ref. 6) showed that the differences between the two are not insignificant for free surface flow problems.) The a_5 term is a time-independent force given by $-G_eAa_5/a_1$. As expected, the special case of the Neumann boundary condition ($\phi_n=0$) corresponds to the traction-free boundary in elasticity and hence is a natural boundary condition. The Dirichlet condition ($\phi=\phi_0$) is implemented merely by enforcing the desired value as a "displacement" boundary condition.

EXAMPLE: TORSION OF PRISMATIC BARS

A simple example involving the torsion of prismatic bars can illustrate the use of the structural analogy. The stress distribution over a non-circular cross section of a twisted bar is determined by finding the stress function $\phi(x,y)$ which satisfies the two-dimensional Poisson equation

$$\nabla^2\phi = -2G\theta \qquad (19)$$

in the cross section and is zero on the boundary. The stresses of interest are obtained by differentiation:

$$\tau_{xz} = \partial\phi/\partial y , \qquad \tau_{yz} = -\partial\phi/\partial x \qquad (20)$$

In Equation (19), G is the shear modulus of the bar, and θ is the angle of twist per unit length. The torsional constant J for the cross section is given by (Ref. 7)

$$J = (2/G\theta) \int_A \phi \, dA \qquad (21)$$

The specific cross section considered here is the equilateral triangle of altitude "a" (Figure 1). (This is not the same "a" that appears in Equation (1).) For this region, Equation (19) can be solved in closed form (Ref. 7) to yield

$$\phi = -G\theta\,[(x^2+y^2)/2 - (x^3-3xy^2)/2a - 2a^2/27] \qquad (22)$$

Along the x-axis, the stresses are obtained from Equation (20) as

$$\tau_{xz} = 0 \tag{23}$$

$$\tau_{yz} = 3G\theta\ (2ax/3 - x^2)/2a \tag{24}$$

The maximum stress occurs at the middle of the sides of the triangle ($x=-a/3$); hence

$$\tau_{max} = G\ \theta\ a/2 \tag{25}$$

The torsional constant is obtained by substituting Equation (22) into Equation (21):

$$J = a^4/15\sqrt{3} \tag{26}$$

For the numerical experiment, the following parameters were chosen:

$a = 0.09$ m
$G = 80$ GPa
$\theta = 0.04$ rad/m

Although symmetry would require modeling only one-sixth of the triangle, the upper half was modeled with the finite element mesh shown in Figure 2. The element used (NASTRAN's IS2D8) is the standard two-dimensional, eight-node, quadratic, isoparametric, plane stress membrane element available in many finite element structural analysis computer programs. In the NASTRAN implementation (Ref. 8) used for this example, nodal stresses are computed by extrapolating from stresses computed directly at the Gauss integration points. When two or more elements are connected to a given point, the nodal stresses obtained for the various elements are averaged. A 3x3 array of Gauss points was selected.

Since ϕ was represented by u, the x-component of displacement, all other degrees of freedom at each node were fixed.

According to Equations (14) and (15), the elastic material properties of each element were chosen as

$$G_e = 1\ , \qquad E_e = 10^{-5} \tag{27}$$

Equation (19) is a special case of the general form (1) with

$$g = 2\,G\,\theta\ , \qquad a = b = 0 \tag{28}$$

Hence, from Equation (16), we must apply a "force" to each node given by

$$F_x = 2\,G\,\theta\,G_e\,V \tag{29}$$

(This example shows why it is important to distinguish between G_e, the "shear modulus" specified on the data card for the element, and G, the actual shear modulus for the bar.) This body "force", which is proportional to the volume assigned to each node, is most conveniently specified as a gravitational load, particularly when a consistent, rather than lumped, loading is desired. Since a gravitational field applies the load $\rho_e g_0 V$ to each node, where ρ_e is the element mass density and g_0 is the acceleration due to gravity, it follows that ρ_e and g_0 must be specified so that

$$\rho_e\,g_0 = 2\,G\,\theta\,G_e = 6.4 \tag{30}$$

Thus, since both constants are otherwise arbitrary,

$$\rho_e = 1\ , \qquad g_0 = 6.4 \tag{31}$$

The element thickness is arbitrary since both the "stiffness" matrix and the "load" are proportional to it.

The actual stresses τ_{xz} and τ_{yz} given by Equation (20) may be obtained using the two-dimensional stress-strain law for plane stress elasticity

$$\begin{Bmatrix} \sigma_{xx} \\ \sigma_{yy} \\ \sigma_{xy} \end{Bmatrix} = \begin{bmatrix} 1 & -1 & \\ -1 & 1 & \\ & & 1 \end{bmatrix} \begin{Bmatrix} u_{,x} \\ v_{,y} \\ u_{,y} + v_{,x} \end{Bmatrix} \tag{32}$$

where the elastic constants of Equation (27) have been used, and v (the y component of displacement) is everywhere constrained to zero. Hence, since ϕ is represented by u,

$$\begin{cases} \sigma_{xx} = u_{,x} = \phi_{,x} \\ \sigma_{yy} = -u_{,x} = -\phi_{,x} \\ \sigma_{xy} = u_{,y} = \phi_{,y} \end{cases} \tag{33}$$

That is, the stresses designated by the finite element program as σ_{xy} and σ_{yy} (in the global coordinate system) correspond, respectively, to τ_{xz} and τ_{yz}, the shear stresses of interest.

The finite element calculation of the torsional constant using Equation (21) requires the numerical integration of the stress function ϕ over the cross section. For a finite element mesh having N grid points, this integral can be approximated by

$$J = (2/G\theta) \sum_{i=1}^{N} \phi_i A_i \tag{34}$$

where ϕ_i is the value of ϕ (the solution) at point i, and A_i is the area assigned to that point. The area A_i can be easily obtained from the applied "load" vector, since a gravitational field applies a force F_i at point i given by

$$F_i = \rho_e g_0 t A_i \tag{35}$$

where t is the element thickness. Thus,

$$J = (2/G \theta \rho_e g_0 t) \sum_{i=1}^{N} \phi_i F_i \tag{36}$$

where the summation is equal to the dot product of the finite element solution vector and the applied force vector. In NASTRAN, the calculation of J can be made using a simple DMAP ALTER, which is listed in Figure 3. Since, by symmetry, only half of the cross section was modeled, the result obtained using Equation (36) must be doubled to account for the unmodeled half.

The complete NASTRAN data deck used to solve this problem (including the ALTER to calculate the torsional constant) is listed in Figure 3. The coordinate system used for the grid point locations has been translated 30 mm to the left relative to the coordinate system shown in Figures 1 and 4.

The finite element solution thus obtained is compared to the exact solution computed from Equation (24) in Figure 4, which shows a plot of the shear stress τ_{yz} along y = 0 plotted as a function of x. The finite element curve was smoothed slightly by fitting a B-spline curve through the nodal stresses (Ref. 9, 10). The agreement is clearly excellent. The torsional constant obtained by NASTRAN was 252.2 cm^4, which differs by about 0.12% from the exact value of 252.5 cm^4 calculated using Equation (26).

For this particular example, a heat conduction analogy could also be employed. However, for programs like NASTRAN whose heat conduction capability does not allow for convenient specification of uniform heat sources over 2-D elements (the thermal analog of a gravitational field), the user would have the burden of specifying at each point a heat input proportional to the area assigned to that point. For irregular meshes and those modeled with isoparametric elements (for which consistent loads are needed), this burden is substantial.

REFERENCES

1. Mason, J.B.: "The Solution of Heat Transfer Problems by the Finite Element Method Using NASTRAN," Report X-321-70-97, NASA Goddard Space Flight Center, Greenbelt, MD, February 1970.

2. Everstine, G.C.; Schroeder, E.A.; and Marcus, M.S.: "The Dynamic Analysis of Submerged Structures," *NASTRAN: Users' Experiences*, NASA TM X-3278, September 1975, pp. 419-429.

3. Everstine, G.C.: "A NASTRAN Implementation of the Doubly Asymptotic Approximation for Underwater Shock Response," *NASTRAN: Users' Experiences*, NASA TM X-3428, October 1976, pp. 207-228.

4. Marcus, M.S.: "A Finite-Element Method Applied to the Vibration of Submerged Plates," *J. Ship Research*, vol. 22, no. 2, 1978, pp. 94-99.

5. Everstine, G.C.: "Structural Analogies for Scalar Field Problems," *Int. J. Num. Meth. in Engrg.*, vol. 17, no. 3, March 1981, pp. 471-476.

6. Zarda, P.R.; and Marcus, M.S.: "Finite Element Solutions of Free Surface Flows," *Sixth NASTRAN Users' Colloquium*, NASA CP-2018, October 1977, pp. 27-52.

7. Timoshenko, S.; and Goodier, J.N.: *Theory of Elasticity*, 2nd ed., McGraw-Hill Book Company, Inc., New York, 1951.

8. Hurwitz, M.M.: "Additions to the NASTRAN User's Manual and Theoretical Manual for a Thermostructural Capability for NASTRAN Using Isoparametric Finite Elements," NSRDC Report 4134, Naval Ship R&D Center, Bethesda, MD, 1973.

9. McKee, J.M.; and Kazden, R.J.: "G-Prime B-Spline Manipulation Package -- Basic Mathematical Subroutines," DTNSRDC Report 77-0036, David W. Taylor Naval Ship R&D Center, Bethesda, MD, 1977.

10. McKee, J.M.: "Updates to the G-Prime B-Spline Manipulation Package," David W. Taylor Naval Ship R&D Center, Bethesda, MD, October 1977.

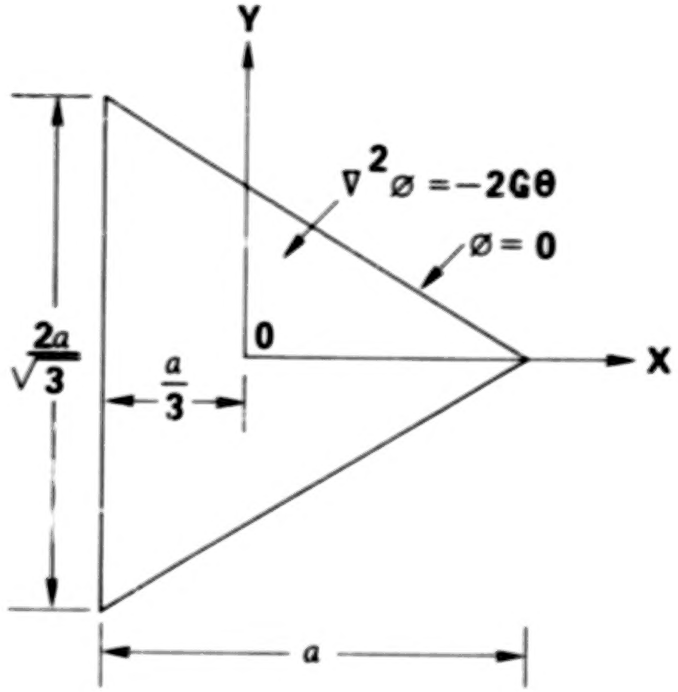

Figure 1 - Torsion of Triangular Prism

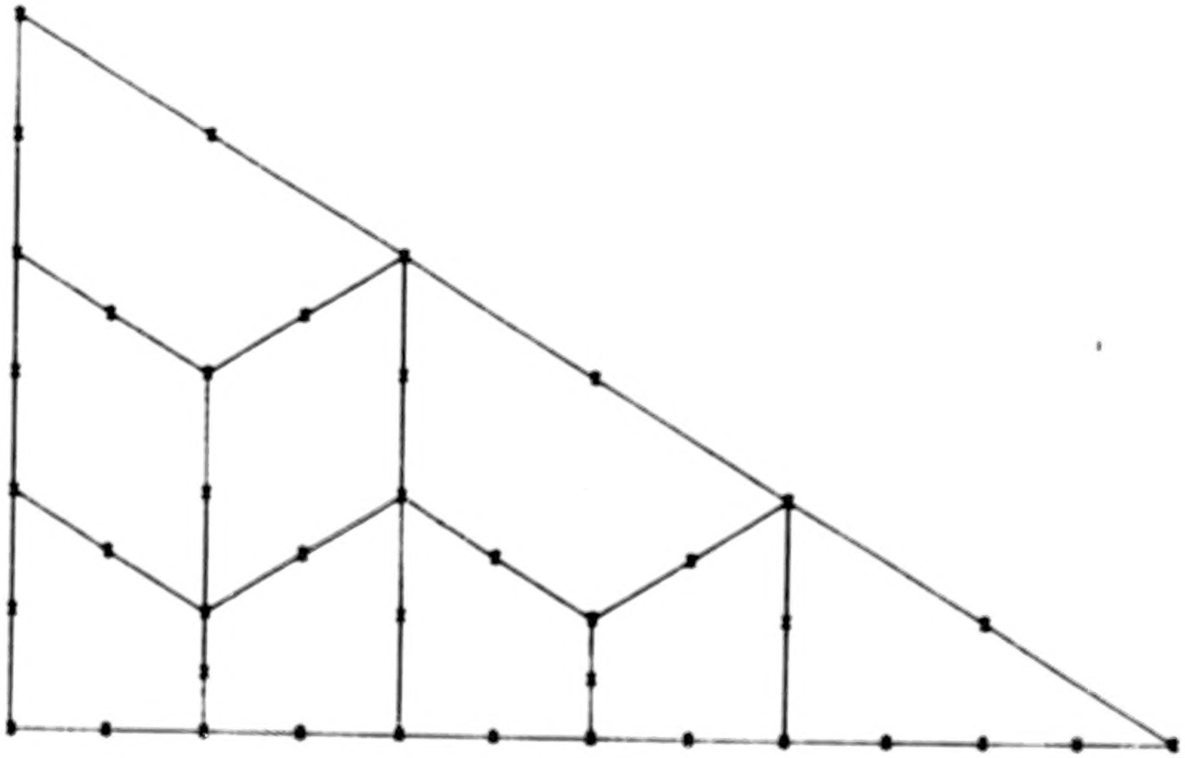

Figure 2 - Finite Element Mesh for Triangular Cross Section

BLANK PAGE

BLANK PAGE

BLANK PAGE

```
ID NASTRAN,DEMO
APP DISP
SOL 1,0
  ALTER 111 $ .R.F. 1, NAVY/NASTRAN LEVEL 15
$       TORSIONAL CONSTANT (TC)
  MPYAD UGV,PG,/TC1/C,N,1/C,N,1/C,N,0/C,N,1 $
  ADD TC1,/TC/C,N,(0.19531,0.0) $    (2/(G*THETA*RHOE*GZERO*T))**2
  MATPRN TC,,,,// $  TORSIONAL CONSTANT
  ALTER 121 $   R.F. 1, NAVY/NASTRAN LEVEL 15
$       STRESS AVERAGING AT GRID POINTS
  STRSAVG EQEXIN,OES1/OESAVG $
  OFP OESAVG,,,,, //V,N,CARDNO $
  SAVE CARDNO $
  ENDALTER $
TIME 10
CEND
TITLE=2-D POISSON EQUATION (TORSION OF TRIANGULAR PRISM)
SPC=13
LOAD=12
DISP=ALL
OLOAD=ALL
STRESS=ALL
BEGIN BULK
APPISO  1
CIS2D8  1       1       3       1       11      13      2       8       +1
+1      12      9       3
CIS2D8  2       1       5       3       13      15      4       9       +2
+2      14      10      3
CIS2D8  3       1       7       5       15      24      6       10      +3
+3      19      16      3
CIS2D8  4       1       13      11      20      22      12      17      +4
+4      21      18      3
CIS2D8  5       1       15      13      22      24      14      18      +5
+5      23      19      3
CIS2D8  6       1       22      20      27      29      21      25      +6
+6      28      26      3
CIS2D8  7       1       24      22      29      35      23      26      +7
+7      32      30      3
CIS2D8  8       1       29      27      33      35      28      31      +8
+8      34      32      3
CIS2D8  9       1       35      33      37      40      34      36      +9
+9      39      38      3
GRAV    12              6.4     1.0
GRDSET                                                  23456
GRID    1
GRID    2                               .00433
GRID    3                               .017321
GRID    4                               .025981
GRID    5                               .034641
GRID    6                               .043301
GRID    7                               .051962
GRID    8                       .0075
GRID    9                       .0075   .01299
GRID    10                      .0075   .030311
GRID    11                      .015
GRID    12                      .015    .00433
GRID    13                      .015    .00866
GRID    14                      .015    .017321
GRID    15                      .015    .025981
GRID    16                      .015    .043301
GRID    17                      .0225
GRID    18                      .0225   .01299
GRID    19                      .0225   .030311
GRID    20                      .03
GRID    21                      .03     .00866
GRID    22                      .03     .017321
GRID    23                      .03     .025981
GRID    24                      .03     .034641
GRID    25                      .0375
GRID    26                      .0375   .01299
GRID    27                      .045
GRID    28                      .045    .00433
GRID    29                      .045    .00866
GRID    30                      .045    .025981
GRID    31                      .0525
GRID    32                      .0525   .01299
GRID    33                      .06
GRID    34                      .06     .00866
GRID    35                      .06     .017321
GRID    36                      .0675
GRID    37                      .075
GRID    38                      .075    .00866
GRID    39                      .0825
GRID    40                      .09
MAT7    11      1.E-5   1.0                     1.0
PARAM   COUPMASS1
PIS2D8  1       11      1.0
SPC1    13      1       1       THRU    7
SPC1    13      1       16      24      30
SPC1    13      1       35      38      40
ENDDATA
```

Figure 3 - Listing of NASTRAN Deck

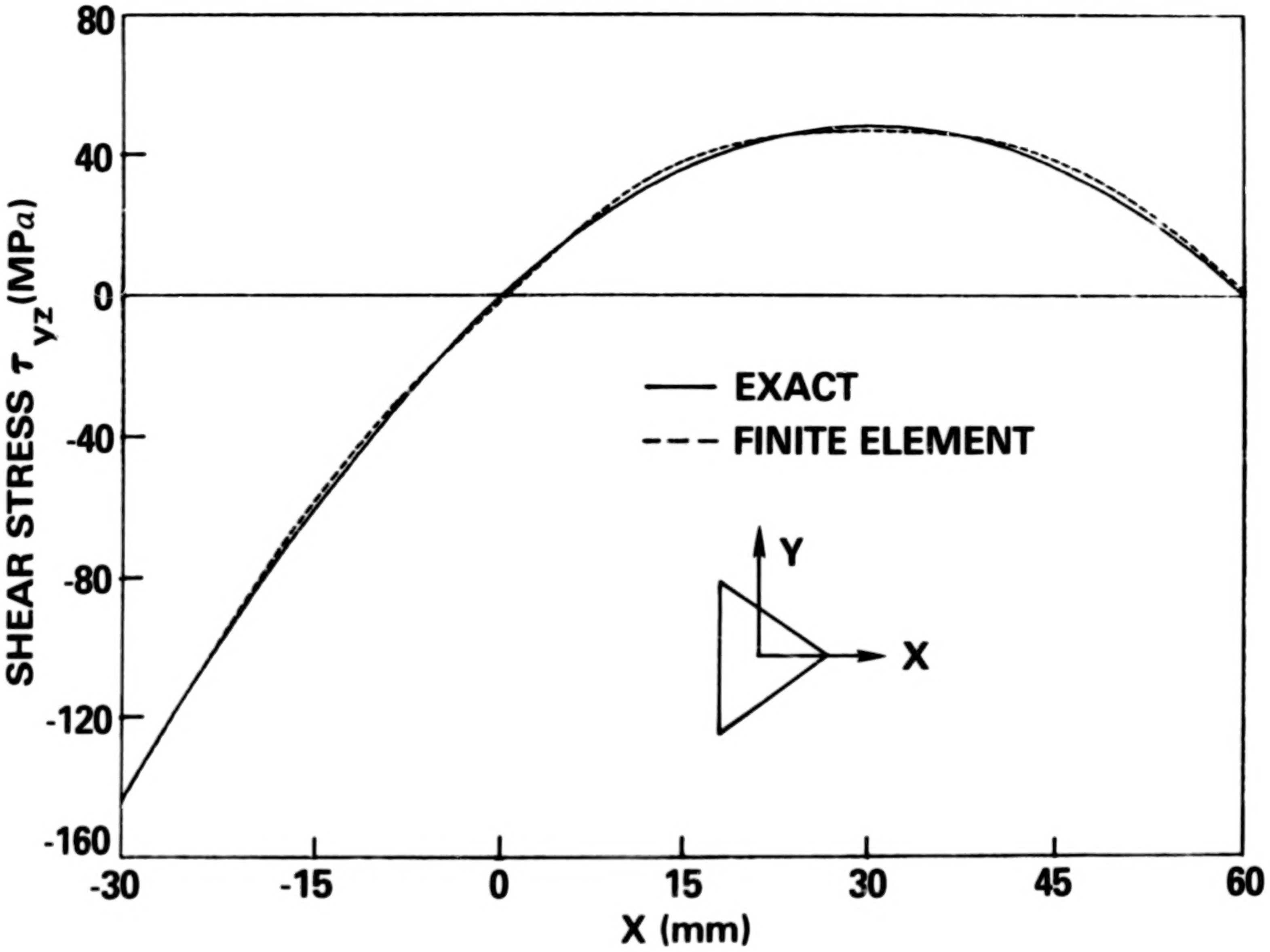

Figure 4 - Shear Stress τ_{yz} Along y = 0: Comparison of Finite Element and Exact Solutions

A NEW CAPABILITY FOR ELASTIC AIRCRAFT AIRLOADS VIA NASTRAN

* Hugh C. Briggs

and

** Lance E. Chrisinger
Air Force Institute of Technology
Wright-Patterson AFB Ohio 45433

ABSTRACT

A new Direct Matrix Abstract Program for NASTRAN has been written that calculates internal stresses and airloads for a flexible wing. The difficulties encountered in interfacing the doublet lattice solution to the aerodynamic problem to the finite element solution to the structural problem are discussed. A brief numerical example is included.

INTRODUCTION

This paper describes a new capability to calculate aircraft airloads including airframe flexibility effects. The primary motivation for this capability is to provide load vectors for large, whole aircraft structural models. By using the large model itself, the construction of an intermediate or secondary aircraft model is avoided. The use of existing aerodynamic and structural capabilities in NASTRAN avoids a requirement for external storage of the large amounts of data. This procedure has been implemented in a new Direct Matrix Abstraction Program constructed from the Static Analysis and Flutter Rigid Formats, augmented by a new module.

The problem at hand is to find the deformed shape of an aircraft under static unknown airloads given a point in the sky, a structural model and an aero model. This is a fluid-structure interaction problem since the aero forces change with the structural deformation and the deformation changes with the aerodynamic loads.

Solutions to such problems are required in several areas of structural analysis and design. Preliminary design of an aircraft requires repeated solutions based on simple models as the form of the aircraft is finalized. A second example is Damage Tolerance Analysis which typically requires an analysis on a much larger scale. In this process, safe crack growth lives are predicted based on internal stresses for the structure under service loads.

---

* Assistant Professor of Aeronautics

** Graduate Student

Current solution practices for this interaction problem are of two kinds due largely to the state of early development of the capability. Several design codes exist which are capable of solving this problem as a subset of their general stability and control capability. Typically such codes use simplistic models and theories to minimize the problem size and solution time. This is in line with the iterative and tentative nature of the design work itself. When faced with the large scale problem of calculating whole aircraft internal loads, analysts must resort to the use of multiple computer codes. Usually a large aero code and a large structural code are run iteratively, with data conversion programs run in between. This process is slow and tedious and requires considerable engineering expertice and program development.

As structural and aero computer analysis techniques mature, new computer codes are becoming available that are capable of solving the complete large scale interaction problem internally. This paper describes the alteration of NASTRAN, an existing code which is capable of both types of analysis separately, to include the analysis of a deformable wing under airloads.

Present NASTRAN Capabilities

Several rigid formats exist which are pertinent to this particular form of fluid-structure interaction. The Static Analysis Rigid Format is useful for calculating structural deformation using a given load vector but includes minimal load generation capability. The Flutter Rigid Format calculates airloads but presumes harmonic motion in the natural modes. Similarly, Transient Aeroelastic Response analysis is carried out in the frequency domain. Although nearly all the building blocks of elastic airloads determination seem to be present, no one rigid format will work.

On the module level, the specific capabilities from these rigid formats are available. The static structural solution and case control modules form the basis for the new program. Complex valued airloads at a given frequency are available by several theories which are useful here at zero frequency. Interpolation by splines exists in the flutter rigid format where it is used to map the structural displacement vector to displacements at the aerodynamic grid points. Lastly, several modules exist for post solution recovery of structural and aerodynamic data.

Interfacing Problems

Using such widely differing theories for the structure and the fluid creates various problems at their interface. This is due to the different physical variables represented in the two regions. Therefore, the node spacing will be different in these regions and subject to different construction guidelines. Furthermore, the nodal unknowns will be different which causes most of the difficulty in representing the interface continuity conditions. The nodal unknowns in the structural region are displacements and the equations represent force equilibrium at the nodes. In the aero region, the unknowns are flow singularity strengths and the equations represent no flow through the wing surface.

Continuity is required in both the interface forces and the interface displacements and is the source of the interaction between the two problem regions. Simply stated, the fluid pressures must be converted to a structural load vector and structural displacements must be input to the aerodynamic theories as boundary motion.

The second of these is done by mapping the structural displacement vector into displacements defined at the aerodynamic points. This process is aggravated by the differences between the structural model and the aerodynamic model. For example, only the primary wing structure may have been modelled or the structural boundary conditions may be approximate and unsuited to the aerodynamic calculations.

Interfacing in the reverse direction requires mapping the aerodynamic pressures given at the aerodynamic points into a structural force vector. This necessitates the construction of an area matrix and the handling of pressures on the unmodelled secondary structure. A primary concern will be the preservation of the total load and moments through the transformation.

The tremendous capabilities of NASTRAN will introduce several interfacing difficulties. For example, the available aerodynamic theories have varying degrees of freedom and planform coverage. The degree of planform segmentation in the mapping of pressures to forces will have a large influence on bookkeeping and programming. Aerodynamic bodies can generate center line loads or surface distributed pressures and must be interfaced to either shell or beam structural bodies. Management of the mapping of pressures from several wing panels and an aileron to the wing box will be complicated by the lack of secondary structure in the model.

Capabilities of the New DMAP Sequence

The primary goals of our efforts were the implimentation of a calculation loop, control of the loop termination and demonstration of the module communications and sequencing.

Realization of the sequence requires the construction of a new module containing all assumptions about the transformation of pressures to forces. The module is invoked once outside the loop and builds the transformation matrix and several recovery matrices. For the present work, the module has been simulated by user supplied, and externally generated, data blocks. As a result of the many interfacing problems, the sequence is limited to a wing along in each of the structural and aerodynamic models. The planform of the structural model must match that of the aerodynamic model. This is easily accomplished with crude extensions of the structural model.

As stated, the new DMAP has been constructed from several rigid formats. Although only a brief summary of the program can be given here, a complete listing is included as an appendix. The problem initiation follows the Static Analysis Rigid Format with the addition of the calculation of the airloads from the Flutter Rigid Format. This includes construction and decomposition of the structural stiffness and construction of the aero influence coefficients. The new module which will calculate the transformation from aero pressures to structural loads has been temporarily replaced by user supplied data blocks and a few matrix operations. A new control loop has been created to repeat the calculation of zero frequency airloads for the current displacement vector, create the structural load vector and calculate new displacements by back substitution into the decomposed stiffness matrix. Since the displacements represent increments due to the elastic airloads, the loop terminates when the displacement norm goes to zero approximately. Post processing includes calculation of total load coefficients as a well as normal data recovery from the Static Analysis Rigid Format.

The primary results provided by the new program are the structural displacements and the aerodynamic pressures. The post-solution recovery includes the lift coefficient and pitch and roll moment coefficients. All standard structural recovered data such as stresses and member forces are available.

A Numerical Example

The results for a simple three dimensional wing at Mach 0.2 and 2 degrees angle of attack are presented to illustrate the fluid-structure interaction problem at hand and the capabilities of the new sequence.

The structural model (Fig. 1&2) consists of three spars with caps and webs and membranes for upper and lower surface coverage. The aerodynamic model (Fig 3) is a uniform 7 x 9 grid of boxes based upon the subsonic doublet lattice method run at very nearly zero frequency.

The main calculation loop consists of repeated back substitution into the decomposed aerodynamic influence equations and structural equilibrium equations. The loop terminates when the displacement vector norm does not change to some tolerance. Table I presents an example of the norm convergence.

Final tip chord displacement and representative chordwise and spanwise pressure distributions are presented in Fig 4, 5 & 6.

Conclusion

This new NASTRAN capability will allow use of a large structural model in the construction of its aerodynamic load vector. The determination of stresses to the full detail of the model and the avoidance of the construction of an intermediate model are additional benefits. Since the very capable and widely supported NASTRAN program is used, no new programs or languages are needed.

Loop	Norm
1	20.069
2	.92205
3	.09327
4	.00920
5	.000837
6	.000094

Note:

Maximum change in displacement for the last pass was -2.347×10^{-6}

Table I. Convergence of the Displacement Norm

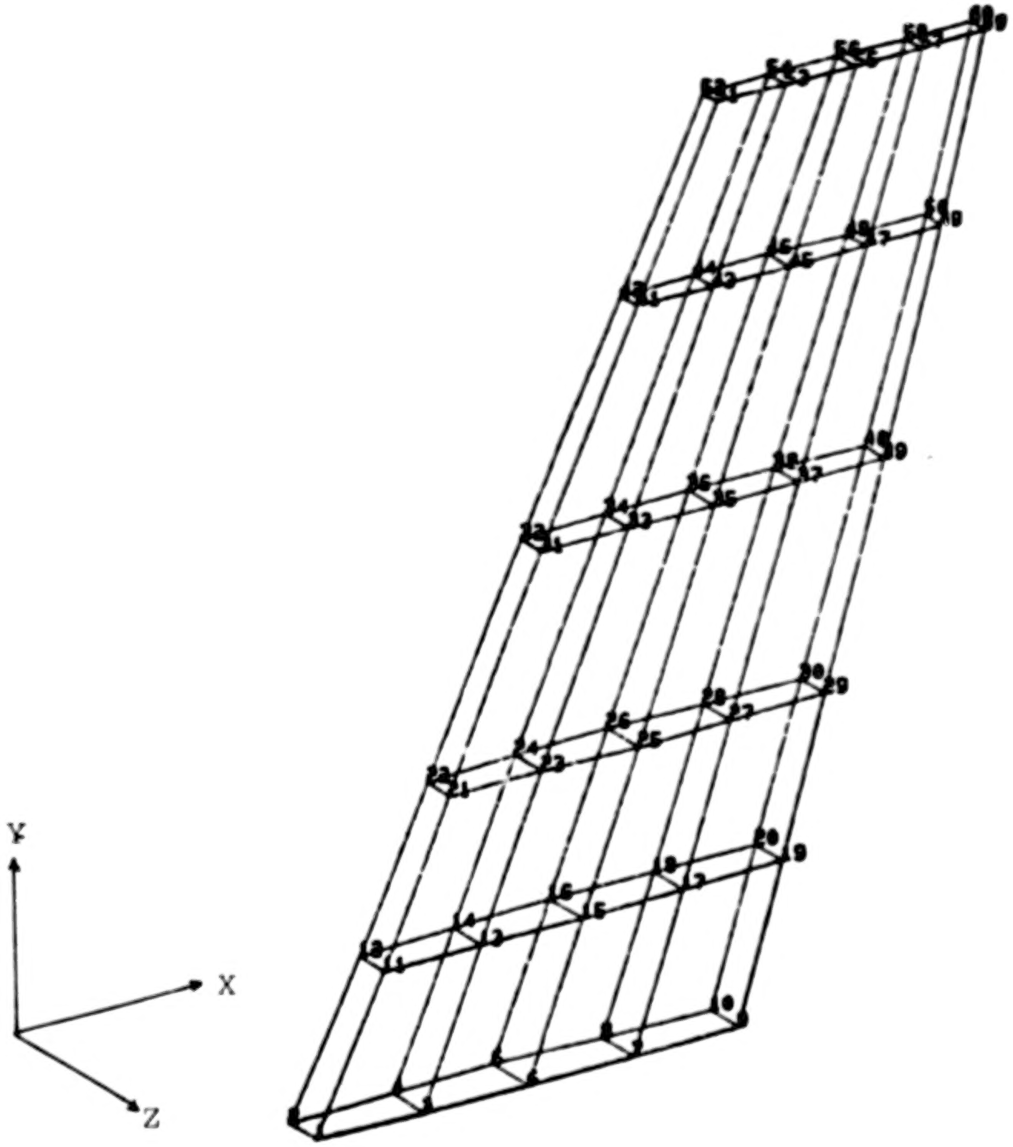

Figure 1. WING MODEL

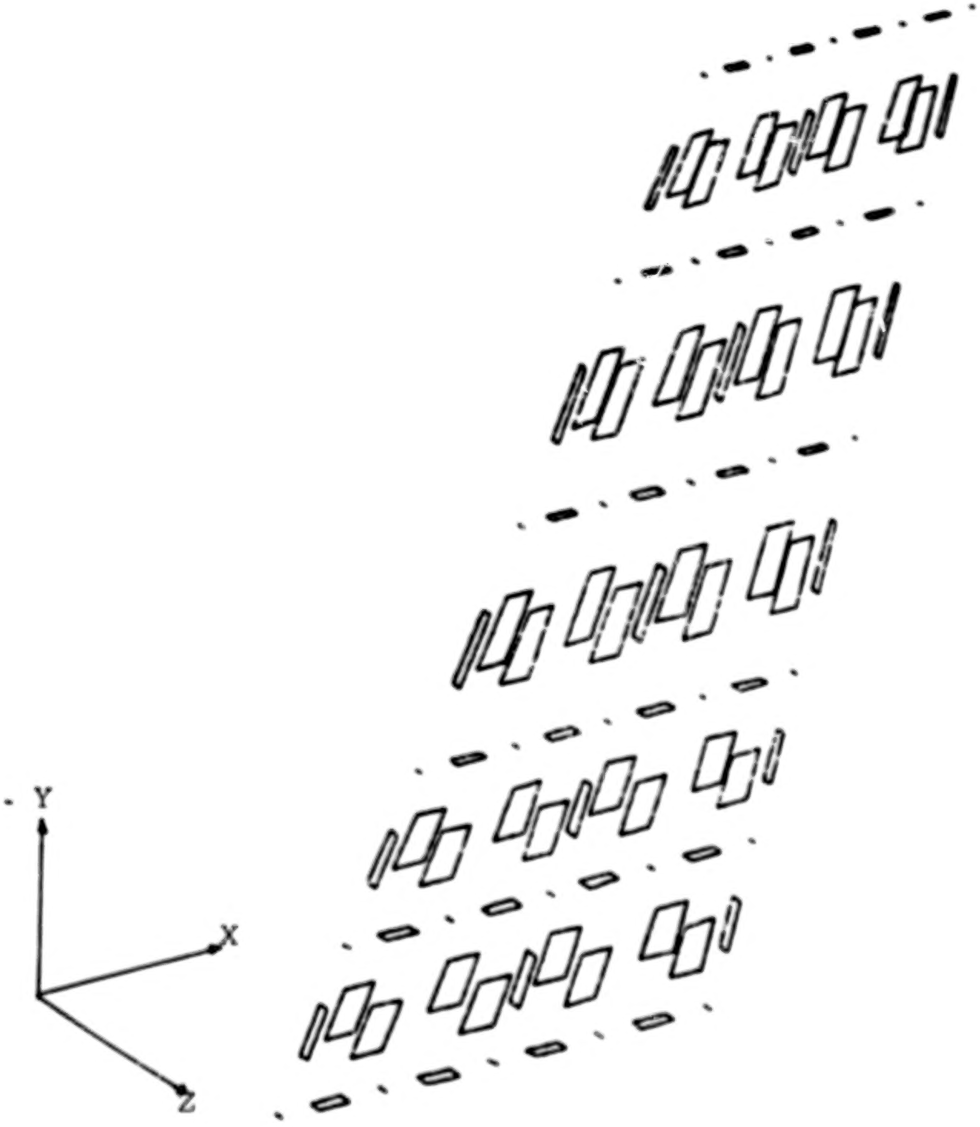

Figure 2. WING MODEL, EXPLODED VIEW

BLANK PAGE

BLANK PAGE

BLANK PAGE

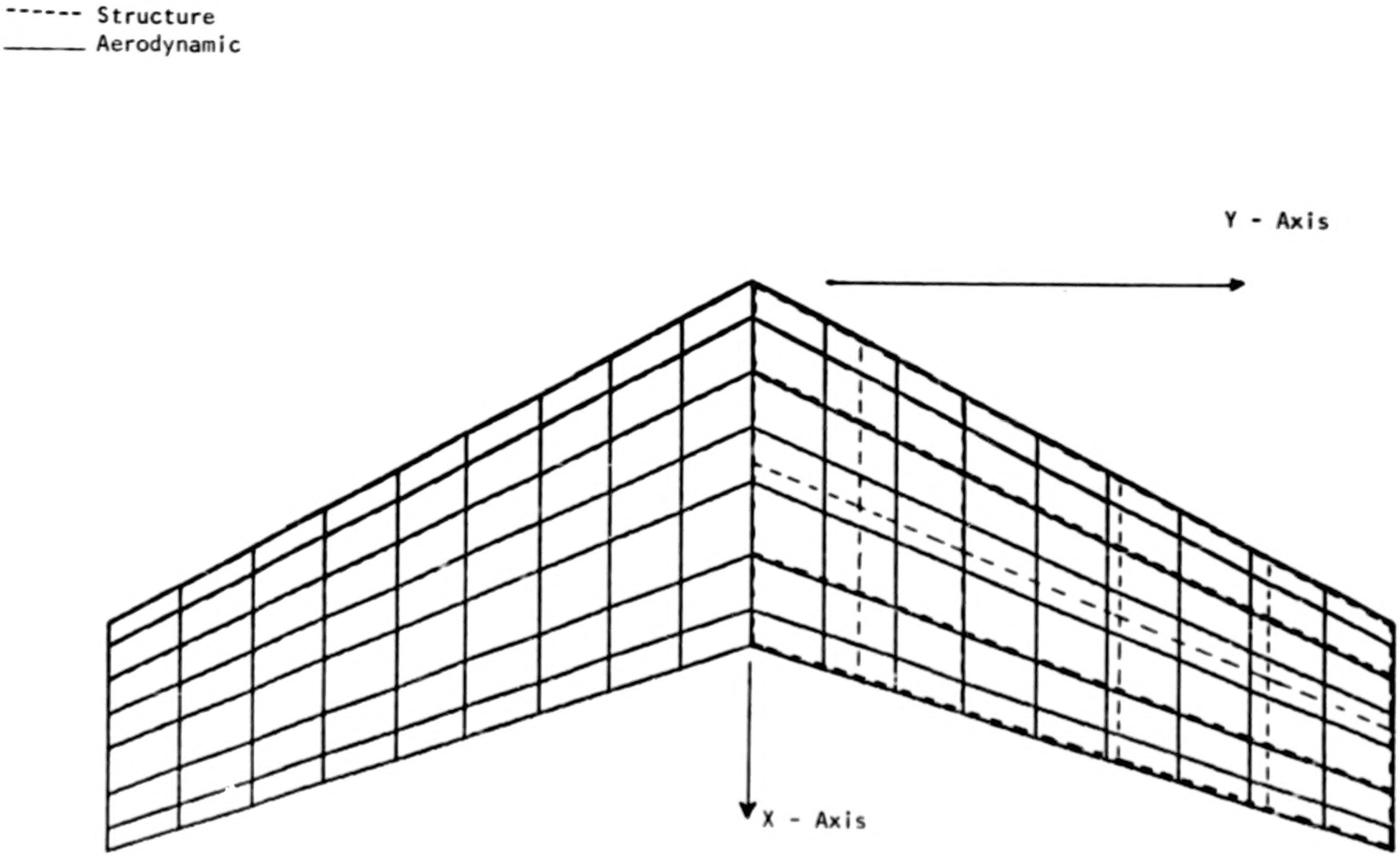

Figure 3. Projected View of Structural and 63-Box Aerodynamic Model.

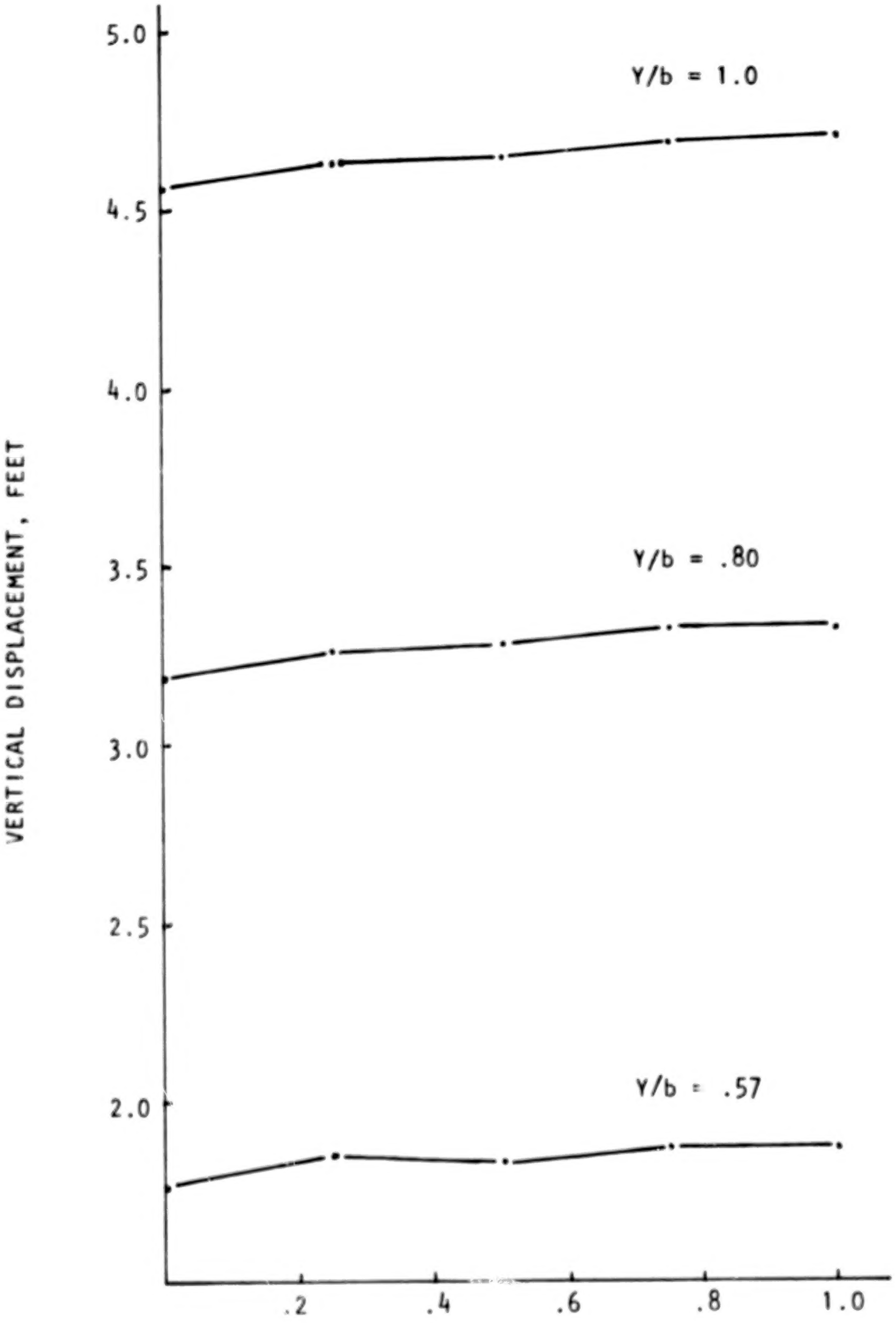

Figure 4. VERTICAL DISPLACEMENTS

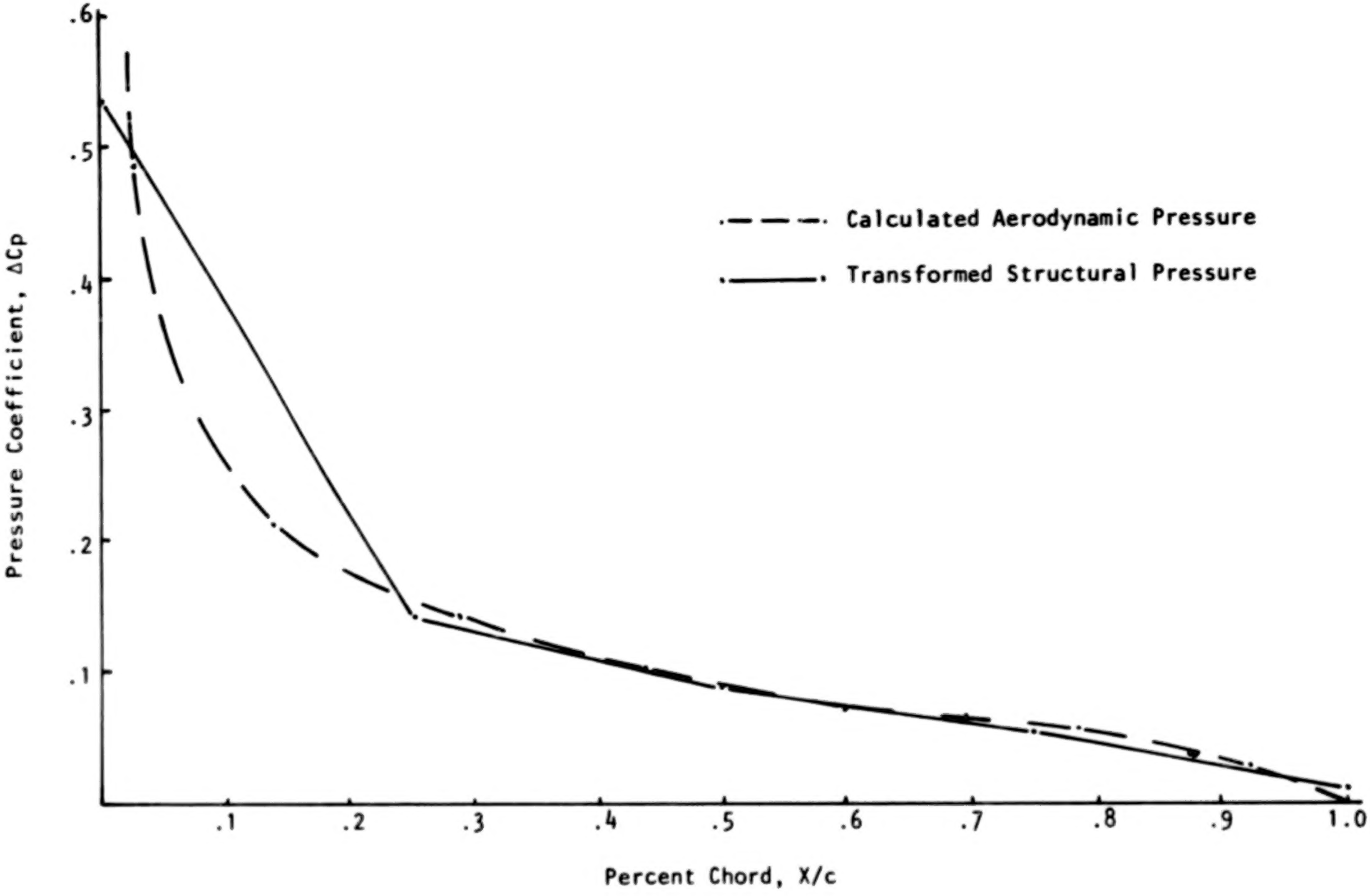

Figure 5. CHORDWISE PRESSURE DISTRIBUTION

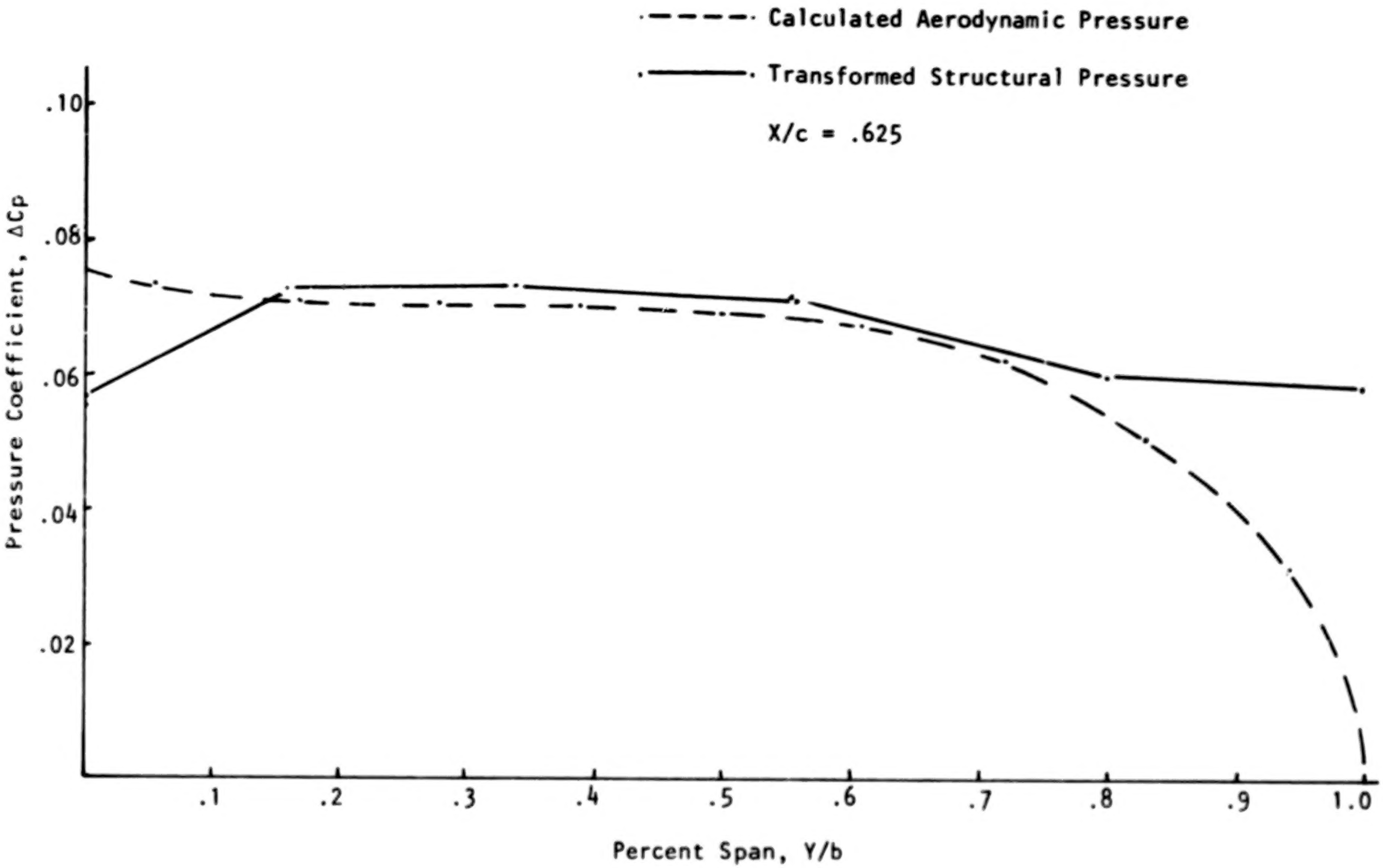

Figure 6. SPANWISE PRESSURE DISTRIBUTION

APPENDIX A

```
LEVEL 2.0 NASTRAN DMAP COMPILER - SOURCE LISTING


OPTIONS IN EFFECT:  GO       ERR=2   NOLIST  NODECK  NOREF   NOOSCAR

     1  BEGIN     $

     2  GP1       GEOM1,GEOM2,/GPL,EQEXIN,GPDT,CSTM,BGPDT,SIL/V,N,LUSET/  V,N,
                  NOGPDT $

     3  SAVE      LUSET,NOGPDT $

     4  COND      ERROR1,NOGPDT $

     5  GP2       GEOM2,EQEXIN/ECT $

     6  PARAML    PCDB//C,N,PRES/C,N,/C,N,/C,N,/V,N,JUMPPLOT $

     7  GP3       GEOM3,EQEXIN,GEOM2/,GPTT/V,N,NOGRAV $

     8  TA1       ECT,EPT,BGPDT,SIL,GPTT,CSTM/EST,GEI,GPECT,/V,N,LUSET/   V,N,
                  NOSIMP/C,N,1/V,N,NOGENL/V,N,GENEL $

     9  SAVE      NOGENL,NOSIMP,GENEL $

    10  COND      ERROR1,NOSIMP $

    11  PARAM     //C,N,ADD/V,N,NOKGGX/C,N,1/C,N,0 $

    12  PARAM     //C,N,ADD/V,N,NOMGG /C,N,1/C,N,0 $

    13  EMG       EST,CSTM,MPT,DIT,GEOM2,/KELM,KDICT,MELM,MDICT,,/V,N,NOKGGX/ V,
                  N,NOMGG/C,N,/C,N,/C,N,/C,Y,COUPMASS/C,Y,CPBAR/C,Y,CPROD/  C,Y,
                  CPQUAD1/C,Y,CPQUAD2/C,Y,CPTRIA1/C,Y,CPTRIA2/C,Y,CPTUBE/ C,Y,
                  CPQDPLT/C,Y,CPTRPLT/C,Y,CPTRBSC $

    14  SAVE      NOKGGX,NOMGG $

    15  COND      JMPKGGX,NOKGGX $

    16  EMA       GPECT,KDICT,KELM/KGGX,GPST $

    17  LABEL     JMPKGGX $

    18  COND      ERROR1,NOMGG $

    19  EMA       GPECT,MDICT,MELM/MGG,/C,N,-1/C,Y,WTMASS=1.0 $

    20  COND      LGPWG,GRDPNT $

    21  GPWG      BGPDT,CSTM,EQEXIN,MGG/OGPWG/V,Y,GRDPNT=-1/C,Y,WTMASS $
```

```
LEVEL 2.0 NASTRAN DMAP COMPILER - SOURCE LISTING

22  OFP       OGPWG,,,,,//V,N,CARDNO $

23  LABEL     LGPWG $

24  EQUIV     KGGX,KGG/NOGENL'$

25  COND      LBL11,NOGENL $

26  SMA3      GEI,/KGGY/V,N,LUSET/V,N,NOGENL/C,N,-1 $

27  ADD       KGGX,KGGY/KGG $

28  LABEL     LBL11 $

29  PARAM     //C,N,MPY/V,N,NSKIP/C,N,0/C,N,0 $

30  PARAM     //C,N,SUB/V,N,DESINT/C,N,0/C,N,1 $

31  PURGE     99BBR,D1JE,D2JE/DESINT $

32  PARAM     //C,N,MPY/V,N,NOCAMBER/C,N,1/C,Y,ICAMB=-1 $

33  PURGE     CAMBER/NOCAMBER $

34  GP4       CASECC,GEOM4,EQEXIN,GPDT,BGPDT,CSTM/RG,,USET,ASET/V,  N,LUSET/
              V,N,MPCF1/V,N,MPCF2/V,N,SINGLE/V,N,OMIT/V,N,REACT/V,N,NSKIP/V,
              N,REPEAT/V,N,NOSET/V,N,NOL/V,N,NOA/C,Y,SUBID $

35  SAVE      MPCF1,MPCF2,SINGLE,OMIT,REACT,NSKIP,REPEAT,NOSET,NOL,NOA $

36  GPSP      GPL,GPST,USET,SIL/OGPST/V,N,NOGPST $

37  SAVE      NOGPST $

38  COND      LBL4,NOGPST $

39  OFP       OGPST,,,,,//V,N,CARDNO $

40  LABEL     LBL4 $

41  EQUIV     KGG,KNN/MPCF1/MGG,MNN/MPCF1 $

42  COND      LBL2,MPCF1 $

43  MCE1      USET,RG/GM $

44  MCE2      USET,GM,KGG,MGG,,/KNN,MNN,, $

45  LABEL     LBL2 $
```

```
LEVEL 2.0 NASTRAN DMAP COMPILER - SOURCE LISTING

46  EQUIV    KNN,KFF/SINGLE/MNN,MFF/SINGLE $

47  COND     LBL3,SINGLE $

48  SCE1     USET,KNN,MNN,,/KFF,KFS,,MFF,, $

49  LABEL    LBL3 $

50  EQUIV    KFF,KAA/OMIT/ MFF,MAA/OMIT $

51  PURGE    GO/OMIT $

52  COND     LBL5,OMIT $

53  PARAM    //C,N,PREC/V,N,PREC $

54  VEC      USET/V/C,N,F/C,N,O/C,N,A $

55  PARTN    KFF,V,/KOO,,KOA,KAAB $

56  DECOMP   KOO/LOO,UOO/C,N,1/C,N,0/V,N,MIND/V,N,DET/V,N,NDET/V,N,SING $

57  SAVE     MIND,DET,NDET,SING $

58  FBS      LOO,UOO,KOA/GO/C,N,1/C,N,-1/V,N,PREC/V,N,PREC $

59  MPYAD    KOA,GO,KAAB/KAA/C,N,1/C,N,1/C,N,1/V,N,PREC $

60  SMP2     USET,GO,MFF/MAA $

61  LABEL    LBL5 $

62  COND     LBL6,REACT $

63  RBMG1    USET,KAA,MAA/KLL,KLR,KRR,MLL,MLR,MRR $

64  RBMG2    KLL/LLL/ $

65  RBMG3    LLL,KLR,KRR/DM $

66  RBMG4    DM,MLL,MLR,MRR/MR $

67  LABEL    LBL6 $

68  DPD      DYNAMICS,GPL,SIL,USET/GPLD,SILD,USETD,TFPOOL,,,,,,EED,EQDYN/V,
             N,LUSET/V,N,LUSETD/V,N,NOTFL/V,N,NODLT/V,N,NOPSDL/V,N,NOFRL/V,
             N,NONLFT/V,N,NOTRL/V,N,NOEED/C,N,123/V,N,NOUE $

69  SAVE     LUSETD,NOUE,NOEED $
```

```
    LEVEL 2.0 NASTRAN DMAP COMPILER - SOURCE LISTING


 70  COND      ERROR2,NOEED $

 71  EQUIV     GO,GOD/NOUE/GM,GMD/NOUE $

 72  READ      KAA,MAA,MR,DM,EED,USET,CASECC/LAMA,PHIA,MI,OEIGS/C,N,MODES/V,N,
               NEIGV $

 73  SAVE      NEIGV $

 74  OFP       OEIGS,LAMA,,,,//V,N,CARDNO $

 75  COND      ERROR4,NEIGV $

 76  MTRXIN    CASECC,MATPOOL,EQDYN,,TFPOOL/K2PP,M2PP,B2PP/V,N,LUSETD/V,N,
               NOK2PP/V,N,NOM2PP/V,N,NOB2PP $

 77  SAVE      NOK2PP,NOM2PP,NOB2PP $

 78  EQUIV     M2PP,M2DD/NOA/B2PP,B2DD/NOA/K2PP,K2DD/NOA $

 79  GKAD      USETD,GM,GO,,,,,K2PP,M2PP,B2PP/,,,GMD,GOD,K2DD,M2DD,B2DD/C,N,
               CMPLEV/C,N,DISP/C,N,MODAL/C,N,0.0/C,N,0.0/C,N,0.0/V,N,NOK2PP/V,
               N,NOM2PP/V,N,NOB2PP/ V,N,MPCF1/V,N,SINGLE/V,N,OMIT/V,N,NOUE/C,
               N,-1/C,N,-1/ C,N,-1/C,N,-1 $

 80  GKAM      USETD,PHIA,,LAMA,DIT,M2DD,B2DD,K2DD,CASECC/MHH,BHH,KHH,AAAAA/V,
               N,NOUE/C,Y,LMODES=0/C,Y,LFREQ=0./C,Y,HFREQ=0./V,N,  NOM2PP/V,N,
               NOB2PP/V,N,NOK2PP/V,N,NONCUP/V,N,FMODE/C,Y,KDAMP $

 81  SAVE      NONCUP,FMODE

 82  ADD       AAAAA,CAMBER/PHIDH/C,Y,AOAP=(1.0,0.0)/C,Y,BETA=(1.0,0.0) $

 83  APD       EDT,EQDYN,ECT,BGPDT,SILD,USETD,CSTM,GPLD/EQAERO,ECTA,BGPA,SILA,
               USETA,SPLINE,AERO,ACPT,FLIST,CSTMA,GPLA,SILGA/V,N,NK/V,N,NJ/V,
               N,LUSETA/V,N,BOV $

 84  SAVE      NK,NJ,LUSETA,BOV $

 85  PARAM     //C,N,MPY/V,N,PFILE/C,N,0/C,N,1 $

 86  COND      SKPPLT,JUMPPLOT $

 87  PARAM     //C,N,MPY/V,N,PLTFLG/C,N,0/C,N,1 $

 88  PLTSET    PCDB,EQAERO,ECTA/PLTSETA,PLTPARA,GPSETSA,ELSETSA/V,N,NSIL1/V,N,
               JUMPPLOT $

 89  SAVE      NSIL1,JUMPPLOT $
```

```
    LEVEL 2.0 NASTRAN DMAP COMPILER - SOURCE LISTING


 90  PRTMSG   PLTSETA // $

 91  COND     SKPPLT,JUMPPLOT $

 92  PLOT     PLTPARA,GPSETSA,ELSETSA,CASECC,BGPA,EQAERO, ,,,,/PLOTX2/V,N,
              NSIL1/V,N,LUSETA/V,N,JUMPPLOT/V,N,PLTFLG/V,N,PFILE $

 93  SAVE     PFILE,JUMPPLOT,PLTFLG $

 94  PRTMSG   PLOTX2 // $

 95  LABEL    SKPPLT $

 96  COND     ERROP2,NOEED $

 97  GI       SPLINE,USET ,CSTMA,BGPA,SIL , ,GM,GO/GTKA/V,N,NK/V,N,LUSET $

 98  PARAM    //C,N,ADD/V,N,DESTRY/C,N,0/C,N,1/ $

 99  AMG      AERO,ACPT/AJJL,SKJ,D1JK,D2JK/V,N,NK/V,N,NJ/V,N,DESTRY/ $

100  SAVE     DESTRY $

101  PARAM    //C,N,SUB/V,N,INEQ/C,N,0/C,N,1 $

102  TRNSP    GTAKT/GTAK $

103  EQUIV    D1JK,CPPH/DESINT $

104  ADD      SAS,CPPH/THA/C,Y,ALPHA=(1.0,0.0)/C,Y,BETA=(-1.0,0.0) $

105  MPYAD    THA,SKJ,/TTAA/C,N,1/C,N,1/C,N,0/C,N,1 $

106  MPYAD    TTSAS,GTAK,/TSTAP/C,N,0/C,N,1/C,N,0/C,N,1 $

107  ADD      TSTAP,B9999/TSTA/C,Y,OC/C,Y,BETA=(0.0,0.0) $

108  MPYAD    AICMT,TTAA,/ATHA/C,N,1/C,N,1/C,N,0/C,N,1 $

109  MPYAD    TTAA,VTRA,/TVERA/C,N,0/C,N,1/C,N,0/C,N,1 $

110  MPYAD    TTAA,VTHA,/TVEHA/C,N,0/C,N,1/C,N,0/C,N,1 $

111  PARAM    //C,N,ADD/V,N,XQHHL/C,N,1/C,N,0 $

112  AMP      AJJL,SAS,D1JK,D2JK,GTKA,PHIDH,D1JE,D2JE,USETD,AERO/QHHLI,QKHLI,
              QHJLI/V,N,NOUE/V,N,XQHHL/V,Y,GUSTAERO=+1 $

113  SAVE     XQHHL $
```

BEST DOCUMENT AVAILABLE

```
LEVEL 2.0 NASTRAN DMAP COMPILER - SOURCE LISTING


114  MPYAD     CPPM,OKHLI,/OKKKI/C,N,1/C,N,1/C,N,0/C,N,1 $

115  MPYAD     TSTA,OKKKI,/PG/C,N,0/C,N,1/C,N,0/C,N,1 $

116  PARAMR    //C,N,MPY/V,N,RCAREA/V,Y,RC/V,Y,WAREA $

117  PARAMR    //C,N,MPY/V,N,OAREA/V,Y,WAREA/V,Y,0 $

118  PARAMR    //C,N,MPY/V,N,ORCAREA/V,N,RCAREA/V,Y,0 $

119  MPYAD     GTAK,OKKKI,/ELFL/C,N,0/C,N,1/C,N,0/C,N,1 $

120  MATPRN    OKKKI,ELFL,,,// $

121  GP4       CASECC,GEOM4,EQEXIN,GPDT,BGPDT,CSTM/RG,YS,USET,ASET/V,N,LUSET/
               V,N,MPCF1/V,N,MPCF2/V,N,SINGLE/V,N,OMIT/V,N,REACT/V,N,NSKIP/V,
               N,REPEAT/V,N,NOSET/V,N,NOL/V,N,NOA/C,Y,SUBID $

122  SAVE      MPCF1,MPCF2,SINGLE,OMIT,REACT,NSKIP,REPEAT,NOSET,NOL,NOA $

123  COND      ERROR9,NOL $

124  PARAM     //C,N,AND/V,N,NOSR/V,N,SINGLE/V,N,REACT $

125  PURGE     KFR,KLR,DR,DM/REACT/GM/MPCF1/GO,KOO,LOO,PO,UOOV,RUOV/OMIT/PS,
               KFS,KSS/SINGLE/QG/NOSR $

126  COND      LBL14,GENEL $

127  GPSP      GPL,GPST,USET,SIL/OGPST/V,N,NOGPST $

128  SAVE      NOGPST $

129  COND      LBL14,NOGPST $

130  OFP       OGPST,,,,,// $

131  LABEL     LBL14 $

132  EQUIV     KGG,KNN/MPCF1 $

133  COND      LBL15,MPCF2 $

134  MCE1      USET,RG/GM $

135  MCE2      USET,GM,KGG,,,/KNN,,, $

136  LABEL     LBL15 $
```

BEST DOCUMENT AVAILABLE

```
LEVEL 2.0 NASTRAN DMAP COMPILER - SOURCE LISTING


138  COND      LBL16,SINGLE $

139  SCE1      USET,KNN,,,/KFF,KFS,KSS,,, $

140  LABEL     LBL16 $

141  EQUIV     KFF,KAA/OMIT $

142  COND      LBL17,OMIT $

143  SMP1      USET,KFF,,,/GO,KAA,KOO,LOO,,,,, $

144  LABEL     LBL17 $

145  EQUIV     KAA,KLL/REACT $

146  COND      LBL18,REACT $

147  RBMG1     USET,KAA,/KLL,KLR,KRR,,, $

148  LABEL     LBL18 $

149  RBMG2     KLL/LLL $

150  COND      LBL19,REACT $

151  RBMG3     LLL,KLR,KRR/DM $

152  LABEL     LBL19 $

153  COPY      PG/PGI/DESINT $

154  PURGE     ULVI,UOOVI/IMEQ $

155  PURGE     PSI,ORI/IMEQ $

156  JUMP      LOOPTOP $

157  LABEL     LOOPTOP $

158  COND      FINIS,ELOOP $

159  SSG2      USET,GM,YS,KFS,GO,DM,PG/QR,PO,PS,PL $

160  SSG3      LLL,KLL,PL,LOO,KOO,PO/PHIOH,UOOV,RULV,RUOV/V,N,OMIT/
               V,Y,IRES=-1/V,N,NSKIP/V,N,EPSI $

161  SAVE      EPSI $

162  COND      LBL20,IRES $
```

```
LEVEL 2.0 NASTRAN DMAP COMPILER - SOURCE LISTING


163  MATGPR   GPL,USET,SIL,RULV//C,N,L $

164  MATGPR   GPL,USET,SIL,RUOV//C,N,O $

165  LABEL    LBL21 $

166  ADD      PHIDH,ULVI/ULVT $

167  ADD      PS,PSI/PSTT $

168  ADD      UOOV,UOOVI/UOOVT $

169  COND     LBL30,REACT $

170  ADD      QF,QRI/QPT $

171  LABEL    LBL30 $

172  PARAM    //C,N,ADD/V,N,XQHHL/C,N,1/C,N,0 $

173  AMP      AJJL,SAS,D1JK,D2JK,GTKA,PHIDH,D1JE,D2JE,USETD,AERO/QHHL,QKHL,
              QHJL/V,N,NOUE/V,N,XQHHL/V,Y,GUSTAERO $

174  SAVE     XQHHL $

175  MPYAD    CPPH,QKHL,/QKKK/C,N,1/C,N,1/C,N,0/C,N,1 $

176  MPYAD    TSTA,QKKK,/PG/C,N,0/C,N,1/C,N,0/C,N,1 $

177  ADD      PG,PGI/PGT $

178  ADD      QKKK,QKKKI/QKKKT $

179  MPYAD    PHIDH,PHIDH,/TNORV/C,N,1/C,N,1/C,N,0/C,N,1 $

180  PARAML   TNORV//C,N,DMI/C,N,1/C,N,1/V,N,SOVN $

181  PARAMR   //C,N,SQRT/V,N,VNSR/V,N,SOVN $

182  PRTPARM  //C,N,0/C,N,VNSR $

183  PARAMR   //C,N,LT/V,N,CHLOOP/V,N,VNSR/C,Y,ELOOP///V,N,FLAG $

184  COND     LBL50,FLAG $

185  PARAM    //C,N,ADD/V,N,IHEQ/C,N,0/C,N,1 $

186  PURGE    ULVI,PSI,UOOVI/IHEQ $

187  COND     LBL31,REACT $
```

```
     LEVEL 2.0 NASTRAN DMAP COMPILER - SOURCE LISTING


188  PURGE     QRI/IHED $

189  COPY      QRT/QRI/DESINT $

190  LABEL     LBL31 $

191  COPY      QKKKT/QKKKI/DESINT $

192  COPY      ULVT/ULVI/DESINT $

193  COPY      PGT/PGI/DESINT $

194  COPY      PSTT/PSI/DESINT $

195  COPY      UOOVT/UOOVI/DESINT $

196  REPT      LOOPTOP,10 $

197  LABEL     LBL5P $

198  MATPRN    QKKKT,ULVT,,,// $

199  PARAM     //C,N,ADD/V,N,NSKIP/C,N,0/C,N,1 $

200  JUMP      RECOVERY $

201  LABEL     RECOVERY $

202  SDR1      USET,PGT,ULVT,UOOVT,YS,GO,GM,PSTT,KFS,KSS,QRT/UGV,PGG,QG/
               V,N,NSKIP/C,N,STATICS $

203  PARAM     //C,N,ADD/V,N,NSKIP/C,N,1/C,N,1 $

204  REPT      RECOVERY,1 $

205  GPFOR     CASECC,UGV,KELM,KDICT,ECT,EQEXIN,GPECT,PGG,QG/ONRGY1,OGPFB1/
               C,N,STATICS $

206  OFP       ONRGY1,OGPFB1,,,,// $

207  SDR2      CASECC,CSTM,MPT,DIT,EQEXIN,SIL,GPTT,EDT,BGPDT,,QG,UGV,EST,
               XYCDB,PGG/OPG1,OQG1,OUGV1,OES1,OEF1,PUGV1/C,N,STATICS/V,N,
               NOSORT2=-1 $

208  SAVE      NOSORT2 $

209  COND      LBL21,NOSORT2 $

210  SDR3      OUGV1,OPG1,OQG1,OEF1,OES1,/OUGV2,OPG2,OQG2,OEF2,OES2, $
```

```
LEVEL 2.0 NASTRAN DMAP COMPILER - SOURCE LISTING

211  OFP      OUGV2,OPG2,OQG2,OEF2,OES2,//V,N,CARDNO $

212  SAVE     CARDNO $

213  XYTRAN   XYCDB,OPG2,OQG2,OUGV2,OES2,OEF2/XYPLTT/C,N,TRAN/C,N,PSET/V,N,
              PFILE/V,N,CARDNO $

214  SAVE     PFILE,CARDNO $

215  XYPLOT   XYPLTT// $

216  JUMP     OPLOT $

217  LABEL    LBL21 $

218  OFP      OUGV1,OPG1,OQG1,OEF1,OES1,//V,N,CARDNO $

219  SAVE     CARDNO $

220  COND     P2,JUMPPLOT $

221  LABEL    OPLOT $

222  PLOT     PLTPAR,GPSETS,ELSETS,CASECC,BGPDT,EQEXIN,SIL,PUGV1,,GPECT,OES1/
              PLOTX2/V,N,NSIL/V,N,LUSET/V,N,JUMPPLOT/V,N,PLTFLG/V,N,PFILE $

223  SAVE     PFILE $

224  PRTMSG   PLOTX2// $

225  LABEL    P2 $

226  MPYAD    ATMA,QKKKT,/TFACP/C,N,0/C,N,1/C,N,0/C,N,1 $

227  PARAML   TFACP//C,N,DMI/C,N,1/C,N,1/V,N,CLAA $

228  PARAMR   //C,N,DIV/V,N,CLACP/V,N,CLAA/V,Y,WAREA $

229  MPYAD    TVEMA,QKKKT,/TMACP/C,N,1/C,N,1/C,N,0/C,N,1 $

230  MPYAD    TVERA,QKKKT,/TRACP/C,N,1/C,N,1/C,N,0/C,N,1 $

231  PARAML   TMACP//C,N,DMI/C,N,1/C,N,1/V,N,ACMA $

232  PARAML   TRACP//C,N,DMI/C,N,1/C,N,1/V,N,ACRA $

233  PARAMR   //C,N,DIV/V,N,CMACP/V,N,ACMA/V,N,RCAREA $

234  PARAMR   //C,N,DIV/V,N,CRACP/V,N,ACRA/V,N,RCAREA $
```

```
    LEVEL 2.0 NASTRAN DMAP COMPILER - SOURCE LISTING

235  MPYAD     VGLS,PGF,/TFSGP/C,N,1/C,N,1/C,N,0/C,N,1 $
236  PARAML    TFSGP//C,N,DMI/C,N,1/C,N,1/V,N,ACLS $
237  PARAMR    //C,N,DIV/V,N,CLSGP/V,N,ACLS/V,N,OAREA $
238  MPYAD     VGMS,PGF,/FMSGP/C,N,1/C,N,1/C,N,0/C,N,1 $
239  MPYAD     VTM,FMSGP,/TMSGP/C,N,1/C,N,1/C,N,0/C,N,1 $
240  MPYAD     VTR,FMSGP,/TRSGP/C,N,1/C,N,1/C,N,0/C,N,1 $
241  PARAML    TMSGP//C,N,DMI/C,N,1/C,N,1/V,N,OACMS $
242  PARAML    TRSGP//C,N,DMI/C,N,1/C,N,1/V,N,OACRS $
243  PARAMR    //C,N,DIV/V,N,CMSGP/V,N,OACMS/V,N,ORCAREA $
244  PARAMR    //C,N,DIV/V,N,CRSGP/V,N,OACRS/V,N,ORCAREA $
245  PRTPARM   //C,N,0/C,N,CLACP $
246  PRTPARM   //C,N,0/C,N,CMACP $
247  PRTPARM   //C,N,0/C,N,CRACP $
248  PRTPARM   //C,N,0/C,N,CLSGP $
249  PRTPARM   //C,N,0/C,N,CMSGP $
250  PRTPARM   //C,N,0/C,N,CRSGP $
251  JUMP      FINIS $
252  LABEL     ERROR2 $
253  PRTPARM   //C,N,-2/C,N,FLUTTER $
254  LABEL     ERROR1 $
255  PRTPARM   //C,N,-1/C,N,FLUTTER $
256  LABEL     ERROR4 $
257  PRTPARM   //C,N,-4/C,N,FLUTTER $
258  LABEL     ERROR9 $
259  PRTPARM   //C,N,-3/C,N,STATICS $
260  LABEL     FINIS $
261  END       $
```

NASTRAN ON THE HEP

W. KEITH BROWN
RPK CORPORATION
ATHENS, GEORGIA

SUMMARY

Preliminary plans for the conversion of NASTRAN to DENELCOR's Heterogeneous Element Processor (HEP) are presented. First, a brief history of computer architecture is discussed. This will provide the reader an appreciation for the architecture of the HEP Computer System. Second, a description of the HEP Computer System is provided. Lastly, the preliminary NASTRAN conversion plans for link management, I/O management, memory management, and code optimization are discussed.

INTRODUCTION

The HEP was developed by Denelcor, Inc., and is based on a multiple instruction, multiple data stream architectural design. This design concept is compared in this paper with earlier architectural designs that are based on a single instruction, single data stream concept and on a single instruction, multiple data stream concept. The basic components of the HEP are described and include the Process Execution Module (PEM), the Data Memory Module, and the support processors, all of which are interconnected by a high-speed data switch network.

The conversion plans address the question of a multiple program design versus a single program design. The different I/O subsystems required in NASTRAN are briefly described and memory management of open core on the HEP is also discussed. Lastly, various functional modules and utilities are designated as candidates to be converted for parallelization.

COMPUTER ARCHITECTURES

The first computers executed a single instruction that operated on a single piece of data. This type of architecture is referred to as Single Instruction, Single Data Stream (SISD) and is shown in Figure 1. Use of "look ahead" capabilities helped the throughput of SISD computers but "look ahead" fails to be useful for programs with many test and branch instructions. The next architectural design to be developed is referred to as Single Instruction, Multiple Data Stream (SIMD). This design allows for a single instruction to process multiple data simultaneously. This is shown in Figure 2. A new design concept in computer architecture has been developed and is referred to as Multiple Instruction, Multiple Data Stream (MIMD). This design allows for different instructions to execute in parallel and to operate on different pieces of data simultaneously (see Figure 3).

The HEP is based on a MIMD architecture. A program may take advantage of this capability during execution by establishing processes that may execute in parallel. To allow for interprocess communication, each data memory location has not only a value but also a state associated with it. The state may be "full" or "empty". Before data can be stored, the state of the data memory address must be "empty". Similarly before data can be read, the state of the data memory address must be "full". Arbitration of memory is handled by hardware and does not effect the execution of unrelated instructions.

HEP COMPUTER SYSTEMS

Figure 4 shows the basic components of the HEP computer systems. The Process Execution Module (PEM) is comprised of memory units, control units, and function units. There may be from 1 to 16 PEMs in one HEP Computer System. The memory unit is divided into three parts (see Figure 5) consisting of program, register, and constant memories. All memories of the HEP are comprised of 64-bit words. Program memory ranges from 32K to 1024K words, with a single error correcting and double error detecting (SECDED) capability (see Reference 1). There are 4096 words of constant registers and 2048 general purpose registers. A PEM is capable of processing up to 10,000,000 instructions per second. A PEM can also process up to a maximum of 16 tasks (or jobs) and up to a maximum of 60 user and 60 supervisor processes simultaneously (see Reference 2). A process is equivalent to a program on a SISD computer. A task is a complete user job that may be comprised of many job steps.

"A PEM supports multiple processes by time-multiplexing its control and execution hardware. Each process is periodically given a chance to execute an instruction; the logic of the PEM is pipelined so that several processes are in different phases of instruction execution at any moment. A user may create and terminate processes dynamically without operating system intervention. A minimum of eight processes are required to keep the PEM execution logic fully occupied, and to achieve 10 million instructions per second."[1]

The function unit performs the operations required for executing instructions.

The Switch is a network of programmable nodes used for transmitting messages and data among the PEMs, data memory, and the peripheral subsystems (see Reference 2).

A Data Memory Module contains 32K to 1024K words, SECDED. There may be a maximum of 128 Data Memory Modules per HEP Computer System or a maximum of 128 * 1020K = 131,072K words.

The I/O Cache component is established to buffer data from mass storage devices that have relatively slow transfer rates to the Switch.

The External I/O component provides the interface between mass storage devices and the Switch.

NASTRAN CONVERSION

The conversion of NASTRAN to the HEP will be done by a two phase development approach. The first phase is to get NASTRAN executing on the HEP without optimization for parallelization. The second phase is to optimize NASTRAN for parallelization. Phase one includes the program management design, the I/O management, and memory management. Phase two includes converting designated utilities and NASTRAN functional modules for parallelization. Further consideration is required for this phase.

LINK MANAGEMENT

HEP can have a range of 32K to 1024K words for program memory. Since program memory contains only code and not data, two approaches are being considered for installing NASTRAN. The first approach assumes that NASTRAN will be developed on the HEP as one program and the second approach assumes that NASTRAN will be developed as multiple programs that dynamically chain themselves.

One Program Concept

The CDC, VAX, and UNIVAC versions of NASTRAN have 15 programs that dynamically chain themselves. The programs are referred to as link 1, link 2, ... link 15, respectively. On the UNIVAC, each link has an instruction bank (I-Bank) and a data bank (D-Bank) of memory. Comparison with the UNIVAC is convenient since the UNIVAC I-Bank contains instructions of the program and serves the same purpose as program memory on the HEP. Furthermore, each assembly language instruction on the UNIVAC requires one word of memory and this is true for the HEP also. The total accumulative 36-bit word sizes of the I-Bank and D-Bank for each of the UNIVAC links are shown in Table 1. The combined lengths of the I-Banks for all links is 1,259,509 words. Approximately, 38000 words of code are common among all links. Consequently, approximately 727,509 words are required for NASTRAN to be one program. A question to be addressed is what is the minimum amount of program memory a user should have on his HEP in order to execute NASTRAN. Assuming a one program version of NASTRAN, then approximately 296,491 words of the maximum program memory available remain for future expansions to NASTRAN. For comparisons, the subsonic and supersonic aeroelastic capability installed required approximately 65,000 words of program memory and the substructuring capability required approximately 90,000 words of program memory.

One other point to be made is that the HEP loader will be required to process over 1500 subroutines and approximately 100 labeled common blocks.

Similarly, it can be seen from Table 1 that the total length of the D-Bank is 673,508 words. Approximately 25000 words of memory are common in each of the links and consequently, 323,508 words of data memory is necessary. This is a maximum because the D-Bank will contain data that may be part of the HEP Data Memory Module or the HEP constant registers. These estimates do not include allowances for open core.

Multiple Program Concept

A multiple program concept will be similar to the CDC, VAX, and UNIVAC versions. Each program will be a link for conformity and ease of maintenance. This design concept eliminates the need for large amounts of program memory to be available on the HEP for NASTRAN. The HEP program sizes should be comparable to the UNIVAC link sizes.

I/O MANAGEMENT

NASTRAN may require up to approximately 60 external files to be assigned during a given execution. It may be possible that up to approximately 16 files may be opened simultaneously. Use of most of these files is done through machine dependent I/O. NASTRAN has the following I/O subsystems that support these files:

1. Generalized I/O subsystem (GINO)
2. Matrix packing/unpacking subsystem (PAKUNPK)
3. Substructure I/O subsystem (SOFIO)
4. General purpose plotter I/O
5. Standard Fortran read, write and punch capabilities

Figure 6 shows the relationship of the various I/O subsystems to the NASTRAN functional modules. All modules use the GINO subsystem. Only selected plotting functional modules use the plotter I/O subsystem and only selected substructuring modules use the substructure I/O subsystem. All matrices to be stored and read are referenced through the PAKUNPK capability that packs and unpacks matrix data. PAKUNPK is a preprocessor to the GINO I/O subsystem.

GINO Subsystem

Tables 2 and 3 provide a list of the subroutine interfaces required in the GINO subsystem. Each of these subroutines must be designed for the HEP version of NASTRAN.

PAKUNPK Subsystem

Table 4 provides a list of the subroutine interfaces required in the PAKUNPK subsystem. Each of these subroutines must be designed for the HEP version of NASTRAN.

Substructure I/O Subsystem

Substructure I/O is implemented through the use of Fortran direct access I/O on some of the versions of NASTRAN. In Figure 6, the code that does the I/O is labeled as HEPSIO. HEPSIO must be designed and built.

Plotter I/O

NASTRAN currently only supports the NASTRAN general purpose plotter capability. The I/O requirement for this capability is processed through a direct buffer read and write type of I/O. This must be built on the HEP by making use of the HEP Fortran BUFFERIN and BUFFEROUT statements.

MEMORY MANAGEMENT

Open core is working storage for NASTRAN functional modules. On all versions of NASTRAN, except the VAX version, open core allocation is based upon the memory allocation provided by the user in his JCL. The larger the allocation requested for memory in the JCL, the larger the allocation for open core. The VAX version has all open core defined by a single labeled common block that can be dimensioned as needed. The same concept is recommended for the HEP version.

OPTIMIZATION TECHNIQUES

Table 5 shows candidate utilities for conversion to parallelization. In addition to these, specific functional modules, such as the eigenvalue extraction module and the element matrix generator and assembler, are to be analyzed for conversion. Further study is to be done in this area.

CONCLUDING REMARKS

The HEP Computer System is designed for fast throughput and the ability to solve large and complex problems. The conversion of NASTRAN to the HEP that has been discussed in this paper will be a great asset to those who are potential users of the HEP.

REFERENCES

1. *Heterogeneous Element Processor Principle of Operations*, Publication number 9000001, April 1982.

2. *HEP Concepts and Facilities*, Publication number 9000005, February 13, 1982.

3. *The NASTRAN Programmer's Manual*, NASA SP-222(03), July 1976.

Link	I-Bank	D-Bank
1	98976	133436
2	78344	34150
3	48994	25648
4	61664	23476
5	89738	45291
6	71593	26512
7	67978	25501
8	128814	80430
9	98258	29667
10	70292	25594
11	95959	29263
12	40382	25680
13	124516	75576
14	45726	43908
15	129275	49376
Total	1259509	673508

Common to Each I-Bank is 38000

Common to Each D-Bank is 25000

Table 1. Level 17.7 UNIVAC I and D-Bank Allocations (in 36 Bit-Words)

Entry Point	Description
BCKREC	Positions the requested file backward one logical record
CLOSE	Terminates activity on the requested file
EOF	Writes an end-of-file on the requested file
FILPOS	Positions the requested file to the stated position
FWDREC	Positions the requested file forward one logical record
GETURN	Finds the unit reference number for the requested file
QOPEN	Initiates activity on a requested file
RDBLK	Reads a physical block from the requested file
READ	Reads a logical record or part of a logical record from the requested file
RECTYP	Determines the type of logical record at which the requested file is positioned
REWIND	Rewinds the requested file
SAVPOS	Saves the current position of the requested file
SKPFIL	Positions the requested file forward or backwards a stated number of files
WRITE	Writes a logical record or a part of a logical record to the requested file
WRTBLK	Writes a physical block to the requested file

Table 2. GINO Subsystem Non-Matrix Interfaces

Entry Point	Description
ENDGTB	Terminates processing a string furnished by GETSTB
ENDGET	Terminates processing a string furnished by GETSTR
ENDPUT	Terminates processing a string furnished by PUTSTR
GETSTB	Returns the pointer to the last element in the string
GETSTR	Returns the pointer to the first element of the string
PUTSTR	Allows for writing a string directly into the buffer

Table 3. GINO Subsystem Matrix Interfaces

Entry Point	Description
BLDPK	An initialization call required for each column to be packed
BLDPKI	Supplies a single element of the column to be packed
BLDPKN	Terminates processing of a column
INTPK	An initialization call required for each column to be read and interpreted
INTPKI	Reads successive non-zero elements of the column
PACK	Packs a column of a matrix
UNPACK	Unpacks a column of a matrix
ZBLPKI	Provides a single element of a column to be packed (single matrix capability)
ZNTPKI	Reads successive non-zero elements of the column (single matrix capability)

Table 4. PAKUNPK Subsystem Interfaces

Subroutine	Description
ATEIG	Finds the eigenvector of an upper Hessenberg matrix
BISLOC	Performs a binary search
CDCOMP	Performs a complex matrix decomposition
DECOMP	Performs an unsymmetric matrix decomposition
EGNVCT	Calculates eigenvectors
ELIM	Performs a matrix reduction
FACTOR	Decomposes a matrix into triangular factors
FBS	Forward - backward substitution
GFBS	General forward - backward substitution
GMMATC	General Matrix multiply and transpose - complex
GMMATD	Double precision of GMMATC
GMMATS	Single precision of GMMATC
HSBG	Reduce a matrix to upper Hessenberg form
INVERD	Double precision matrix inversion
INVERS	Single precision matrix inversion
LSPLIN	Produces an interpolation matrix
MPYAD	Matrix multiplication capability
MPY3	Triple matrix multiply
SDCOMP	Symmetric matrix decomposition
SOLVER	Simultaneous equation solution routine
SSPLIN	Produces an interpolation matrix
TRNSP	Matrix transposition

Table 5. Candidate Utilities for Converting to Use of Parallel Processing

SINGLE INSTRUCTION, SINGLE DATA STREAM

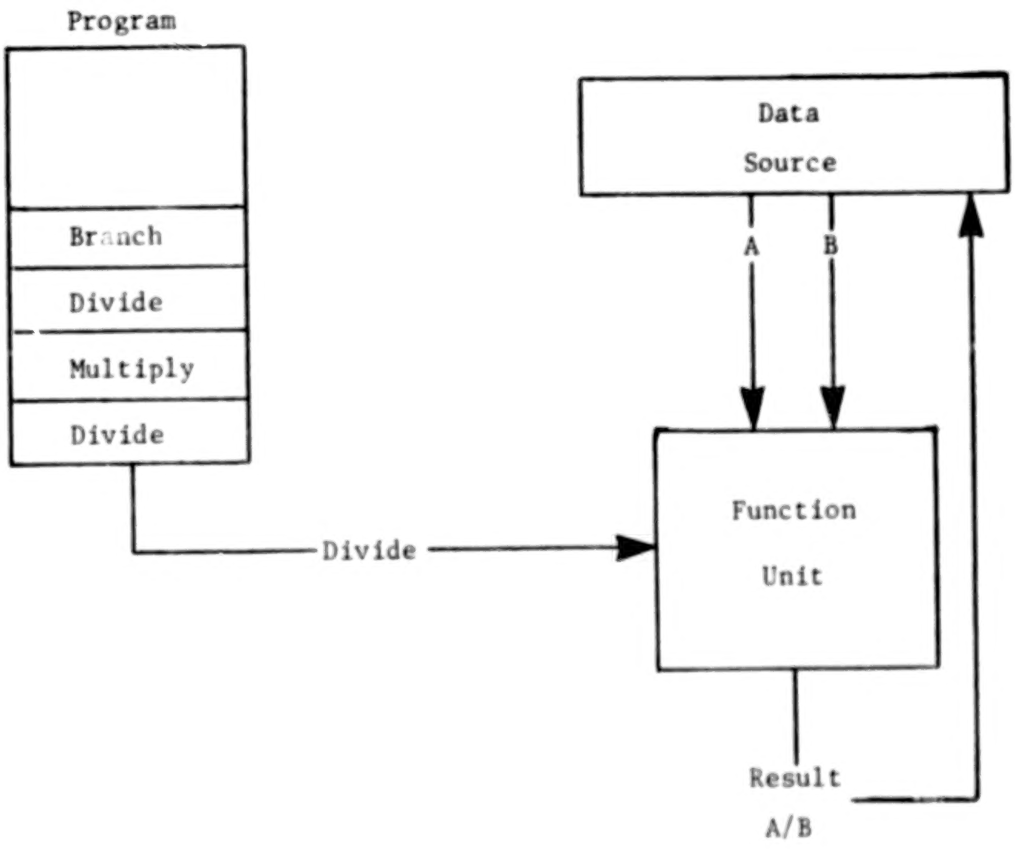

Figure 1

ARCHITECTURE FOR A SISD
COMPUTER SYSTEM

SINGLE INSTRUCTION, MULTIPLE DATA STREAM

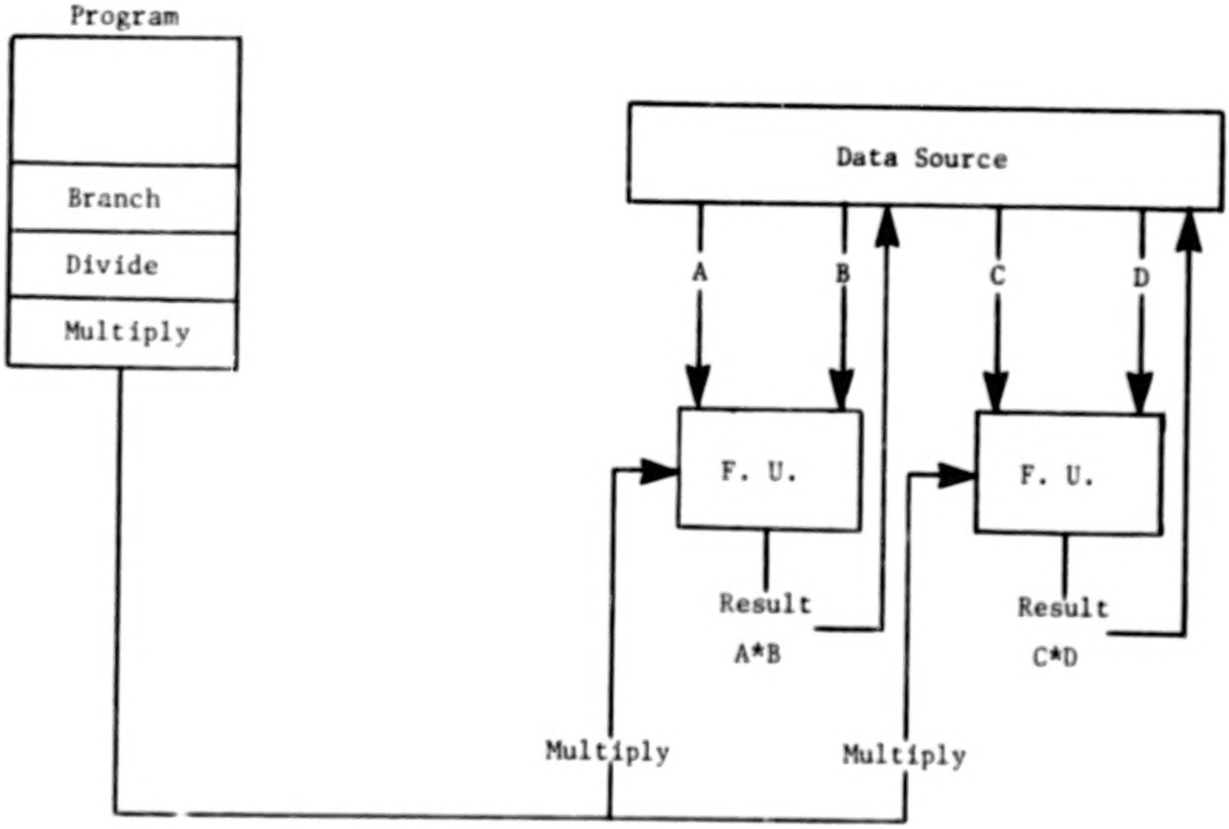

Figure 2

ARCHITECTURE FOR A SIMD
COMPUTER SYSTEM

MULTIPLE INSTRUCTION, MULTIPLE DATA STREAM

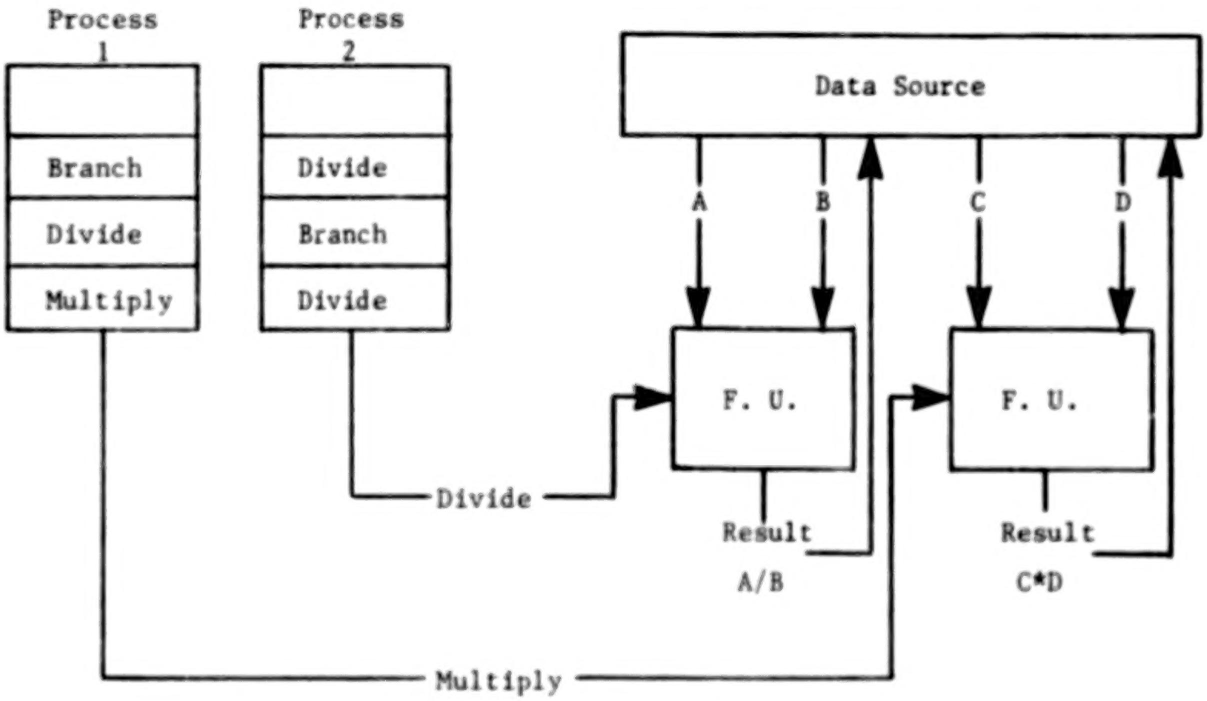

Figure 3

ARCHITECTURE FOR A MIMD
COMPUTER SYSTEM

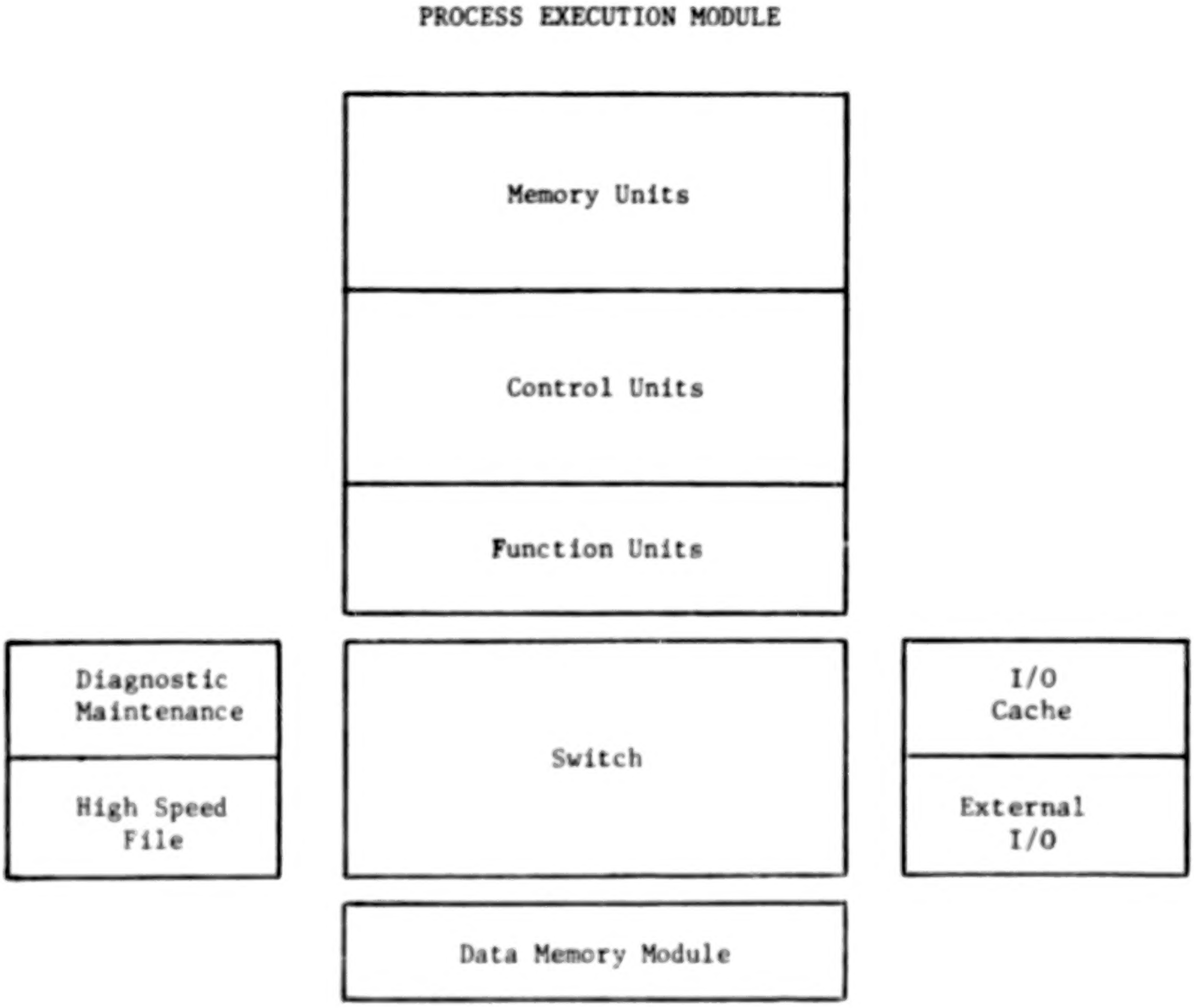

Figure 4

The HEP Computer

PROCESS EXECUTION MODULE STRUCTURE

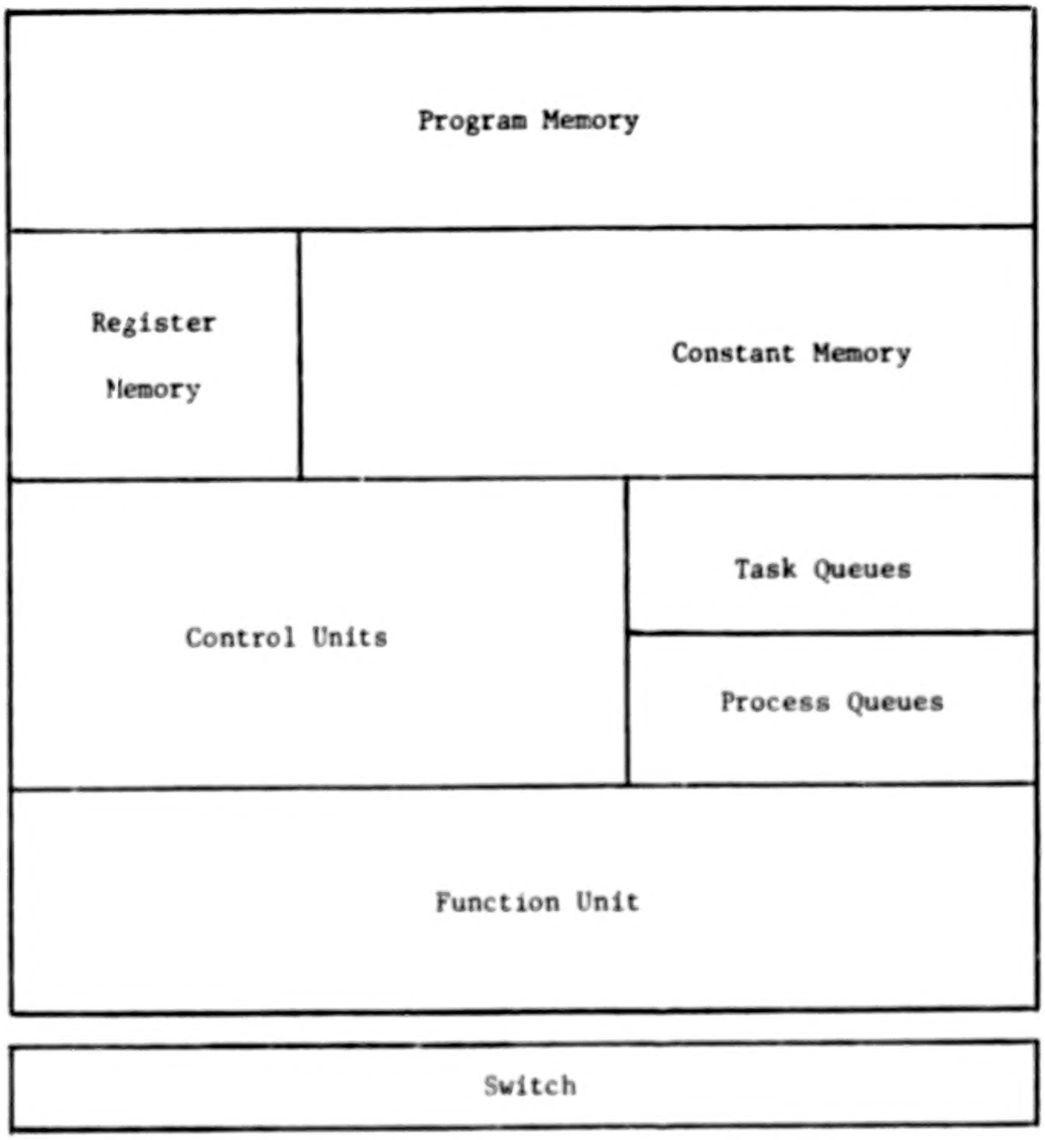

Figure 5

STRUCTURE OF A PEM
COMPUTER SYSTEM

BEST DOCUMENT AVAILABLE

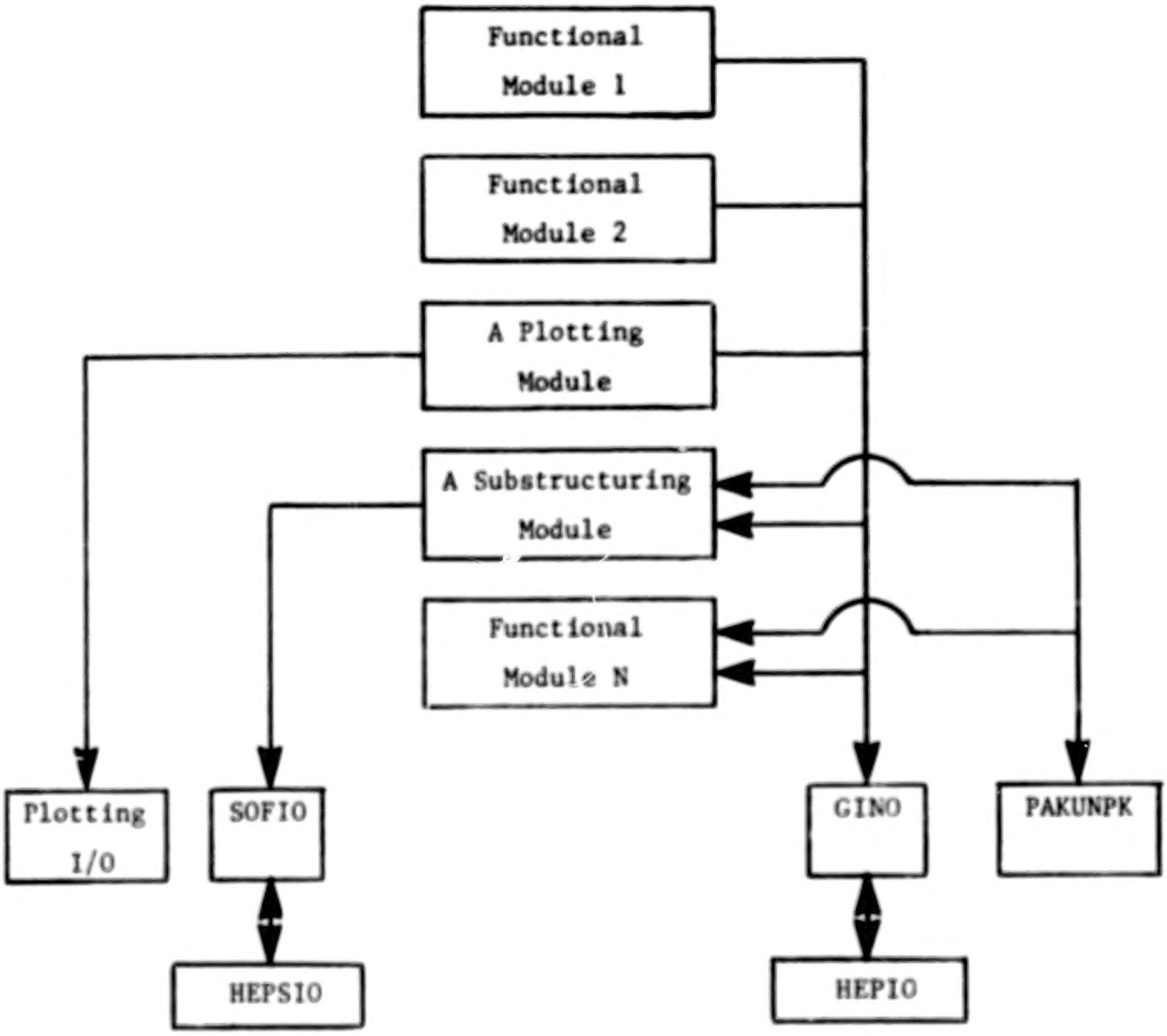

Figure 6

NASTRAN I/O SUBSYSTEMS

THE USAGE OF SUBSTRUCTURING ANALYSES IN THE GET AWAY SPECIAL (GAS) PROGRAM

Nelson J. Ferragut
Goddard Space Flight Center

SUMMARY

The use of automatic multi-stage substructuring analysis (reference 1) was demonstrated for a hypothetical case of a GAS container supported by structural channels with a simulated experimental package inside the container. The GAS Program purpose was stated and potential candidate structures to support experimental packages were discussed. The GAS container model shown in Figure 1 and the substructuring analysis capabilities of NASTRAN make it possible to study the experiments inside the container as well as the design constraints resulting from the support structures holding the containers. The use of substructuring in the GAS Program could be an important factor in increasing the number of flight opportunities.

INTRODUCTION

The U.S. Space Shuttle will be used as a workhorse in space. When fully operational it will perform numerous missions per calendar year. The GAS Program was developed to support self-contained experiments with minimum interfaces with the orbiter and very low cost. The purpose of the GAS as stated in the GAS Users Handbook (reference 2) is to:

- Encourage the use of space by all researchers, private individuals and organizations;
- Foster enthusiasm in younger generation;
- Increase knowledge of space;
- Be alert to possible growth of GAS investigation into a prime experiment;
- Generate new activities unique to space.

The experiments to be flown in the GAS containers will be the primary responsibility of the experimenters. The GAS container is intended to provide an environment to the experimenter; it takes into consideration all requirements for the safety of the U.S. Space Shuttle. The GAS Program personnel must consider the interfaces with the experimenters (or GAS users) and with the Shuttle Transportation System.

The example under consideration is shown in Figure 1 as a subcomponent of an Across-the-Bay structure, which can be considered as a possible carrier of a greater number of cans in a six-pack configuration as shown in the schematic representation in Figure 2. This Across-the-Bay structure was studied further by assuming a twelve-pack configuration using automatic multi-stage substructuring. The additional analysis for the twelve-pack configuration was almost trivial due to the use of substructuring analysis techniques. This paper shows what can be done with substructuring analysis. The substructuring analyses techniques developed in NASTRAN are specially useful in programs such as the GAS Program where the same type of structure will be used in many different flight configurations, many of them unforeseen at this time. By developing proper modeling techniques at this time, we will be able to assist in the development of new flight opportunities for the GAS Program.

DISCUSSION

Two sample problems were considered:

- The first one was shown in Figure 1 and consisted of a substructure which can be built up to form an Across-the Bay structure for the U.S. Space Shuttle.
- The second consisted of half of a structure which could form an Across-the-Bay structure. Symmetry was used to limit the number of degrees of freedom.

The first example was developed to study future interactions with experiments to be flown in the GAS containers. The second example was part of a feasibility study to determine if the GAS containers could be used as an integral part of an Across-the-Bay structure where the GAS containers contribute to the build up of the structure and were assumed to be rigid.

The results in the preliminary phase of the feasibility study were very encouraging. It was shown that with additional structural modifications it could be possible to raise the structural natural frequencies to levels in the neighborhood of 25 Hz.

When the containers were considered to be rigid in the feasibility study (second case), the connections were made from the center of the can to the brackets by assuming offsets in CBAR elements.

In the case of the more detailed container (first case), it was necessary to make sure that all degrees of freedom of rotation in the transition regions between beams and plates would satisfy the Euler's Beam Theory, which states that the rotation across the beam will be the same for all points on a transverse plane with no warping taking place. Also, when applying substructuring, it is important for the proper fit of subcomponents that all points matching at the boundaries have available the same degrees of freedom.

In applying substructuring analysis, care must always be exercised when putting a model together:

- All grid points joining substructures must be expressed in the basic global coordinate systems.
- No singularities must be left unresolved before making a solution run in phase 2.
- For better compatibility of subcomponents all degrees of freedoms must be accounted for at all boundary interfaces.

The model used for 1/8 of a container plus attachments in case 1 consisted of 209 GRID's, 117 CQUAD2's, 107 CTRIA2's and 32 CBAR's. The model used for the feasibility study of an Across-the-Bay structure for the U.S. Space Shuttle considering symmetry and assuming rigid containers (case 2) consisted 42 GRID's and 69 CBAR's.

Table 1 shows the most important parts of the substructuring decks in the NASTRAN runs. The model shown in Figure 1 consists of one eighth (1/8) of the model to be expanded in consecutive runs to obtain one quarter (1/4), one half (1/2) and finally the full model. The model developed has enough detail to be able to model any attachments to the interior and to the exterior of the container.

The second model resulted from a request to look at a twelve-pack configuration after the results were obtained for a six-pack configuration for an Across-the-Bay structure in the U.S. Space Shuttle. The fact that substructuring analyses capabilities were available made it simple to run the new analysis. A new coordinate system was defined using a GRIDSET Card and then the twelve-pack configuration was generated using the SYMTRANSFORM Command.

Some of the structures that are suggested to experimenters to put inside the GAS container are discussed in reference 2. Future work will include the use of some structures actually designed for experiments inside the GAS container. But for now it was only assumed that the experiment could be modeled by a beam structure attached to the top plate of the GAS container.

CONCLUSION

The GAS container has already flown in the STS-3 Shuttle mission on a GAS Beam Structure similar to that shown in Figure 4. Additional flight opportunities are expected in the future and many payload carriers are being considered as potential candidates. The use of substructuring will assist us in the tasks ahead .

Because of future developments in the GAS Program, it will be necessary to evaluate modal synthesis analyses techniques needed to develop simplified models which could be utilized to perform load analyses with U.S. Space Shuttle interfaces and at the same time provide the experimenters with models which could be used to verify the structural integrity of their packages analytically. Further developments are required to achieve these goals. The automatic multistage substructuring analysis has already been used successfully in some tasks in the GAS Program as previously stated, but much work is still required to fulfill future requirements of the GAS Program with greater ease.

REFERENCES

(1) The NASTRAN Users Manual (Level 17.5), NASA SP-222(05), Dec. 1978.

(2) Get Away Special (GAS) Small Self-Contained Payloads Experimenter Handbook, National Aeronautics and Space Administration, Goddard Space Flight Center, October 1979.

Figure 1-A. GAS Structural Model, Cylinder Details

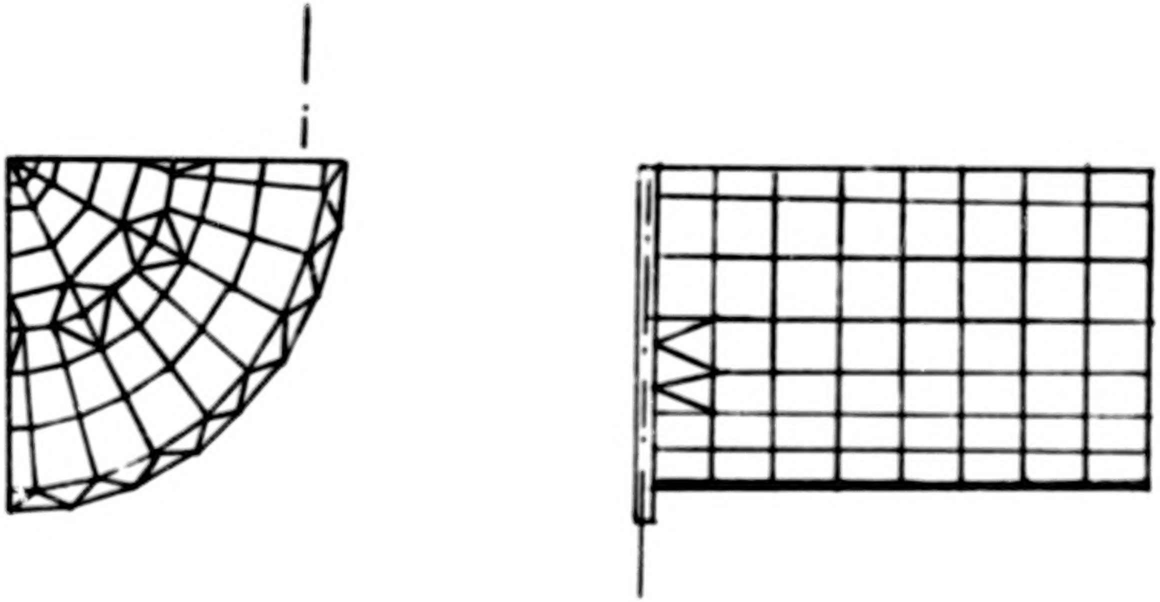

BLANK PAGE

BLANK PAGE

BLANK PAGE

Figure 1-B. GAS Structural Model, Bracket Deatils

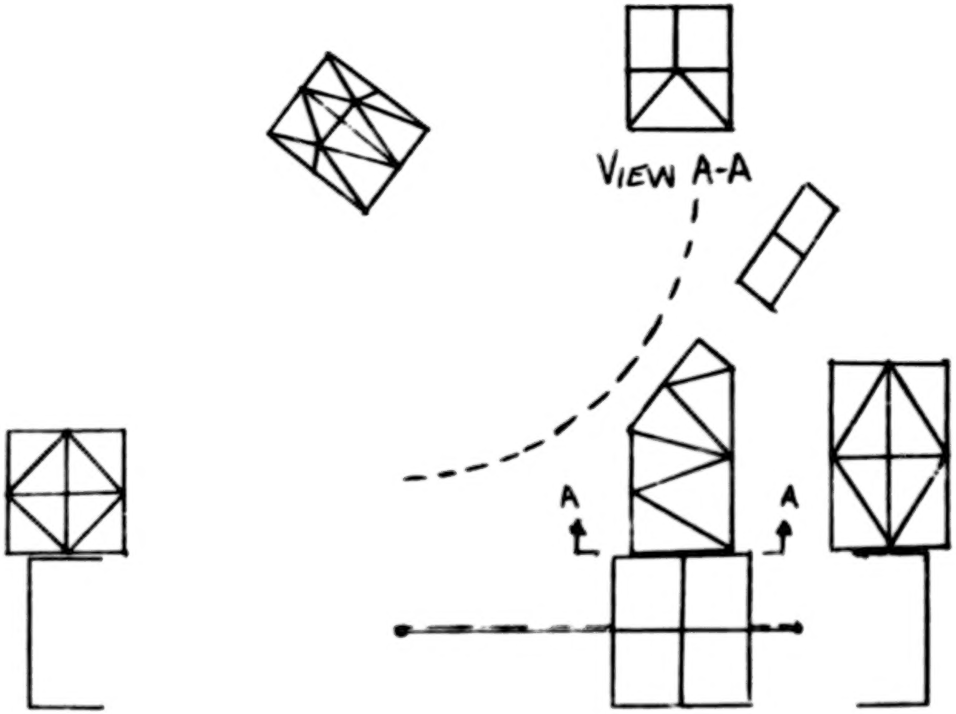

Figure 1-C. GAS Structural Model, Channel Details

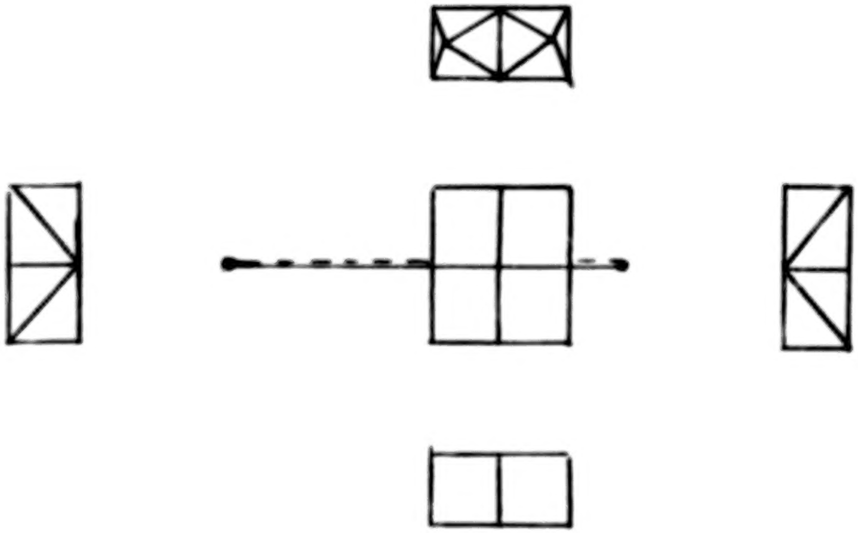

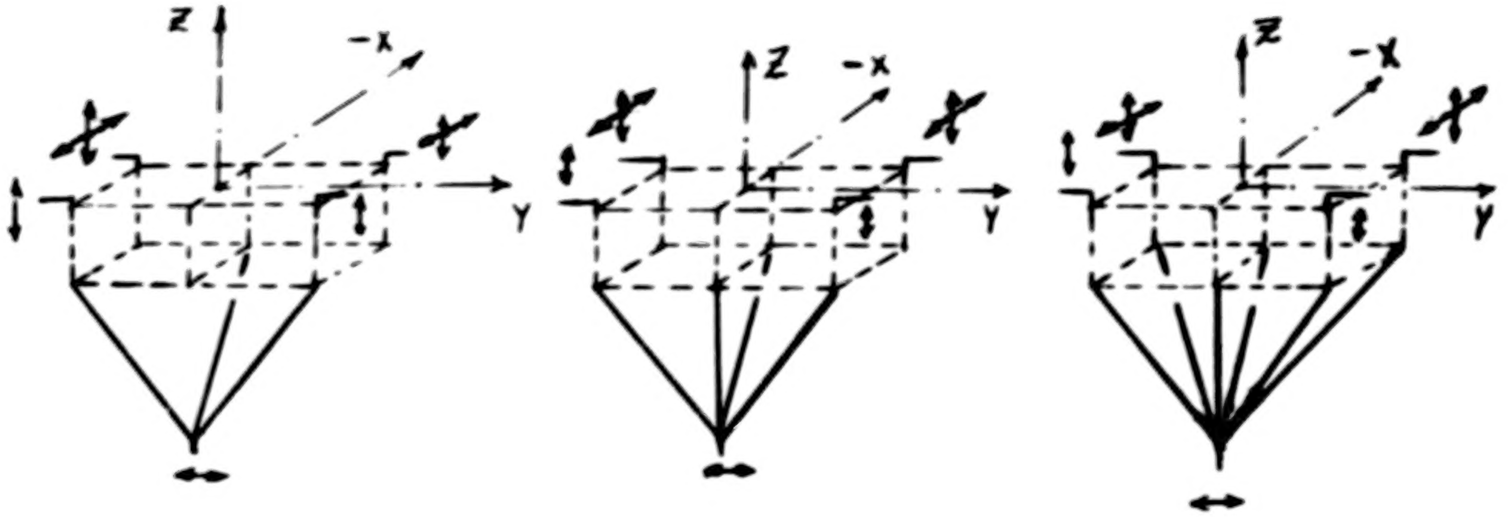

Single Tripod

Single Tripod with Center Member

Double Tripod

Figure 2. GAS Bottom Support Structures for Six-Pack Across-the-Bay Configuration.

BEST DOCUMENT AVAILABLE

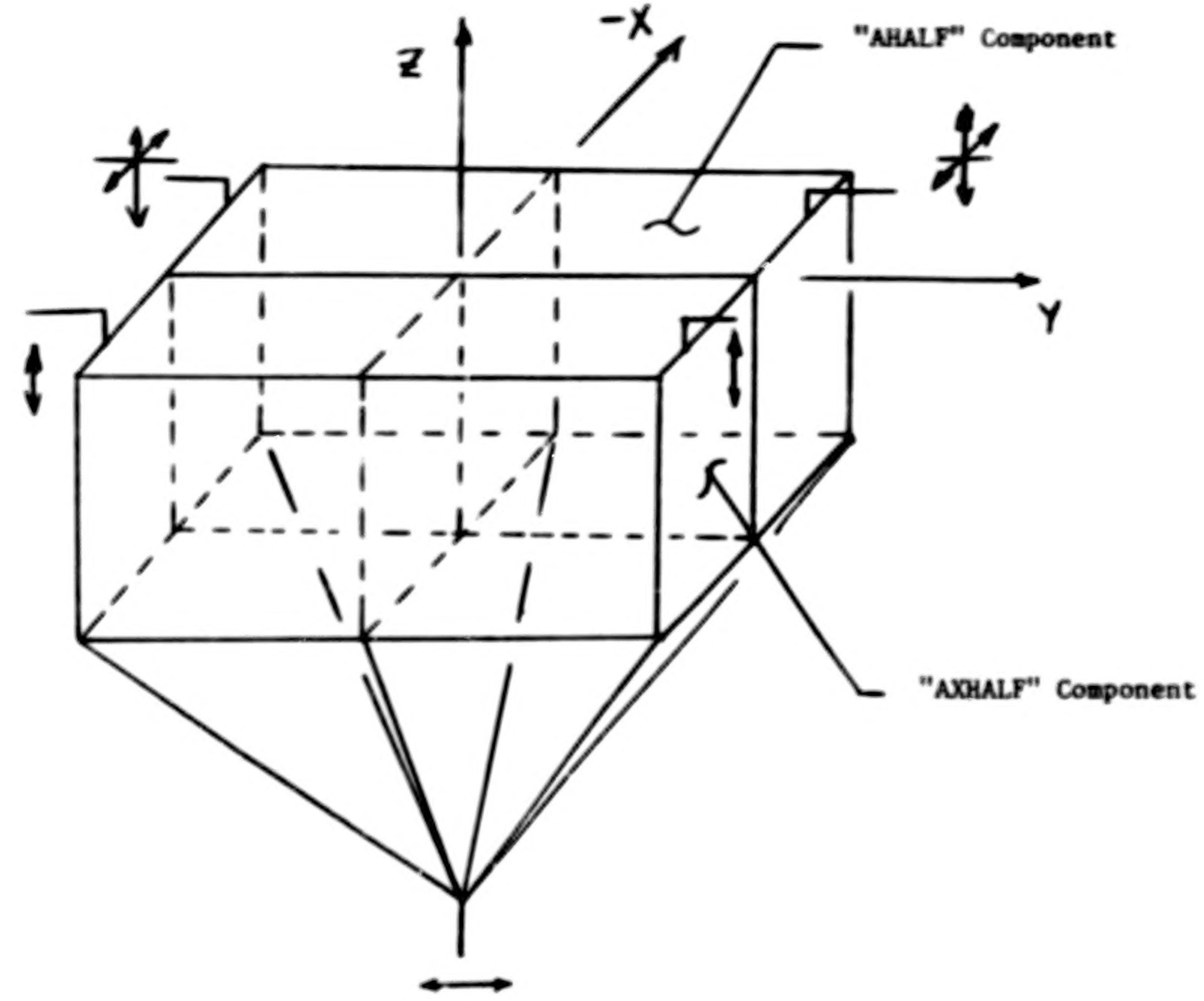

Figure 3. "Two Tripod" Overall Bottom Support for Twelve-Pack Across-the-Bay Configuration

GET AWAY SPECIAL
GAS
CONTAINER/ADAPTER BEAM ASSEMBLY

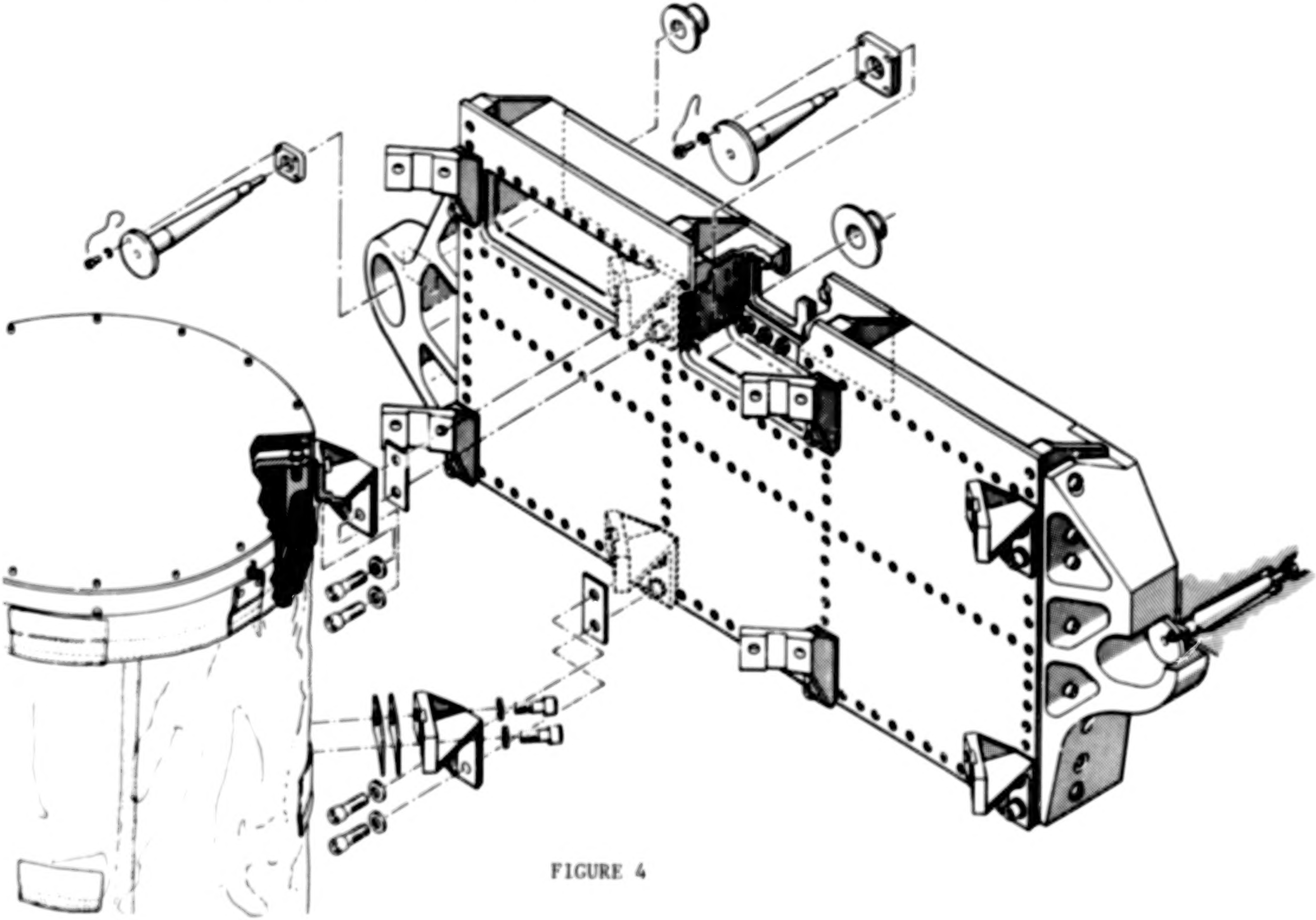

FIGURE 4

213

TABLE 1. SUBSTRUCTURING DECKS

Loading One-Eighth of Container Structure

```
SUBSTRUCTURE PHASE1
SOF(1)=  FT18,4000,NEW
PASSWORD= BCKT
NAME= CE
SAVEPLOT= ALL
SOFPRINT TOC
ENDSUBS
```

Loading the Equivalent Experiment Structure

```
SUBSTRUCTURE PHASE1
SOF(1)=  FT18, 4000
PASSWORD= BCKT
NAME= EXP
SOFPRINT TOC
ENDSUBS
```

Building Up the GAS Container

```
SUBSTRUCTURE PHASE2
SOF(1)=  FT18, 20000
PASSWORD= BCKT
OPTIONS= K,M,P
SOFPRINT TOC
EQUIV CE, XCE
     PREFIX= X
     COMBINE CE,XCE
     NAME= QEX
     TOLER= .001
          COMPONENT XCE
          SYMT= X
SOFPRINT TOC
EQUIV QEX,YQEX
     PREFIX= Y
     COMBINE QEX,YQEX
     NAME= TE
     TOLER= .001
          COMPONENT YQEX
          SYMT= Y
SOFPRINT TOC
```

```
EQUIV TE,ZTE
     PREFIX= Z
     COMBINE TE,ZTE
     NAME= CAN
     TOLER= .001
          COMPONENT ZTE
          SYMT= Z
OUTPUT= 2,7,11,12,14
SOFPRINT TOC
ENDSUBS
```

TABLE 1. SUBSTRUCTURING DECKS

(CONTINUED)

Tie-Up of Experiment with GAS Container

```
     SUBSTRUCTURE PHASE2
     SOF(1)=  FT18, 20000
     PASSWORD= BCKT
     OPTIONS= K,M,P
     SOFPRINT TOC
          COMBINE EXP,CAN
          NAME= GAS
          TOLER= .1
     SOFPRINT TOC
     ENDSUBS
```

Running a Static Solution

```
     SUBSTRUCTURE PHASE2
     SOF(1)=  FT18, 20000
     PASSWORD= BCKT
     SOFPRINT TOC
     SOLVE GAS
     SOFPRINT TOC
     RECOVER GAS
          PRINT CE
               DISP= ALL
               SPCF= ALL
               OLOA= ALL
          PRINT EXP
               DISP= ALL
               SPCF= ALL
               OLOA= ALL
          SAVE CE
     SOFPRINT TOC
     ENDSUBS
```

Recovering Stresses from Basic Substructure

```
     SUBSTRUCTURE PHASE3
     SOF(1)=  FT18, 20000
     PASSWORD= BCKT
     SOFPRINT TOC
     BRECOVER CE
     ENDSUBS
```

USING NASTRAN TO SOLVE SYMMETRIC STRUCTURES WITH NONSYMMETRIC LOADS

by

Thomas G. Butler
BUTLER ANALYSES

This paper deals with reflective dihedral symmetry; not rotational nor cyclic symmetry. There is nothing new about this until we talk about nonsymmetrical loads on symmetrical structures. In principal this too is an old topic, but I choose to talk about it, because I get a look of disbelief from clients when I tell them that I can legitimately confine such analyses to a half, quarter, or an octal segment. I tried to give these people a reference to consult and found none. Such reactions convinced me that it was worth while to air this topic in the open literature.

For completeness sake, I plan to start with a simple example, then explore those areas where the analyst must make his decisions, and conclude with a rather involved application.

In order to convince you that this approach to analysis is legitimate, I offer an argument from strength of materials based on a nonsymmetrically loaded simply supported prismatical beam.

LAW: For reflective dihedral symmetry in linear structures under non-symmetric loads, the response in any part of the whole structure can be determined by solving a unit segment of the symmetrical structure for all permutations of symmetric and antisymmetric boundary conditions with the nonsymmetric load in place for all of them by properly combining results of the permuted solutions.

The nub of this law rests on another law from tensor analysis that says that any nonsymmetric load can be decomposed into a symmetrical set plus an antisymmetrical set.

While in the process of defining, it would be well to distinguish anti-symmetrical from non-symmetrical and to be specific about the kind of symmetry being dealt with.

First of all our concern is for symmetry of elastic deformation. As a consequence, such actions as axial, bending, membrane, and torsional deformations need examining. As such, we will talk in terms of modes of deformation. Modes can be described in general by using "+" and "-" signs for opposite actions. For example, in bending "+" can stand for tension and "-" can stand for compression, or in axial deformation "+" can stand for condensation and "-" can stand for rarefaction, etc.

Symmetry maps the elastic deformations on one side of the plane of symmetry (p.o.s.) into like values on the opposite side of the p.o.s. at corresponding distances perpendicular to the p.o.s.

$D[x=(p-d),y,z] = D[x=(p+d),y,z]$ will be written in abbreviated notation as

$D(p-d) = D(p+d)$ SYMMETRIC ELASTIC DEFORMATION

where D can represent any elastic deformation; p is the location of the p.o.s.; and d is the distance away from the p.o.s., all measured perpendicular to the p.o.s.

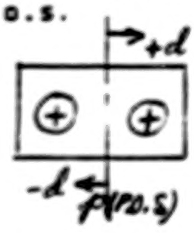

OR

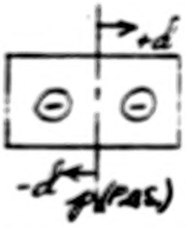

Antisymmetry maps the elastic deformations on one side of the p.o.s. into like values -- but of opposite sign -- on the opposite side of the p.o.s. at corresponding distances perpendicular to the p.o.s.

$D(p-d) = (-1)D(p+d)$ ANTISYMMETRIC ELASTIC DEFORMATION

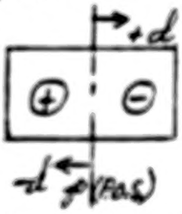

OR

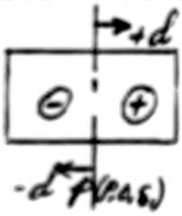

BOUNDARY CONDITIONS AT THE PLANE OF SYMMETRY

The first task is to translate these elastic actions into boundary conditions on displacements at the p.o.s. for the unit segment of the structure. Start with bending in the XY plane for a beam colinear with the x-axis.

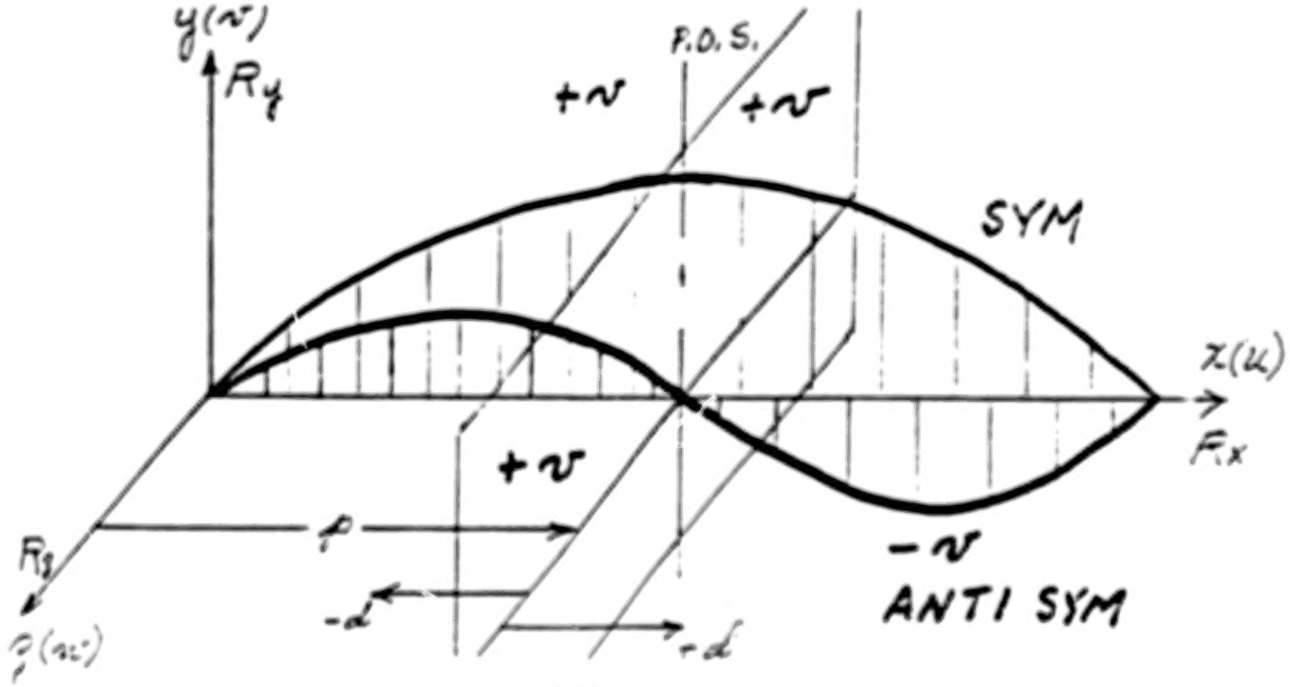

The elastic actions in XY bending require for symmetry that $v(p-d) = v(p+d)$. In the limit as corresponding points approach the p.o.s.

$$\lim_{d \to 0} [v(p-d) = v(p+d)] \implies v(p) \neq 0$$

Since elastic continuity is maintained at the p.o.s., there must be continuity in the slope of v. Corresponding slopes in symmetry are of opposite sign:

$$\frac{\partial v}{\partial x}(p-d) = (-1)\frac{\partial v}{\partial x}(p+d)$$

In the limit as corresponding slopes approach the p.o.s.

$$\lim_{d \to 0} \left[\frac{\partial v}{\partial x}(p-d) = (-1)\frac{\partial v}{\partial x}(p+d)\right] \implies \frac{\partial v}{\partial x}(p-0) = (-1)\frac{\partial v}{\partial x}(p+0)$$

This can be satisfied only if $\frac{\partial v}{\partial x}(p) = 0$. This is equivalent to prescribing that the rotational d.o.f. about the Z axis at the p.o.s. is zero; i.e. $Rz(p) = 0$.

The elastic actions in XY bending require for antisymmetry that

$$v(p-d) = (-1)v(p+d).$$

In the limit at p as corresponding points approach the p.o.s.

$$\lim_{d \to 0} [v(p-d) = (-1)v(p+d)] \implies v(p-0) = (-1)v(p+0).$$

This can be satisfied only if $v(p) = 0$. Intuitively one can affirm that the slope $\frac{\partial v}{\partial x}$ must be allowed to be non-zero at p; therefore the rotational d.o.f. about Z at the p.o.s. must be non-zero; i.e. $Rz(p) \neq 0$.

Turn next to bending in the XZ plane.

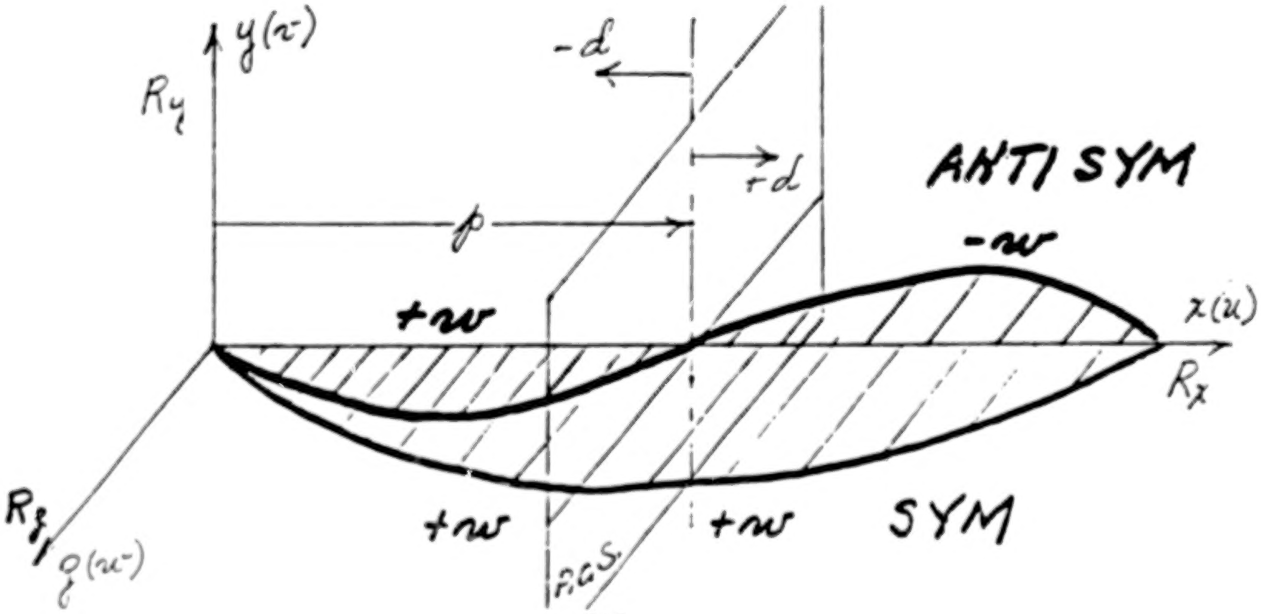

The elastic actions in XZ bending require for symmetry that $w(p-d) = w(p+d)$. In the limit as corresponding points approach the p.o.s.

$$\lim_{d \to 0} [w(p-d) = w(p+d)] \Longrightarrow w(p) \neq 0.$$

Since elastic continuity is maintained at the p.o.s., there must be continuity in the slope of w. Corresponding slopes in symmetry are of opposite sign:

$$\frac{\partial w}{\partial x}(p-d) = (-1)\frac{\partial w}{\partial x}(p+d)$$

In the limit as corresponding slopes approach the p.o.s.

$$\lim_{d \to 0} \left[\frac{\partial w}{\partial x}(p-d) = (-1)\frac{\partial w}{\partial x}(p+d)\right] \Longrightarrow \frac{\partial w}{\partial x}(p-0) = (-1)\frac{\partial w}{\partial x}(p+0)$$

This can be satisfied only if $\frac{\partial w}{\partial x}(p) = 0$; therefore $Ry(p) = 0$.

The elastic actions in XZ bending require for anti-symmetry that $w(p-d) = (-1)w(p+d)$.

In the limit as corresponding points approach the p.o.s.

$$\lim [w(p-d) = (-1)w(p+d)] \Longrightarrow w(p-0) = (-1)w(p+0).$$

This can be satisfied only if $w(p) = 0$.

The slope $\frac{\partial w}{\partial x}(p)$ must be allowed to be non-zero at the p.o.s.; which is equivalent to the condition $Ry(p) \neq 0$.

Turn next to longitudinal deformation in X

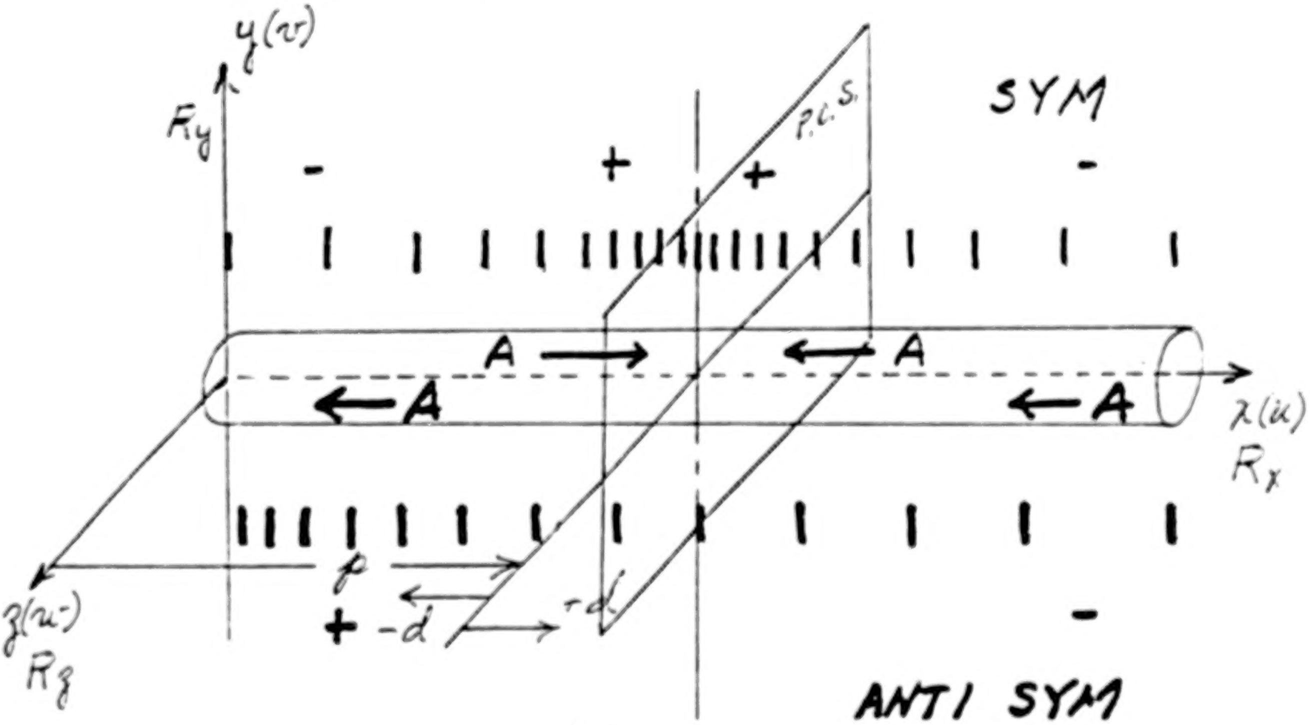

The longitudinal actions in X require for symmetry that both sides be either in condensation or in rarefaction; therefore axial forces, A, are equal and opposite

$$A(p-d) = (-1)A(p+d),$$

but this implies that axial deformations are likewise equal and opposite

$$u(p-d) = (-1)u(p+d).$$

In the limit as corresponding points approach the p.o.s

$$\lim_{d \to 0} [u(p-d) = (-1)u(p+d)] \quad ::> \quad u(p-0) = (-1)u(p+0).$$

this can be satisfied only if $u(p) = 0$.

The longitudinal actions in X require for anti-symmetry that one side be in condensation while the other side is in rarefaction; therefore axial forces, A, are equal

$A(p-d) = A(p+d)$; but this implies that axial deformations are likewise equal

$$u(p-d) = u(p+d).$$

In the limit as corresponding points approach the p.o.s.

$$u(p-0) = u(p+0) \quad ::> \quad u(p) \neq 0.$$

Finally turn to torsion about X.

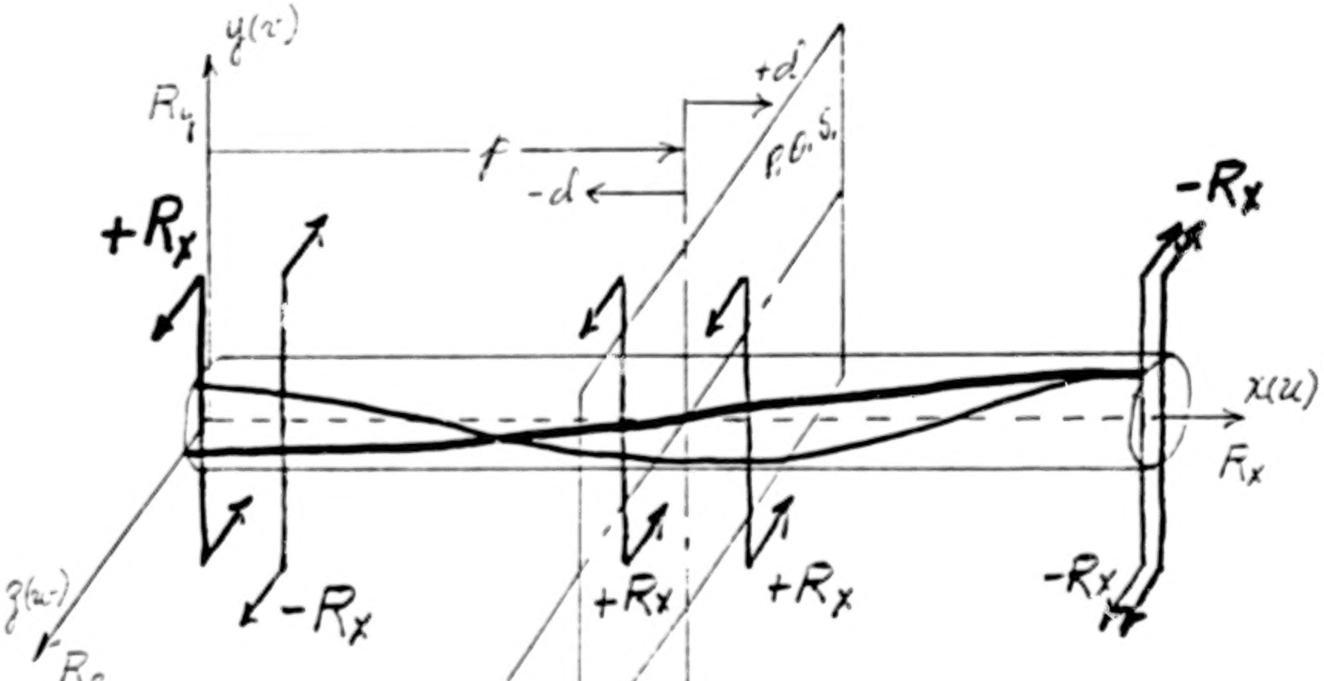

The torsional actions about X for symmetry require that $Rx(p-d) = Rx(p+d)$. In the limit as corresponding points approach the p.o.s.

$$\lim_{d \to 0} [Rx(p-d) = Rx(p+d)] \Longrightarrow Rx(p) \neq 0.$$

For anti-symmetry

$$\lim_{d \to 0} [Rx(p-d) = (-1)Rx(p+d)] \Longrightarrow Rx(p-0) = (-1)Rx(p+0).$$

This can be satisfied only if $Rx(p) = 0$.

All six degrees of freedom have been examined for symmetric and antisymmetric boundary condition requirements at the p.o.s. The results are summarized in a table below.

BOUNDARY CONDITION @ YZ P.O.S.				
D.O.F. No.	SYM	ANTISYM	P.O.S. ORIENTATION	BOUNDARY CONSTRAINT FORCE
1	$u(p)=0$	$u(p)\neq 0$	Perp to p.o.s.	Axial in X
2	$v(p)\neq 0$	$v(p)=0$	In p.o.s.	Trnsv in Y
3	$w(p)\neq 0$	$w(p)=0$	In p.o.s.	Trnsv in Z
4	$Rx(p)\neq 0$	$Rx(p)=0$	About normal to	Tors about X
5	$Ry(p)=0$	$Ry(p)\neq 0$	About axis in	Moment about Y
6	$Rz(p)=0$	$Rz(p)\neq 0$	About axis in	Moment about Z
Total	1,5,6=0 2,3,4≠0	1,5,6≠0 2,3,4=0		

Several generalizations can be noted:

1. When a constraint requirement in a d.o.f. is zero for one condition, it is non-zero for the other condition.
2. For either condition there are always 3 zero and 3 non-zero constraint requirements.
3. Constraint forces at the p.o.s. are those forces that are transmitted to the adjacent segment in the whole structure.
4. Rather than deal in rote quantities for each change of coordinate system, the boundary condition requirements can be expressed in terms of axes imbedded in the p.o.s.: two axes lying in the p.o.s. and an axis normal to the p.o.s.

- Symmetry
  - Zero
    - Translation normal to p.o.s.
    - Rotation about 2 axes lying in p.o.s.
  - Non-zero
    - Translation along 2 axes lying in p.o.s.
    - Rotation about normal to p.o.s.
- Anti-Sym
  - Zero
    - Translation along 2 axes lying in p.o.s.
    - Rotation about normal to p.o.s.
  - Non-zero
    - Translation normal to p.o.s.
    - Rotation about 2 axes lying in p.o.s.

The law that assymetric loads on symmetric structures can be represented by the superposition of partial load conditions can be illustrated by a simply supported prismatic beam with an off-center load.

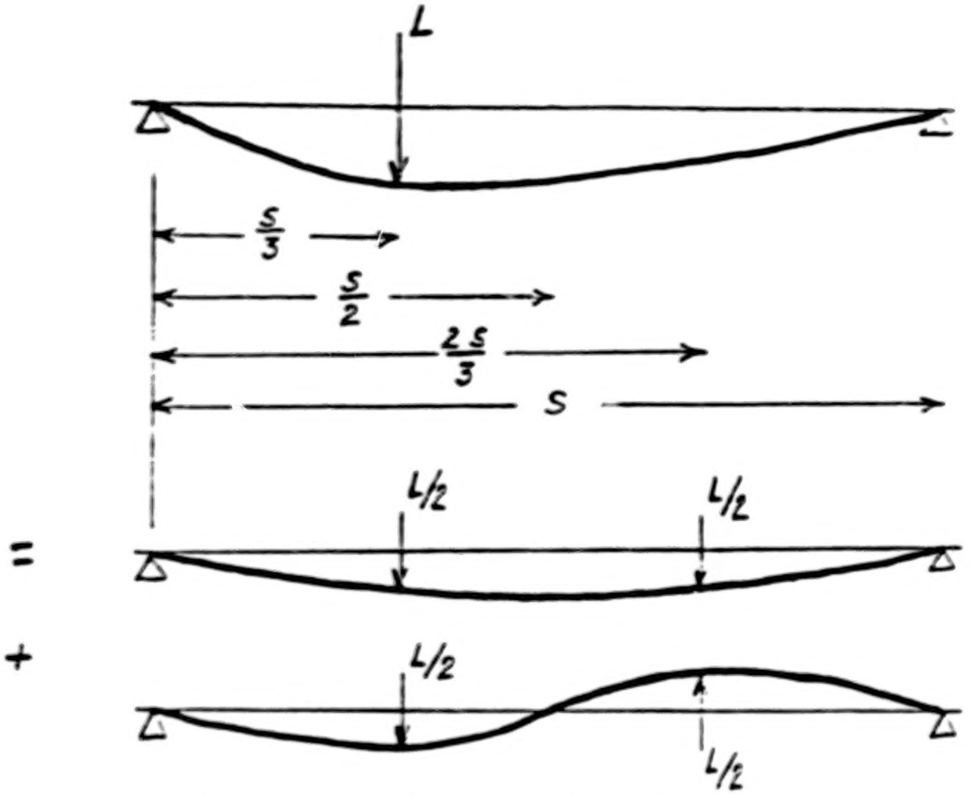

Plan of Analysis Using One Symmetric Half Only
Ingredient case 1. L/2 @ s/3:sym bc @ s/2. Can represent either side.
2. L/2 @ s/3:asym bc @ s/2. Can represent either side.
LH behavior Sym + Asym. Sum F:L/2 + L/2=L. Sum M:2xL/2xs/3=sL/3
RH bahavior Sym - Asym. Sum F:L/2 - L/2=0. Sum M:L/2xs/3-L/2xs/3=0

These statements will now be verified by (1) solving for the slope and deflection of the whole beam, (2) solving for the slope and deflection of the LH half using half load, under symmetric boundary conditions, (3) solving for slope and deflection of the LH half using half load under antisymmetric boundary conditions, (4) evaluating slope and deflection formulas @ S/4, s/2, and 3s/4, (5) adding the symmetric and antisymmetric response and comparing with the response of the LH half of the whole beam, and (6) subtracting the antisymmetric response from the symmetric response and comparing with the response of the RH half of the whole beam.

The slope and deflection of the S-S beam with load L @ s/3 and EI = 1 are:

	x=s/4	x=s/2	x=3s/4
$y'(x)$	$\frac{-53Ls^2}{48x27}$	$\frac{5Ls^2}{24x27}$	$\frac{101Ls^2}{48x54}$
$y(x)$	$\frac{-71Ls^3}{72x72}$	$\frac{-23Ls^3}{36x36}$	$\frac{-119Ls^3}{2x72x72}$

The slope and deflection of the left hand half with half load @ s/3 under symmetric boundary conditions at the plane of symmetry are and evaluated at s/4 and s/2 are:

Sym $y'(x)$	$\frac{-23Ls^2}{36x16}$	0
Sym $y(x)$	$\frac{-29Ls^3}{72x32}$	$\frac{-23Ls^3}{36x36}$

The slope and deflection of the left hand half with half load under anti-symmetric boundary conditions at the plane of symmetry are and evaluated at s/4 and s/2 are:

Anti $y'(x)$	$\frac{-5Ls^2}{64X81}$	$\frac{5Ls^2}{24x27}$
Anti $y(x)$	$\frac{-23Ls^3}{96x216}$	0

To depict the left half full scale behavior @ x=s/4

sum Sym y'(s/4) & Anti y'(s/4) $= -\frac{23Ls^2}{36x16} - \frac{5Ls^2}{64X81} = -\frac{53Ls^2}{48x27}$

and

sum Sym y(s/4) & Anti y(s/4) $= -\frac{29Ls^3}{72x32} - \frac{23Ls^3}{96x216} = -\frac{71Ls^3}{72x72}$

At x = s/2 the sum also checks; e.g.

sum Sym y'(s/2) & Anti y'(s/2) $= 0 + \frac{5Ls^2}{24x27} = \frac{5Ls^2}{24x27}$

and

sum Sym y(s/2) & Anti y(s/2) $= -\frac{23Ls^3}{36x36} + 0 = -\frac{23Ls^3}{36x36}$

Differences are taken in order to use results of the analysis from the left hand half to predict the behavior of the right hand half. Compare differences of the LH half @ x = s/4 with the full scale @ x = 3s/4; e.g.

subtract Sym y'(s/4) & Anti y'(s/4) : $\frac{-23Ls^2}{36\times16} + \frac{5Ls^2}{64\times81} = \frac{-101Ls^2}{36\times72}$

Note: The sign is opposite to that of y'(3s/4), because the calculated slope is in a reflected position wrt plane of sym.

subtract Sym y(s/4) & Anti y(s/4) = $\frac{-29Ls^3}{72\times32} + \frac{23Ls^3}{96\times216} = \frac{-119Ls^3}{2\times72\times72}$

In summary for the beam analysis:

Half symmetry was used.
Non-symmetric load was split into 1/2 Sym & 1/2 Anti-Sym.
L.H. side was the solution segment.
Ingredient S/C 1; Load=L/2 with symmetric bound. cond.
Ingredient S/C 2; Load=L/2 with antisymmetric bound. cond.
Sol'n whole L.H. = 1.0 (S/C 1) + 1.0 (S/C 2)
Sol'n whole R.H. = 1.0 (S/C 1) - 1.0 (S/C 2)
In solving just one segment with 2 different boundary conditions, the same half load is used in both cases.

The representation of the whole structure comes about during the combining of the ingredients. How they should be combined depends upon which segment was chosen as the solution segment, which segment contained the nonsymmetric load, and what part of the whole structure is being synthesized. This will be illustrated for two variations:

SOL'N SEGMENT = LH, LOAD SEGMENT = LH
    LH Whole for defl. & slope = Sym + Antisym
    RH Whole for defl. = Sym + Antisym
    RH Whole for slope = (-1)(Sym - Antisym)
SOL'N SEGMENT = RH, LOAD SEGMENT = LH
    LH Whole for defl. = Sym + Antisym
    LH Whole for slope = (-1)(Sym + Antisym)
    RH Whole for defl. & slope = Sym - Antisym

New wrinkles get introduced when there is more than one p.o.s. When there was one p.o.s. there were 2 ingredient subcases. For two p.o.s.'s the solution segment is a quadrant, and there will be 4 ingredient subcases to solve. For three p.o.s.'s the solution segment is an octant, and there will be 8 ingredient subcases to solve.

Expanding on quarter symmetry there are two possible boundary conditions over the section of the structure at each of two planes of symmetry. Four permutations of combined boundary conditions are possible:

	XZ PLANE OF SYMMETRY	YZ PLANE OF SYMMETRY	ABBREV
1.	Symmetric	Symmetric	SX, SY
2.	Anti-symmetric	Symmetric	AX, SY
3.	Symmetric	Anti-symmetric	SX, AY
4.	Anti-symmetric	Anti-Symmetric	AX, AY

An example is taken with a non-symmetric load in the 3rd quadrant. The load, P, on the whole structure is shown with a shading

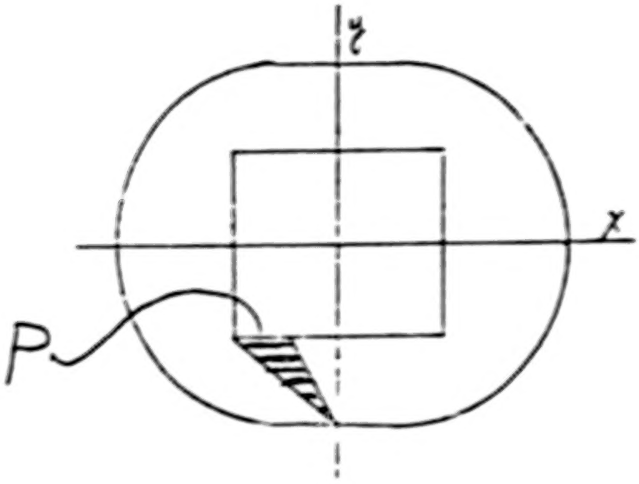

The modes associated with the establishment of boundary conditions for 2 planes of symmetry can be illustrated simply as

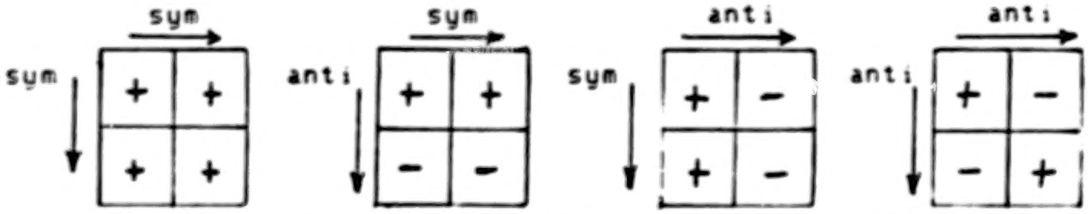

Let quadrant one be the model-quadrant. Four ingredient cases are constructed from the model quadrant with the 4 combinations of boundary conditions and each is given the same nominal load N.

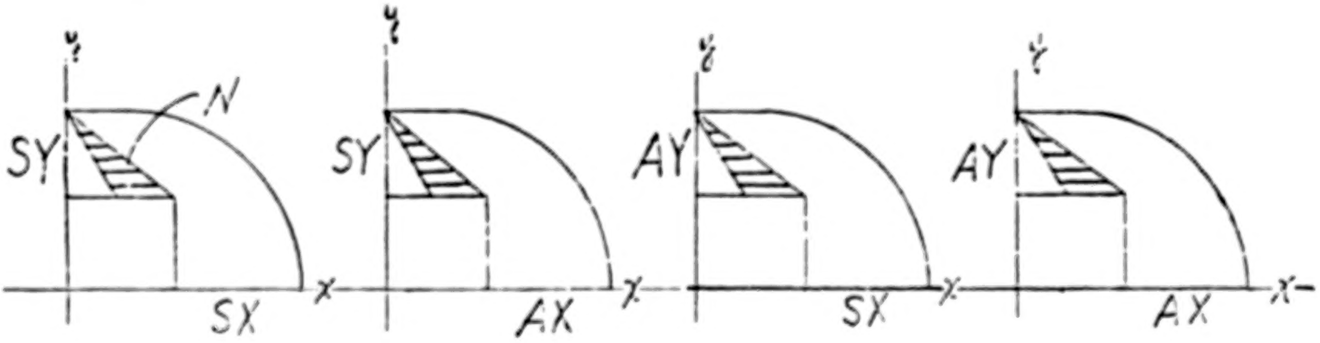

Since I found no guidelines in the literature I had to arrive at my own rules for combining ingredient subcases to represent any quadrant of the structure. There will always be one loaded quadrant and 3 non loaded quadrants. If a given non-symmetric load spans more than one quadrant, take the load as it appears in one quadrant at a time and do a 4 segment decomposition on each and solve the eight subcases then combine the 8 parts together in SUBCOM. The logic used in arriving at the signs to be applied to the coefficients of ingredient subcases for representing the responses in the 4 different quadrants will be taken up as one topic. The logic used in arriving at the magnitudes of of these coefficients will be taken up as another topic. The logic will be developed with respect to a particular example of a skewed load acting in the third quadrant of the structure. The representative structure will be modeled in the first quadrant. I asked myself "What are the signs to use for the ingredients to represent the nonloaded quadrants?" I don't remember the evolution of my thinking, but after I hit on the correct rule, I remember feeling ashamed of myself for being temporarily content with an inexact method earlier on. The nice thing is that the correct rule is a simple rule. The bothersome part in digging out this rule was for the quadrant which was located diagonally across from the loaded quadrant. This nagging problem disciplined my thinking until I finally clicked.

The RULE OF SIGNS is:
There is no change of sign when the response from a given quadrant is reflected about a symmetric boundary to yield the response in an adjacent quadrant. The sign is changed when the response from a given quadrant is reflected about an antisymmetric boundary to yield the response in an adjacent quadrant.

Loads from the 4 component cases must add up to 4N when representing the loaded quadrant which in this case is quadrant 3. Loads from these same 4 component cases must add up to zero in the other 3 quadrants (1, 2, and 4). Therefore the sign of the scale factors must be positive when combining Suhcases to represent quadrant 3;

QUAD 3
+SX, SY
+AX, SY
+SX, AY
+AX, AY

The reflections for quadrant 2 with respect to the signed array from quadrant 3 are about the X axis.

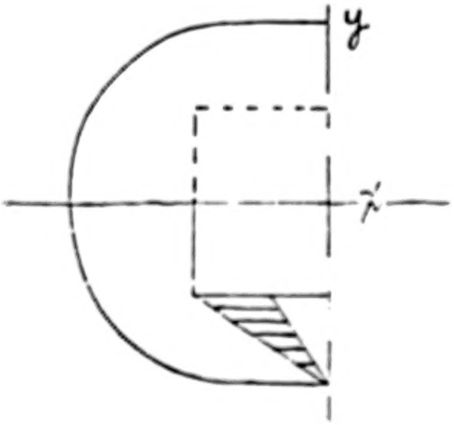

The first case SX,SY keeps a positive sign, because it is a symmetric reflection. The second case AX,SY changes sign and becomes negative, because the reflection with respect to the X axis is antisymetric. Similarly, the third case SX,AY has a symmetric boundary with respect to X and an antisymmetric boundary with respect to Y. But since the reflection is with respect to X in going from quad 3 to quad 2, there is no change of sign. This implies that the antisymetric conditions along Y remain the same in quadrant 2 as they did in quadrant 3 when it is associated with a symmetric reflection in X. Applying this logic to case four gives rise to a change in sign for the AX,AY response in quadrant 2. The coefficient signs for qaudrant 2 are tabulated as

QUAD 2
+SX,SY
-AX,SY
+SX,AY
-AX,AY

The reflections from quadrant 3 to quadrant 4 are about the Y axis so that anti-symmetric reflections with respect to Y change sign accordingly. The tabulation for quadrant 4 is

QUAD 4
+SX,SY
+AX,SY
-SX,AY
-AX,AY

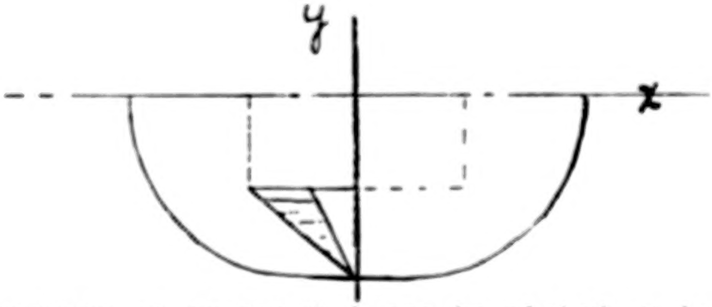

The case for the response in quadrant 1 can be stated in terms of reflections from quadrant 4 or from quadrant 2. The same results are obtained in either case. Referring to the signed tabulation for quadrant 4, the results for quadrant 1 become, as a result of reflecting the signed quantities of quadrant 4 about the X axis

QUAD 1
+SX,SY
-AX,SY
-SX,AY
+AX,AY

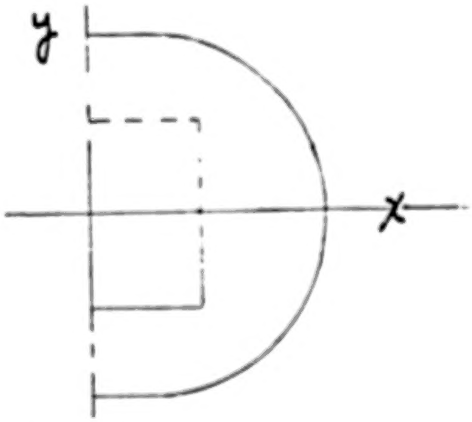

The magnitude of the coefficient, C, depends on the type of symmetry (e.g. half or quarter or octant); the magnitude of the nominal load, N, used in the ingredient subcases; and the magnitude of the ultimate loading, U, as it appears in the whole structure. The magnitude of the coefficient is the same for all components in all four quadrants. The equation to use to have all four components sum to the ultimate in the loaded quadrant for quarter symmetry is:

$$CN(SX,SY) + CN(AX,SY) + CN(SX,AY) + CN(AX,AY) = U$$

$$4CN = U$$

$$C = U/(4N)$$

For the half symmetry case with respect to X, the formula to have both components sum to the ultimate for the loaded half is:

$$CN(SX) + CN(AX) = U$$

$$2CN = U$$

$$C = U/(2N)$$

The extension to octal symmetry becomes $C = U/8N$.

If r stands for the number of reflections then the general formula for RULE OF MAGNITUDE of the coefficient is:

$$C = U/[2^r N],$$

where r is 1 for the one plane of half symmetry, r is 2 for the two planes of quarter symmetry, and r is 3 for the three planes of octal symmetry.

The observations made so far with one and two dimensional elements can easily be extended to three dimensional elements. When modeling with polyhedra there are only 3 translational d.o.f. per grid point. The question arises as to whether the general rules which were developed for grid points having rotational as well as translational d.o.f.'s will apply for polyhedral models. Since pairs of contrained grid points on a solid boundary will produce couples, the zero slope effect will be achieved, so it is possible to satisfy the boundary requirements with only sets of translational constraints at the p.o.s. Look at the table of Boundary Conditions on page 6. For symmetry the only translational zero constraint is on u. But the condition that Ry and Rz be zero must be satisfied in a macro sense if not at the grid point level. Polyhedral elements will have at least a pair of points in each of 3 coordinates, so that a pair of constraints on u when separated by a span in z will produce a restraining couple about Y which will have the effect of constraining Ry to zero. Similarly, a pair of constraints on u when separated by a span in y will produce a restraining couple about Z which will have the effect of constraining Rz to zero. Apply this same reasoning to anti-symmetry and you will be reassured that the displacement constraints on v & w will contain Rx at zero.

The extension of the rule of signs on page 11 to octal symmetry is accomplished by changing the word "quadrant" to "segment". There are two possible boundary conditions over the section of the structure at each of the three planes of symmetry. Eight permutatins of these boundary conditions is possible. Consequently, for the loaded octal segment the signs to combine the eight ingredient subcases are all positive.

Sx,Sy,Sz
Sx,Sy,Az
Sx,Ay,Sz
Sx,Ay,Az
Ax,Sy,Sz
Ax,Sy,Az
Ax,Ay,Sz
Ax,Ay,Az

Changing signs when reflecting across an antisymmetric boundary successively until the octal segment diagonally opposite to the loaded segment is reached, the array of signs become

+Sx,Sy,Sz
-Sx,Sy,Az
-Sx,Ay,Sz
+Sx,Ay,Az
-Ax,Sy,Sz
+Ax,Sy,Az
+Ax,Ay,Sz
-Ax,Ay,Az.

NASTRAN PROCEDURE

Before proceeding to an application we should determine what the implication for all these observations are for setting up a problem within NASTRAN.

The analyst must model a segment with a fraction of the nonsymmetric load in place. If the loaded segment is chosen as the solution segment, the load is oriented as it is specified. If the solution segment is other than the loaded segment the load must be in a properly reflected orientation.

If n is allowed to represent the number of p.o.s.'s, set up 2^n sets of Single Point Constraints (SPC's) for all permutations of symmetric and anti-symmetric boundary conditions at the planes of symmetry.

Set up one load set.

Set up 2^n subcases each with the same load but each with a different one of the SPC sets.

Request OLOAD for checking on the correct assembly of load.

Request SPCFORCES for checking on equilibrium for checking on equilibrium and for the magnitudes of loading across the planes of symmetry.

Arrange the subcases in a logical sequence that will be manageable for the assigning of coefficients when the results are to be combined.

Refer to the RULE OF MAGNITUDE on page 14 for computing the combining coefficients. Refer to the RULE OF SIGNS on page 11 for setting the signs of combining coefficients.

Set up the output sets for the results. If output from individual as well as combined subcases is desired, the Case Control option of SUBCOM should be used. If output from only combined cases is desired, the Case Control option of SYMCOM can be used. A separate combining case is set up for each segment from which results are desired.

The values of scaling coefficients are transcribed to NASTRAN through the Case Control entry of SUBSEQ for SUBCOM cases and SYMSEQ for SYMCOM cases. NASTRAN reads the string of coefficients from left to right and assigns them as amplifiers to the results of preceeding subcases in the order from top to bottom as they appear in the Case Control Packet. This can take on such an abstract appearance that care is needed to ensure that they are in correct sequence. The burden is entirely on the analyst to exercise tidy bookkeeping to ensure proper correspondence.

APPLICATION

These techniques were applied to a thick structure having quarter symmetry which was modeled with polyhedra. Five distinct loads were applied to the structure with varying degrees of symmetry, such that 12 subcases were needed to represent all of the ingredient conditions. A sketch of the loadings is shown by shading and by number

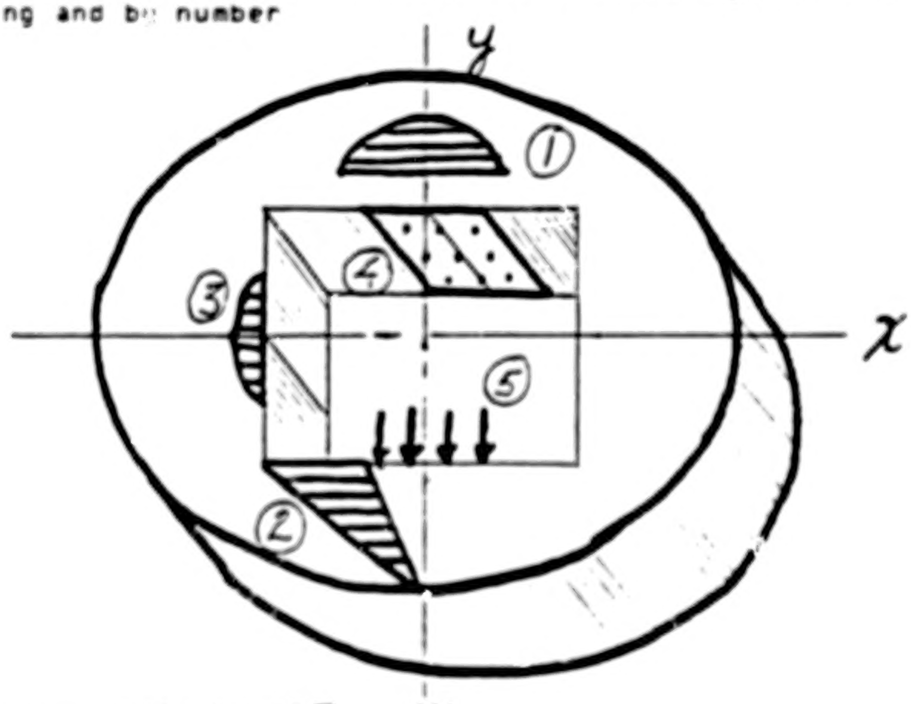

Their symmetry characteristics were as tabulated below:

LOAD NO	RELATION TO P.O.S. XZ	YZ	NUMBER OF INGREDIENT SUBCASES
1	Unsym	Sym	2
2	Unsym	Unsym	4
3	Sym	Unsym	2
4	Unsym	Sym	2
5	Unsym	Sym	2

A quadrant was modeled with a fine mesh of 5 courses of solids through the thickness to obtain detailed stress distributions for studying stress concentrations and fatigue failure. Loads 1 and 4 were combined for one result and loads 2, 3, and 5 were combined for another result. The analyses were successful in that the patterns and levels of stresses were quite reasonable.

CONCLUSION

What does all this special business buy you? A way to quantify the merits is to set up measures such as results per unit cost or results per manhour or results per computer hour. Such management schemes were not used, but some areas are explored that can be useful to evaluate relative merits. Decomposition time varies as the square or the cube of the matrix order N, depending on the density and/or band and/or wave front. A comparison follows.

ESTIMATES OF DECOMPOSITION TIME							
TYPE SYM	LEAST PER INGREDIENT	# ING	NET	MOST PER INGREDIENT	# ING	NET	SAVING
FULL	NXN	1	NXN	NXNXN	1	NXNXN	0
HALF	NXN/4	2	NXN/2	NXNXN/8	2	NXNXN/4	2:1<S<4:1
QTR	NXN/16	4	NXN/4	NXNXN/64	4	NXNXN/16	4:1<S<16:1
OCT	NXN/64	8	NXN/8	NXNXN/512	8	NXNXN/64	8:1<S<64:1

If on the other hand one wanted as detailed a model that could be relied upon to be free of ill-conditioning, then the order of the segment model would be approximately 8,000 d.o.f. Using symmetry would give results comparable to a full scale model of order 16,000 for half symmetry; of order 32,000 for quarter symmetry; and of order 64,000 for octal symmetry. This indicates that as one goes to higher order symmetry in an analysis, one gets more results and uses less time to do the job by taking advantage of symmetry.

Another factor to look at is the analyst's preparation time. It takes less time to set up a smaller solution segment. It takes more time to set up more boundary conditions. It takes more time to set up more subcases and combining cases with coefficients. Once the model is complete, however, the entire job can be run as a single submittal so the handling is no more demanding. The evaluation of the results of the job becomes easier because the parceling of results from the combining cases makes the job more tractable.

A disadvantage to call to your attention is in getting a report on the load as it is associated in a combining subcase. OLOAD does not report on the equivalent combined load from a combining subcase. The user must engage in one of two routes which are not completely free of human error in order to get a report on the equivalent combined load. He can set up a dummy subcase and do the combining of the load with the bulk data LOAD card and by assigning amplifying coefficients according to those used in the combining sequence statement and call for OLOAD in this dummy subcase.
Alternatively, he can take the output of the PG vector from successive loops through module SSG1, and write a DMAP packet to scale the components and sum them to produce a combined load to check.

It appears that the advantages outweigh the disadvantages so that I would recommend that if you find that this paper has reduced the running of a symmetry problem to a useful routine, you might employ it more and enjoy some of its benefits. One can be assured that his solution is not compromised for having used symmetry. All parts of the solution are contained in the result after the combining has been accomplished.

T. G. Butler March 5, 1982.

EVALUATION AND REDUCTION
OF
ERRORS INDUCED
BY THE
GUYAN TRANSFORMATION

GARY L. FOX

Director
Engineering and Computational Sciences
Division

NKF Engineering Associates, Inc.

SUMMARY

The Guyan Reduction refers to a method used to reduce the number of degrees of freedom in a structural model for dynamic anlysis. Experience has shown that, if the method is properly employed, then this reduction method does in fact provide a "reasonably" accurate approximation of the dynamic characteristics of the unreduced model.

This paper presents a method that provides an accurate estimate of the error in each mode of the reduced eigenvalue problem and, in addition, gives first order correction terms that greatly improve the accuracy of the eigenvectors and eigenvalues. The method is demonstrated by standard COSMIC NASTRAN® DMAP Alters to Rigid Format 3, Real Normal Mode Analysis. Comparative computer time, modal extraction vs error analysis, is discussed for the VAX-11/780 version of COSMIC NASTRAN.

INTRODUCTION

Consider the well-known system of linear equations with constant coefficients

$$[M]\ [\ddot{X}\} + [K]\ [X\} = [P(t)\} \qquad (1)$$

where: $[M]$ = Mass matrix
$[K]$ = Stiffness matrix
$[X\}$, $[\ddot{X}\}$ = Displacement, acceleration vector
$[P(t)\}$ = Load vector

In the notation used here, {] is a row vector and { } is a scalar quantity. A matrix multiplication, {] [ ] [} results in a scalar, as indicated by the left and right elements; similarly, [} {] would indicate a matrix result. In the text a scalar will often be written without the braces.

In current finite element models the degrees of freedom represented by Equation (1) are often many thousand. This large number of equations is usually a result of the finite element technique itself rather than being necessary for a sufficiently accurate solution to a dynamic problem.

In a short, but significant paper [1], Robert Guyan suggested that a transformation be applied to the mass matrix that was based on partitioning the stiffness matrix. This reduction of the number of degrees of freedom for a dynamic analysis is cost effective, in terms of computer time, when the system of equations is reduced by a factor of four or more.

Computing efficiency is therefore a central issue to the consideration of any reduction process. A numerical procedure for estimating the error must not be excessive. It is felt that the method presented here meets this basic requirement, provided that a modal analysis is required as part of the solution process. Even if the direct methods are to be used for the dynamic analysis, a modal analysis is often performed.

Modal analysis provides an insight into the dynamic behavior of a complex system, provides a means by which a finite element model may be checked for errors, or provides a basis for estimating the response of the system to a specific, simple excitation. Modal analysis plays a central role in the U.S. Navy's Dynamic Design Analysis Method (DDAM) as well as many other well-known techniques of enforced motion boundary problems that use shock response spectra as a statistical technique for dynamic analysis.

In addition, the system response to transient or harmonic excitation may be calculated by an eigenvector expansion. Eigenvector expansion techniques are also cost effective when a number of different load conditions are analyzed for a given set of equations. Also, numerical studies indicate that errors in frequency and errors in amplitude have the same magnitude [2].

It is shown below that the Guyan transformation is the first term of a series expansion, the second term being the first order correction. This correction term is used to improve the accuracy of the Guyan transformation as well as to provide a single number that represents the dynamic accuracy of each mode. Note that the Guyan transformation, when applied to the stiffness matrix, is exact, as can be seen from simple matrix partitioning.

DERIVATION OF THE CORRECTION TERM

It is the assumption that the analyst wishes to calculate a significant number, say 10 percent, of the lowest modes represented by the homogeneous form of Equation (1),

$$[M]\,\{\ddot{X}\} + [K]\,\{X\} = 0 \tag{2}$$

Presume that the eigenvalue, Equation (2), is partitioned into two sets, the "0" set of DOF to be omitted and the "a" set of DOF to be retained in the Guyan Reduction, i.e.,

$$\begin{bmatrix} \bar{K}_{aa} & K_{ao} \\ K_{oa} & K_{oo} \end{bmatrix} \begin{Bmatrix} \bar{\phi}^{i}_{a} \\ \bar{\phi}^{i}_{o} \end{Bmatrix} = \bar{\lambda}^{i} \begin{bmatrix} \bar{M}_{aa} & M_{ao} \\ M_{oa} & M_{oo} \end{bmatrix} \begin{Bmatrix} \bar{\phi}^{i}_{a} \\ \bar{\phi}^{i}_{o} \end{Bmatrix} \tag{3}$$

where $\bar{\lambda}^i$ is the true eigenvalue and

$$\{\bar{\phi}^i\} = \left[\begin{matrix} \bar{\phi}^i_a \\ \bar{\phi}^i_o \end{matrix}\right\}$$ is the true eigenvector for the i^th mode

The reader is reminded that the solution of the reduced equations using the Guyan reduction is

$$[K_{aa}]\,\{\phi^i_a\} = \lambda^i\,[M_{aa}]\,\{\phi^i_a\} \tag{4}$$

where: $[K_{aa}] \equiv [\overline{K}_{aa}] + [K_{ao}\,G_{oa}]$

$[M_{aa}] \equiv [\overline{M}_{aa}] + [G^T_{oa}\,M_{oa}] + [M_{ao}\,G_{oa}] + [G^T_{oa}\,M_{oo}\,G_{oa}]$

$[G_{oa}] \equiv -[K_{oo}{}^{-1}\,K_{oa}]$

Consider the exact solution of Equation (3) in partitioned form by solving e second set of equations for $\{\phi^i_o\}$ in terms of $\{\phi^i_a\}$

$$\{\bar{\phi}^i_o\} = -[K_{oo} - \bar{\lambda}^i M_{oo}]^{-1}\,[K_{oa} - \bar{\lambda}^i M_{oa}]\,\{\bar{\phi}^i_a\} \tag{5}$$

The first term of the matrix product indicated above can be expanded in a power series

$$[K_{oo}(I_{oo} - \bar{\lambda}^i\,K^{-1}_{oo}\,M_{oo})]^{-1} = [I_{oo} + \bar{\lambda}^i\,K^{-1}_{oo}\,M_{oo} + \dots]\,[K^{-1}_{oo}] \tag{6}$$

Substituting Equation (6) into Equation (5) for the i^th eigenvalue and eigenvector

$$\{\bar{\phi}^i_o\} = [G_{oa}]\{\bar{\phi}^i_a\} + \bar{\lambda}^i\,[E_{oa}]\{\bar{\phi}^i_a\} + \text{higher order terms in } \bar{\lambda}^i \tag{7}$$

where

$$[E_{oa}] = -[K^{-1}_{oo}]\,[M_{oo}K^{-1}_{oo}\,K_{oa} - M_{oa}]$$

The first term on the right in Equation (7) provides an approximation of $\bar{\phi}_o^i$ correct to first order in λ^i.

$$\{\bar{\phi}^i\} \cong \begin{bmatrix} \bar{\phi}_a^i \\ G_{oa} \quad \bar{\phi}_a^i \end{bmatrix} \tag{8}$$

The second term is the second order correction to this approximation. The condition that the term containing $[E_{oa}]$ in Equation (6) be small can be expressed as

$$[I_{oo}] \gg \bar{\lambda}^i \, [K_{oo}^{-1} \, M_{oo}] \tag{9}$$

and from (7) that

$$[G_{oa}] \gg \bar{\lambda}^i \, [E_{oa}] \tag{10}$$

Assuming that the second term, $[M_{oa}]$ in the error matrix, $[E_{oa}]$, is proportional to $[M_{oo}]$ Equation (10) reduces to Equation (9). Equation (9) is thus the condition that a particular eigenvalue be accurate for a specific set of omitted DOF. The lower the λ^i and larger the product $[K_{oo}^{-1} \, M_{oo}]$, the more accurate the eigenvalue and therefore the eigenvector.

Equation (9) points out the well-known dependency of the Guyan reduced error on frequency within a given class of modes (i.e., longitudinal, torsional, etc.); the lower the mode, the lower the error. Another well-known rule, to keep all large masses in the a-set, is also confirmed by this equation. The influence of the stiffness term, however, is not easily evaluated.

Two examples that illustrate the difficulty that the analyst faces in choosing an a-set are: (1) on what basis would a mass be compared to a rotational moment of inertia; and (2) how accurate are the modes associated with a stiff and massive section of a structure--a common occurrence in structures. With these unknowns, the analyst needs an accurate evaluation of the error involved in this method.

Equation (7) is in terms of the exact solution of Equation (2), $\bar{\lambda}^i$ and $\{\bar{\phi}^i\}$. Let $\{\phi^i\}$ and λ^i be the solution of Equation (4),

$$\{\bar{\phi}^i\} = \{\phi^i\} + \{\Delta\phi^i\}$$

and (9a)

$$\bar{\lambda}^i = \lambda^i + \Delta\lambda^i$$

Equation (7) becomes

$$\begin{aligned}\{\bar{\phi}_o^i\} = {} & [G_{oa}]\{\phi_a^i\} + \lambda^i\,[E_{oa}]\{\phi_a^i\} \\ & + [G_{oa}]\{\Delta\phi_a^i\} + \Delta\lambda^i\,[E_{oa}]\{\phi_a^i\} \\ & + \lambda^i\,[E_{oa}]\{\Delta\phi_a^i\} + \Delta\lambda^i\,[E_{oa}]\,\{\Delta\phi_a^i\} \\ & + \text{higher order terms}\end{aligned} \tag{7a}$$

The first term on the right provides the theoretical basis for the Guyan transformation. The last four terms are small compared to the first two if the condition (10) is met. Clearly, then, the second term in Equation (7a) is the first order correction term to the Guyan Transformation. This term will now be used to provide a measure of the effect of this error for each mode.

Consider the i^{th} eigenvalue given by Rayleigh's quotient.

$$\lambda^i = \{\phi^i]\;[K]\{\phi^i\}\;/\;\{\phi^i]\;[M]\{\phi^i\} \tag{11}$$

Taking the natural log of Equation (11) yields

$$\ell n\,\lambda^i = \ell n\,K_g^i - \ell n\,M_g^i \tag{12}$$

Where K_g^i = i^{th} generalized stiffness

M_g^i = i^{th} generalized mass

Taking differentials of Equation (12) provides the relationship in error between the eigenvalue, λ^i, and stiffness and mass weighted eigenvector,

$$\frac{d\lambda^i}{\lambda^i} = \frac{1}{K_g^i}\,dK_g^i - \frac{1}{M_g^i}\,dM_g^i \tag{13}$$

Writing the differential of the first term of Equation (13) yields

$$dK_g^i = \sum_{\ell,m} d(\phi_\ell^i)\;K_{\ell m}\;\phi_m^i + \sum_{\ell,m} \phi^i\;K_{\ell m}\;d(\phi_m^i) \tag{14}$$

Since the two terms in Equation (14) are identical,

$$dK^i_g = 2\{\phi^i]\ [K]\{d\phi^i\} \tag{15}$$

Similarly

$$dM^i_g = -2\{\phi^i]\ [M]\{d\phi^i\}$$

It is now required to evaluate

$$\{d\phi^i\} = \begin{Bmatrix} d\phi^i_a \\ d\phi^i_o \end{Bmatrix}$$

to first order in λ^i. Using the Guyan transformation, $\{\bar{\phi}_o\} \equiv [G_{oa}\}\ \{\phi_a\}$ in the second of Equation (3).

$$\{0\} = \lambda[M_{oa}]\{\phi_a\} + \lambda[M_{oo}][G_{oa}]\{\phi_a\} \tag{16}$$

By pre-multiplying Equation (16) by $[G_{oa}]^T$ and adding it to the first of Equation (3), one finds that to first order in λ, incorporating Equation (9a)

$$[K_{aa}]\{\phi_a\} = \lambda[M_{aa}]\{\phi_a\} \tag{17}$$

It is therefore seen that

$$\{d\phi_a\} \equiv \{0\} \tag{18}$$

From Equation (7)

$$\{d\phi^i_o\} \equiv \lambda^i\ [E_{oa}]\{\phi^i_a\} \tag{19}$$

Therefore, from Equations (18) and (19)

$$\{d\phi^i\} = \left\{\begin{array}{c} \{0\} \\ \hline \lambda^i\ [E_{oa}]\ \{\phi^i_a\} \end{array}\right\} \tag{20}$$

and

$$\{\phi^i\} = \begin{Bmatrix} \{\phi\}_a^i \\ \hline [G_{oa}]\,\{\phi_a^i\} \end{Bmatrix} \tag{21}$$

Evaluation of the first term of Equation (13) using Equations (14), (20), and (21) yields

$$dK_g^i \equiv \lambda^i \, \{\phi_a^i][K_{ao}\, E_{oa} + G_{oa}\, K_{oo}\, E_{oa}][d\phi_a^i\} \tag{22}$$

The term in brackets is zero, i.e.,

$$dK_g^i \cong 0 \tag{23}$$

to first order in λ. The error in λ, to first order of λ, is due to the second term in Equation (13), i.e.,

$$\frac{d\lambda^i}{\lambda^i} = -\frac{1}{M_g^i} \; \{\phi^i] \; [M] \; [d\phi^i\} \tag{24}$$

Equation (24) illustrates the fact that the error in each element of the vector $[d\phi^i\}$ must be mass weighted in order to evaluate the significance of such term.

NUMERICAL EXAMPLES

The bending modes of a five-cell cantilever beam is considered. The physical parameters of the beam are shown in Figure 1.

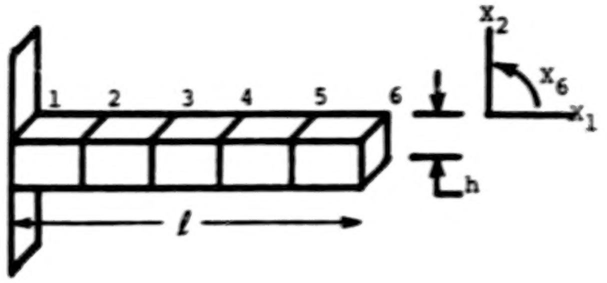

$h = 0.86$	Depth and width of beam
$\ell = 8.66025$	Length of beam
$\phi = 7.28E-4$	Mass density of beam
$I = h^4/12 = 0.0456$	Second moment of area
$A = h^2 = 0.7396$	Cross sectional area
$E = 3.0E+7$	Modulus of elasticity
$\lambda_i = c_i^4 \; EI/A$	ith theoretical eigenvalue
$c = 1.875, 4.694,$ $7.85, 10.996$	First theoretical four eigenvalue coefficients

Figure 1. Five-Cell Beam

The NASTRAN computer code was used for the numerical calculations because of the powerful DMAP compiler available and the generality of the results. The Guyan Transformation is available through the use of Alter statements, which allow the evaluation of the error simply by performing matrix manipulations.

Many elements in NASTRAN offer two options for the form of the mass matrix: lumped parameter or coupled mass. The bulk data parameter COUPMASS identifies the elements for which coupled mass matrices are to be used. The first four eigenvalues of the finite element model are compared to the coupled mass results in Table 1.

Table 1. Comparison of Theoretical and FEM Coupled Mass Eigenvalues

MODE NO.	THEORETICAL	FEM (COUPLED MASS)	$\Delta\lambda/\lambda$
1	5.50829E6	5.50839E6	1.81E-5
2	2.16363E8	2.16547E8	8.50E-4
3	1.69667E9	1.70827E9	6.84E-3
4	6.51554E9	6.66659E9	2.32E-2

Let the 10-DOF system (5 translational and 5 rotational) be Guyan reduced to 4 degrees of freedom and evaluate the estimated and "actual" error. The "actual" error is defined as the difference in frequency between the 10-DOF system and the Guyan reduced system. Table 2 shows the four eigenvalues and the predicted and actual error. The analysis set is defined as 6-2, 5-2, 4-2, and 3-2, the first number being the grid point and the second number the direction.

Table 2. Comparison Between Predicted and Actual Guyan Reduction Error

MODE NO.	EIGENVALUE	ACTUAL $\Delta\lambda/\lambda$	PREDICTED $\Delta\lambda/\lambda$
1	5.50856E6	3.09E-5	3.22E-5
2	2.17408E8	3.98E-3	3.89E-3
3	1.86197E9	8.62E-2	7.55E-2
4	1.01909E10	5.29E-1	2.73E-1

The accuracy with which the error is predicted decreases with increasing predicted error. Also, as expected, the error increases as the mode number increases. Small studies of the actual error have led to the "rule of thumb" that in a Guyan reduced model, the lower 50 percent of the modes in the reduced model are reasonably accurate, similar to the above result.

As an additional numerical example, let concentrated masses of 1.0 E-1 and 1.0 E-2 be located at grid points 2 and 4. These masses are large compared with the mass of a cell, 4.7 E-4. A Guyan reduction to the 3-DOF of 2-2, 4-2, and 6-2 yields the results shown in Table 3.

Table 3. Predicted and Actual Error for the Five-Cell Beam With Two Concentrated Masses

MODE NO.	EIGENVALUE	ACTUAL $\Delta\lambda/\lambda$	PREDICTED $\Delta\lambda/\lambda$
1	1.6754E6	1.06E-4	1.06E-4
2	1.9465E7	9.50E-4	9.40E-4
3	1.5367E8	2.11E-2	2.05E-2

Notice that all three modes are acceptable for normal engineering practices. This accuracy is surprising when compared to the "rule of thumb" mentioned above. The analysis set included the two large mass points as well as the extreme point of the model.

ACCURACY IMPROVEMENT

The first order correction terms for each eigenvector and eigenvalue, as given by Equations (20) and (24), respectively, when added to the original values, produce results of higher accuracy. The preceding problem is used to provide a numerical example of this technique. Table 4 shows the results.

Table 4. Comparison of Corrected Eigenvalues and Eigenvectors (Translational Degrees of Freedom Only)

		ACTUAL	REDUCED	CORRECTED
	T2-2	.079 043	.079 045	*(1)
M	T3-2	.261 771	.261 822	.261 776
O	T4-2	.496 462	.496 668	*
D	T5-2	.746 667	.746 114	.746 670
E	T6-2	1.000 000	1.000 000	*
1	λE6(2)	1.675 229	1.675 406	1.675 228
	$\Delta\lambda/\lambda$	0.0	1.06E-4	5.97E-7
	T2-2	-.188 478	-.188 305	*
M	T3-2	-.164 285	-.161 416	-.163 820
O	T4-2	.135 814	.136 368	*
D	T5-2	.551 465	.545 963	.551 790
E	T6-2	1.000 000	1.000 000	*
2	λE6(2)	1.944 648	1.946 488	1.944 659
	$\Delta\lambda/\lambda$	0.0	9.46E-4	5.66E-6
	T2-2	.019 266	.018 408	*
M	T3-2	-.132 795	-.117 919	-.130 236
O	T4-2	-.137 034	-.132 191	*
D	T5-2	.320 375	.293 898	.322 948
E	T6-2	1.000 000	1.000 000	*
3	λE6(2)	1.504 932	1.536 720	1.505 240
	$\Delta\lambda/\lambda$	0.0	2.11E-2	6.64E-4

NOTE: (1) Same as reduced; see Equation (18).

(2) Multiply λ by 10 raised to the power indicated.

As can be seen, the accuracy is improved substantially—the least accurate, Mode 3, by nearly a factor of 100.

DMAP LISTING

The DMAP Alters used to produce the numerical examples are shown in Figure 2. Although the procedure is straightforward, a few comments will likely aid the reader. Line numbers refer to the successive lines of the alter.

Line 2. DUM is input via DMI cards; the module, LAMX, does not use it since the first parameter is negative. See the COSMIC/NASTRAN user's manual for a description of LAMX.

Lines 3 and 4. WAM is the radian natural frequency column matrix; MGEN, the generalized mass column matrix.

Line 9. MGI is a square, diagonal matrix with the inverse of the generalized mass of the i^{th} mode in i,i position.

Line 10. LAMD is a square diagonal matrix of eigenvalues.

Line 14. EOA is as defined in Equation (7).

Line 20. ERMN is the scalar error for each mode calculated by Equation (24).

Line 24. PH1O is the "corrected" O-set eigenvectors.

Line 26. LAMD1 is the "corrected" set of eigenvalues.

The bulk data for this example is given in Figure 3.

COMPUTATIONAL COMPARISON

Two problems were used to provide a general guideline to costs (computer time) using this method as compared to the eigenvalue analysis. Since the Guyan reduction is applicable for both direct and modal analysis, and the Givens method is indicated for a small a-set, this method was used for comparison. The small model consisted of 10 DOF in the f-set and 4 DOF in the a-set and 4 modes extracted. The large model consisted of 8092 in the f-set and 203 DOF in the a-set and 75 modes extracted. Table 5 provides a summary of the time required for the major operations. Included, for comparison, is the time required for the modal analysis. The relative time required for the error check vs the modal analysis is clearly dependent on model size. The majority of time is spent in FBS, indicating that the error analysis is roughly the cost of a static analysis.

```
LINE      ALTER 78

  1       UPARTN       USET,MFF/,MOA,,MOO/V,N,MA=F/V,N,M1=A/V,N,M2=0 $
  2       LAMX         DUM,LAMA/LAMB/-1 $
  3       PARTN        LAMB,PWV,/,,WAM,/1 $
  4       PARTN        LAMB,PMV,/,,MGEN,/1 $
  5       TRNSP        WAM/WAMT $
  6       TRNSP        MGEN/MGENT $
  7       MPYAD        MGEN,MGENT,/MG/0/1/0 $
  8       MPYAD        WAM,WAMT,/LAM/0/1/0 $
  9       DIAGONAL     MG/MGI/C,Y,OP/-.5 $
 10       DIAGONAL     LAM/LAMD/C,Y,OP/1.0 $
 11       MPYAD        MGI,LAMD,/LDM/0/1/0 $
 12       MPYAD        MOO,GO,/MGM/0/1/1/2 $
 13       ADD          MOA,MGM/MOM $
 14       FBS          LOO,,MOM/EOA////2 $
 15       SMPYAD       PHIA,MOA,EOA,PHIA,,/ENN1/4////1/1 $
 16       SMPYAD       PHIA,EOA,MGM,PHIA,,/ENN2/4////1/1 $
 17       ADD          ENN1,ENN2/ENN
 18       DIAGONAL     ENN/DENN/C,Y,OP $
 19       MPYAD        LDM,DENN,/ERMN/1///2 $
 20       MATGPR       GPL,USET,SIL,ERMN//A $
 21       MPYAD        GO,PHIA,/P1/0 $
 22       MPYAD        PHIA,LAMD,/PL/0 $
 23       MPYAD        EOA,PL,/P2/0 $
 24       ADD          P1,P2/PHIO $
 25       MPYAD        LAMD,ERMN,/DEL/0 $
 26       ADD          DEL,LAMD/LAMD1/(-1.0,0.0) $
 27       UMERGE       USET,PHIA,PHIO/PHIF/*F*/*A*/*0* $
 28       MATPRN       PHIA,PHIO,PHIF,LAMD,LAMD1// $
          ENDALTER
          $
```

Figure 2. DMAP Alter for Error Evaluation and Reduction

```
GUYAN REDUCTION ERROR ANALYSIS                                  APRIL  20, 1982   NASTRAN 12/29/81    PAGE      3
        BEAM 15 DOF

                                   S O R T E D   B U L K   D A T A   E C H O
 CAR
 COUNT        .   1  ..   2  ..   3  ..   4  ..   5  ..   6  ..   7  ..   8  ..   9  ..  10  .
   1-         ASET1   1       2000
   2-         ASET1   2       2000    4000    6000
   3-         CBAR    101     10      1000    2000    .0      100.0   .0      1
   4-         CBAR    102     10      2000    3000    .0      100.0   .0      1
   5-         CBAR    103     10      3000    4000    .0      100.0   .0      1
   6-         CBAR    104     10      4000    5000    .0      100.0   .0      1
   7-         CBAR    105     10      5000    6000    .0      100.0   .0      1
   8-         CONM2   201     2000            1.E-1
   9-         CONM2   202     4000            1.E-2
  10-         DMI     DUM     0       1       1       1               1       1
  11-         DMI     DUM     1       1       1.
  12-         DMI     PHV     0       2       1       1               5       1
  13-         DMI     PHV     1       4       1.
  14-         DMI     PWV     0       2       1       1               5       1
  15-         DMI     PWV     1       2       1.
  16-         EIGR    10      GIV     .0      1.E10           4                       EIGR
  17-         +EIGR   MAX
  18-         GRID    1000            .0      .0      .0              123456
  19-         GRID    2000            1.73205 .0      .0              345
  20-         GRID    3000            3.46410 .0      .0              345
  21-         GRID    4000            5.19615 .0      .0              345
  22-         GRID    5000            6.92820 .0      .0              345
  23-         GRID    6000            8.66025 .0      .0              345
  24-         MAT1    1       3.E+7           .33     7.38E-4
  25-         PARAM   COUPMASS1
  26-         PARAM   OP      SQUARE
  27-         PBAR    10      1       .7396   .0456   .0456
              ENDDATA
```

Figure 3. Bulk Data Listing of Example 2

Table 5. Time Required for the Major Operations (VAX-11/780)

OPERATION/LINE NUMBER	TIME (SEC)	
	SMALL MODEL*	LARGE MODEL
12	0.5	755
13	0.5	761
14	1.0	31,487
15	1.0	5,935
16	1.0	8,650
MODAL ANALYSIS	60	79,200

* Times are only approximate since the timing data is printed out rounded off to integer seconds.

CONCLUSIONS

In summary, it has been shown that a method exists that provides a useful, cost effective method for estimating the error induced by the Guyan Reduction. The method presented produces a single number for the error in each mode, making it easy for the analyst to evaluate the accuracy of the reduced model that will produce reliable results.

In addition, with a minor amount of additional computational effort, the eigenvectors and eigenvalues can be improved dramatically in accuracy, the error associated with the corrected modes being on the order of $(\Delta\lambda/\lambda)^2$.

ACKNOWLEDGEMENTS

The author is indebted to Tom Butler for his many helpful suggestions and to Russ Miller for continued computational support during the many months that this investigation spanned.

REFERENCES

1. Guyan, Robert J., "Reduction of Stiffness and Mass Matrices," AIAA Journal, Vol. 3, No. 2.

2. NASTRAN Theoretical Manual, Section 11.3 (available from COSMIC, Suite 112, Barrow Hall, Athens, Georgia 30602).

ON RESTARTS IN NASTRAN

P. R. Pamidi* and M. M. Lin
Computer Sciences Corporation

ABSTRACT

The checkpoint/restart capability available in NASTRAN is very sophisticated. Many improvements and enhancements to this capability have been made recently with a view to increasing its efficiency and usefulness. Some important features resulting from these changes are discussed in this paper. In particular, the paper describes the different types of restarts available in NASTRAN and explains how they are handled both in the Rigid Format and DMAP environments. The paper also describes and illustrates the output of restart runs.

INTRODUCTION

The checkpoint/restart feature available in NASTRAN is a very sophisticated and useful capability. The purpose of this feature is to enable a user to checkpoint a NASTRAN run and then restart it (with or without changes in data) by executing only those modules that need to be executed for the restart.

There are several situations in which the use of the checkpoint/restart feature may be desirable. Some of these are listed below:

1. The user may wish to perform his analysis task in two or more stages by specifying scheduled exits in one or more runs.
2. The user may want to ensure that unscheduled exits (resulting from such causes as data errors, insufficient time, insufficient core or hardware failures) will not require him to repeat his entire analysis.
3. The user may wish to rerun his problem by making limited changes in his data.

The checkpoint/restart feature is referenced in several places in the NASTRAN documentation. The user may refer to Sections 2.2 and 3.1 of Reference 1, Sections 1.10 and 7.1 of Reference 2 and Sections 6.4, 11.4.3, 13.5.3 and 13.5.6 of Reference 3 for discussions of the various items related to the use of this feature.

---

* Present affiliation: RPK Corporation

Many improvements and enhancements to the checkpoint/restart capability have been made recently with a view to increasing its efficiency and usefulness. These are all incorporated in the latest release of NASTRAN (Release Apr. 1982). Some important features resulting from these changes are discussed in this paper. In particular, the paper describes the different types of restarts available in NASTRAN and explains how they are handled both in the Rigid Format and DMAP environments. It is hoped that this discussion will result in a better understanding of the checkpoint/restart capability in NASTRAN and lead to more widespread and effective use of this excellent feature.

AUTOMATED CHECKPOINTING IN RIGID FORMATS

The Rigid Format DMAPs no longer employ explicit CHKPNT instructions to checkpoint specific data blocks. Instead, a single PRECHK ALL instruction is used in each Rigid Format to automatically checkpoint all output data blocks from each functional module and PURGE instruction and all secondary data blocks from each EQUIV instruction (see page 5.7-10a of Reference 1). This elegantly accomplishes two important and distinct objectives:

a. Every output data block is checkpointed.*

b. Every output data block that is checkpointed is checkpointed immediately after the DMAP instruction that generated it.

It should be noted that the above two objectives are prerequisites for efficient and satisfactory execution of restarts, particularly unmodified restarts. (A detailed discussion on the types of restarts is given later in the paper). These objectives were not achieved consistently in earlier versions of NASTRAN thereby resulting in inefficient and unsatisfactory restarts.

INCREASED CHECKPOINTING BY USE OF PURGE INSTRUCTIONS IN RIGID FORMATS

All Rigid Formats have been revamped by the addition of PURGE instructions in several appropriate locations in the DMAP. These PURGE instructions in conjunction with the PRECHK ALL instruction discussed earlier result in increased checkpointing in all Rigid Formats. As a matter of fact, checkpointing is now done right till the very end of the DMAP in all Rigid Formats. The net result of this in a checkpoint run is to push the reentry point as far downstream into the DMAP in each Rigid Format as practicable. This ensures that, when a restart is made, the restart run will result in the execution of as few modules as possible thus contributing greatly to the efficiency of the restart.

---

* The only exceptions to this are the CASESS, CASEI and CASECC data blocks appearing as output in substructure analyses.

TYPES OF RESTART

The type of a restart is determined automatically by the program by comparing the input data of the restart run with that of the checkpoint run. The user need not be concerned about the manner in which this is done, but may be interested in knowing the resulting type.

The types of restarts presently recognized in NASTRAN (Release Apr. 1982) are summarized in the following table.

Types of Restarts in NASTRAN

Restart data compared to checkpoint data	Resulting Type of restart	Applicable Environment	
		Rigid Format	DMAP
No effective changes	Unmodified Restart	Yes	Yes
Effective changes only to Case Control Deck and/or Bulk Data Deck	Modified Restart	Yes	Yes
Change in Rigid Format	Modified Restart with Rigid Format Switch	Yes	No

In earlier versions of NASTRAN, an additional type of restart, called the Pseudo Modified Restart, was recognized for cases involving changes only in output requests. This is no longer done since it can now be quite elegantly handled as a special case of the Modified Restart.

The manner in which a restart is handled by the program depends on its type and on its environment (Rigid Format or DMAP environment). This is discussed in the following sections.

RESTARTS IN RIGID FORMAT ENVIRONMENT

Module Execution Decision Table (MEDT) and Mask Word

The heart of the restart logic in the Rigid Format environment is the Module Execution Decision Table (MEDT) associated with each Rigid Format. The MEDT for each Rigid Format can be looked upon as a "matrix" with m "rows" and n "columns" where m is the number of DMAP instructions in the Rigid Format and n is the number of "bits" used to control the restart logic. Thus, each "row" of this matrix corresponds to a DMAP instruction in that Rigid Format and each "column" corresponds to a restart bit. The value of m is different for different Rigid Formats. At present, n is taken to be 155. Bits 1 through 62 are assigned to represent changes in Case Control and Bulk Data Decks, bits 63 through 93 are assigned to represent Rigid Format switches and bits 94 through 155 are assigned to represent file or data block requirements. The actual assignment of the specific bits for each Rigid Format is determined by the Card Name Restart Table, the Rigid Format Change Restart Table and the File Name Restart Table associated with that Rigid Format. (See Sections 1.10 and 7 of Reference 2).

Each "element" in the above MEDT "matrix" is set to 1 if the change represented by the corresponding bit (for bits 1 through 93) affects the corresponding DMAP instruction or if the file or data block corresponding to that bit (for bits 94 through 155) is generated by the corresponding DMAP instruction. Otherwise, the "element" is set to 0.

When the data for a restart run is processed by the program, a mask word that is 155 bits long is first constructed. The Card Name and Rigid Format Change Restart Tables are used to turn on bits in the 1-93 bit portion of this word to represent corresponding changes in data. The 94-155 bit portion of this mask word is initially set to 0.

The MEDT is always used in conjunction with the mask word. The manner in which it is used depends upon the type of restart. This is discussed in detail below.

Unmodified Restart

An unmodified restart involves no effective changes to the data. The execution in this type of restart resumes at the reentry point*. The MEDT data is not used in this case.

It is useful to distinguish between two types of unmodified restarts. These are described below.

- Unmodified restart in which the reentry point is not within a DMAP loop

This is the simplest type of restart possible. In this case, the execution flags for all DMAP instructions prior to the reentry point are turned off and the execution flags for all DMAP instructions from the reentry point onwards are turned on. All input files or data blocks required for the restart already exist on the ØPTP (Old Problem Tape) and will be retrieved. Appendices 1, 2, and 4 illustrate the typical output for this type of restart.

- Unmodified restart in which the reentry pont is within a DMAP loop.

In this case, *initially*, the execution flags for all DMAP instructions prior to the reentry point are turned off and the execution flags for all DMAP instructions from the reentry point onwards are turned on. This is so indicated in the DMAP source listing. However, *subsequently*, the DMAP instructions prior to the reentry point and within the DMAP loop are recognized and their execution flags are turned on. The user is informed about this in the output as shown in Appendix 3. Note, however, that the execution *does* resume at the reentry point, even though DMAP instructions prior to this point are turned on. DMAP instructions within the DMAP loop and prior to the reentry point are executed only if additional passes in the loop need to be executed. If the restart is within the last pass of the DMAP loop, obviously DMAP instructions within the loop and prior to the reentry point are not executed though their execution flags are on.

All input files or data blocks required by the restart already exist on the ØPTP and will be retrieved.

---

* The reentry point for a restart is the last reentry point specified in the restart dictionary. It is an integer equal to the instruction number of the DMAP instruction at which the restart will resume execution. (See Section 2.2 of Reference 1).

Appendices 1 through 4 illustrate the typical output for this type of restart.

Modified Restart

This type of restart involves one or more effective changes to the data in the Case Control Deck and/or in the Bulk Data Deck. In this case, all DMAP instructions from the reentry point onwards have their execution flags turned on. In addition, this type of restart generally requires that certain DMAP instructions prior to the reentry point be also turned on, depending on the specific data changes involved. The DMAP instructions that need to be so turned on are determined by comparing the 1-62 bit portion of the mask word with the corresponding portion of each "row" of the MEDT "matrix" prior to the reentry point. The DMAP source listing provided in the output indicates all the DMAP instructions whose execution flags are initially turned on by the above procedure.

Once the DMAP instructions are initially turned on as described above, the program checks to see if all the required input data blocks are either being generated by prior modules or are available on the 0PTP for retrieval. If so, no additional DMAP instructions need to be turned on. If, however, there are any input data blocks that are neither being generated by prior modules nor are available on the 0PTP, the program turns on bits corresponding to these data blocks in the 94-155 bit portion of the mask word by using the File Name Restart Table associated with the Rigid Format. This portion of the mask word is then compared with the corresponding (94-155 bit) portion of each "row" of the MEDT "matrix" prior to the reentry point in order to determine the additional DMAP instructions that need to be turned on to generate the data blocks in question.

After the additional DMAP instructions are turned on as described in the above paragraph, the process is repeated until it is ensured that all the required input data blocks are either generated by prior modules or can be retrieved from the 0PTP.

All the DMAP instructions that are turned on as per the above logic (by the use of the File Name Restart Table) are identified and listed in the restart output just after the DMAP source listing. This is shown in Appendix 7.

Those input files or data blocks that are needed for the restart and that are available on the 0PTP are retrieved.

Appendices 5, 6, 7 and 4 illustrate the typical output of a modified restart.

It should be noted that the execution in a modified restart will start at the first module in the DMAP sequence whose execution flag is turned on. Generally, this is before the reentry point.

Modified Restart with Rigid Format Switch

This type of restart involves a switch from one Rigid Format to another. It may or may not involve effective changes to the data in the Case Control Deck and/or in the Bulk Data Deck.

The most important point to recognize in this type of restart is that the reentry point is quite meaningless since it was determined in relation to another Rigid Format. This is handled in the program by resetting the reentry point to an extremely high value which, for all practical purposes, can be considered to be infinite. As a result, all DMAP instructions in the restart are considered to be before the reentry point and no DMAP instructions are considered to exist after the reentry point.

Once this important change is made, this type of restart is handled in the program in exactly the same manner as a modified restart. Thus, all the required DMAP instructions are turned on by a consideration of the mask word and the MEDT data for the restart Rigid Format as per the logic described earlier for modified restart.

Appendix 8 in conjunction with Appendices 6 and 7 and 4 illustrates the typical output for this type of restart.

Use of DMAP ALTERs in Restarts

Because different types of restarts are handled differently by the program, the user should be careful in the use of DMAP ALTERs in restarts.

In the case of an unmodified restart in which the reentry point is not within a DMAP loop, the only DMAP instructions that are flagged for execution are those that are beyond (and include) the reentry point. Hence, a DMAP ALTER will be flagged for execution only if it is beyond the reentry point and will be ignored if it is before the reentry point.*

---

* The user can ensure that a DMAP ALTER in an unmodified restart is flagged for execution by suitably deleting the latter part of the restart dictionary so that the reentry point is before the DMAP ALTER. This, of course, will, in general, cause more modules to be executed in the restart.

In the case of an unmodified restart in which the reentry point is within a DMAP loop, the only DMAP instructions flagged for execution are those that are beyond (and include) the reentry point and those that are before the reentry point but within the DMAP loop. Hence, a DMAP ALTER will be flagged for execution only if it is beyond the reentry point or before it but within the DMAP loop. Otherwise, it will be ignored.*

In the case of a modified restart and a modified restart with Rigid Format switch, a DMAP ALTER will be flagged for execution regardless of its position in the DMAP with respect to the reentry point.

RESTARTS IN DMAP ENVIRONMENT

Restarts in DMAP environment are much easier to handle than restarts in Rigid Format environment. Unlike a Rigid Format, the modules and their sequence in a DMAP are, by definition, not predetermined. Hence an MEDT is meaningless for a DMAP. There is therefore also no need for using a mask word in handling a restart in DMAP environment.

Unmodified Restart

An unmodified restart in DMAP environment is handled by the program exactly like an unmodified restart in Rigid Format environment. This applies to both types of unmodified restarts - those in which the reentry point is not within a DMAP loop and those in which the reentry point is within a DMAP loop.

Modified Restart

The effect of changes in the Case Control Deck and/or in the Bulk Data Deck on particular modules in a modified restart in DMAP environment cannot be determined since the DMAP itself is not predefined. Hence, it is assumed that the changes will affect the entire DMAP which, therefore, needs to be re-executed. This is accomplished in the program by re-setting the reentry point to zero and treating this case as an unmodified restart. This causes the entire DMAP to be re-executed. Because of this, the need for a modified restart in DMAP environment is questionable except to reuse a large Bulk Data Deck from the ØPTP.

---

* See footnote on the previous page.

OUTPUT FROM RESTART RUNS

The output resulting from restart runs has been made much more meaningful to the user. Specific items are discussed below:

- Unsorted and sorted Bulk Data Deck echo

ECHØ=BØTH (in the Case Control Deck) has been made the default for restart runs. Since the only bulk data cards that the user submits in a restart run are those that represent deletions from and/or additions to the Bulk Data Deck already on the ØPTP, the unsorted echo of the Bulk Data Deck is the only way of identifying these deletions and/or additions. (The user can, of course, override the default by specifying, for example, ECHØ=SØRT or ECHØ=NØNE).

- Automatic output of the DMAP source listing

The LIST option on the XDMAP card (see page 5.7-14 of Reference 1) has been made the default for restart runs. This causes the DMAP source listing to be automatically output on the print file. There is no longer any need, therefore, to turn on DIAG 14 (in the Execution Control Deck) for this purpose. The DMAP source listing is useful in a restart run since the user can identify the DMAP instructions that are flagged for execution as described earlier in the paper. (The user can suppress the output of the DMAP source listing by ALTERing in an XDMAP card with NØLIST option).

- Identification of the type of restart

The output of the restart run clearly identifies the restart by type (see earlier discussion in the paper) and also lists the effective data changes (if any) that control the restart. The output distinguishes between effective changes made to the Case Control Deck and those made to the Bulk Data Deck. Appendices 1, 5 and 8 illustrate this output for all possible types of restart.

- Identification (in the DMAP source listing) of DMAP instructions initially flagged for execution in the restart

The DMAP source listing (that is automatically output by default in a restart) identifies those DMAP instructions that are initially flagged for execution by the symbol * on the left of the DMAP instruction names. (It should be emphasized that a DMAP instruction marked with the symbol * is only flagged for execution; whether it actually gets executed or not is decided by the logic in the DMAP).

The DMAP source listing also identifies those DMAP instructions that are processed only at DMAP compilation time, but are not actually executed. These instructions are identified by the symbol + on the left of the DMAP instruction names. (DMAP instructions BEGIN, FILE, LABEL, PRECHK and XDMAP are the only instructions that belong to this category).

Messages output just after the DMAP listing inform the user about the use of the above mentioned symbols. Appendices 2 and 6 illustrate this output.

- Identification of additional DMAP instructions flagged for execution

The DMAP instructions flagged for execution and indicated by the symbol * in the DMAP source listing (see discussion above) are those that are initially flagged as such by the restart logic. Additional DMAP instructions may need to be flagged for execution in order to generate certain required data blocks in the case of modified restarts or to accomplish looping in unmodified restarts involving DMAP looping. Such instructions are appropriately identified in the output. Appendices 3 and 7 illustrate such cases.

- Listing of files or data blocks retrieved from the ØPTP

The input files or data blocks that are required for the restart and that are retrieved from the ØPTP are listed in the output. Appendix 4 illustrates this type of output.

SUMMARY

The important features of the checkpoint/restart capability resulting from recent improvements and enhancements are discussed. In particular, the types of restarts available in NASTRAN are described and the manner in which they are handled by the program is explained. The paper also describes and illustrates the output of restart runs.

REFERENCES

1. The NASTRAN User's Manual, (Level 17.5), NASA SP-222(05), December 1978.

2. The NASTRAN Programmer's Manual, (Level 17.5), NASA SP-223(05), December 1978.

3. Field, E. I., Herting, D. N., and Morgan, M. J., NASTRAN User's Guide, (Level 17.5), NASA Contractor Report 3146, June 1979.

```
*** USER INFORMATION MESSAGE 4143, THIS IS AN UNMODIFIED RESTART.
```

Appendix 1. Output of an unmodified restart indicating the type of restart

```
TEST OF UNMODIFIED RESTART                          FEBRUARY 16, 1982   RELEASE  APR. 1982    PAGE     8

   LEVEL 2.0 NASTRAN DMAP COMPILER - SOURCE LISTING

  15  INPUTT2  /D,,,,/ S
  16  MATPRN   A,B,,,// S
  17  MATPRN   C,,,,// S
  18  MATPRN   D,,,,// S
  19  INPUTT2  /E,F,,,/-3// S
  20  MATPRN   E,F,,,// S
  21  INPUTT2  /TABLE1,,,,/-5// S
  22  MATPRN   TABLE1,,,,// S
  23  INPUTT2  /TABLE2,TABLE3,,,/-6// S
  24  MATPRN   TABLE2,TABLE3,,,// S
  25  INPUTT2  /TABLE4,TABLE1,,,/-7// S
  26  MATPRN   TABLE4,TABLE1,,,// S
+ 27  LABEL LOOP S
  28  INPUTT2  /MATRIX,TABLE5,,,/-8// S
* 29  MATPRN   MATRIX,TABLE5,,,// S
* 30  REPT  LOOP,2 S
* 31  INPUTT2  /MATRIX,TABLE5,,,/-8// S
* 32  END   S

+ INDICATES DMAP INSTRUCTIONS THAT ARE PROCESSED ONLY AT DMAP COMPILATION TIME.
* INDICATES DMAP INSTRUCTIONS THAT ARE FLAGGED FOR EXECUTION IN THIS UNMODIFIED RESTART.
```

Appendix 2. Output of an unmodified restart with the DMAP source listing

```
     TEST OF UNMODIFIED RESTART                          FEBRUARY 16, 1982   RELEASE  APR. 1982    PAGE      9


 *** USER INFORMATION MESSAGE 4148
     NOTE THAT ADDITIONAL DMAP INSTRUCTIONS (NOT INDICATED BY AN * IN THE DMAP SOURCE LISTING)
     NEED TO BE FLAGGED FOR EXECUTION SINCE THIS UNMODIFIED RESTART INVOLVES DMAP LOOPING AND
     THE REENTRY POINT IS WITHIN A DMAP LOOP.  SUCH INSTRUCTIONS ARE IDENTIFIED BELOW.
     HOWEVER, THE EXECUTION WILL RESUME AT THE LAST REENTRY POINT (DMAP INSTRUCTION NO.   29).

   28   INPUTT2
```

Appendix 3. Output of an unmodified restart (with the reentry point within a DMAP loop) indicating the additional DMAP instructions that are flagged for execution

```
TEST OF UNMODIFIED RESTART                    FEBRUARY 16, 1982   RELEASE  APR. 1982    PAGE     10


THE FOLLOWING FILES FROM THE OLD PROBLEM TAPE WERE USED TO INITIATE RESTART

   FILE NAME  REEL NO.  FILE NO.

    TABLES     (PURGED)
    MATRIX           1          27
    XVPS             1          28

          **NO ERRORS FOUND - EXECUTE NASTRAN PROGRAM**
```

Appendix 4. Output of a restart indicating the files (or data blocks) retrieved from the ØPTP (Old Problem Tape)

```
     DELTA WING          RESTART                                                MARCH   1, 1982   RELEASE  APR. 1982    PAGE     11
     NASTRAN DEMONSTRATION PROBLEM NO. 1-4-1A

     LOAD ON LEADING EDGE

*** USER INFORMATION MESSAGE 4144. THIS IS A MODIFIED RESTART.

CASE CONTROL AND BULK DATA DECK  CHANGES AFFECTING THIS RESTART ARE INDICATED BELOW.


EFFECTIVE CASE CONTROL DECK CHANGES
-----------------------------------

MASK WORD - BIT POSITION ---- FLAG NAME ---- PACKED BIT POSITION

   15
                3             LOADS                    39
               17             POUTS                    19
               31             NOLCOPS                  31

EFFECTIVE BULK DATA DECK CHANGES
--------------------------------

NONE
```

Appendix 5. Output of a modified restart indicating the type of restart

```
DELTA WING          RESTART                                           MARCH  1, 1982  RELEASE  APR. 1982   PAGE     19
NASTRAN DEMONSTRATION PROBLEM NO. 1-1-1A

LOAD ON LEADING EDGE

    LEVEL 2.0 NASTRAN DMAP COMPILER - SOURCE LISTING


  140  PRTMSG    PLOTX2// $

+ 141  LABEL     P2 $

+ 142  LABEL     LOOPEND $

  143  COND      FINIS,COUNT $

  144  REPT      LOOPTOP,360 $

* 145  JUMP      FINIS $

+ 148  LABEL     ERROR2 $

  149  PRTPARM   //-2/*STATICS* $

+ 150  LABEL     ERROR3 $

* 151  PRTPARM   //-3/*STATICS* $

+ 152  LABEL     ERROR4 $

  153  PRTPARM   //-4/*STATICS* $

+ 154  LABEL     ERROR5 $

  155  PRTPARM   //-5/*STATICS* $

+ 156  LABEL     FINIS $

* 157  PURGE     DUMMY/MINUS1 $

* 158  END       $


+ INDICATES DMAP INSTRUCTIONS THAT ARE PROCESSED ONLY AT DMAP COMPILATION TIME.

* INDICATES DMAP INSTRUCTIONS THAT ARE FLAGGED FOR EXECUTION IN THIS MODIFIED RESTART.
```

Appendix 6. Output of a modified restart with the DMAP source listing

BLANK PAGE

BLANK PAGE

BLANK PAGE

```
     DELTA WING              RESTART. REAL EIGENVALUE ANALYSIS                    MARCH   1, 1982   RELEASE  APR. 1982    PAGE      19
     NASTRAN DEMONSTRATION PROBLEM NO. 1-1-1B

             RIGID FORMAT SWITCH FROM 1 TO 3

*** USER INFORMATION MESSAGE 4147
    NOTE THAT ADDITIONAL DMAP INSTRUCTIONS (NOT INDICATED BY AN * IN THE DMAP SOURCE LISTING)
    NEED TO BE FLAGGED FOR EXECUTION IN ORDER TO GENERATE CERTAIN REQUIRED DATA BLOCKS.
    SUCH INSTRUCTIONS AND THE ASSOCIATED DATA BLOCKS ARE IDENTIFIED BELOW.

TO GENERATE DATA BLOCK MAA       - TURN ON THE EXECUTE FLAG FOR THE FOLLOWING DMAP INSTRUCTIONS

   60  XEQUIV
   61  COND
   63  SMP2

TO GENERATE DATA BLOCK MFF       - TURN ON THE EXECUTE FLAG FOR THE FOLLOWING DMAP INSTRUCTIONS

   43  XPURGE
   55  XEQUIV
   56  COND
   57  SCE1

TO GENERATE DATA BLOCK MNN       - TURN ON THE EXECUTE FLAG FOR THE FOLLOWING DMAP INSTRUCTIONS

   50  XEQUIV
   51  COND
   53  MCE2

TO GENERATE DATA BLOCK MR        - TURN ON THE EXECUTE FLAG FOR THE FOLLOWING DMAP INSTRUCTIONS

   65  COND
   69  RBMG4

TO GENERATE DATA BLOCK MLL       - TURN ON THE EXECUTE FLAG FOR THE FOLLOWING DMAP INSTRUCTIONS

   66  RBMG1
```

Appendix 7. Output of a modified restart indicating the additional DMAP instructions that are flagged for execution

```
     DELTA WING              RESTART, REAL EIGENVALUE ANALYSIS              MARCH   1, 1982   RELEASE  APR. 1982    PAGE     12
     NASTRAN DEMONSTRATION PROBLEM NO. 1-1-1B

             RIGID FORMAT SWITCH FROM 1 TO 3

  *** USER INFORMATION MESSAGE 4145, THIS IS A MODIFIED RESTART INVOLVING RIGID FORMAT SWITCH.

  CASE CONTROL AND BULK DATA DECK CHANGES AFFECTING THIS RESTART ARE INDICATED BELOW.

  EFFECTIVE CASE CONTROL DECK CHANGES
  -----------------------------------

  MASK WORD - BIT POSITION ---- FLAG NAME ---- PACKED BIT POSITION

     15
                  4             METHODS              62
                 17             POUTS                19
  EFFECTIVE BULK DATA DECK CHANGES
  --------------------------------

  MASK WORD - BIT POSITION - CARD/PARAM NAME - PACKED BIT POSITION

     3
                 23             EIGR                 61
```

Appendix 8. Output of a modified restart with Rigid Format switch indicating the type of restart

1. Report No
NASA CP-2249

2. Government Accession No

3. Recipient's Catalog No

4. Title and Subtitle
Tenth NASTRAN® Users' Colloquium

5. Report Date
November 1982

6. Performing Organization Code

7. Author(s)

8. Performing Organization Report No

10. Work Unit No

9. Performing Organization Name and Address
Computer Software Management and Information Center
University of Georgia
Athens, GA 30602

11. Contract or Grant No

13. Type of Report and Period Covered
Conference Publication

12. Sponsoring Agency Name and Address
National Aeronautics and Space Administration
Washington, D.C. 20546

14. Sponsoring Agency Code

15. Supplementary Notes

16. Abstract

This publication is comprised of papers presented at the Tenth NASTRAN® Users' Colloquium held at the Marriott Hotel, New Orleans, Louisiana, May 13-14, 1982. The authors discuss the general application of finite element methodology and the specific application of NASTRAN to a wide variety of static and dynamic structural problems.

17. Key Words (Suggested by Author(s))
NASTRAN, structures
Finite element analysis
Substructuring
Colloquium

18. Distribution Statement
Unclassified - Unlimited

Subject Category 39

19. Security Classif (of this report)
Unclassified

20. Security Classif (of this page)
Unclassified

21. No of Pages
273

22. Price*
A12

* For sale by the National Technical Information Service, Springfield, Virginia 22161

NASA-Langley, 1982

268